The Regioselective Dimerisation of Phenol

A Thesis Presented to the University of Glasgow
for the Degree of Doctor of Philosophy

David John Marshall Williams

November 2006

The polymerisation of 2,6-dimethylphenol for the production of carbon-carbon and carbon-oxygen coupled biphenol compounds is currently catalysed on an industrial scale using homogeneous phase copper/diamine complexes. These homogeneous systems are however unable to yield useful polymers from phenols with only one or no *ortho*-substituent. The stereoselective polymerisation of 2- and/or 6-unsubstituted phenols has been a challenge since the late 1950's.

For the production of biphenol from phenol, both direct dehydrogenation and oxidative dehydrogenation can be envisaged. Catalytic systems for the selective carbon-carbon dimerisation of phenol are currently undeveloped. A commercial one-step regioselective synthesis of biphenol compounds from phenol would dramatically reduce production costs since phenol is a relatively cheap and readily available starting material. The aim of this research project was to develop a catalyst system(s) capable of selectively generating 4,4'-biphenol, 2,2'-biphenol and 4-phenoxyphenol from phenol, exploiting the compounds different molecular shapes and dimensions. Biphenols are used as lubricants, fuel additives, antioxidants, polymerisation intermediates and fungicides.

This research project studied the one-step regioselective synthesis of biphenol compounds from phenol using the zeolite catalysts: Zeolite-Y and ZSM-5, the clays: Montmorillonite and Attapulgite and the mesoporous catalyst MCM-41. Zeolites are crystalline aluminosilicates whose structures contain molecular sized and shape selective cavities that can be used as molecular sieves and/or the location of active sites for heterogeneous catalysis. Shape selectivity was important for the dimerisation of phenol to biphenols.

This investigation has demonstrated that the regioselective dimerisation of phenol can be realised using metal-ion exchanged zeolites and clays as catalysts. A new reaction mechanism has been proposed which demonstrates the need for both water and oxygen. The oxygen was required to oxidise Cu^{1+} back to Cu^{2+} and water used to convert Brønsted acid sites back to Lewis base sites in order to complete the catalytic cycle. The results from this research project suggest the coupling of phenoxy radicals coordinated to the catalyst. The yield of phenolic dimers was controlled by the position of active sites and therefore adsorbed phenoxy radicals.

Solvents used to dissolve the phenol had a considerable impact on the selectivity of phenol dimerisation. These solvent effects had not previously been investigated. Acetonitrile was found to be not only a solvent but also a catalyst modifier. The solvent used did not however affect the rate of reaction, rate-determining step or conversion of phenol. The selectivity of phenol dimerisation catalysed by Cu/Zeolite-Y or Cu/Attapulgite was due to the competitive adsorption between water, the solvent and phenol at copper exchanged sites.

Thank you Professor David Jackson for all your help and guidance. There was never an occasion when you were too busy to discuss aspects of my research or ask some difficult questions to concentrate the mind. Thank you also for combining forces with Gail to ensure I always gave my best. Thank you Gail Paterson, although you will soon be Gail Williams, for everything. I only wish we could jointly receive 'The PhD'. Thank you Mum and Dad for your encouragement and continued support, especially in the difficult moments. Thank you Jan and Bruce Paterson for your support, meals and beer!

I was lucky enough to have my PhD funded by Sumitomo Chemical Ltd., who are based in Japan. Thank you Dr Carsten Stöcker and Makoto Kitano for your continued interest in the project and taking the time to read all of those reports.

Thank you Ron Spence, Andy Monaghan, Arran Canning, Dan Rosenberg, Elaine Opara, Elaine Vass, Elaine Gelder, Sharon Burns, Gemma Parker and Sreekala Rugmini for all your help.

Figures

Equations

Tables

1 Introduction

'Catalysis is the acceleration of a chemical reaction by a small quantity of a substance, which may take part in the reaction, but in the end is not changed by the reaction.'[1] In homogeneous catalysis the reactants and catalyst form a single phase; in heterogeneous catalysis they are in different phases. Catalysts provide an alternative reaction pathway for which the activation energy is lower. This increases the rate at which the reaction approaches equilibrium but does not alter the position of equilibrium.

Heterogeneous catalysts are solid porous materials, for example zeolites and clays or impregnated materials, for example Rh/SiO_2. Reactant molecules have to be transported from the bulk to the active sites of the catalyst and products removed. The selectivity of a solid catalyst for a particular reaction or desired product is often unrivalled. The complex reaction kinetics and mechanisms of heterogeneous catalysis mean however that catalyst selection is still often empirical and based on prior experience or analogy.[1] Catalyst porosity, pore structure and size and the shape and type of reactor must be considered for each system. 'Recent years have witnessed a phenomenal growth in the use of inorganic solids as reaction media for organic transformations'.[2] Indeed, the future of synthetic organic chemistry depends on the development of heterogeneous media.[3] The inorganic solids are catalysts used to enhance the rate of reaction, improve product selectivity and therefore help the drive towards a cleaner and *greener* chemical industry.

This thesis documents the development of a range of inorganic heterogeneous catalysts for the regioselective dimerisation of phenol. There are currently no commercial catalysts capable of catalysing the dimerisation of phenol either to carbon-carbon or carbon-oxygen coupled dimers.

1.1 Biphenol production

Homogeneous phase copper/diamine complexes catalyse the polymerisation of 2,6-dimethylphenol (DMP) on an industrial scale (Figure 1).

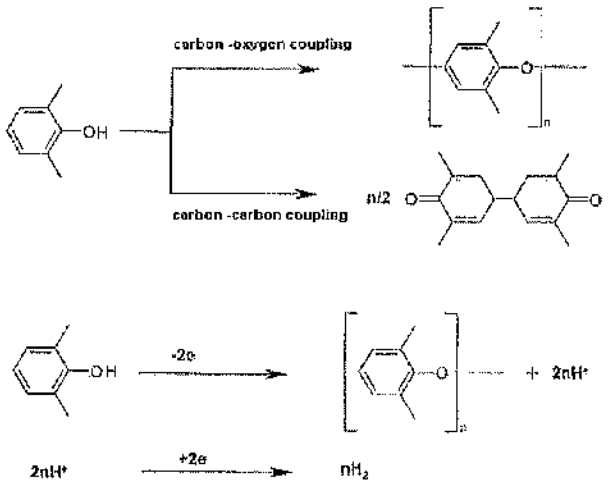

Fig. 1[4] The polymerisation of 2,6-dimethylphenol.

These homogeneous systems are however unable to yield useful polymers from phenols with only one or no *ortho*-substituent. The stereoselective polymerisation of 2- and/or 6-unsubstituted phenols has been a challenge since Hay's pioneering work in the late 1950's.[5] The enzymatic tyrosinase model complexes are selective for the carbon-oxygen coupling of phenols although other systems also offer potential.[6] The catalytic oxidative polymerisation of phenols is regarded as a clean and efficient process for the synthesis of phenolic polymers. A heterogeneous catalytic system would eliminate the need for product and catalyst separation and has the potential to reduce byproduct formation. 'The ever growing number of patents filed on the use of heterogeneous copper catalysts witnesses their renewed interest due to their selectivity and low ecotoxicity.'[7] 'The conditions are however demanding, the homogeneous polymerisation uses molecular oxygen and coordinating ligands such as amines that have the potential to cause leaching of metal species from a heterogeneous system. Catalytic systems for the selective carbon-carbon dimerisation of phenol are as yet undeveloped. A commercial one-step regioselective synthesis of biphenol compounds

from phenol would dramatically reduce production costs. Phenol is a relatively cheap and readily available starting material.

For the production of biphenol from phenol, both direct dehydrogenation and oxidative dehydrogenation can be envisaged. Direct dehydrogenation reactions are usually endothermic and operated at elevated temperatures. Operating *catalytic* dehydrogenation reactions at raised temperatures unfortunately increases coke formation and therefore the possibility of catalyst deactivation.

$$2\ C_6H_5OH \rightarrow HO(C_6H_4).(C_6H_4)OH + H_2$$

Oxidative dehydrogenation (ODH) is the alternative route.

$$2\ C_6H_5OH + \tfrac{1}{2}O_2 \rightarrow HO(C_6H_4).(C_6H_4)OH + H_2O$$

Most ODH reactions use temperatures ca. 200 K lower than direct dehydrogenation reactions. This is an important advantage for an industrial scale process; lower temperatures mean lower fuel costs and coking should be less prominent although there are inherent disadvantages to the ODH process. Combustion of the feedstock and a concern about explosive limits mean there are few if any industrial processes for dehydrogenation that involve an oxidation step.

1.1.1 Uses of 4,4'- and 2,2'-biphenol and 4-phenoxyphenol

Biphenols are used as lubricants, fuel additives, antioxidants, polymerisation intermediates and fungicides.[8] The high melting point and crystallinity of 4,4'-biphenol provides high heat distortion resistance, important at electrical contacts in polyether liquid crystal displays (LCDs) and many other electronic devices including mobile phones and computers.[9] The reliable and economic production of 4,4'-biphenol is therefore important for the development of related growth areas within the electronics industry. The dimer 4-phenoxyphenol is used in the preparation of pesticides and as an intermediate in manufacture of many pharmaceutical compounds.

1.1.2 Current manufacturing routes

The current manufacturing route to 4,4'-biphenol uses the oxidative coupling of 2,6-di-*tert*-butylphenol and subsequent debutylation.[10] The dimer 4-phenoxyphenol is manufactured by the condensation of sodium phenolate with 4-chlorophenol.[11] No information was available for the manufacturing route to or uses of 2,2'-biphenol. The current production of 4,4'-biphenol is 7000 Ton/year at ca. £10 kg^{-1}, production of 4-phenoxyphenol is 30 Ton/Year at ca. £25 kg^{-1}. Both 4,4'-biphenol and 4-phenoxyphenol are classified as fine chemicals.

1.2 Zeolite and clay catalysts

This research project studied the one-step regioselective synthesis of biphenol compounds from phenol using the zeolite catalysts: Zeolite-Y and ZSM-5, the clays: Montmorillonite and Attapulgite and mesoporous catalyst MCM-41. The properties of these materials are summarised in Table 1.

Table 1[12-14] Properties of Zeolite Y, ZSM5, MCM-41, Montmorillonite and Attapulgite.

Name	*Description*	*Dimensions*	*Si:Al ratio*
Zeolite-Y	Synthetic form of the zeolite - Faujasite. Consists of four tetrahedrally orientated 12-ring openings.	12-ring aperture has a diameter of 0.74 nm. Internal supercage has a diameter of ~1.3 nm.	Between 1.5 and 3.
ZSM-5	Most siliceous common zeolite. Consists of two intersecting 10-ring tunnel systems.	10-ring aperture has a diameter of 0.55-0.6 nm.	Between 25 and 2000.
MCM-41	Hexagonal, unidimensional mesopores.	Aperture has a diameter of 1.6-10 nm.	A high Si:Al ratio
Montmorillonite (Smectite)	Layered structure. Octahedral sheet positioned between two tetrahedral sheets. Pillaring is possible.	Pillaring provides a space of ~0.8 nm between layers	A high Si:Al ratio
Attapulgite (Palygorskite)	Silica tetrahedra in double chains linked through oxygens at their longitudinal edges, ribbon characteristic.	Channels are many nm long.	A high Si:Al ratio

Zeolites are crystalline aluminosilicates whose structures contain molecular sized and shape selective cavities that can be used as molecular sieves and/or the location of active sites for heterogeneous catalysis. Shape selectivity is important for the dimerisation of phenol to biphenols. The aim of this research project has been to develop a catalyst system(s) capable of selectively generating 4,4'-biphenol, 2,2'-biphenol and 4-phenoxyphenol from phenol, exploiting the compounds different molecular shapes and dimensions.

There are many naturally occurring and synthetic zeolites all of which have a three dimensional, polymeric structure of tetrahedral SiO_4 and AlO_4^- units linked by shared oxygens, the most basic of which is the sodalite cage (Figure 2). Access to this cage is through a six-membered ring, the aperture of which has a diameter of ~0.25 nm and

the internal diameter of the cage is 0.66 nm. To maintain electrical neutrality these structures contain framework cations, usually Na^+. These cations can however be replaced using ion-exchange techniques.

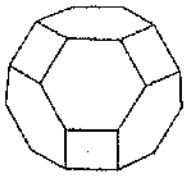

Fig. 2 The sodalite cage.

Zeolites are potential Lewis and Brønsted solid acids and bases. These properties are ultimately controlled by the Si:Al ratio. A high Si:Al ratio is obtained by removing some of the framework aluminium which produces an acidic zeolite. If the number of AlO_4^- species is increased then a basic zeolite can be created. The basic properties are enhanced if Na^+ is replaced with large cations such as Cs^+.

Clays occur abundantly in nature and like zeolites their high surface area, sorptive and ion-exchange properties are increasingly been exploited for catalytic applications. Clay minerals are crystalline, layered silicates. Smectites are a group of clay minerals with a dioctahedral or trioctahedral 2:1 layered structure of which montmorillonite is the most important.[2] Montmorillonite has a high cation-exchange capacity (CEC) and good swelling properties. Montmorillonites were used extensively for petroleum processing during the 1930's and 40's before zeolites began to replace them as more thermostable alternatives. Clay catalysts are however undergoing a revival as it becomes increasingly important for any new catalytic process to be environmentally benign.[15]

The MCM-41 materials possess a regular, uniform array of hexagonal unidimensional mesopores that can be varied in diameter from approximately 1.6 to 10nm[12]. These materials bridge the gap between uniform microporous and amorphous mesoporous materials. A paper by Szegedi and co-workers[16] reported the synthesis and characterisation of MCM-41 materials containing transition metals. Similarly, Karthik and colleagues[17] reported the characterisation of Co,Al-MCM-41. There was an important difference between the acidic properties of these two catalysts. The preparations of both materials were analogous apart from the inclusion of aluminium

into one of the catalysts. Using DRIFT spectra of chemisorbed pyridine (Figure 3), Karthik *et al.*.[17] showed that Co,Al-MCM-41 contained both Brønsted and Lewis acid sites.

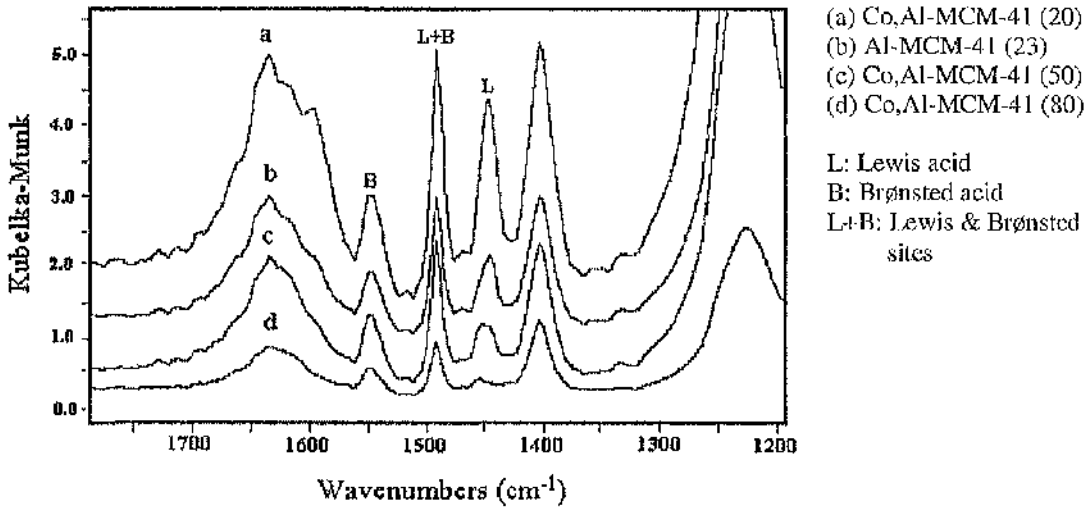

Fig. 3 DRIFT spectra of pyridine adsorption region of mesoporous materials.

In contrast, the FT-IR spectra of adsorbed pyridine on samples of Co- and Cu-MCM-41 (Figure 4) indicated the presence of only Lewis acid sites. Szegedi and co-workers[16] concluded that Co- and Cu-MCM-41 catalysts contain no Brønsted acid sites.

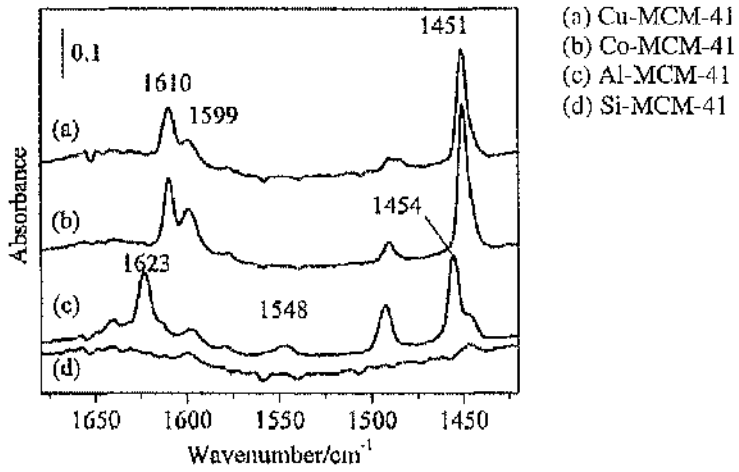

Fig. 4 FT-IR spectra of adsorbed pyridine on samples (a)-(d).

Other zeolites are currently at the forefront of design and application. Recently reported has been 'ITQ-15: The first ultra-large pore zeolite with a bi-directional pore system formed by intersecting 14 and 12-ring channels...'[18] The pore topology of ITQ-15 zeolite displays a 14-ring channel that is intersected perpendicularly by a 12-ring pore. Acid sites have been introduced into its framework to provide catalytic activity.

1.2.1 Shape selectivity

The shape selectivity of reactions catalysed by zeolites and clays can be provided by reactant selectivity, two types of product selectivity and restricted transition-state selectivity.[19] Zeolites can be both size and shape selective catalysts. The effective catalytic pore size is temperature dependent, for H/ZSM5 this has been calculated by Webster *et al.*.[19] to be between 6.62 and 7.27 Å at 573 K. At a temperature of 643 K the minimum pore diameter was reported to increase to more than 7.64 Å. The same temperature change increased the pore intersection dimensions from 8.17 by 8.88 Å to 9.08 by 9.09 Å.

Reactant selectivity describes potential exclusion of reactant molecules on the basis of their size compared to the dimensions of the pore opening. Figure 5 illustrates reactant selectivity.

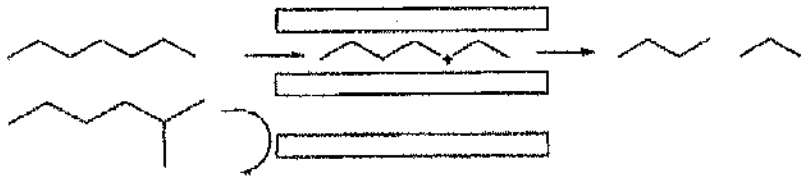

Fig. 5[19] Reactant selectivity provided by zeolites and clays.

Preferential diffusion occurs when two or more, often isomers form within the pore structure of a zeolite or clay that have significantly different diffusivities (Figure 6). This is also referred to as configurational diffusion controlled product selectivity.

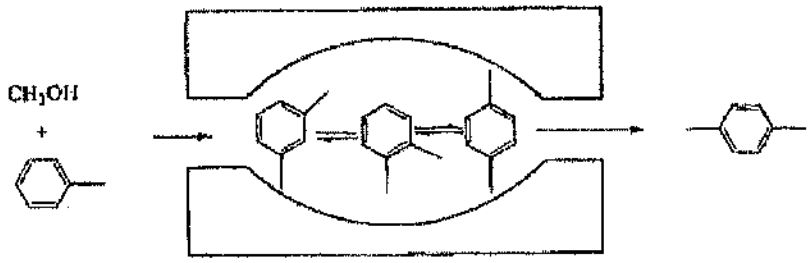

Fig. 6[19] Configurational diffusion controlled product selectivity provided by zeolites and clays.

The second type of product selectivity is size-exclusion, characterised by the confinement of a reaction product, as illustrated in Figure 7.[20]

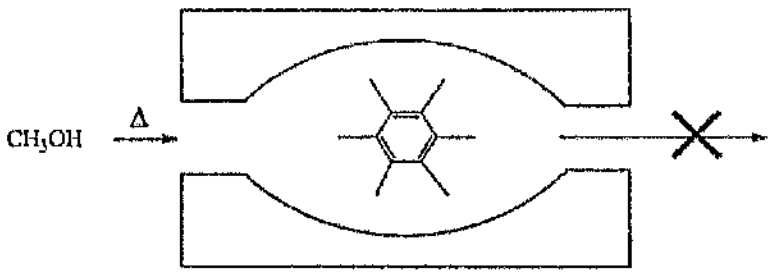

Fig. 7[19] Size exclusion product selectivity provided by zeolites and clays.

Finally, transition-state selectivity describes when one or more transition states is too large to be contained within the pores or intersections of the zeolite or clay.[19]

Despite these classifications specific experimental data is important. Many authors have reported catalytic reactions within, and diffusion of molecules through, zeolite and clay catalysts involving molecules that have molecular dimensions larger than the reported maximum pore dimensions of the material. These discrepancies have been ascribed to thermal vibrations and distortion of the crystal lattice and/or adsorbate molecules.

1.2.2 Catalyst preparation

Pure siliceous mesoporous materials consist of a neutral framework and are therefore of limited use. Modification of the amorphous walls and inclusion of heteroatoms allows useful and diverse catalytic materials to be created. Isomorphous substitution of Al^{3+} for Si^{4+} creates negative charges that must be balanced by cations.[17] These cations can be protons, sodium or transition metal ions amongst others. The incorporation of transition or early transition metals within zeolitic materials allows the generation of redox properties and possible synthesis of bifunctional catalysts.[21] The metals can occupy extra-framework sites or be incorporated into the support structure of the material. The process of ion-exchange involves the exchange of extra-framework cations, usually Na^{+} ions for protons or transition metal ions. Isomorphous substitution incorporates transition metal cations into the skeleton structure although this is normally only possible during the initial synthesis of the support.[21]

Lee and co-workers[22], Baba *et al.*.[23], Zhanpeisov *et al.*.[24] and Li *et al.*.[25] all reported similar catalyst preparation techniques. The same techniques were used for the preparation of the zeolite and clay catalysts used for this research project. The kinetic analysis of exchange processes between sodium ions from Zeolite A and cadmium, copper and nickel ions from solution was reported by Biskup and co-worker[26]. The application of their study was water purification but the principles are relevant to our own catalyst preparation. Since metal ions are more hydrated in solution than in the zeolite, cations entering the zeolite can do so only with reduction to their hydration sphere. The rate of cation-exchange depends therefore not only on the affinity of cation for zeolite but also on the number of hydration 'n' and energy of dehydration. Biskup and co-worker[26] reported that cation-exchange processes were controlled by chemical reaction rather than by diffusion.

After the process of ion-exchange, zeolite and clay catalysts are often calcined to remove the structural template molecules and carrier molecules for the metal ion, e.g. acetate or nitrate from the catalyst. During calcination any sodium ions present that were previously inaccessible for ion-exchange become redistributed over the zeolite surface and made accessible. During calcination it is also possible to remove alumina from the structure, although this process can often provide important stabilisation of the catalyst.[27]

1.2.3 Metal-ion leaching

Removal of cations under experimental conditions from the zeolite or clay support is known as leaching. This process depends not only on the structural position and function of the cations within the zeolite material but also the solvent used. If cations are solublised in the channels and pores of the support then subsequent reactions may need to be considered as homogeneous.

Sobczak *et al.*.[21] published data in 2004 that confirmed the leaching of Cu-species during the hydroxylation of phenol using various copper containing MCM-41 zeolites. Norena-Franco and co-workers[28] reported an absence of leaching using similar catalysts for the same hydroxylation of phenol reaction, however it should be noted that the preparation methods for the two copper-containing catalysts were different. Norena-Franco *et al.*[28] synthesised the catalysts using a hydrothermal method, Sobczak *et al.*[21] prepared their catalysts at room temperature. Catalysts prepared hydrothermally are typically more stable than those prepared at room temperature[21]. Leaching of metal ions from zeolites and clays occurs via solvation. Norena-Franco and co-workers[28] used acetonitrile as their solvent, whereas Sobczak *et al.*[21] used water. Acetonitrile is a less effective ligand for the leaching of metal ions compared to water.[28]

1.2.4 Characterisation

Many techniques can be used to probe and characterise zeolites and clays, these include X-ray Diffraction (XRD), Fourier-Transform Infra-red (FT-IR), Brunauer-Emmett-Teller (BET), Magic Angle Spinning Nuclear Magnetic Resonance (MAS NMR), Transmission Electron Microscopy (TEM) and Temperature Programmed Desorption using ammonia as a probe (NH_3-TPD). Triantafyllidis *et al.*[29] used all of these techniques to characterise a range of ZSM-5 catalysts. Since ca. 1980 many authors have observed that the catalytic performance of metal containing catalysts is strongly dependent on the method of catalyst preparation and activation which the aforementioned characterisation techniques can be used to confirm.[30] It is not possible to operate all characterisation techniques *in situ* and it is not always necessary, however care must be taken when characterising catalysts outside the *normal* catalytic operating conditions.

The Brunauer-Emmett-Teller (BET) method of characterisation can be used to probe the structures of zeolites and clays. BET analysis is supported by a kinetic model for the adsorption process proposed by Langmuir[31] in 1916 in which the surface of the solid was regarded as an array of adsorption sites. A dynamic equilibrium was postulated in which the rate of adsorption was equal to the rate of desorption.[32] Using BET analysis the surface area and average pore diameter of a material can be obtained. It is important to note that accurate BET analysis requires the material to exhibit a 'type II' adsorption isotherm. Zeolites, clays and other similar materials exhibit particularly well-defined 'type I' adsorption isotherms. For a type I isotherm uptake does not increase continuously, as it does in type II, instead it reaches a limiting value. For this reason BET analysis is particularly useful for comparison between for example Na, H and Cu-forms of zeolites and clays but not the accurate calculation of surface area, pore diameter or the comparison between different support structures. As suggested by Gregg and Sing[32] 'it is perhaps the very breadth of its scope which has led to a somewhat uncritical application of the method...this is particularly true of those solids which contain very fine pores.'

X-ray diffraction (XRD) relies on the principle that every crystalline material has its own characteristic X-ray diffraction pattern. This analytical technique allows structures to be checked against one another or compared with an internationally accepted collection of simulated diffraction patterns. The database for these XRD powder patterns is extensive although many factors influence the diffraction pattern obtained, including the Si/Al ratio and therefore the value of comparing obtained patterns with simulated patterns is limited.

Powder X-ray diffraction is most often applied in heterogeneous catalysis to identify and confirm known phases using standard fingerprint techniques. There is however a wealth of additional information potentially available, including identification of novel phases, determining catalyst stoichiometry, identifying the location of coke, confirming micro-structural characteristics of catalysts, the application of Debye Functional Analysis and combining X-ray adsorption and diffraction methods[33]. Much of the more detailed information depends however on the suitability of the system to *in situ* structural characterisation within the constraints of X-ray diffraction techniques.

Dealumination of a zeolite can be confirmed by XRD and involves the removal of tetrahedrally coordinated aluminiums from the zeolite framework. This affects the physiochemical, ion-exchange and catalytic properties of the material. The XRD patterns of dealuminated samples are characterised by a shift in peak position (Figure 8).

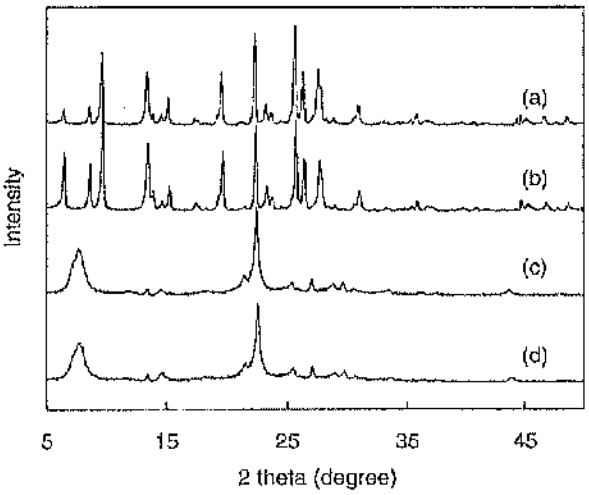

Fig. 8[34] X-ray diffraction patterns of (a) parent MOR, (b) dealuminated MOR, (c) parent BEA, (d) dealuminated BEA sample.

Dealumination is often achieved using acid treatment with an aqueous HCl solution and then calcination in air. Realumination is sometimes possible[34].

The majority of copper ions in copper exchanged zeolites exist as single cations located at structural cationic sites.[35] Bulanek *et al.*[35] summarised results from numerous authors, concluding that the appearance of two dominant peaks in the H_2-TPR of Cu-zeolites represent a two stage reduction of copper, $Cu^{2+} \rightarrow Cu^{+} \rightarrow Cu^{0}$ and not two different types of Cu^{2+} ions. Figure 9 provides the data obtained by Bulanek *et al.*[35] for the H_2-TPR profiles of Cu-Na-MFI. Only the Cu-Na-MFI zeolite with the highest concentration of copper exhibited splitting of the low temperature peak, reported to indicate the one-step reduction of Cu^{2+} to Cu-metal, confirmed by Sárkány *et al.*.[36]

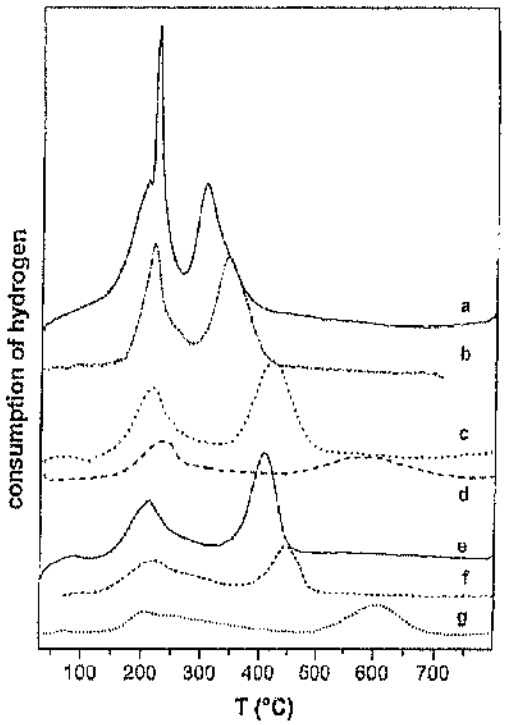

(a) CuNa-MFI-14.1-0.59-3.63
(b) CuNa-MFI-14.1-0.52-3.05
(c) CuNa-MFI-14.1-0.37-2.23
(d) CuNa-MFI-14.1-0.19-1.13
(e) CuNa-MFI-22.6-0.50-1.96
(f) CuNa-MFI-22.6-0.28-1.10
(g) CuNa-MFI-22.6-0.26-1.05

Fig. 9[35] H_2-TPR profiles of Cu-Na-MFI.

Bulanek *et al.*[35] concluded that the redox properties of the exchanged Cu ions are different to those of the Cu oxide dispersed throughout the zeolite. The structure of CuO species was analogous to supported Cu on amorphous carriers including SiO_2 and Al_2O_3. Tailoring the redox properties of copper and other transition metal ions is possible although complex.

1.2.5 Metal oxidation state

The two common and robust techniques used to establish the oxidation state of a metal within any heterogeneous catalyst are Ultra-Violet Visible Near-Infrared (UV/Vis/NIR) and Fourier Transform Infrared (FTIR) spectroscopy.[37-39] UV/Vis/NIR spectroscopy is not suitable for use with all transition metals but it does confirm the presence of Cu^{2+} species. The UV/Vis/NIR spectra of copper containing Zeolite-Y samples were obtained by Mesu[39] for a range of copper loadings (Figure 10). The active species was a Cu^{2+}/Histidine complex with the Cu^{2+} d-d transition band observable between wavelengths of 14,500 and 15,300 cm^{-1} depending on the Cu^{2+}/His content.

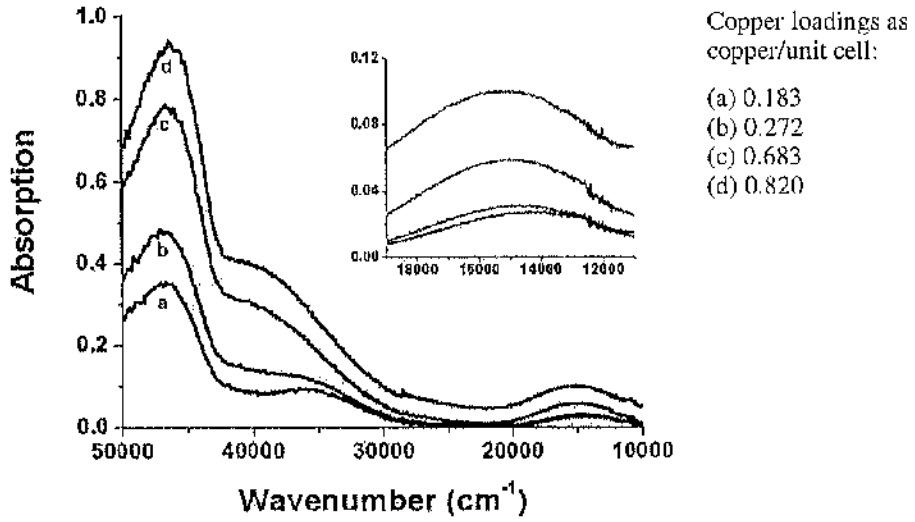

Fig. 10[39] UV/Vis/NIR adsorption spectra of Cu^{2+}/His immobilised in Zeolite-Y. The insert shows the Cu^{2+} d-d transition band.

The d-d transition band was sensitive to the hydration state of the zeolite and Cu^{2+} loading suggesting the presence of at least two different Cu^{2+} species. After drying samples of the zeolites in a desiccator, Mesu[39] observed a red-shift of the transition band, whilst rehydration caused back-shift to the original position. Electron-spin resonance (ESR), Extended X-ray adsorption fine structure (EXAFS), Infrared (IR) and Raman spectroscopy were also used to characterise the metal sites.[39]

Using infrared spectroscopy it is possible to distinguish between Cu^{2+} and Cu^{+}. Five Fourier Transform Infrared Spectra (FTIR) of Cu/ZSM-5 are shown in Figure 11. After calcination in oxygen the IR bands at 970 cm^{-1} for Cu^{+} and 918 cm^{-1} for Cu^{2+} were detected suggesting that whilst most of the copper was present as Cu^{2+} some existed as Cu^{+}. The peaks of interest are highlighted.

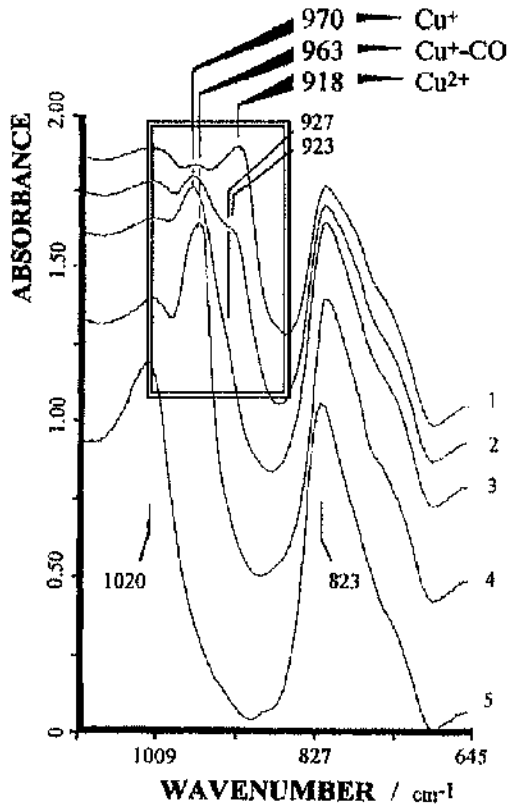

(1) calcined in O_2
(2) addition of 0.50cm^3 H_2O into Ar line at 293K followed by outgassing in Ar flow at 773K for 10mins
(3) continuation of outgassing at 773K for 11hrs
(4) treatment at 293K in 0.979% CO/He flow for 30mins followed by 20min purge with Ar
(5) total reduction in H_2

Fig. 11[40] FTIR spectra of Cu/ZSM-5.

Other IR and UV-Vis-NIR spectra of Cu/ZSM-5 (Figure 12) were recorded by Palomino *et al.*.[38]

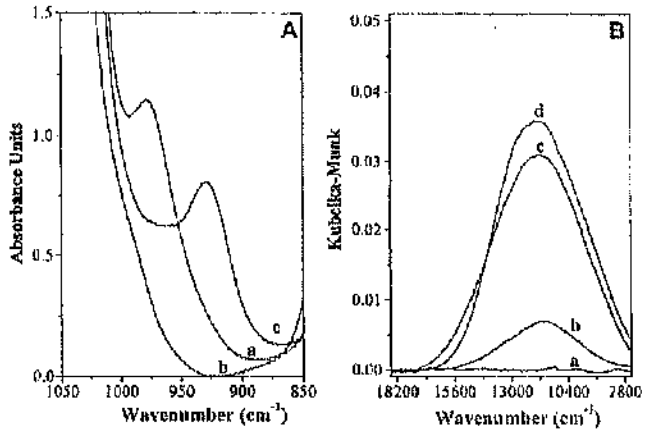

(A) Evolution of the IR spectra in the 1050−850 cm^{-1} range upon interaction with adsorbates. Sample activated at 673 K (curve a), after interaction with H_2O (curve b) and subsequent O_2 dosage (curve c). (B) Evolution of the vis−near-IR spectra, in the d−d region, curves a−c as in part A. Curve d reports the spectrum obtained on the fresh sample activated at 300 K for comparison.

Fig. 12[38] FTIR spectra of Cu/ZSM-5.

As before the IR band at ~980 cm^{-1} was assigned to Cu^{+} and the band at ~920 cm^{-1} to Cu^{2+}. The lack of any peak in spectrum 'b' suggests the solvation effect of water had moved the copper ions away from the zeolite walls. Spectrum 'd' confirmed Cu^{2+} species in a fresh sample of Cu/ZSM-5 activated at 300 K.

1.2.6 Coking

There are four reasons for the deactivation of zeolite and clay catalysts during commercial processes[41]:

(i) poisoning of the active sites either by feed impurities or carbonaceous deposits

(ii) limited access of reactants to active sites due to partial or complete blockage of pores by carbonaceous deposits or extra-framework species from dealumination etc.

(iii) framework alteration

(iv) sintering of supported metals.

Carbonaceous deposits or coke are the principle cause of deactivation for processes involving the conversion of hydrocarbons. All reactions involving organic compounds and solid acid catalysts are accompanied by the formation of by-products, deposited on the surface of the catalyst that provoke deactivation. These by-products are widely referred to as *coke*, defined as carbonaceous compounds, polyaromatic or non polyaromatic formed during a reaction which are responsible for catalyst deactivation[42]. The rate of deactivation depends not only on the relative rate but also the mode of coke formation. The effect of coke is more pronounced when deactivation is due to pore blockage compared to active site coverage[42]. Coking, deactivation rates and the composition of coke depend on the pore structure of the zeolite or clay.

1.2.6.1 Formation of coke, the types and location

It is difficult to accurately evaluate the effect of pore structure on the rate of coke formation since it is not possible to manufacture zeolites with the same acidity but different pore structures. It is however possible to conclude that the rate of coke formation is greater when (i) the space available for its formation, for example in cavities or at channel intersections is greater and (ii) the intermediates in coke formation diffuse more slowly through the support[42]. Since the acid sites in zeolites are located in cavities or channel intersections, the size difference between these cavities and the pore apertures must be considered. The greater the difference, the greater the possibility of trapping coke. Zeolite-Y and ZSM-5 have pore apertures approximately half the diameter of the corresponding cavity or channel intersection[41]. Rollmann and Walsh[43] concluded that the ratio of coke formed to that of alkane converted was ca. 1 for all large-pore zeolites. This reduced to a ratio of 0.05 for small-pore zeolites.

Coke composition depends on the catalyst and system although general observations can be made. When the coke content is low the coke is non-aromatic and the hydrogen-to-carbon (H/C) ratio is >1. At high coke contents the coke is polyaromatic and the H/C ratio closer to 1. Coke is more likely to be aromatic for large pore zeolites whilst for all zeolites the H/C ratio decreases with increasing time-on-stream (TOS).

Guisnet and Magnoux[42] characterised coke as either soluble or insoluble in methylene chloride (CH_2Cl_2). The soluble coke was compounds with up to and including six aromatic rings. The authors concluded that the soluble coke molecules were intermediates in the formation of insoluble coke. Insoluble coke was therefore not formed at low coke contents and the aromaticity of soluble coke increased with coke content. For reasons of basicity and volatility the soluble coke molecules were located within the pores of the zeolite. Deactivation of the catalytic system was due to the limited or blocked access of reactant molecules to active sites, not from the poisoning of an active site.

The coking and deactivation of zeolites depends not only on pore structure but also on TOS, temperature, pressure, the type of reactants and the strength and density of

active sites. More recently, Guisnet and Magnoux[44] have characterised the mode of coke formation as dependent on temperature. At low reaction temperatures (≤473 K) the H/C ratio of the coke was close to that of the reactants and it was therefore concluded that coke formation involved mostly condensation and rearrangement steps. The deposits were not polyaromatic and their retention due mainly to strong adsorption and their low volatility or solubility. At low reaction temperatures the composition of coke depended on the reactant(s) and reaction products. Since the coke was located inside the zeolite pores, less than 5% could be recovered through direct Soxhlet extraction with methylene chloride. At high reaction temperatures (>623 K) coke was polyaromatic. Formation involved hydrogen transfer and dehydrogenation in addition to condensation and rearrangement steps. The composition of coke was independent of the reactant(s) and was instead determined by the size and shape of the catalyst pores[41]. When using zeolites insoluble coke molecules often form via the condensation of soluble coke molecules. At intermediate temperatures coke formation occurs via both low and high temperature modes. During n-heptane cracking at 723 K, the number of coke molecules that cause complete deactivation of H/Zeolite-Y and H/ZSM-5 was close to the number of strong acid sites so also active sites. For H/MOR and H/ERI it was 7-8 times smaller; deactivation of these catalysts was probably due to pore blockage.

It is possible to define four modes of pore blockage, limited (1) or no (2) access for reactant molecules to the active sites of a cage or intersection which contains a molecule of coke and limited (3) or no (4) access for reactant molecules to the active sites of a cage or intersection which *do not* contain a molecule of coke. These are depicted in Figure 13.

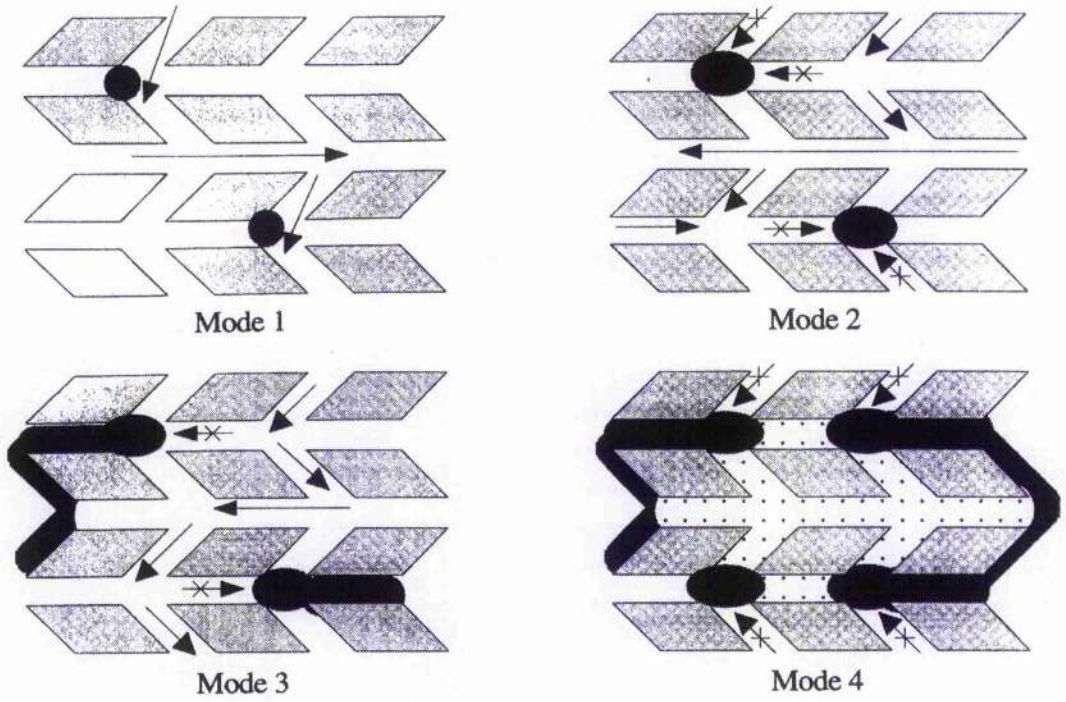

Fig. 13[41] Four possible modes of deactivation by carbonaceous deposits in H/ZSM-5.

Identifying the location of coke is important. The literature[42, 45, 46] reports that *ex situ* X-ray powder diffraction can be used to confirm the deposition of coke within the channel systems of ZSM-5 structures as evidenced by monoclinic to orthorhombic transformations. Using fresh and coked H/ZSM-5 samples Lucas *et al.*[45] correlated the decreasing intensity of a shoulder on the main reflection with increasing coke content.

For H/Zeolite-Y the acid sites are of more than one strength. The strongest acid sites are the most active and therefore the first to be deactivated and so coke has a high toxicity at low coke content. Deactivation of zeolites and clays by coke depends therefore on both the acidity and pore structure of the catalyst.

Coke does not always have a detrimental effect on catalytic activity and selectivity. The coke molecules within zeolites are relativity small and therefore the reactivity of these molecules remains high allowing them to participate in the main reaction. Toluene disproportionation using a MFI zeolite at high temperature and high coke content provided excellent selectivity towards paraxylene. The coke molecules block outer surface acid sites that are non-shape selective and improved the sieving properties of the zeolite[46].

1.2.6.2 Coke removal

Deactivation by coke is reversible. Coke is generally removed by oxidation, unfortunately this regeneration is often incomplete due to the secondary effects of water present at high temperatures. For these reasons limiting the deactivation of catalysts by coking and reducing the need for regeneration are important economic objectives for industrial catalyst manufacturers[44].

The choice of operating conditions, in particular temperature, are important if the detrimental effects of water produced by coke oxidation are to be minimised[47]. Dealumination and structural alterations as a result of water present at high temperatures must be avoided if catalytic activity and selectivity are to be restored successfully. Three types of reactions have been identified in the oxidation of coke[47]. Firstly the formation of oxygenated compounds by partial oxidation of polyaromatics which begins at ca. 433 K. Secondly the condensation of polyaromatics and their oxidation products which occurs above 523 K. Thirdly the decarbonylation and decarboxylation of oxygenated compounds that occurs only at temperatures above 573 K. A large source of hydrogen comes from coke molecules oxidised at ca. 433 K. A two-stage regeneration, first at low and then high temperature limits the contact time between the catalyst and steam at elevated temperatures. This reduces catalyst degradation.

The catalytic oxidation of toluene over CuNaH/Zeolite-Y catalysts was studied by Antunes *et al.*[48]. They concluded that copper sites were involved in oxygen activation and improved both the oxidation of toluene and coke. The temperature required for complete oxidation of toluene to CO_2 was reduced by ca. 100 K by increasing the copper loading from 1 to 8% w/w (Figure 14). The temperature required to oxidise the coke within the zeolite was also reduced by ca. 100 K for the same increase in metal loading.

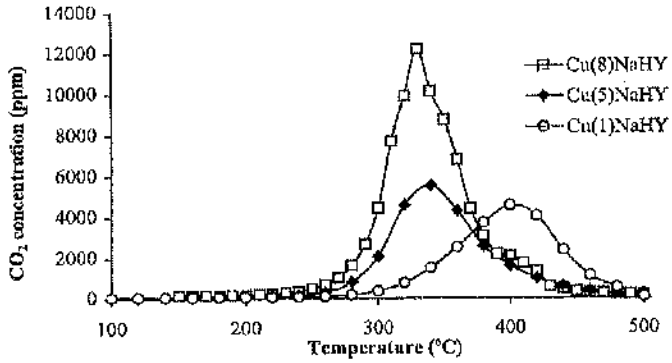

Fig. 14[48] The influence of copper loading on the temperature required to remove coke formed after 6hr of toluene oxidation at 523K.

1.2.6.3 Characterisation of coke

Various spectroscopic techniques including FTIR, UV-VIS and MAS ^{13}C NMR have been used to characterise the chemical composition of coke within zeolites. There are also various techniques used to remove coke trapped in zeolite pores for subsequent analysis. Treatment of the coked zeolite with an organic solvent or an inert gas flow at high temperature allows recovery of only a small fraction of coke compounds. The alternative is to destroy the zeolite framework by ball-milling or acid treatment. The soluble coke components can then be analysed using standard Gas Chromatography (GC), High Performance Liquid Chromatography (HPLC) and/or Mass Spectrometry (MS)[42].

The scheme below (Figure 15) illustrates the techniques used by Guisnet and Magnoux[42] to characterise the compounds responsible for zeolite deactivation.

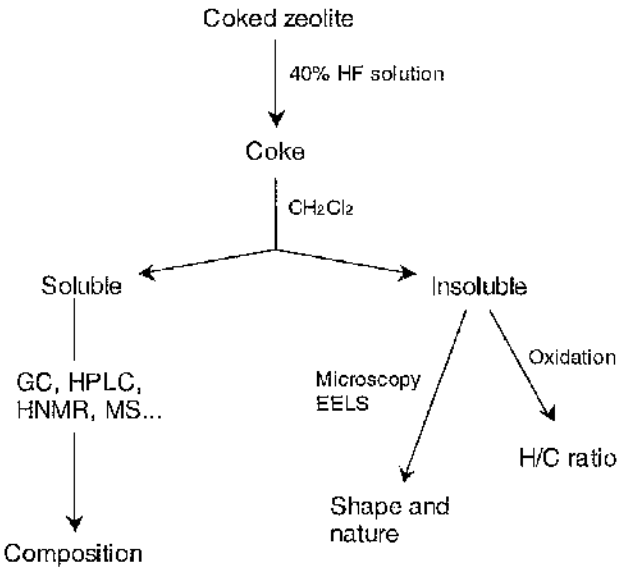

Fig. 15 Characterisation of coked zeolites.

Coke generally consist of a large number of compounds difficult to separate from the catalyst, this makes their identification and characterisation difficult[44]. The elemental composition of coke (CH_x) formed during hydrocarbon transformations can be obtained by qualitative analysis of CO_2 and H_2O resulting from combustion, sometimes combined with oxygen consumption[44]. From the elemental composition, useful information about chemical identity can be obtained, for example the average degree of aromaticity.

1.3 Adsorption and dimerisation of phenol and its analogues

The oxidative coupling of phenol was reported in 1983 by Armstrong *et al.*.[49] The researchers used metal ion oxidants amongst others to oxidise phenol. The highest yields of 4,4'-biphenol and 2,2'-biphenol were attained using $[Ce(NO_3)_6]^{2-}$ as the oxidant, which produced 38% 4,4'-biphenol and 48% 2,2'-biphenol. Heterogeneous catalysis was not used although the importance of an appropriate solvent was alluded to.

The coupling of 2,6-dimethylphenol has one obvious advantage over the dimerisation of unsubstituted phenol. The presence of *ortho*-substituents prevents coupling at carbons-2 and 6 whilst large and bulky substituents also prevent carbon-oxygen coupling. Using 2,6-dimethylphenol, Hay[4] reported high yields of the carbon-carbon coupled diphenoquinone using butyronitrile as a solvent and a copper/amine catalyst in the presence of oxygen at 373 K. The diphenoquinone product was reported to be insoluble and precipitated from solution during the homogeneous catalytic reaction. For phenol there is the possibility of *ortho*, *meta* or *para* coupling. The oxygen atom of the OH group means that the benzene ring is electron rich at the *ortho* and *para* positions, carbons 1, 5 and 3.[49] The spin density at the *para* position has been shown to be nearly twice that of the *ortho*-position.[50] Radicals are reportedly formed during the dimerisation of phenol and its derivatives which, using molecular orbital theory, should couple at the site of highest spin density.[51] It is therefore possible that for phenol and its derivatives where both the *ortho* and *para* positions are free, the *para*-coupled products will dominate.

Most catalysts used for oxidative polymerisations are transition metal salts, usually Cu or Mn. The other requirements are often a base, an amine ligand and the presence of oxygen. Polymerisation is however possible under anaerobic conditions. Benzene, toluene and isopropanol have all reportedly been used as solvents for these reactions although carbon-oxygen coupled products were the target compounds. For phenols with only one *ortho* substituent and an open *para*-position, oxidative polymerisation is also possible, however the polymer is usually highly branched and coloured.

1.3.1 Adsorption onto zeolites and clays

Zeolites and clays contain molecular sized cavities. These cavities are both size and shape selective. The internal dimensions of the pores, channels and interlamellar spacings of the zeolites and clays used were reported in Section 1.2. The molecular dimensions of phenol, 4,4-biphenol, 4-phenoxyphenol and 2,2-biphenol are therefore an important consideration (Figures 16-19). The dimensions were obtained from The Cambridge Structural Database (CSD)[52] and represent distances from the centre of each atom.

Fig. 16

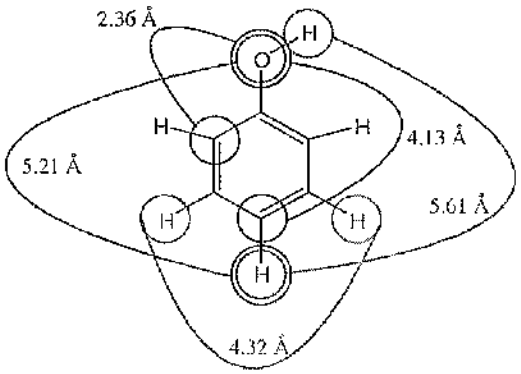

Fig. 18

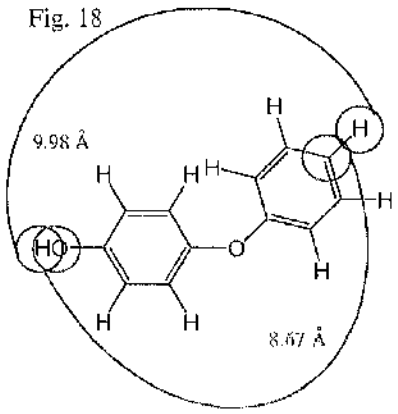

Fig. 17

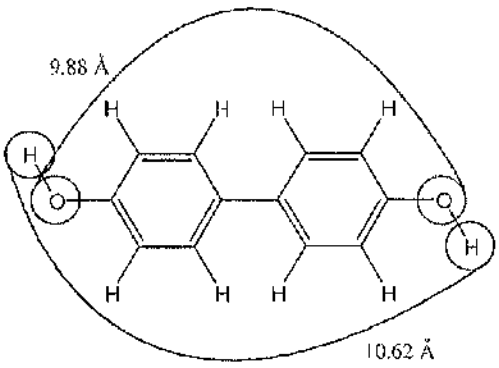

Fig. 19

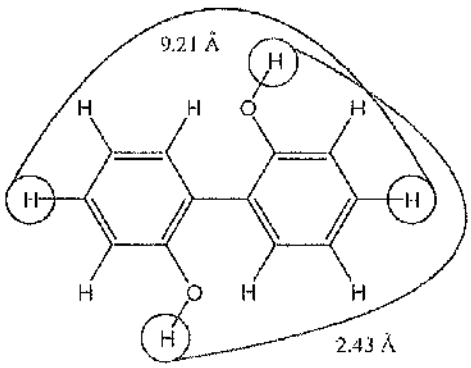

Using an energy minimisation approach, both 2,2'- and 4,4'-biphenol are assumed *twisted*, with a 30° angle between the two aromatic rings. The crystallographic data confirms the 2,2'-biphenol molecule is twisted but suggests the 4,4'-biphenol molecule is *flat*, with the two aromatic rings in the same plane.

The adsorption of phenol over zeolite and clay catalysts is understandably necessary for their regioselective dimerisation. Choudhary *et al.*[53] reported the diffusion and sorption of straight and branched chain compounds in the liquid phase onto H/ZSM-5 was strongly influenced by the chain length and critical molecular size of sorbate molecules. They also reported that the diameter of the molecule maybe smaller than that of the channel pore but entrance not possible and vice-versa. The sorption of phenol onto ZSM-5 and MCM-41 has also recently been reported by Ghiaci *et al.*[54].

Research by Fujiyama *et al.*[55] provided an adsorption study of 2,6-di-*tert*-butylphenol (BOH) onto the surface of Na-MCM-41. Although other papers including those by Roostaei *et al.*[56] and Shen *et al.*[57] have mentioned and referenced to the adsorption of phenol onto different surfaces, the application of their work here is limited. The method employed by Fujiyama *et al.*[55] used 0.2 g of catalyst and 1 mmol of phenol dissolved in 20 cm^3 of acetonitrile. The mixture was heated to 313 K in a stirred tank batch reactor (STR) and a sample taken after 24 hours for analysis by HPLC.

The adsorption of molecules such as phenol and 4,4'-biphenol onto zeolites and clays can occur at both internal and external sites. Assuming that the adsorption of such molecules occurs at the site or in the presence of cations, both internal and external sites must be considered. The total cation-exchange capacity (CEC) and the external CEC (ECEC) can be measured using either Ming and Dixon[58] or Haggerty and Bowmann[59] methods of calculation. For a sample of ZSM-5 material with a SiO_2/Al_2O_3 ratio of 31, the calculated CEC is 650 mmol kg^{-1} and the ECEC is equal to 40 mmol kg^{-1}. [54]

A recently published paper by Beutel *et al.*[60] reported the interaction of phenol with NaX zeolite. The interactions were studied using ^{1}H MAS NMR, ^{29}Si MAS NMR and ^{29}Si CP MAS NMR spectroscopy. In the conclusion of their work, Beutel and co-workers[60] suggested that phenol adsorbed in the pores of zeolite NaX underwent H-

bonding via the hydroxyl group to basic oxygen atoms within the zeolite support structure. Evidence was also given showing that the hydrogen atoms of phenol and/or phenolate anions were in close proximity to silicon framework atoms. This was explained by either the interaction between the π-electrons of the aromatic ring of the adsorbate with Na^+ cations and/or by the interaction of the hydrogen atoms of the aromatic ring with oxygen atoms of the 12-membered ring of the supercage. Beutel *et al.*[60] were able to deduce from the ^{29}Si CP MAS spectra that when the thermal treatment temperature was raised from 493 to 593 K, phenol was entirely deprotonated and linear Na^+ --- ^-OPh complexes were formed. Similar studies by Perez-Ramirez *et al.*[61] on Fe-ZSM5 catalysts, using ^{27}Al MAS NMR spectroscopy, both before and after activation provide confirmation that the support structure is little affected by calcination and therefore also activation processes.

1.3.2 Dimerisation using zeolites and clays

The selectivity of reactions catalysed by shape selective zeolites such as ZSM-5 and Zeolite-Y and clays, is largely dependent on intra-crystalline mass transfer processes. In the liquid phase, zeolite crystals are largely surrounded by bulk liquid containing the reactant molecules. For a catalytic reaction to occur these reactant molecules must leave the liquid phase and enter the zeolite channels. Molecules inside the zeolite channels are considered as single strings of sorbed molecules. The critical molecular size and polarity of the sorbate molecules is crucial for allowing diffusion and sorption from the liquid phase. The diameter of the reactant molecule may however be smaller than that of the channel pore but entrance not possible. Alternatively, the diameter of the reactant molecule may be larger than that of the channel pore but entrance feasible as illustrated in Figure 20.

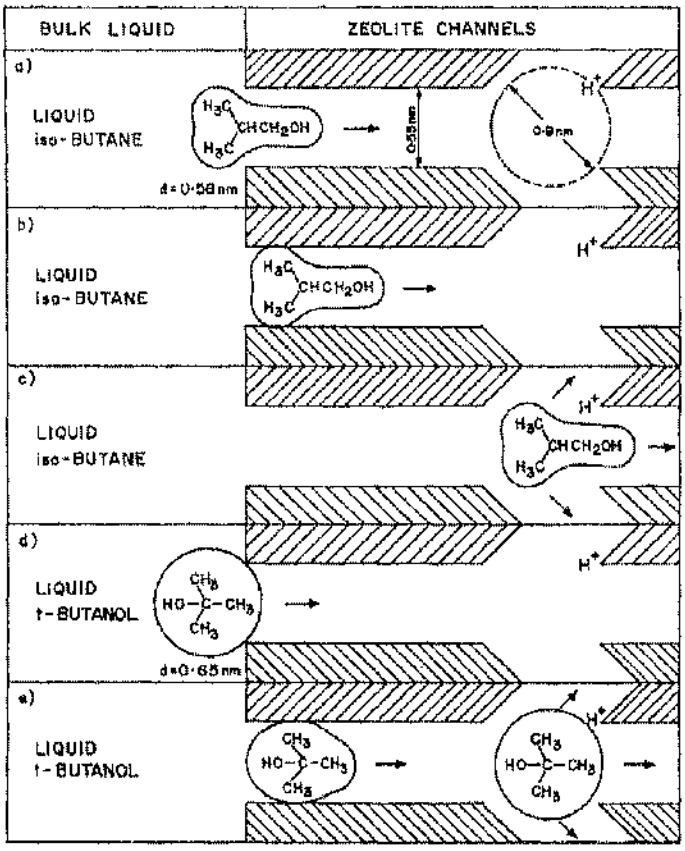

Fig. 20[52] Entry of sorbate molecules into H/ZSM-5.

Research by Kohara *et al.*[62] and Fujiyama *et al.*[55] was concerned with the oxidative dehydrogenation of 2,6-di-*tert*-butylphenol (BOH). Both groups used Cu ion-exchanged Na/MCM-41 to study the liquid-phase catalytic oxidation of 2,6-di-*tert*-butylphenol. Copper and silver were chosen in preference to precious metals due to their relatively poor capacity for combustion and so consequently the formation of coke. Kohara *et al.*[62] confirmed that the addition of alkali metals increased the catalytic activity for BOH oxidation. An induction period was reported for both the production of 4,4'-dihydroxy-3,3'-,5,5'-tetra-*tert*-butyl-biphenyl (H_2DPQ) and the further oxidised product 3,3'-,5,5'-tetra-*tert*-butyl-4,4'-biphenoquinone (DPQ), although H_2DPQ was the first to be detected in the reaction mixture. Catalytic activity and selectivity were reported to depend on the copper content of the catalyst and the different alkali metals added.

The research published by Fujiyama *et al.*[55] highlighted the liquid-phase oxidation of 2,6-di-*tert*-butylphenol using Ti and V incorporated mesoporous silicates and hydrogen peroxide, originally published by Reddy.[63] Also mentioned was the liquid-phase oxidation of benzene catalysed by Cu-supported mesoporous silicates and aluminosilicates using gaseous oxygen and ascorbic acid as the reductant. Fujiyama *et al.*[55] reported using Cu impregnated MCM-41 with the addition of potassium hydroxide for the oxidative dehydrogenation of BOH. Fujiyama *et al.*[55] gave a clear indication that the mesopores of the catalyst offer a 'reaction field substantially preferable for 4,4'-dihydroxy-3,3'-,5,5'-tetra-*tert*-butyl-biphenyl (H_2DPQ) formation in comparison with the bulk solution.' Also reported was the ability to vary the relative yields of H_2DPQ and 3,3'-,5,5'-tetra-*tert*-butyl-4,4'-biphenoquinone (DPQ) by the addition of different alkali metals and varying the methods of their addition.

The liquid-phase oxidation of 2,6-di-tert-butylphenol over Cu-impregnated solid inorganic catalysts provides a useful comparison to the dimerisation of phenol to biphenol. To consider the relative selectivity of *ortho* and *para* coupling, other molecules such as pyridine and aniline must however be considered. These molecules should be directly analogous to phenol and able to couple at both *ortho* and *para* positions.

The solid acid catalysed condensation of phenylhydroxylamine with aniline was studied by Smith *et al.*[64] (Figure 21).

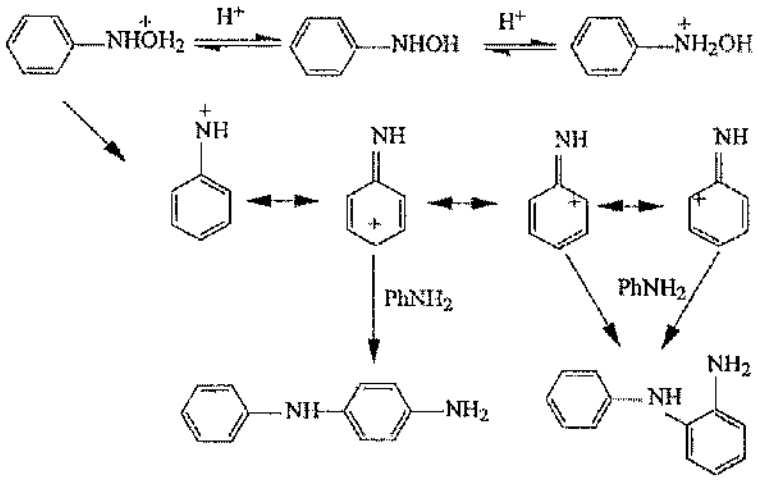

Fig. 21[64] Proposed reaction mechanism for the condensation of phenylhydroxylamine with aniline.

Reactions were carried out at 433 K in a liquid-phase batch reactor using aniline as the solvent. The selectivity towards *p*-aminodiphenylamine (*p*-ADPA) was 100% when using Nafion or H/ZSM-5 as the solid acid, although yields were low for both. Using H/Zeolite-Y improved the yield of *p*-aminodiphenylamine but reduced selectivity to ca. 50%. Smith *et al.*[64] also reported the condensation of nitrosobenzene with aniline using an acid clay, Filtrol. Products included *p*-ADPA, *o*-ADPA, azoxybenzene and azobenzene. Yields of *p*-ADPA varied between 3.8 and 44.0% depending on reaction conditions. Using a fixed-bed reactor produced the highest selectivities and moderate yields of *p*-ADPA in comparison to the stirred tank batch reactor. The authors confirmed no reaction occurred between the products, *p*-ADPA, *o*-ADPA, azoxybenzene and azobenzene and the active surfaces of Filtrol.

The oxidative dehydrogenation of pyridine has also been considered. Preparation of 2,2'-bipyridys is the subject of a patent[65] owned by Imperial Chemical Industries Ltd. from 1971. The selectivity towards 2,2'-bipyridys was thought to be controlled by bonding between the nitrogen atoms and catalyst surface, directing coupling at the *ortho* positions. Research by Gillard and co-workers[66], published in 1988 suggested that with the correct catalyst this process could be adapted for the production of 4,4'-bipyridys. Gillard *et al.*[66] used natural sand from Loch Aline as a catalyst, supplied by BDH. It was recently suggested that the catalysed coupling of pyridine reported by Gillard *et al.*[66] was probably due to ion-exchanged metals on the weakly acidic silica support. Other recent publications[67, 68] have reported arene dimerisation using transition metal ion-exchanged acidic supports.

The adsorption and reaction of monosubstituted benzenes and related 4,4'-disubstituted biphenyls using transition metal, ion-exchanged montmorillonite was investigated by Soma *et al.*[67]. Two adsorption complexes of benzene were reported, types I and II. Using Electron Spin Resonance (ESR) and resonance Raman, Soma *et al.*[67] confirmed that type II benzene was the poly-*p*-phenylene cation radical and type I benzene was the reduced form of poly-*p*-phenylene. For 4,4'-dimethoxybiphenyl there were also two different species, conversion between which was possible in the presence of water. The Raman spectra of species I and II were almost identical except for the inter-ring C-C stretching band. Soma and co-workers[67] suggested that species II had a strong interaction with its surroundings. This implied adsorption of species II

to the Cu^{+} ion and/or silicate surface of the catalyst. Species I was more susceptible to water and was readily reduced to neutral 4,4'-dimethoxybiphenyl, implying it was free and therefore desorbed from the catalyst surface. The copper ions of Cu/Montmorillonite remained reduced in the presence of both species.

Also studied has been the absorption of anisole over Cu^{II}/Montmorillonite.[67] With enough space between the anisole cation radical and its neighbouring active sites, it was able to react with a neutral anisole molecule to form 4,4'-dimethoxybiphenyl. This is oxidative dehydrogenation and the water produced during formation of the cation radical is then used to neutralise the radical and regenerate Cu^{2+} (Figure 22).

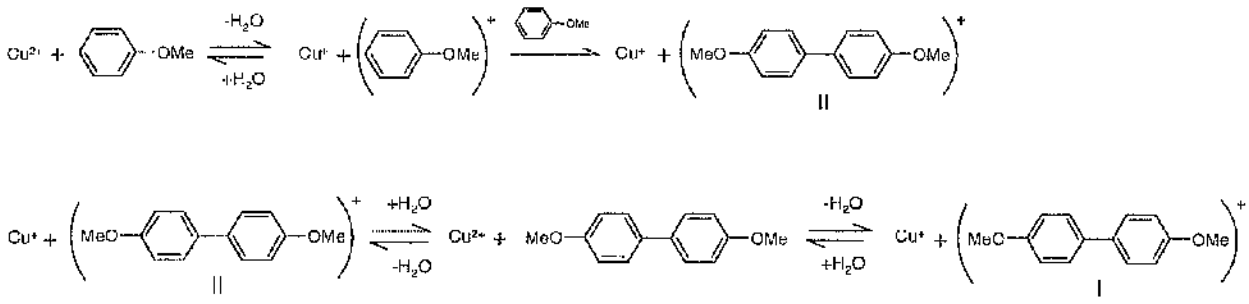

Fig. 22[67] Reaction mechanism for the formation of 4,4'-dimethoxybiphenyl using Cu^{2+} sites.

1.3.3 Reaction mechanisms

Fujiyama *et al.*[55] and Kohara *et al.*.[62] proposed the same reaction scheme (Figure 23) for the oxidative polymerisation of 2,6-di-*tert*-butylphenol using Cu/MCM-41.

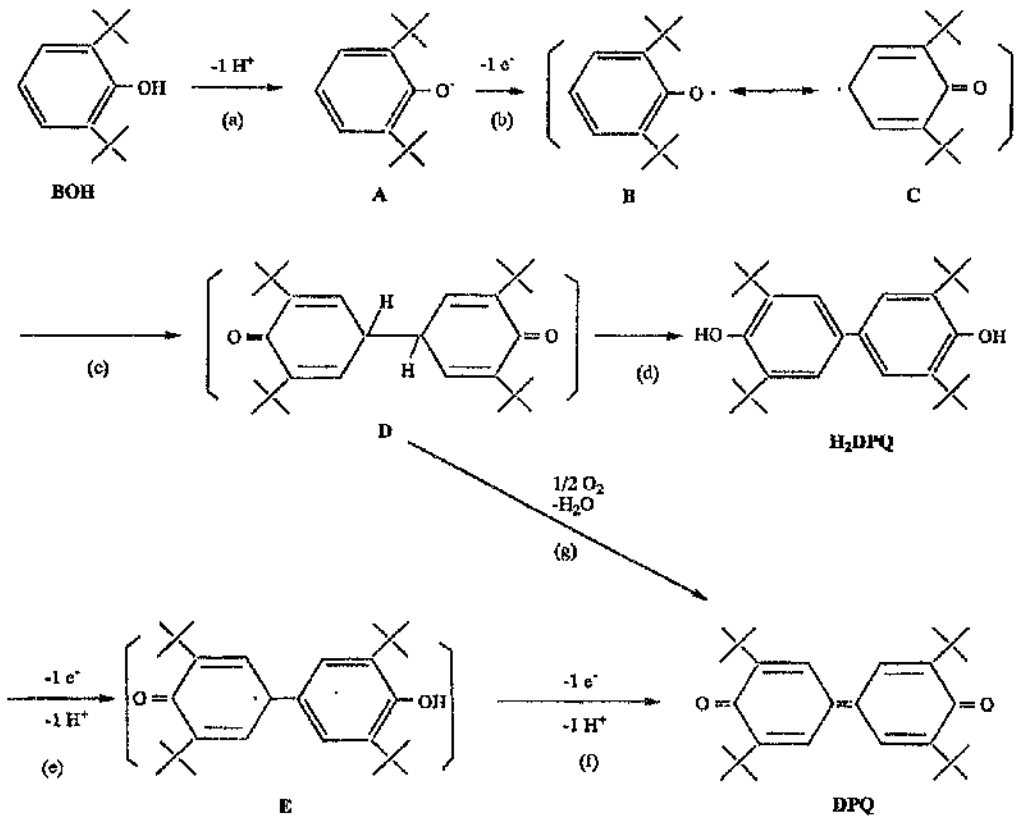

Fig. 23[55] Oxidative polymerisation of 2,6-di-*tert*-butylphenol using Cu/MCM-41.

A recent review paper by Kodayashi *et al.*[6] focused on the homogeneous catalysed, oxidative polymerisation of phenols. The reaction mechanisms and selectivity to carbon-oxygen or carbon-carbon coupled products were discussed (Figure 24), neither of which are yet fully understood. Three reaction mechanisms were proposed that included radical and ionic reactions.

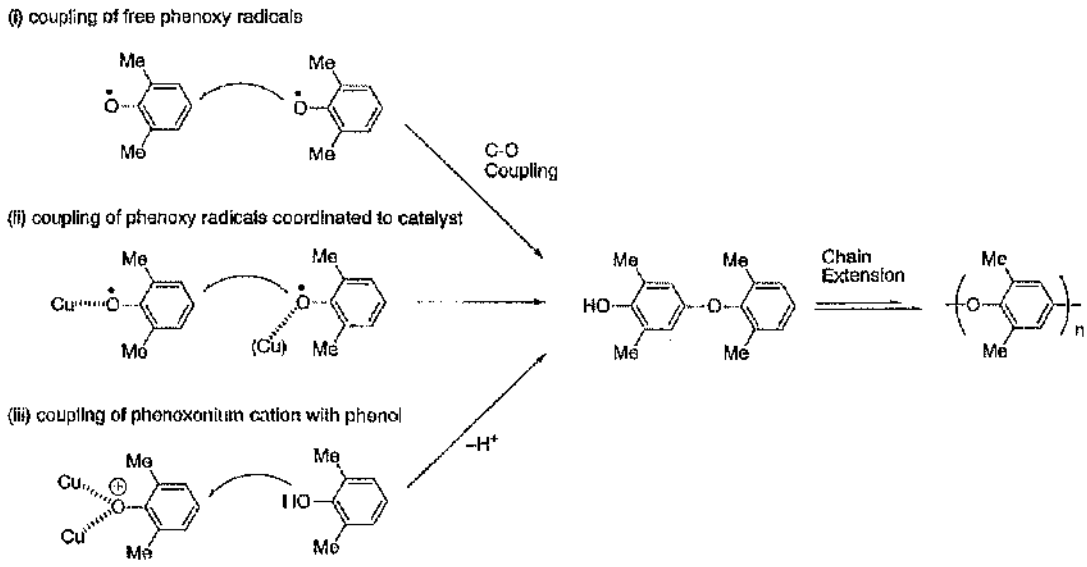

Fig. 24[6] The three reaction mechanisms proposed for the C-O selectivity of 2,6-dimethylphenol.

A recent publication by Baesjou *et al.*[69] reported reaction mechanism (iii) Figure 24, to be the only coupling mode that explained high selectivity towards C-O coupling. With reference to Figure 24 (ii), the coupling of phenoxy radicals coordinated to the catalyst complex had been investigated by Hay *et al.*[70], Price and Nakaoka[71] and Tsuchida *et al.*[72] amongst others. All three groups studied the coupling of 2,6-dimethylphenol (DMP) although there is no adequate or concurrent evidence for whether the coordination of the phenoxy radical to the catalyst provides carbon-oxygen or carbon-carbon coupling selectivity. Tsuchida *et al.*[72] proposed that oxidative polymerisation proceeds via a Michaelis-Menten type reaction mechanism (Figure 25).

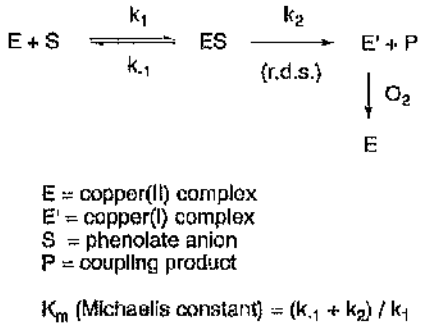

Fig. 25[6] Oxidative polymerisation via a Michaelis-Menten type reaction mechanism.

Analysis of the kinetic data suggested that carbon-oxygen coupling was preferred when at least one radical was coordinated to copper, whilst the coordination of 2,6-dimethylphenol was controlled by addition of pyridine to the reaction mixture.

The third coupling mechanism, Figure 24 (iii), was originally proposed by Kresta *et al.*[73] and Challa *et al.*[69] and suggests formation of a phenoxonium cation. From evidence provided by Electron Spin Resonance (ESR) studies, this coupling mechanism will only afford the carbon-oxygen coupled product. Reedijk *et al.*[74] also studied these reactions and like Challa *et al.*[69] used a copper(II) nitrate/ N-methylimidazole catalyst for the oxidative polymerisation of DMP. Both concluded that the complex only reacted with 2,6-dimethylphenol in the presence of water even under a nitrogen atmosphere. Reedijk *et al.*[74] and Baesjou *et al.*[69] also excluded the coupling of (coordinated) phenoxy radicals with each other leading to carbon-oxygen coupling. They confirmed this by treatment of 2,6-dimethylphenol with benzoyl peroxide, a radical initiator. As a result the carbon-carbon coupled diphenoquinone (DPQ) was the main product, whereas in the copper-catalysed reaction less than 5% DPQ was formed. Other radical initiators or oxidants include *tert*-butylhydroperoxide (Bu^tOOH) and *meta*-chloroperbenzoic acid (m-CPBA)[75].

Reaction mechanisms for the coupling of phenoxy radicals coordinated to the catalyst (ii) and the coupling of a phenoxonium cation with phenol (iii) are based on the assumption that coupling of the free phenoxy radicals of DMP results in carbon-carbon coupling.[6] Evidence for this comes from results published by Waters *et al.*[76] for the oxidation of DMP with alkaline ferricyanide and benzoyl peroxide. The carbon-carbon coupled dimer DPQ was produced in 45-50% yield, although the other half of the oxidised material was a yellow, no-ketonic polymer probably based on the carbon-oxygen coupled dimer. Waters *et al.*[76] also reported the oxidation of DMP with only benzoyl peroxide which afforded the carbon-carbon coupled dimer DPQ as the sole product in 60% yield. Despite this the other authors report complex experimental results and provide conflicting interpretations such that it should not be presumed that carbon-carbon coupling is a result of free radical formation.

A paper published by Baesjou *et al.*[69] provides an alternative evaluation of the mechanistic pathways proposed for the oxidative coupling of DMP (Figure 26).

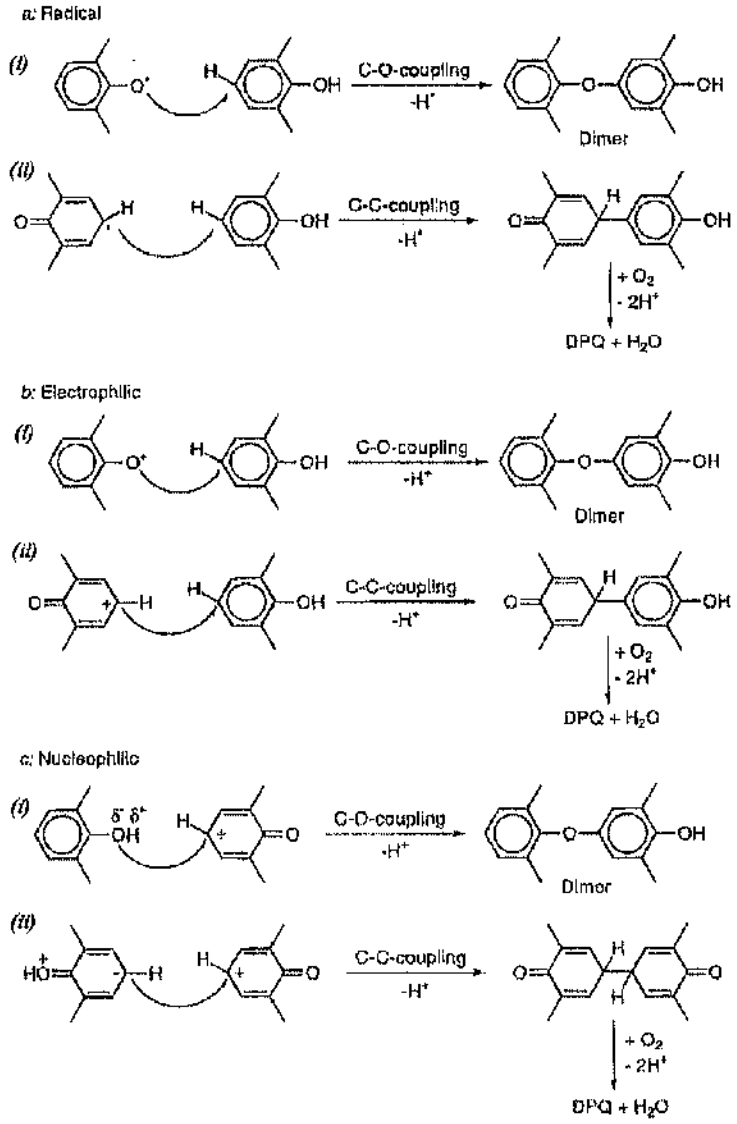

Fig. 26[69] Mechanistic pathways proposed for the oxidative coupling of 2,6-dimethylphenol.

The authors Baesjou *et al.*[69] conclude that pathways (a)(i), b(i)&(ii) and c(ii) are not viable mechanisms and so carbon-oxygen coupling was only possible via nucleophilic attack [c(i)], whilst carbon-carbon coupling required radical formation [a(ii)]. A recent paper by Kubota *et al.*[77] concluded unlike Baesjou *et al.*[69] that controlled radical coupling between two molecules of $[Cu\text{-}OAr]^+$ produced 4-phenoxyphenol. Both authors however suggested the formation of a Cu^I complex as an intermediate.

The authors Kobayashi and Higashimura[6] reviewed the homogeneous catalytic oxidation of 2,6-dimethylphenol using monooxygenase model complexes and proposed a cyclic reaction mechanism for regeneration of Cu^{II} from Cu^{I} (Figure 27).

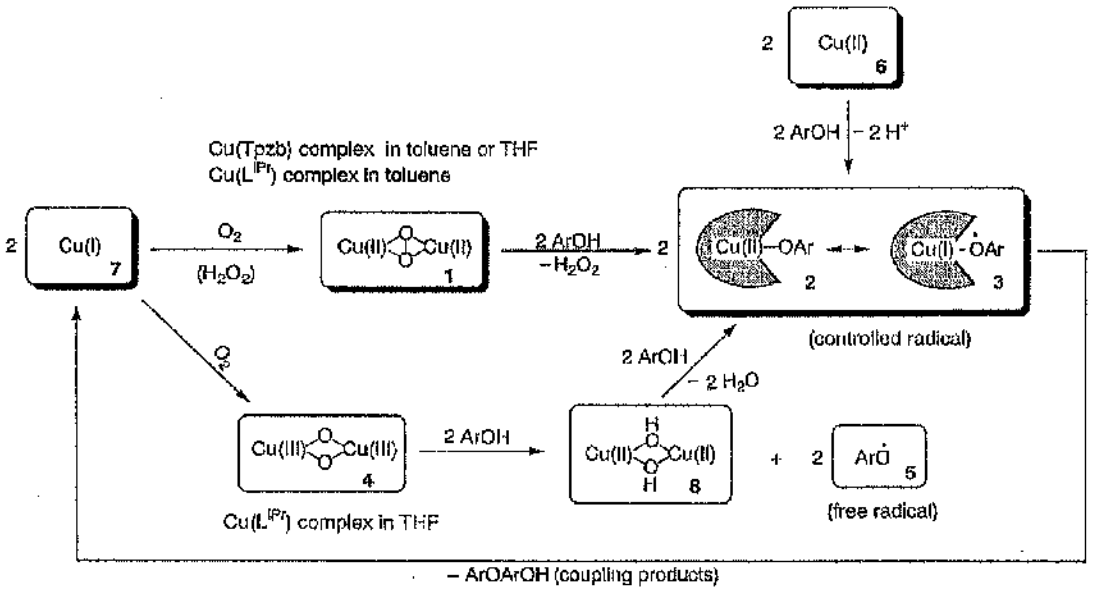

Fig. 27[6] Postulated mechanism for the catalytic oxidation of 2,6-dimethylphenol by a copper complex.

Higashimura *et al.*[78] have also recently reported the radical-controlled oxidative polymerisation of phenol using the (1,4,7-triisoproyl-1,4,7-triazacyclononane) copper(II) dichloride ($Cu(tacn)Cl_2$) catalyst (Figure 28).

Entry	Monomer	Oxidation System	Time (h)	Conv.[b] (%)	Yield[c] (%)	Dimer Ratio[d]				
						p-2	o-2	pp-2	po-2	oo-2
1	p-1	Cu(tacn)Cl/O_2[e]	1	2.8	0.14	63	3	5	21	8
2	p-1	AIBN[f]	71	3.8	0.35	15	14	2	48	21
						p-4	o-4	oo-22	oo-13	
3[g]	p-2	Cu(tacn)Cl/O_2[e]	0.5	15	10	93	7	0	0	
4[g]	p-2	AIBN[f]	120	27	15	82	4	2	12	

[a] Oxidative polymerization of p-1 (1.20 mmol) or p-2 (0.60 mmol) in toluene (1.2 g) at 40 °C.
[b] Conversion of monomer.
[c] Total yield of dimers.
[d] Dimers shown below.
[e] Cu(tacn)Cl_2 (0.0030 mmol) and 2,6-diphenylpyridine (0.030 mmol) under dioxygen (1 atm).
[f] Oxidized by an equivalent molar of AIBN to p-1 or p-2 under nitrogen.
[g] Refs. 16 and 17.

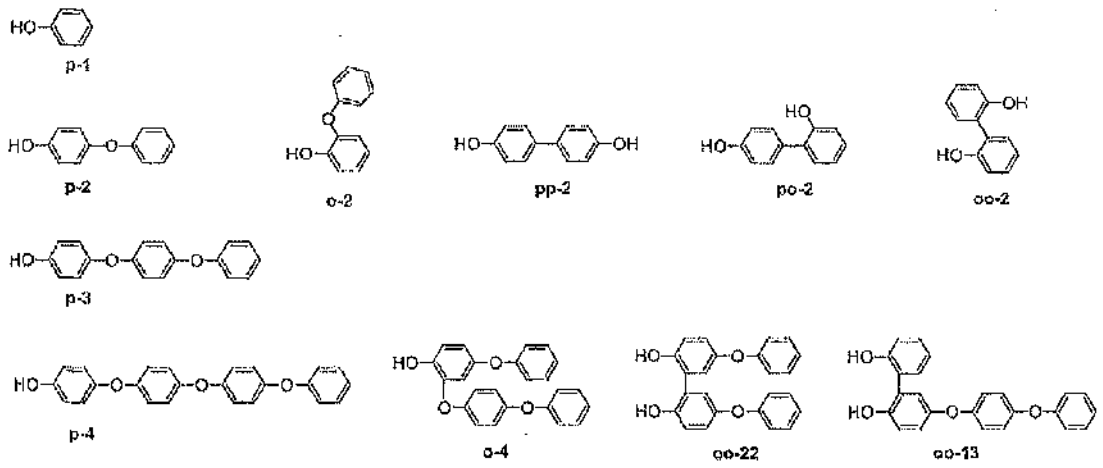

Fig. 28[78] Dimer formation. The dimers and oligomers of phenol and dimers of 4-phenoxyphenol.

Research recently reported by Gamez *et al.*[79] concerned the oxidative polymerisation of 2,6-dimethylphenol. The oxidative coupling reactions were catalysed by organic copper(II) complexes, without the use of zeolites or clays. Despite this, the results and discussion given suggest acetonitrile to be a suitable solvent. Indeed the activity of catalysts was greatly improved with the use of acetonitrile. The authors suggested that acetonitrile could act as a labile ligand for the copper ions and favour the 'scattering' of water so by helping to prevent hydrolysis and subsequent catalyst deactivation. Gamez *et al.*[79] indicated that increasing the quantity of water present in the reaction mixture caused a progressive deactivation of the catalysts due to the formation of inactive copper(II) hydroxide. Water was nevertheless recognised as the co-product of the oxidative coupling reaction.

1.3.4 Properties of 4,4'- and 2,2'-biphenol and 4-phenoxyphenol

For a more complete understanding of the phenoxyl radical recombinations that maybe responsible for the production of 2,2'- and 4,4'-biphenol and 4-phenoxyphenol, the redox behaviour and acidic properties of these biphenols must be known. Biphenols have two theoretical pK_a values. A pK_a value indicates the strength of an acid on a logarithmic scale using $\log_{10}(1/K_a)$ where K_a is the acid dissociation constant; the higher the pK_a value the weaker the acid. The two pK_a values, pK_{a1} and pK_{a2} correspond to HO-Ph-Ph-OH and $^{-}$O-Ph-Ph-OH. Jonsson *et al.*[8] reported the pK_a of phenol to be 10.0; pK_{a1} and pK_{a2} for 2,2'-biphenol as 7.6 and 13.7 and for 4,4'-biphenol pK_{a1} and pK_{a2} were quoted as 9.7 which was almost identical to phenol. Das[80] and Pal *et al.*[81] however reported two pK_a values for 4,4'-biphenol and Pal *et al.*[81] estimated pK_{a1} and pK_{a2} values for 2,2'-biphenol to be 7.5 and 14.7 and those for 4,4'-biphenol to be 9.4 and 14.1. The same authors rationalised the different pK_a values of 2,2'- and 4,4'-biphenol by the presence and absence respectively of intramolecular hydrogen bonding.

Jonsson *et al.*[8] also calculated the pK_a values of phenoxyl radicals, quoted as 6.3 and 10.0 for 4,4'- and 2,2'-biphenol respectively. Compared to phenol, the 4-phenoxyl radical in the *para* position is electron-withdrawing whilst the effect of the 2-phenoxyl radical in the *ortho* position is negligible. Jonsson *et al.*[8] reported the 'O-H' Bond Dissociation Energies (BDE) of 2,2'-biphenol to be 372 kJ mol^{-1}, 4,4'-biphenol as 349 kJ mol^{-1} and phenol as 365 kJ mol^{-1}. Jonsson *et al.*[8] and Pal *et al.*[81] both calculated the BDE for 4,4'-biphenol as less than that for 2,2'-biphenol. The weaker 'O-H' bond in 4,4'-biphenol demonstrates its suitability as an antioxidant. Das[80] elucidated one other important correlation that can be drawn from the two pK_a values of 4,4'-biphenol. An increase of ca. 5 pH units for the second pK_a value to 14.1 confirms the planar conformation of 4,4'-biphenol. The negative charge from one deprotonation is delocalised over the whole molecule and resists the second deprotonation. Das[80] also commented on the limited solubility of 4,4'-biphenol in neutral and acidic solutions but its free solubility at alkaline pH, although slow thermal oxidation took place in the presence of dissolved oxygen.

The formation of the phenoxyl radical is possible either via cleavage of the ArO-H bond or by a one electron transfer from the phenolate anion to the oxidant (Figure 29).[80]

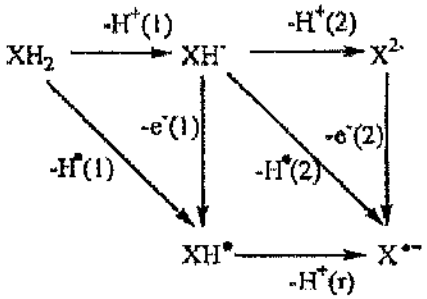

Fig. 29[81] Thermodynamic cycle for diprotic acids.

1.4 Improving catalytic activity and selectivity

The polymerisation of phenol has been and is still an important target for the field of polymer synthesis. Catalysts used include CuCl/pyridine, N,N`-bis(salicylidene) ethylenediamine iron (Fe(salen)) complexes and enzymes such as horseradish peroxidase (HRP). It is however not possible for these catalysts to control the regioselective coupling of phenoxy radical intermediates. There are a number of possible dimerisation products, as shown in Figure 30.

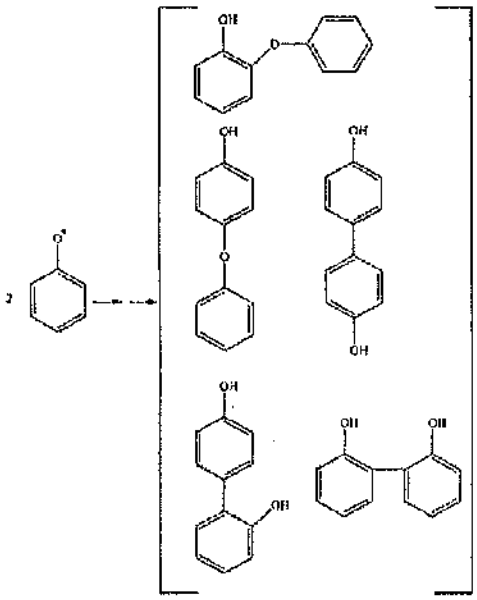

Fig. 30[8] The viable products of phenoxyl radical recombination.

Catalysts affect the kinetics of chemical reactions and can therefore be designed to direct selectivity.[82] Kodayashi *et al.*[6] suggested that if a catalyst generates and regenerates only a nucleophilic active oxygen intermediate, which then reacts with phenols to give *controlled* radicals without formation of *free* radicals, the stereoselectivity of the subsequent coupling may be entirely regulated.

Boccuzzi *et al.*[7] suggested a number of heterogeneous alternatives to the homogeneous copper salt catalysts currently used by industry to polymerise 2,6-dimethylphenol. These require an excess of oxidising agents such as silver, lead, manganese oxides or copper(II) complexes all in the presence of dioxygen whose function is to oxidise the highly stabilised copper(I) to copper(II) and regenerate the base. The heterogeneous catalysts used by Boccuzzi *et al.*[7] were 8% Cu/SiO_2 and

Cu/SiO_2-TiO_2. The starting material was 2,6-dimethylphenol and the target product was the carbon-oxygen coupled poly-2,6-dimethyl-1,4-phenylene ether although the unreduced catalyst provided significant quantities of the carbon-carbon coupled diphenoquinone product despite significant leaching of copper.

1.4.1 Water

The preparation technique for catalysts has an important impact on the catalyst surfaces and distribution/type of active sites. These properties are also affected by post-preparation treatments including calcination, used to remove template and carrier molecules for example acetate. The temperatures required for calcination are ca. 720 K and so any water present will be removed. The catalyst will however regain some of this water if the sample is returned to and stored in the laboratory without a controlled atmosphere.

The position of transition metal ions in hydrated zeolites was studied by Mortier.[83] The hydrated metal ions present in cation-exchanged zeolites are always located at *accessible* sites. After preparation and to dehydrate cation-exchanged zeolites, heating should be slow in order to avoid hydrolysis of the *waters of hydration*.[84] This allows the metal ions to be distributed evenly over the surfaces of the catalyst, although some hydrolysis is inevitable. Dealumination is the removal of alumina whilst the crystallinity of the zeolite is retained. This is possible at temperatures above 730 K and in the presence of steam or by acid extraction[27] although some zeolites, including HZSM-5 are highly resistant to such processes[85]. In addition to removing the water of constitution from the structure, surface hydroxyl groups can also be removed, allowing Brønsted acid sites to be converted to Lewis acid sites. This process will occur at temperatures greater than 673 K (Figure 31).

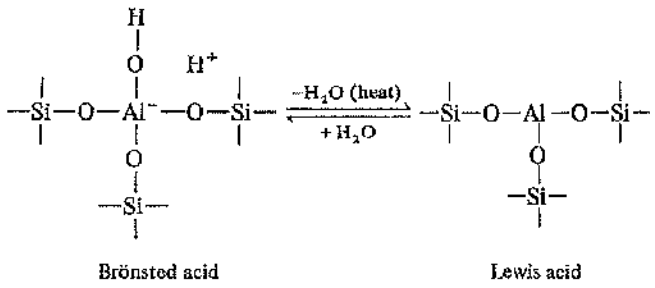

Fig. 31[86] The conversion of Brønsted acid sites to Lewis acid sites.

Zeolites and other microporous crystalline materials that have undergone ion-exchange with reducible cations can form bifunctional catalysts, displaying both metal and Brønsted acid functionality after reduction.[27] For aluminosilicates and other similar mixed-oxide catalysts the source of acidity may be rationalised using a theory originally developed by Linus Pauling describing the isomorphous substitution of a trivalent aluminium ion for a quadrivalent silicon ion. The resulting net negative charge within the lattice must be stabilised by cations, such as protons. The dissociation of water forming a hydroxyl group on the aluminium atom can provide these protons. The structure then contains tetrahedrally coordinated silicon and aluminium atoms and provides Brønsted acidity. It is the heating of this structure that removes the so-called *water of constitution* that converts Brønsted acidity to Lewis acidity.

The interaction between these aluminium sites and hydrocarbons is also important (Figure 32).

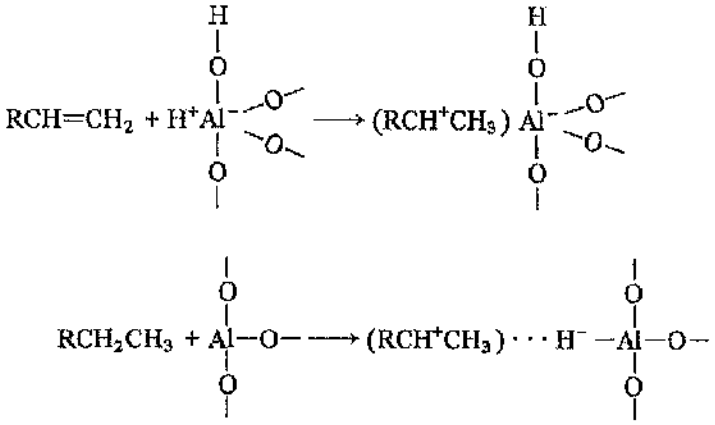

Fig. 32[86] Adsorption of an alkene at Brønsted and Lewis acid sites.

Removing the *water of hydration* from the surfaces of the catalyst may or may not be necessary to allow the adsorption of hydrocarbons. Zeolite and clay catalysts are hydrophilic which encourages the adsorption of water during or prior to a reaction, providing stabilisation and therefore sometimes a lowering of catalyst performance.[87] For copper exchanged zeolites, the cations remain as Cu^{II} ions during dehydration. The production of Cu^{I} is however possible and is often achieved using 'autoreduction', described in detail by Larsen *et al.*[88]. Autoreduction of Cu^{II} to Cu^{I} with 40-60% conversion is achieved by heating the catalyst above 698 K in a flow of helium or under vacuum. Water reduces the ability of montmorillonite to oxidise phenol because the water acts as a Lewis base.[89]

Catalyst activity and the rate of deactivation were reported by Girotti *et al.*[87] to depend on the water content in the liquid phase fraction of the reaction mixture. A water concentration of 0.88 wt.% was considered the upper limit.[87] Increasing the reaction temperature removes more water but may also increase the desorption rate of products and reactants.[56] Lucas *et al.*[90] demonstrated that water could reduce the deactivation rate of H/ZSM-5 catalysts by converting Brønsted acid sites into Lewis acid sites so by reducing coke formation. Das and co-worker[91] concluded that the presence of water reduced the occurrence of side reactions and improved the catalyst stability during the selective synthesis of para-ethylphenol from phenol and ethanol using zeolite catalysts.

1.4.2 Acidity

Kodayashi *et al.*[6] provided evidence that the coupling of free phenoxy radicals and coordinated phenoxy radicals under basic conditions favoured carbon-oxygen coupling. In comparison, the coupling of free phenoxy radicals and phenoxonium cations from the two-electron oxidation with phenol under acidic conditions favoured carbon-carbon coupling. Figure 33 illustrates the effect of acidic and basic conditions on the oxidative polymerisation of DMP using Ag_2CO_3 on celite.

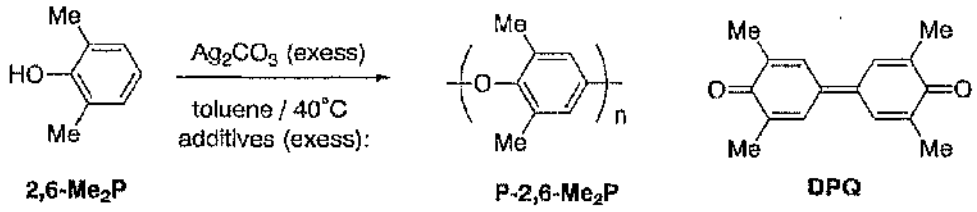

additives	P-2,6-Me_2P		DPQ	total yield (%)
$nC_5H_{11}NH_2$	>99	/	~0	93%
(no addition)	50	/	50	74%
CH_3CO_2H	0	/	100	79%

Fig. 33[6] Oxidative polymerisation of 2,6-Me_2P (0.8mmol) with 50wt% Ag_2CO_3 (2.4mmol) in the absence and presence of acid and base (16mmol) in toluene (16g) at 40°C under argon for 24-48hrs.

Addition of a base ($C_5H_{11}NH_2$) improved the selectivity towards carbon-oxygen coupled products. Kodayashi *et al.*[6] referenced Baesjou *et al.*[69] who concluded that with limited amine present the conditions were acidic, owing to the Lewis-acidity of the copper(II) ion. In excess amine the acidity was reduced and carbon-oxygen coupling was favoured. The strength and number of Lewis acid sites in zeolites and clays vary with pH as do their ability to oxidise phenol. The oxidation of phenol was maximised at pH value 2 – 3.5 and >8.[92]

1.4.3 Temperature

In 1956 Hay[4] and co-workers discovered that 2,6-dimethylphenol could be oxidatively polymerised to a high molecular weight, linear poly(phenylene oxide) (PPO) at room temperature using a copper(I) salt as a catalyst in the presence of oxygen (Figure 34). Small amounts of diphenoquinone, the carbon-carbon coupled product, were detected. Diphenoquinone became the dominant product at temperatures above 373 K.

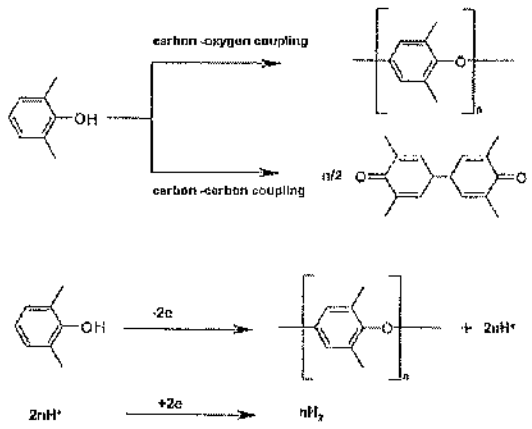

Fig. 34[4] The oxidative coupling of 2,6-dimethylphenol and formation of carbon-carbon and carbon-oxygen coupled products.

1.4.4 Alkali metals

Fujiyama *et al.*[55] and Kohara *et al.*[62] reported the addition of alkali metals into the feedstock solution or onto the Cu-Na/MCM-41 catalyst surfaces increased catalytic activity for phenol oxidation. Neither Fujiyama *et al.*[55] or Kohara *et al.*[62] provided an explanation for the observed increase in catalytic activity. Hayashibara and co-workers[93] also studied the effect of alkali promoters but on Cu-Na/ZSM5 catalysts for the oxidation of benzyl alcohol. They suggested that the copper and alkali cooperated in the partial oxidation of benzyl alcohol rather than functioning separately. Hayashibara *et al.*[93] also suggested that the alkali forced Cu ions within the zeolite to locate at sites more accessible to reactant molecules. This slowed the deactivation of Cu-Na-ZSM5 by impeding the formation of carbonaceous deposits on the zeolite surfaces. Similarly the role of potassium added to a Ce-Na/ZSM-5 catalysts for the partial oxidation of benzyl alcohol was studied by Idaka *et al.*.[94] They also concluded that whilst potassium reduced catalytic activity it prevented the build-up of coke on the surface of high Ce-loaded Na/ZSM-5 catalysts and so prolonged catalytic life. For low Ce-loaded Na/ZSM-5 the addition of potassium as CH_3COOK promoted catalytic activity.[94] The effects of alkali metals added to Cu/Zeolite-Y were similar. Xu and co-workers[95] reported that alkali metals increased the amount of adsorbed oxygen species responsible for the partial oxidation of benzaldehyde. An atomic K/Cu ratio of 4 was reported to provide maximum catalytic activity when added to Na/ZSM-5.[96]

1.4.5 Number and strength of acid sites

The flexible nature of the acid-base bond between the zeolite and adsorbed phenol molecule may control product selectivity and the Brønsted or Lewis acidity of the zeolite or clay maybe responsible for catalytic activity. Reddy and co-workers[97] investigated the alkylation of phenol with methanol over molybdenum oxide supported on Na/Zeolite Y. A series of MoO_3 catalysts with Mo loadings between 2 and 16% were prepared by impregnation of the support using an aqueous ammonium heptamolybdate solution at pH 8. The Na/Zeolite-Y used had a SiO_2/Al_2O_3 ratio of 5.2. The authors reported that it was well established that the alkylation of phenol was sensitive to the acidic and basic properties of the catalyst. Strong acidity favoured C-alkylation whilst basic catalysts were found to promote O-alkylation. Using an acidic catalyst the oxygen of the phenol will *attack* the catalytic surface. The orientation of the then adsorbed phenol molecule means further reaction with this molecule without desorption can only involve the carbon and hydrogen atoms of the benzene ring. Reddy *et al.*[97] reported from their own studies that an increase in the *number* of acid sites on the zeolite support caused an increase in the selectivity to C-alkylation. A significant increase in the *strength* of available acid sites generated an increase in O-alkylation selectivity. They concluded that C-alkylation was governed by the type of phenol adsorption on the catalyst surface that depended on its acidic strength. On highly acidic catalysts the phenol ring adsorbed parallel to the surface thus decreasing the likelihood of substitution at the *ortho*, *meta* and *para*-positions and promoting formation of the ether[97]

From the NH_3-TPD profiles of MoO_3/Na/zeolite-Y catalysts, Reddy and co-workers[97] established the relative strength of the acid sites. As MoO_3 loading increased, the number of acid sites was seen to decrease due to pore blocking. In contrast, at higher MoO_3 loadings the strength of acid sites increased. Product selectivities and conversions at different MoO_3 loadings were also recorded.

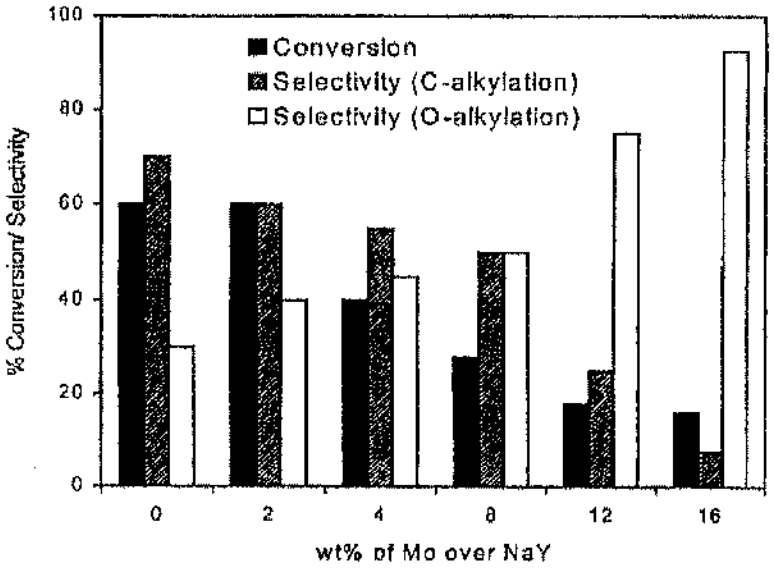

Fig. 35[97] Alkylation of phenol over various Mo/NaY catalysts. Reaction temperature of 673K, WHSV: 0.035 mol $h^{-1}g^{-1}$.

Reddy and co-workers[97] concluded, with reference to a publication by Parton *et al.*,[98] that product distribution between O- and C-alkylation (Figure 35) depended on the acid/base properties and pore size of the zeolites in addition to Weight Hourly Space Velocity (WHSV), phenol to MeOH ratio, time on stream and temperature. The dimerisation of phenol to 4,4'-biphenol, 2,2'-biphenol and 4-phenoxyphenol is a form of alkylation and the alkylation of phenol is a reaction sensitive to the acid-base properties of the catalysts used[17].

2 Experimental

2.1 Analytical techniques

A total of eight analytical techniques were used to characterise and confirm the properties of fresh and spent catalysts. *Fresh* is used to describe a catalyst before reaction and *spent* refers to a catalyst after reaction.

2.1.1 X-ray Diffraction

The X-ray Diffraction (XRD) patterns of powdered samples of the catalysts were measured at room temperature on a Siemens D5000 diffractometer using a stationary Cu K_α source and a movable detector over a range of 2θ values from 5 to 45° using a step size of 0.02° and a step time of 1.5 seconds.

The intensity of diffracted radiation was measured by the detector as a function of 2θ between the incoming and diffracted beams. The atoms in a crystal are arranged in a regular pattern. Atoms that are on the crystal planes provide constructive interference of the scattered X-ray beam. The intensity of the diffracted beam depends on the number of electrons and so type of atom and its relative position. The position of the diffracted beam depends on the size and shape of the crystal unit cell. All crystalline compounds therefore have a unique, fingerprint diffraction pattern. For powdered samples the alignment of a small fraction of particles in a given crystal plane at any given value of 2θ provides constructive interference.[99, 100]

2.1.2 Atomic Adsorption Spectroscopy

Atomic Absorption Spectroscopy (AAS) relies upon two processes, (i) the production of free atoms from the sample and (ii) the adsorption, by these atoms, of radiation from an external source.[100] The method used to convert analytes in solution to free atoms in the flame is summarised in Figures 36 & 37.

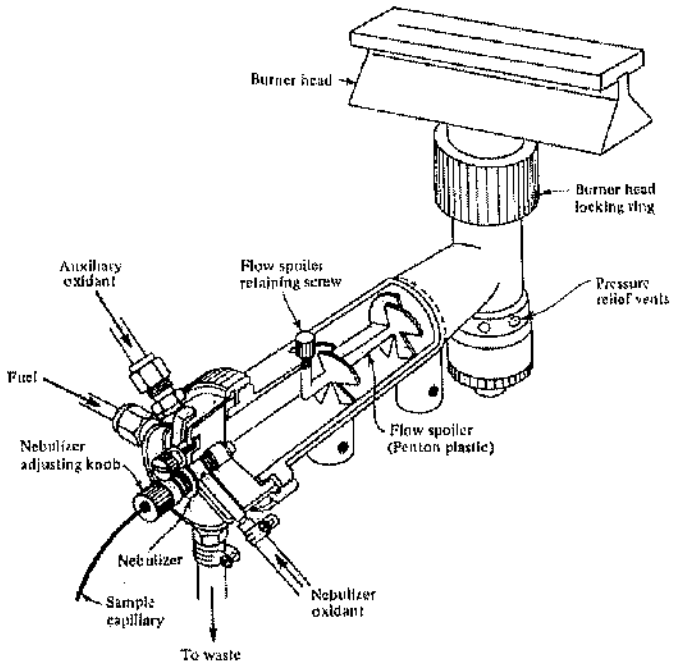

Fig. 36[100] Slot burner and expansion chamber of a flame atomic absorption spectrometer.

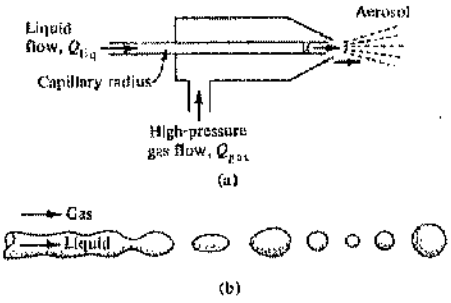

Fig. 37[100] Magnification of (a) the pneumatic nebuliser and (b) breakdown of liquid filament into droplets from Figure 36.

The adsorption of radiation by free atoms in the flame, removed from their chemical environment without ionisation, involves a transition of these atoms from the highly populated electronic ground state to an excited state. Using specialised software, the instrument is able to convert the atomic adsorption spectrum that consists of a series of resonance lines to a digital absorbance readout calibrated to a series of external standards, run prior to the sample of unknown concentration. The instrument used was a Perkin-Elmer, 1100B Atomic Adsorption Spectrometer.

Element Mode:	Flame	Replicates:	3
Element:	Ag /Cu	Oxidant:	Air
Wavelength (nm):	328.1 /324.8nm	Fuel Flow (L/min):	2.5
Slit (nm):	0.7	Oxidant flow (L/min):	8.0
Lamp current (MA):	4	Calibrations:	1,2 & 5
Integration time (sec):	3.0		

2.1.3 Hydrofluoric acid digestion

Hydrofluoric acid (HF) was used to dissolve the aluminosilicate catalytic support. Having dissolved the support, any metal species from the ion-exchange or coke from the reaction were dissolved into solution. Atomic Absorption Spectroscopy (AAS) of the filtrate provided quantitative elemental analysis for copper, silver or nickel.

Hydrofluoric acid is *very toxic* and *corrosive*. For these reasons the dissolutions were done at the Scottish Universities Environmental Research Centre (SUERC). To each 0.50 g sample of catalyst, ca. 2 ml of HF was added and the solution heated to 343 K for 3-5 hours until all material had dissolved. The solutions were then heated to dryness and made up with 50 ml of 0.2 mol L^{-1} HNO_3 to allow safe handling. The AA spectrum of each sample filtrate was then obtained. This was done in the Chemistry Department at the University of Glasgow.

2.1.4 Thermogravimetric analysis

Thermogravimetric analysis (TGA) provides a quantitative measurement of weight change against temperature or time. A sample changes weight due to physical or chemical bond making or breaking, made possible at elevated temperatures. The weight of the sample is continuously recorded. A horizontal quartz beam holds a crucible for the sample the other end of which passes into the transducer coil of an electromagnetic balance. A pair of photosensitive diodes detect any movement of this beam (Figure 38). It was possible to control the atmosphere around the sample and direct a portion of the exit gas stream from the chamber to a mass spectrometer (MS) for analysis.

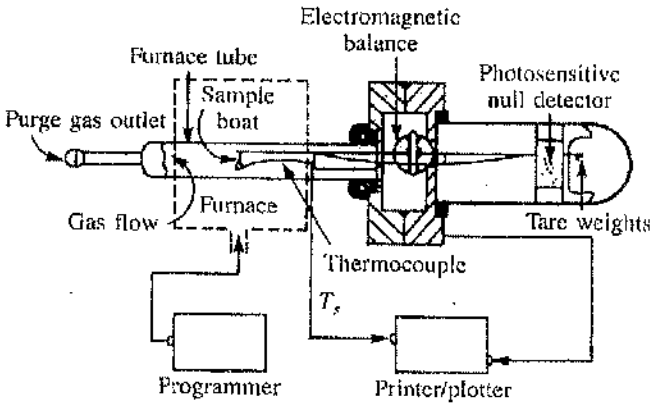

Fig. 38[100] Schematic of a thermogravimetric analyser.

The samples of catalyst were heated from room temperature to 1273 K at 10° min^{-1} in a flow of 2%O_2/Ar using a SDT Q600 TGA machine. The mass spectrometer (European Spectrometry Systems Ltd., 'evolution') was programmed to monitor mass/charge (m/z) ratios of 18 (water), 28 (carbon monoxide), 41 (acetonitrile), 44 (carbon dioxide), 94 (phenol) and 186 (biphenol).

2.1.5 Mass spectrometry

A mass spectrometer creates gaseous ion fragments of a sample. A mass analyser is then used to separate the ions produced in the ion source according to their m/z ratios. A quadrupole mass analyser as used, consists of four electrically conducting parallel rods. One diagonally opposite pair is positively charged, the other pair negatively charged. An rf oscillator modifies the region between the four rods to appear as oscillating hyperbolic potentials (Figure 39). Resolution is a function of the number of cycles an ion undergoes in the field, the lighter the ion the less cycles.

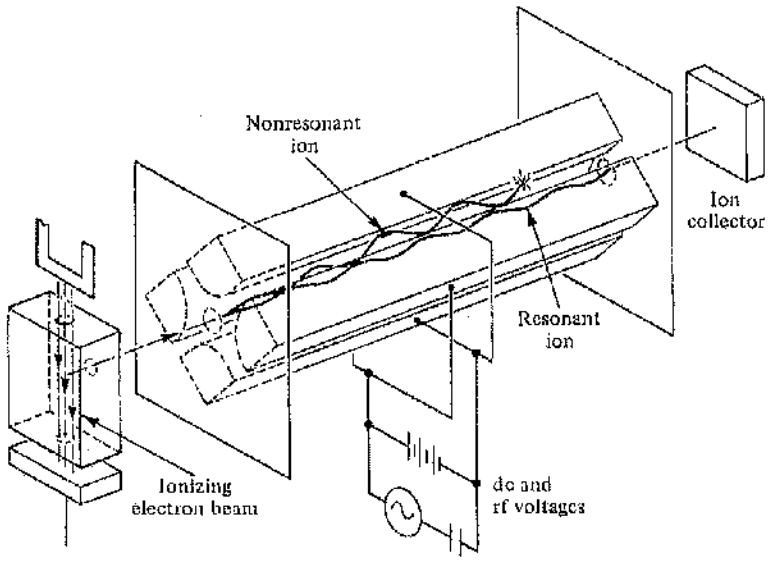

Fig. 39[100] Schematic of a quadrupole mass analyser.

2.1.6 UV/Vis/NIR spectroscopy

The diffuse reflectance UV spectra of the powdered catalysts were obtained using a Varian, Cary 500 Scan spectrophotometer with *Praying Mantis* attachment. The spectra were recorded between 35,000 and 7,500 cm^{-1}. The diffuse reflectance of electromagnetic radiation is shown schematically in Figure 40.

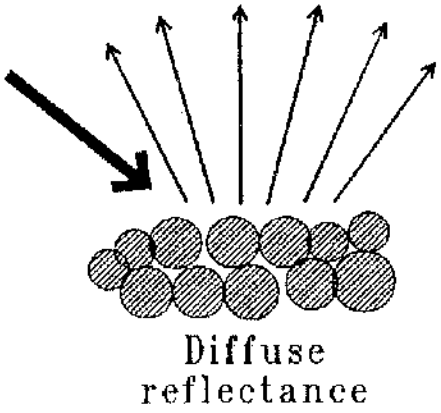

Fig. 40[99] Diffuse reflectance spectroscopy on a powdered catalyst sample.

The scattered radiation is collected by the ellipsoidal mirror of the *Praying Mantis* and focussed on the detector. Figure 41 illustrates the component parts of the *Praying Mantis* attachment.

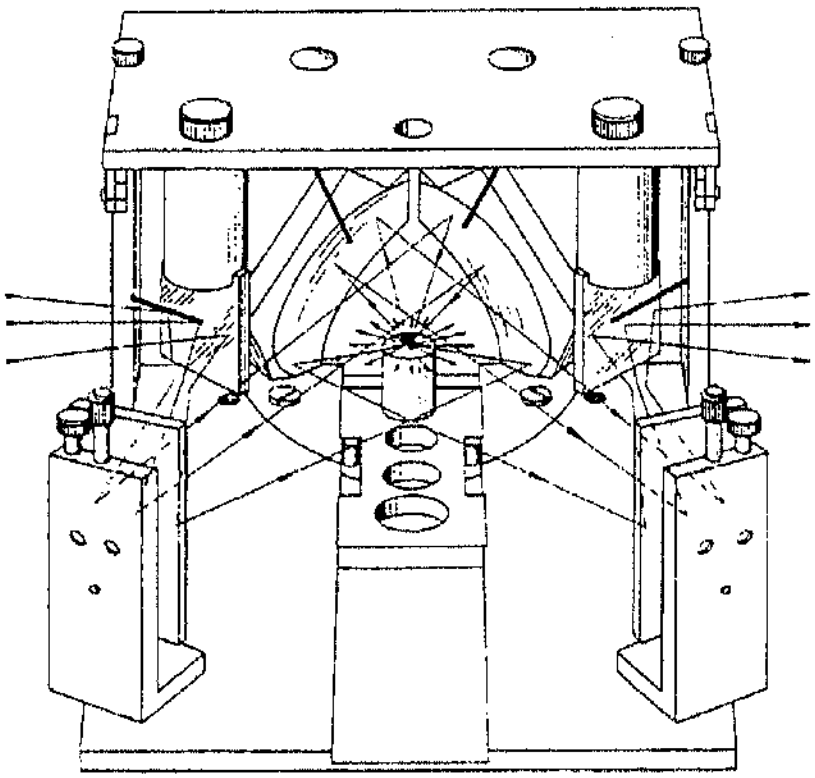

Fig. 41[101] Praying Mantis attachment.

The absorption spectrum was described by the Kubelka-Munk function (Equation 1).

Equ. 1 Kubelka-Munk function.

$$\frac{K}{S} = \frac{(1-R_\infty)^2}{2R_\infty}$$

K is the absorption coefficient, a function of the frequency ν

S is the scattering coefficient

R_∞ is the reflectivity of a sample of infinite thickness, measure as a function of ν

If *S* does not depend on ν then the Kubelka-Munk function transforms the measured spectrum R_∞ into the absorption spectrum K(ν).[99]

2.1.7 BET analysis

The Brunauer Emmett Teller (BET) analysis of catalysts is often used to measure surface area and pore diameters. Accurate BET analysis requires the material to exhibit a Type II adsorption isotherm. Zeolites and other similar materials exhibit particularly well-defined Type I isotherms. For a Type I isotherm uptake does not increase continuously as it does for Type II, instead uptake reaches a limiting value. The BET analysis of zeolites and clays will therefore only be used to compare the pore diameters and surface areas of catalysts before and after reactions.

Using a Flowprep 060 Micrometrics Gemini BET machine, ca. 0.04 g of catalyst was placed in a tube of known volume, heated and degassed overnight at 383 K. After calibration of the equipment the sample was then cooled with liquid nitrogen and a known volume of nitrogen gas introduced into the tube. The pressure was measured throughout this procedure and the sequence repeated with successive pulses of nitrogen.

The accompanying software calculated the BET surface area, pore size and pore volume of the catalyst using the volume of the tube, temperature and volume of nitrogen introduced with each pulse. The expected pressure in the absence of any

adsorption was calculated and compared to the observed pressures for vials containing catalyst.

2.1.8 Nuclear Magnetic Resonance

Nuclear Magnetic Resonance (NMR) relies on the characteristic absorption of energy by certain spinning atomic nuclei in a strong magnetic field when irradiated by a second, weaker and perpendicular magnetic field. The characteristic adsorption patterns allow identification of atomic configurations in molecules[100]. Used simply the patterns from compounds of known structure can be related to the patterns obtained from samples of unknown composition. The NMR spectra of 4,4'-biphenol, 4-phenoxyphenol and the then unknown compound $C_{18}H_{14}O_3$ were obtained using Bruker, DPZ400 equipment.

2.2 Catalyst preparation and characterisation

Five catalyst supports, Zeolite-Y, ZSM-5, Attapulgite, Montmorillonite and MCM-41 were purchased in their sodium form (Table 2). The Zeolite-Y, Attapulgite and Montmorillonite were purchased from Catal International Ltd, ZSM-5 from Zeochem and MCM-41 from Aldrich.

Table 2 Specification of the five catalyst supports.

Support	*Specification*
Zeolite-Y	Zeolite Y (Na Form) CT-427
ZSM-5	Zeocat PZ-2/40
Attapulgite	Catalyst Grade Attapulgite Ref. D-1430
Montmorillonite	Catalyst Grade Montmorillonite Ref. D1440
MCM-41	Aluminosilicate, mesostructured hexagonal framework, MCM-41 type, Ref. 643653

To maintain electrical neutrality these support structures contain framework cations. These cations are usually sodium and can be replaced by ion-exchange techniques with a range of other cations including hydrogen, copper, silver and nickel. A total of twenty-three catalysts were prepared and tested (Table 3).

Table 3 Summary of the twenty-three catalysts prepared and tested.

Support / *Metal*	*Zeolite-Y*	*ZSM-5*	*Attapulgite*	*Montmorillonite*	*MCM-41*
Na	✓	✓	✓	✓	
H	✓	✓	✓	✓	
Cu	✓ 1, 5, 6 & 8%	✓ 4%	✓ 1, 3 & 5%	✓ 6 & 9%	✓ 5%
Ni	✓ 5%				
Ag	✓ 1(10%), 2(18%) & 3(18%)				

After preparation all catalysts were heated at 10° min^{-1} to 723 K and calcined for 5 hours in a flow of air. The airflow was >1 L min^{-1}.

2.2.1 Methods of ion-exchange

The ion-exchange of sodium for hydrogen, copper, silver or nickel required sodium nitrate ($NaNO_3$), ammonium nitrate (NH_4NO_3), copper acetate ($Cu(CH_3CO_2)_2.H_2O$), silver acetate ($Ag(CH_3CO_2).H_2O$) and nickel acetate ($Ni(CH_3CO_2)_2.H_2O$), all purchased from Aldrich.

H/zeolites and clays. The Na/zeolite or clay (25 g) was treated three times with 0.2 L of a 1 mol L^{-1} NH_4NO_3 aqueous solution at 348 K by reflux for 1 hour. A 100 ml round bottom flask with magnetic stirrer, water condenser and oil bath were used. The sample was filtered then washed after each reflux with 0.5 L of de-ionised water, filtered again and the catalyst dried at 353 K overnight. This was repeated twice before the sample was heated at 10° min^{-1} to 723 K and calcined at 723 K for 5 hours in a flow of air using a tubular furnace.

Cu/zeolites and clays. The Na/zeolite or clay (25 g) was first pre-treated with 0.2 L of a 1 mol L^{-1} $NaNO_3$ aqueous solution at 348 K by reflux for 1 hour to ensure the Na content of the Na/zeolite or clay was 100%. The sample was filtered then washed after the reflux with 0.5 L of de-ionised water, filtered again and the catalyst dried at 353 K overnight. This was repeated before the copper ion-exchanged Na/zeolite or clay was then prepared using 0.3 L of an aqueous copper acetate solution in a round bottomed flask with magnetic stirrer, water condenser and oil bath. The concentration of this solution varied depending on the metal loading required. The sample was filtered and washed with 0.5 L of de-ionised water, filtered again and the catalyst dried at 353 K overnight. The sample was heated at 10° min^{-1} to 723 K and calcined at 723 K for 5 hours in a flow of air using a tubular furnace.

Four Cu/Zeolite-Y catalysts were prepared. Starting with Na/Zeolite-Y the material was refluxed once with 0.3 L of an aqueous solution of copper acetate at a concentration sufficient to produce the predetermined copper loading. Cu/Zeolite-Y was prepared with w/w metal loadings of 1, 5, 6 and 8%, using 0.02, 0.10, 0.21 and 0.42 mol L^{-1} solutions. All other copper catalysts were prepared by the same method. A 0.08 mol L^{-1} solution was used for Cu(4%)/ZSM-5 and 0.07 mol L^{-1} solution for Cu(5%)/MCM-41. For the Attapulgite catalysts 0.01, 0.21 and 0.55 mol L^{-1} solutions were used for 1, 3 and 5% Cu/Attapulgite. Aqueous copper acetate solutions of 0.05

and 0.08 mol L^{-1} were used for 6 and 9% Cu/Montmorillonite. These concentrations were for the preparation of 25 g of catalyst using 0.3 L of distilled water.

Ag/zeolites. Three Ag/Zeolite-Y catalysts were prepared with increasing silver loading. Starting with 25 g of Na/Zeolite-Y the material was refluxed once, twice or three times with 0.3 L of a 0.17 mol L^{-1} aqueous silver acetate solution. These catalysts will subsequently be referred to as Ag-1(10%)/Zeolite-Y, Ag-2(18%)/Zeolite-Y and Ag-3(18%)/Zeolite-Y respectively.

Ni/zeolites. The procedure used for the preparation Ni/zeolites was the same as that described for Cu/zeolites and clays except a 0.42 mol L^{-1} aqueous nickel acetate solution replaced the copper solution.

All catalysts were calcined after preparation and stored in screw top jars without a controlled atmosphere. During this time the natural hygroscopic nature of the catalysts was considered to cause complete re-hydration.

2.2.2 Characterisation

The atomic scale composition and structure of a surface determine its catalytic properties. An atom by atom characterisation of the surface would provide the data for a complete understanding of the catalytic system. For the development of an industrial catalyst the emphasis is however often different. Chemical and physical characterisation is required to identify the properties responsible for active, inactive, selective and unselective catalysts.[99]

The metal loading, crystalline structure, metal oxidation state and surface area of catalysts were determined. The metal loading of catalysts was established using HF digestion and Atomic Absorption Spectroscopy explained in Sections 2.1.2 and 2.1.3. The crystalline structures of fresh and spent catalysts were confirmed using X-ray diffraction (Section 2.1.1) and surface area estimated using BET analysis (Section 2.1.7). The oxidation state of metal ion exchanged catalysts was investigated using UV/Vis/NIR Spectroscopy (Section 2.1.6). The electronic configurations of the metal must first be considered.

The electronic configurations of Cu, Cu^{+} and Cu^{2+} are

Cu	[Ar] $4s^{1}$ $3d^{10}$
Cu^{+}	[Ar] $4s^{0}$ $3d^{10}$
Cu^{2+}	[Ar] $4s^{0}$ $\mathbf{3d^{9}}$

The important characteristic of Cu^{2+} is the partially filled d-orbital for which the d-d transition of electrons is observable using UV/Vis/NIR spectroscopy. This provides a distinctive band at wavelengths between ~10,000 and 15,000 cm^{-1} (~1,000 and 650 nm), confirming the presence of Cu^{2+} but not the presence or absence of Cu^{+}-species. The common oxidation states of silver are Ag, Ag^{1} and Ag^{2+}. Copper and silver are both in Group 11 of the periodic table and so the metals and ions have comparable electronic configurations. The electronic configuration of Ag is [Ar] $5s^{1}$ $4d^{10}$. It is however not possible to confirm the oxidation state of nickel ions by the same method. Ni, Ni^{+} and Ni^{2+} all have a $3d^{8}$ electronic configuration. Without a change in the d-shell configuration the d-d transition of electrons observable using UV/Vis/NIR spectroscopy will be indistinguishable. All UV/Vis/NIR spectra were obtained at room temperature. During reaction, the catalyst temperature ranged from 308 to 408 K. Temperature is however unlikely to affect the oxidation state of copper below ca. 400K.[38]

Thermal analysis of fresh and spent catalyst material was used to confirm the presence of coke (Sections 2.1.4 and 2.1.5) and HF digestion used to separate this coke from the catalyst support as explained in Section 2.1.3.

2.3 Phenol and biphenol adsorption

The liquid-phase adsorption of phenol was studied using a 100 ml round bottomed flask and trickle bed reactor. Using High Performance Liquid Chromatography (HPLC) for analysis it was not possible to observe the adsorption of phenol over any of the zeolite or clay catalysts using these reactors. To ensure complete saturation of the catalyst and encourage removal of solvent, phenol and products of dimerisation from the catalyst, a Flooded Bed Reactor was commissioned.

2.3.1 Flooded Bed Reactor

The catalyst was loaded into the reactor, a stainless steel tube 100 mm in length with an internal diameter of 4 mm (Figure 42). The reactants were fed up through the catalyst bed by a HPLC pump. Before the column was attached to the liquid feed line the system was flushed with acetone and then with the acetonitrile, chloroform or aqueous solution of phenol and the pump was calibrated for a flow of 1.0 ml min^{-1}. The 0.7 g of catalyst was held in place by two metal frits located inside the end caps of the tube. The adsorption studies were done at 298 K using the furnace to maintain a constant temperature, accurately controlled via the thermocouple in the catalyst bed.

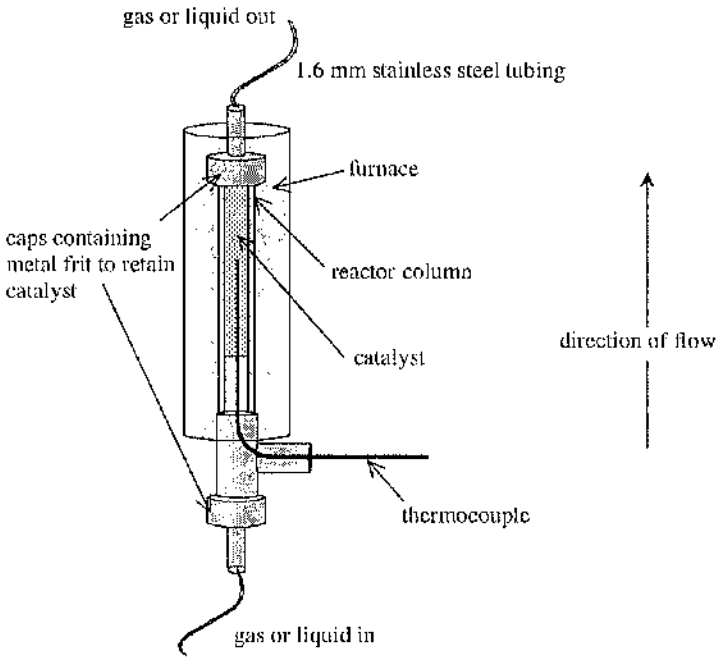

Fig. 42 Flooded Bed Reactor.

As solution was passed up through the column the powdered catalysts were compressed. The Cu(6%)/Zeolite-Y catalyst was compressed to occupy a length of ca. 75 mm. Inherent with this compaction was a pressure drop across the bed of ca. 12 bar. This was typical for all zeolite catalysts whilst for the clay catalysts the pressure drop was ca. 3 bar. These pressures remained constant throughout the adsorption experiments.

The exit solution was collected over 45 min in eighteen aliquots collected for 2.5 min each. These samples were then analysed by HPLC and the concentration of phenol or biphenol in solution calculated. Data was also collected when no catalyst was used and the column left empty.

2.3.2 Process variables

The adsorption of phenol, 4,4'-biphenol, 2,2'-biphenol and 4-phenoxyphenol was studied over twelve catalysts (Table 4).

Table 4 Summary of the different catalysts and adsorbates studied.

Support / *Metal*	*Zeolite-Y*	*ZSM-5*	*Attapulgite*	*Montmorillonite*
Na	Phenol 4,4'-biphenol	Phenol 4,4'-biphenol	Phenol	Phenol
H	Phenol 4,4'-biphenol	Phenol 4,4'-biphenol	Phenol	Phenol
Cu	Phenol 4,4'-biphenol 2,2'-biphenol 4-phenoxyphenol	Phenol 4,4'-biphenol	Phenol 4,4'-biphenol 2,2'-biphenol 4-phenoxyphenol	Phenol

The adsorption of phenol over Na/Zeolite-Y was studied at three concentrations, 0.004, 0.03 and 0.07 mol L^{-1} and using water, acetonitrile and chloroform as the solvents for phenol.

2.4 Dimerisation of phenol

The dimerisation of phenol to 4,4'-biphenol, 2,2'-biphenol and 4-phenoxyphenol was studied using the flooded bed reactor. All catalysts prepared and listed in Section 2.2, Table 3 were tested for their catalytic activity and selectivity.

2.4.1 Reaction methodology

The dimerisation of phenol to 4,4'-biphenol, 2,2'-biphenol and 4-phenoxyphenol was studied using the Flooded Bed Reactor, as described in Section 2.3.1, Figure 42. Phenol is a solid at room temperature so a solvent was required for a liquid phase reaction. Only two solvents were considered to be suitable, denoted by an asterisk (Table 5).

Table 5 Solvents considered.

Solvent	Chemical Formula	Boiling Point (K)	Price (£ L^{-1})	Comments
Water	H_2O	373	-	Poor solubility of 4,4'-biphenol
Ethanol	CH_3CH_2OH	351	9	Oxidise (aldehyde to carboxylic acid)
Benzene	C_6H_6	353	17	React as phenol
Acetone	CH_3COCH_3	329	8	Aldol condensation
Chloroform *	$CHCl_3$	334	10	Low boiling point at atmospheric pressure
Octanol	$CH_3(CH_2)_6CH_2OH$	469	21	Oxidise (aldehyde to carboxylic acid)
2-Ethyl-hexanol	$CH_3(CH_2)_3CH(C_2H_5)\text{-}CH_2OH$	457	16	Oxidise (aldehyde to carboxylic acid)
2-Propanol (IPA)	$(CH_3)_2CHOH$	355	11	Dehydrogenation possible
Ethoxyethane (diethyl ether)	$CH_3CH_2\text{-}O\text{-}CH_2CH_3$	308	35	Low boiling point
2-Methoxy-2-methylpropane	$CH_3\text{-}O\text{-}C(CH_3)_2CH_3$	328	28	Low boiling point
Acetonitrile *	CH_3CN	355	9	Decompose to cyanide

Solutions of phenol in chloroform, phenol in acetonitrile and phenol in acetonitrile *and* chloroform were prepared at five different concentrations.

For a standard reaction the reactor was loaded with 0.7 g of catalyst and heated in air to 348 K at 10° min^{-1}. The temperature of the catalyst bed was maintained at 348 K using the furnace, controlled by the thermocouple inside the reactor. A 0.04 mol L^{-1} phenol in acetonitrile, chloroform or acetonitrile *and* chloroform solution was pumped up through the catalyst bed at 0.5 ml min^{-1}. The liquid pressure in the reactor was maintained at 20 bar g by a pressure relief valve. Samples of the exit stream were taken at regular intervals for analysis by HPLC. Time zero corresponded to the initial flow of solution out of the reactor.

Chloroform solution. The methodology using a chloroform solution was modified to take account of poor product solubility. The solution was pumped through the bed for 45 min. The flow was stopped and the pump and lines flushed with acetonitrile. Acetonitrile was directed to the reactor and the catalyst bed flushed for 10 min at 1 ml min^{-1} whilst samples of the exit stream were taken. As the solubility of 4,4'-biphenol in chloroform was particularly poor, acetonitrile was used to encourage the removal of 4,4'-biphenol and the other dimers from the system. At changeover the flow of solution from the reactor was instantaneous. This two-phase cycle was repeated and after three complete cycles the flow was stopped and the catalyst discharged. At 0.5 ml min^{-1} the Liquid Hourly Space Velocity (LHSV) was 33 hr^{-1}.

Acetonitrile or *mixed chloroform* and *acetonitrile solutions.* These were pumped through the catalyst bed for 90 min. There was no flush used as poor solubility was not an issue. At 0.5 ml min^{-1} of acetonitrile solution the Liquid Hourly Space Velocity (LHSV) was 33 hr^{-1}.

The Piping and Instrumentation Drawing (P&ID) diagram (Figure 43) shows all components of the rig.

Fig. 43 Flooded Bed Reactor.

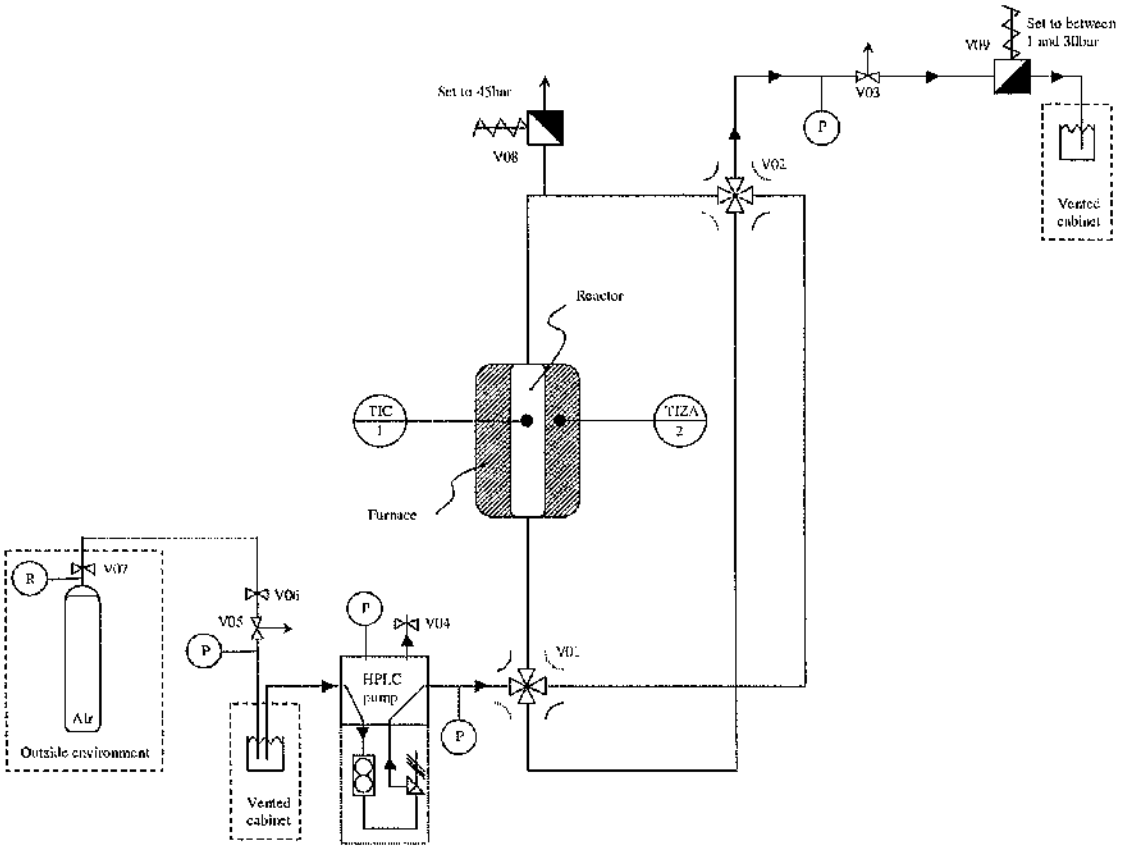

2.4.2 Process variables

The activity and selectivity of all catalysts was established using the standard experimental conditions explained in Section 2.4.1. Table 6 summarises the other experimental conditions under which the catalysts Cu(6%)/Zeolite-Y and Cu(5%)/Attapulgite were studied.

Table 6 Summary of the process variables used.

Catalyst / *Variable*	*Cu/Zeolite-Y*	*Cu/Attapulgite*
Solvent	Chloroform, acetonitrile, chloroform and acetonitrile mix, butyronitrile, propionitrile.	Chloroform, acetonitrile.
Metal loading	1, 5, 6 & 8% w/w	1, 3 % 5% w/w
Temperature	308, 328, 348, 388 and 408 K	
Phenol Concentration	0.02, 0.04, 0.08, 0.16, 0.32 mol L^{-1}	0.02, 0.04, 0.08 mol L^{-1}
Low temperature pre-treatment	Pre-treatment at 348 K in air, oxygen or nitrogen.	
High temperature pre-treatment	Pre-treatment at 723 K in air or nitrogen	
Pre-treatment with 4,4'-biphenol, 2,2'-biphenol or 4-phenoxyphenol	Acetonitrile, 4,4'-biphenol, 2,2'-biphenol, 4-phenoxyphenol, water.	Not investigated
Added alkali	Potassium acetate	No alkali added
Pressure	1, 10, 20 and 30 bar g	20 bar g
Water and peroxide	Phenol to water ratio and phenol to peroxide ratio was 1:2, added to the feedstock.	Not investigated

Low temperature pre-treatment. The catalyst was heated to 348 K at 10^{o} min^{-1} in a flow (100 ml min^{-1}) of air, oxygen or nitrogen. The catalyst was then held at 348 K for 30 min in the gas flow. The acetonitrile, chloroform or acetonitrile *and* chloroform solution was degassed simultaneously with the same gas supply but at a reduced flow rate of 10 ml min^{-1}. After 30 min the degassed solution was pumped into the reactor following the procedure for a chloroform or acetonitrile solution (Section 2.4.1).

High temperature pre-treatment. The catalyst was heated to 723 K at 10^{o} min^{-1} in a flow (100 ml min^{-1}) of air, oxygen or nitrogen. The catalyst was then held at 723 K for 90 min in the gas flow. The acetonitrile, chloroform or acetonitrile *and* chloroform solution was degassed simultaneously with the same gas supply but at a reduced flow rate of 10 ml min^{-1}. After 90 min the reactor was cooled to 348 K and the degassed solution was pumped into the reactor following the procedure for a chloroform or acetonitrile solution (Section 2.4.1).

Pre-treatment with 4,4'-biphenol, 2,2'-biphenol or 4-phenoxyphenol. The catalyst was heated in air to 348 K at 10^{o} min^{-1}. With the temperature held at 348 K, pure acetonitrile or a 0.04 mol L^{-1} solution of 4,4'-biphenol, 2,2'-biphenol or 4-phenoxyphenol in acetonitrile or chloroform was pumped through the catalyst bed at 1 ml min^{-1} for 30 min, at a liquid pressure of 20 bar g. After 30 min the flow was stopped and the pump and lines flushed with the solution of phenol in acetonitrile. The phenol solution was pumped into the reactor following the general procedure for an acetonitrile solution (Section 2.4.1).

2.4.3 Homogeneous phase reactions

A 100 ml round bottomed flask, oil bath, hot plate and magnetic stirrer were used. A water-cooled condenser was used to minimise solvent loss. The flask was heated to 348 K and 45 ml of the 0.04 mol L^{-1} acetonitrile solution and 0.169 g of copper acetate were added. The ratio of copper to phenol was 1:1. The temperature was held at 348 K and after 90 min a sample of the solution was taken for HPLC analysis.

2.4.4 Metal-ion leaching

The leaching of copper and silver from Zeolite-Y supported catalysts was investigated using the Flooded Bed Reactor as described in Section 2.4.1. The exit solution from the reactor was collected for 6 hours, the metal ion concentration in solution determined using Atomic Absorption Spectroscopy and the percentage loss of metal from the catalyst support calculated. This technique has been widely reported in the literature.[102]

2.5 High Performance Liquid Chromatography

High Performance Liquid Chromatography (HPLC) was used to analyse all samples from the liquid phase dimerisation of phenol to 4,4'-biphenol, 2,2'-biphenol and 4-phenoxyphenol and the adsorption studies. A schematic of the HPLC instrumentation used is given in Figure 44. Chromatographic separation in HPLC relies upon the interactions between sample molecules and both the mobile and stationary phases. A variable wavelength, Ultraviolet-Visible spectrometer was used as the detector.

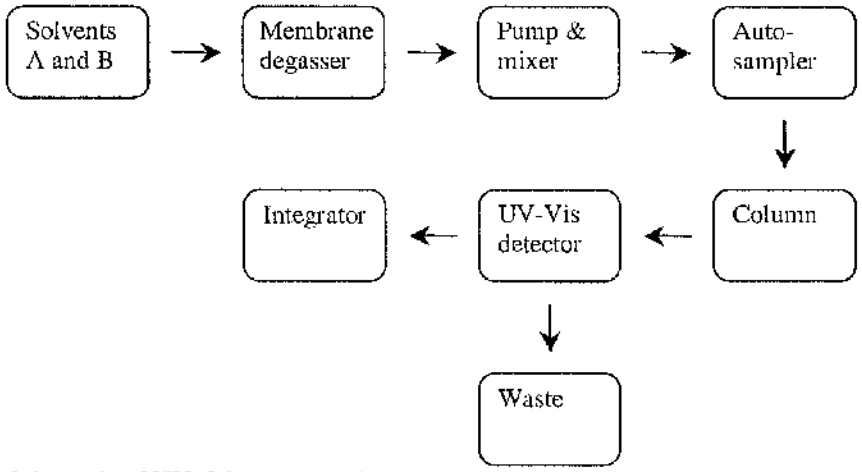

Fig. 44 Schematic of HPLC instrumentation.

2.5.1 Equipment and procedure

A binary mobile phase was used, solution A: 0.1% trifluoroacetic acid in water and B: 0.1% trifluoroacetic acid in acetonitrile. The trifluoroacetic acid was purchased from Aldrich, the HPLC grade water and acetonitrile were purchased from Fisher Scientific. Capillary tubing made from Polyetheretherketone (PEEK) connected the solvent reservoirs, membrane degasser and pump. Solvent was drawn through the degasser by the pump. The in-line vacuum degasser used was manufactured by LDC Analytical. The vacuum gradient generated causes dissolved gases to permeate out of the mobile phase, across the tubing membrane and into the degassing chamber. Removing dissolved gases from the mobile phase helped prevent the formation of bubbles in the HPLC system. Air bubbles in the pumpheads cause incorrect solvent gradients and bubbles moving through the stationary phase of the column under pressure produce channels that reduce the chromatographic separation of samples. Bubbles in the detector contribute to a noisy baseline.

The HPLC pump used was manufactured by Gilson; modules 305, 306, 811C and 805 were used. The pumps supply solvent at constant flow rates and accurate composition at operating pressures in the range 100 – 6000 psi. To prevent pressure pulsation, a compressible dead volume component was incorporated. Modules 305 and 306 were single piston reciprocating pumps (Figure 45) supplying solvents A and B to a low-volume mixing chamber for high pressure mixing. The flow rate was 1 ml min^{-1} and the solvent gradient was A/B = 60/40 with linear change over 30 min to A/B = 0/100 (held for 20 min). Stainless steal capillary tubing was used to connect the pump and autosampler.

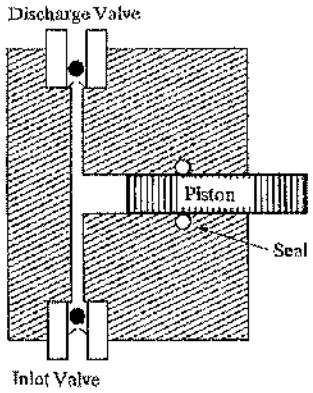

Fig. 45[103] A single piston reciprocating pump.

A Waters 717 Autosampler was used to increase sample throughput and improve assay precision. An autosampler makes it possible to deliver samples to the head of the column without stopping or disturbing the mobile phase flow and with minimal sample carryover between injections. The Waters autosampler uses an integral loop-loading configuration in which the injection needle forms an integral part of the injection loop (Figure 46). This means the entire volume (5 µl) of loaded sample is injected and the injection valves and loops are continually flushed during solvent cycles, reducing sample carryover.

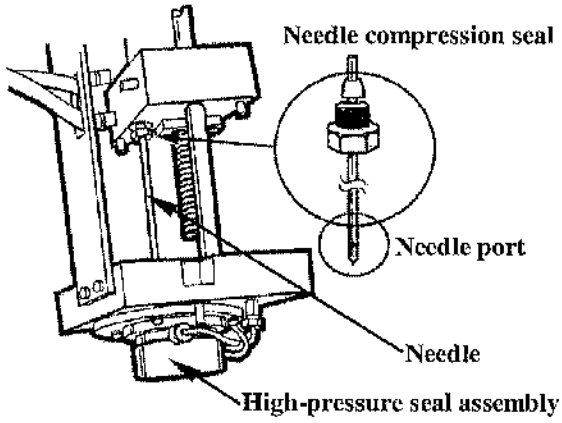

Fig. 46[104] The needle and high-pressure seal assembly.

The chromatographic separation of samples was achieved using a Reverse-Phase Supelcosil LC-ABZ+' HPLC column, purchased from Aldrich. The column temperature was not controlled and small variations in absolute retention times were therefore apparent. Results were normalised by running the standards of known concentration prior to every set of reaction samples. Reverse-phase chromatography uses a hydrophobic bonded packing and a polar mobile phase. As the hydrophobic character of solutes increase, retention times increase and so hydrocarbons are retained more strongly than alcohols. The driving force for retention is not the favourable interaction between solute and stationary phase; hydrocarbons are forced onto the stationary phase by changes in mobile-phase composition.

A variable wavelength, Thermo Separation Products, Spectra Series UV-2000 Ultraviolet-Visible spectrometer was used as the detector. A deuterium lamp produced continuous, intense UV radiation over the wavelength range 190-400 nm. The detection wavelength used was 262 nm, selected after obtaining the individual UV spectrum of phenol, 4,4'-biphenol, 2,2'-biphenol and 4-phenoxyphenol in acetonitrile. The optical system used in the UV-2000 detector (Figure 47) compares the signal from the reference photodiode with the signal from the sample photodiode.

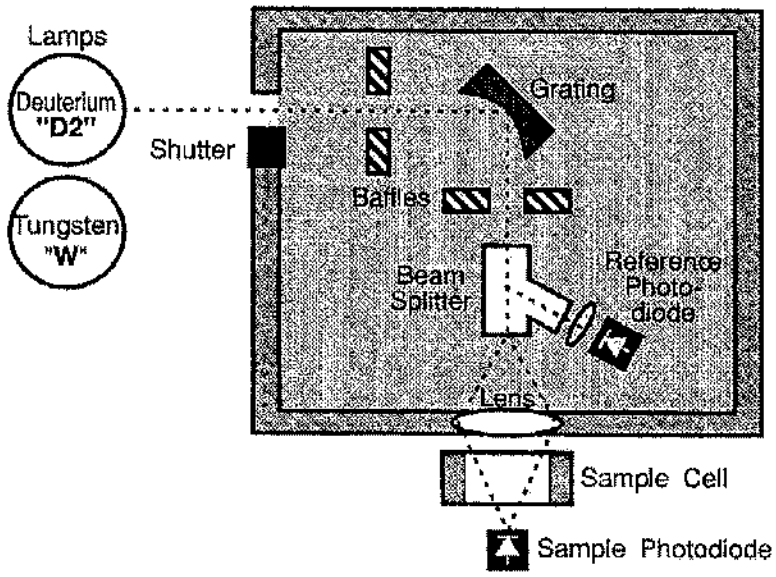

Fig. 47[105] The optical system for the UV2000 detector.

In summary,

- Mobile Phase: Solution A; 0.1% trifluoroacetic acid/H_2O
  Solution B; 0.1% trifluoroacetic acid/CH_3CN
- A flow rate of 1 ml min^{-1}
- Elution method: A/B = 60/40 (hold 0 min)
  ↓ 30 min
  A/B = 0/100 (hold 20 min)
- Injection volume: 5 µl
- Detection: UV 262 nm

The absorption of UV radiation by the separated solutes phenol, 4,4'-biphenol, 2,2'-biphenol and 4-phenoxyphenol obeys the Beer-Lambert law (Equation 2).

$A = \varepsilon c l$ where A = sample absorbance
ε = Molar Extinction Coefficient
l = flowcell path length
c = sample concentration

Therefore $A \propto c$

Absorbance was converted to a digital signal by the detector and sent to an integrator for processing. Using a series of standards, concentration was plotted against absorbance. Peak separation was good ensuring the Thermo Separation Products - Data Integrator accurately calculated the area under each peak.

The integrator settings used for analysis all reaction samples was,

- Attenuation: 512
- Chart Speed: 0.25
- Auto-zero at: 0.01 min

For the analysis of soluble coke after HF digestion of the support, attenuation was changed to 32.

2.5.2 Data analysis

Figures 48 to 51 are typical examples of the calibration graphs used to calculate the concentration of phenol, 4,4'-biphenol, 2,2'-biphenol and 4-phenoxyphenol in a reaction sample.

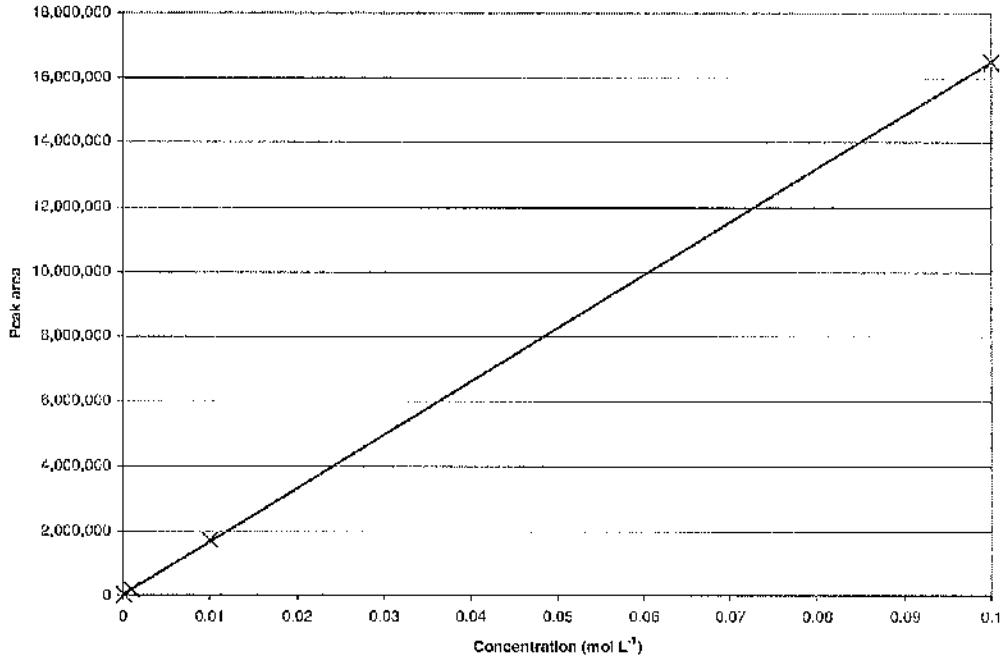

Fig. 48 Calibration graph for phenol.

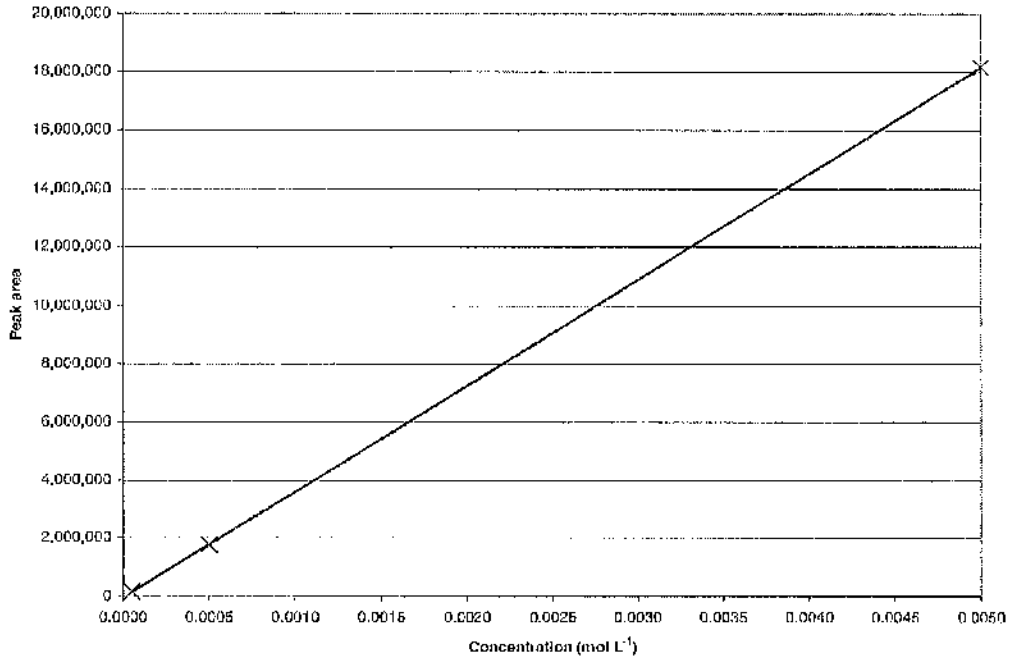

Fig. 49 Calibration graph for 4,4'-biphenol.

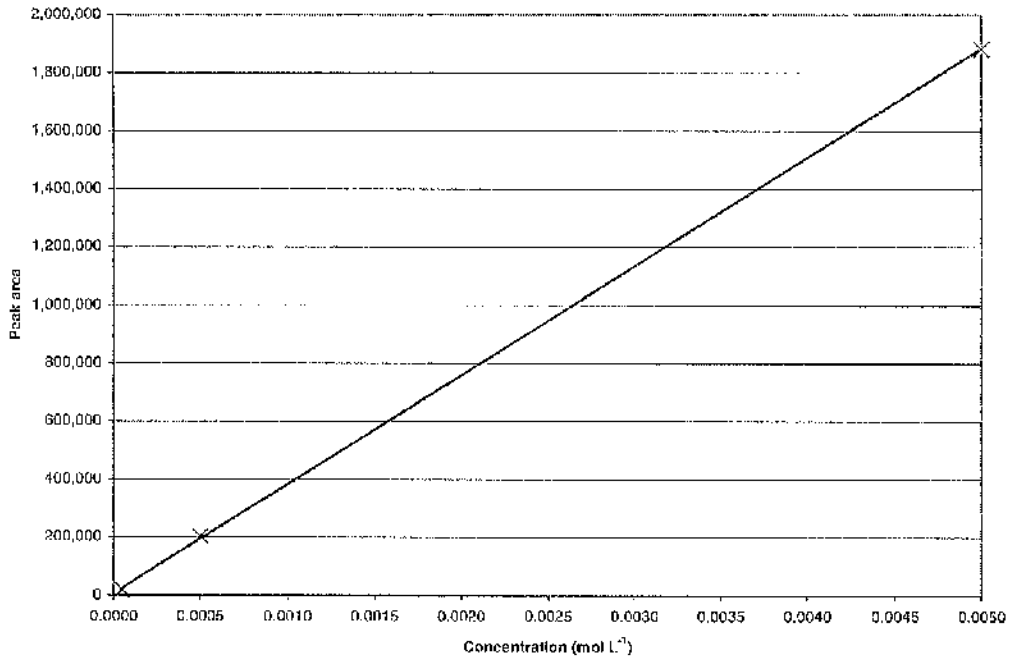

Fig. 50 Calibration graph for 2,2'-biphenol.

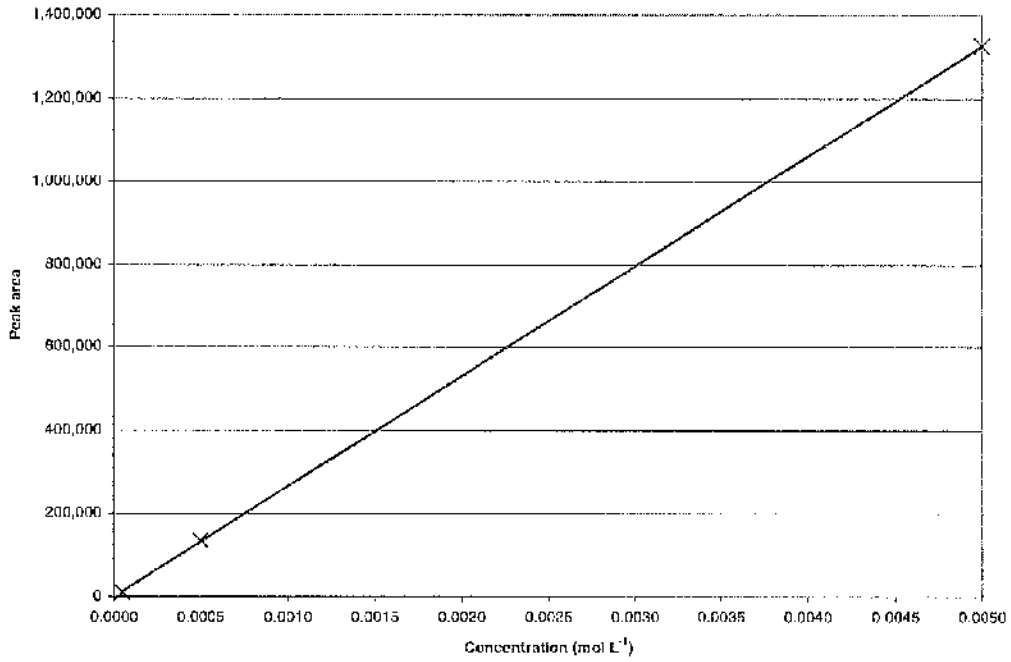

Fig. 51 Calibration graph for 4-phenoxyphenol.

The data used to plot these calibration graphs is reproduced in Tables 7 and 8.

Table 7 Phenol calibration standards.

Concentration (mol L^{-1})	Peak area
0.1	16489236
0.01	1724557
0.001	188688
0.0001	20933

Table 8 Calibration standards for 4,4'-biphenol, 2,2'-biphenol and 4-phenoxyphenol.

Concentration (mol L^{-1})	Peak area		
	4,4'-biphenol	2,2'-biphenol	4-phenoxyphenol
0.005	18158639	1883066	1325943
0.0005	1760452	201340	134356
0.00005	149720	17512	10491

The relative retention times of compounds confirmed their identity (Table 9).

Table 9 Compounds and their relative retention times.

Compound	*Retention time /min*
Phenol	6.6
4,4'-biphenol	8.6
2,2'-biphenol	11.4
4-phenoxyphenol	14.4

The HPLC analysis of reaction samples was capable of separating phenol, 4,4'-biphenol 2,2'-biphenol and 4-phenoxyphenol and other byproducts from the dimerisation of phenol. A typical integrator printout (Figure 52) had five of six other peaks between 6 and 15 min that were considered to be other dimers and trimers of phenol, some examples of which are given in Figure 53.

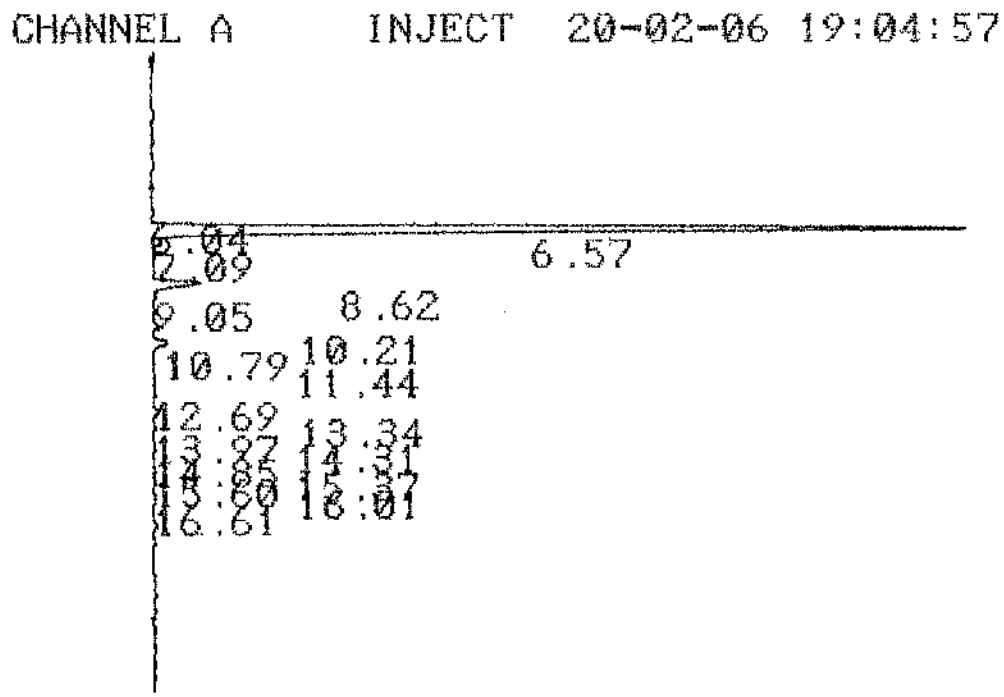

Fig. 52 A typical HPLC integrator printout during the dimerisation of phenol using Cu(6%)/Zeolite-Y.

Fig. 53 Dimers and trimers of phenol.

4,4'-biphenol

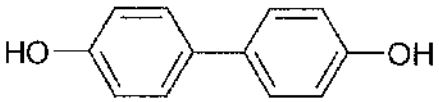

2,2'-biphenol

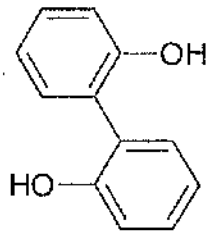

4-phenoxyphenol

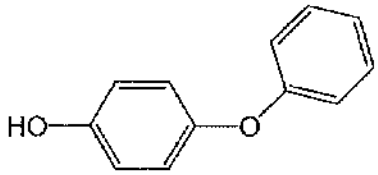

2,4'-Biphenol

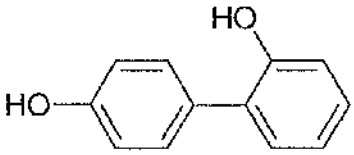

2-phenoxyphenol

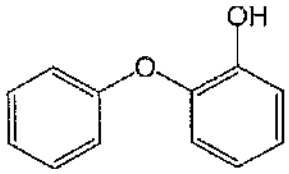

3-phenoxyphenol

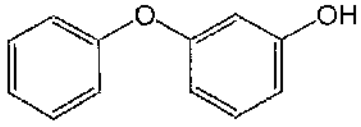

Examples of phenolic trimers.

1.

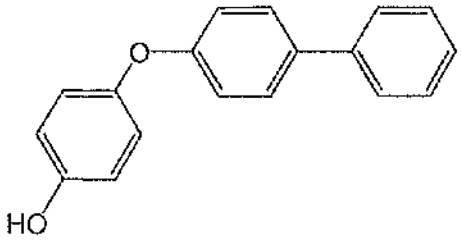

2.

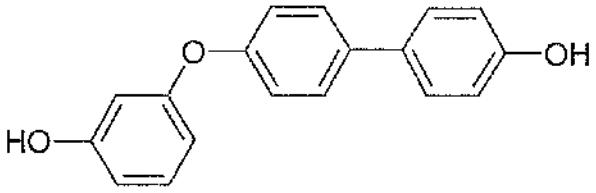

3.

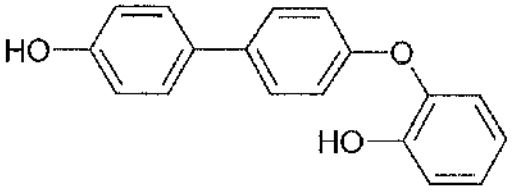

4.

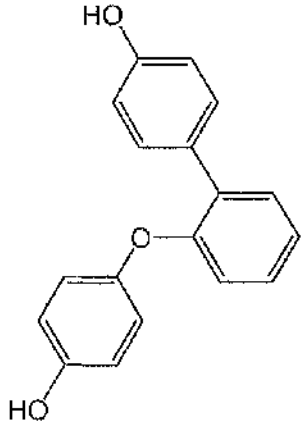

5.

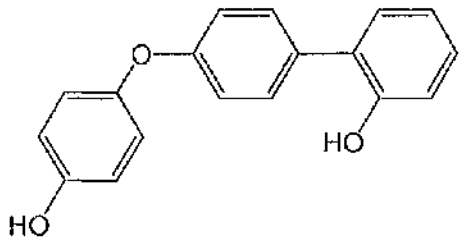

The individual peaks were not assigned to specific dimers or trimers although one trimer (Figure 54) was isolated by rotary evaporation and solid-phase distillation of a reaction sample[106]. NMR and Mass Spectrometry were then used to determine its structure.

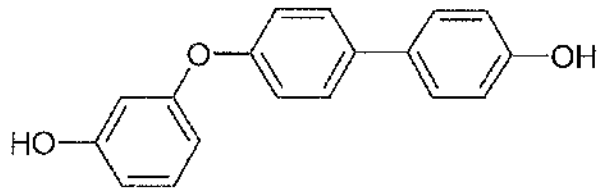

Fig. 54 Isolated trimer.

The retention time of this trimer was 7.2 min. Retention times between 6 and 15 min were therefore likely to be dimers and trimers of phenol but these compounds could not be purchased for calibration.

2.5.3 Presentation of data

For every experiment a results table was used to present the conversion of phenol data and selectivity to 4,4'-biphenol, 2,2'-biphenol and 4-phenoxyphenol. The yield of each dimer can be calculated by multiplying conversion with selectivity. The conversion of phenol was calculated using Equation 3.

$$\text{Conversion (\%)} = \left[\frac{\text{moles of phenol IN} - \text{moles of phenol OUT}}{\text{moles of phenol IN}} \right] \text{x } 100$$

Selectivity was calculated using Equation 4.

$$\text{Selectivity (\%)} = \left[\frac{\text{moles of dimer OUT x 2}}{\text{moles of phenol IN} - \text{moles of phenol OUT}} \right] \text{x } 100$$

Only data from the first cycle of chloroform solution and acetonitrile flush was shown for each experiment (Table 10). All data collected using an acetonitrile or mixed acetonitrile and chloroform solution was shown (Table 11). When conversion of phenol was less than 1% (<1) the accurate calculation of dimer selectivity was not possible. If 4,4'-biphenol, 2,2'-biphenol or 4-phenoxyphenol were detected at <1% phenol conversion the letter *t* was used to denote a *trace* amount.

Table 10 Cu(6%)/Zeolite-Y –chloroform.

Time (min)	Conversion (%)	Selectivity (%)		
		4,4'-biphenol	2,2'-biphenol	4-phenoxyphenol
0-5	22	t	0	t
5-10	17	t	0	t
10-15	12	t	0	2
15-30	6	t	0	1
30-45	6	t	0	2
45-50				
50-55	-	t	0	t
55-60	-	1	0	t

Table 11 Cu(6%)/Zeolite-Y –acetonitrile.

Time (min)	Conversion (%)	Selectivity (%)		
		4,4'-biphenol	2,2'-biphenol	4-phenoxyphenol
0-5	16	14	0	4
5-10	17	12	1	3
10-15	12	13	1	4
15-30	6	13	1	4
30-45	4	12	2	5
45-60	3	12	2	4
60-90	2	12	2	5

2.6 Detection and characterisation of coke

Removing the coke from the catalyst was necessary before characterisation was possible. Refluxing the catalyst using Soxhlet extraction with acetonitrile had failed to remove any soluble coke. HF digestion was therefore used to liberate both the soluble and non-soluble coke from the catalyst. After HF digestion the samples were centrifuged and the nitric acid solution removed. The solid was then dissolved in 20 ml of acetonitrile and a sample taken for HPLC analysis. A sample of the remaining insoluble coke was taken for Carbon/Hydrogen/Nitrogen (CHN) analysis.

2.7 Catalyst Regeneration

Both *in situ* and *ex situ* regeneration of catalyst activity was attempted. For the *in situ* regeneration, a standard reaction using an acetonitrile solution was run, after which flow was stopped and the reactor cooled to room temperature. Acetonitrile was pumped through the catalyst bed for 3 hours at a flow rate of 0.5 ml min^{-1}. Samples were taken and analysed by HPLC to confirm when the exit stream ran clear of phenol. The catalyst was dried at 348 K in a 100 ml min^{-1} flow of 2%O_2/Ar for 12 hours. Still *in situ* the catalyst was then heated to 773 K at 10° min^{-1} in a 100 ml min^{-1} flow of 2%O_2/Ar and calcined at 773 K for 5 hours. After cooling to 348 K, the gas flow was stopped and the acetonitrile solution fed to the reactor at 0.5 ml min^{-1} for 90 min with samples of the exit stream taken at regular intervals.

For the *ex situ* regeneration the catalyst was discharged from the reactor after flushing with acetonitrile and dried overnight at 348 K in air. The catalyst was placed in a tubular furnace and heated to 773 K at 10° min^{-1} in a 1 L min^{-1} flow of air and calcined at 773 K for 5 hours. After cooling the catalyst was removed from the furnace and exposed to atmosphere for 1 week before being reloaded into the reactor and the second, standard 90 min reaction performed.

3 Results

3.1 Phenol and biphenol adsorption studies

The adsorption of phenol, 4,4'-biphenol, 2,2'-biphenol and 4-phenoxyphenol was studied over a range of catalysts.

3.1.1 Adsorption of phenol

The liquid phase adsorption of phenol over Na, H and Cu(6%)/Zeolite-Y and Na, H and Cu(4%)/ZSM-5 was studied using a chloroform solution (Figure 55). The data for H/Zeolite-Y corresponds to the *secondary y-axis*.

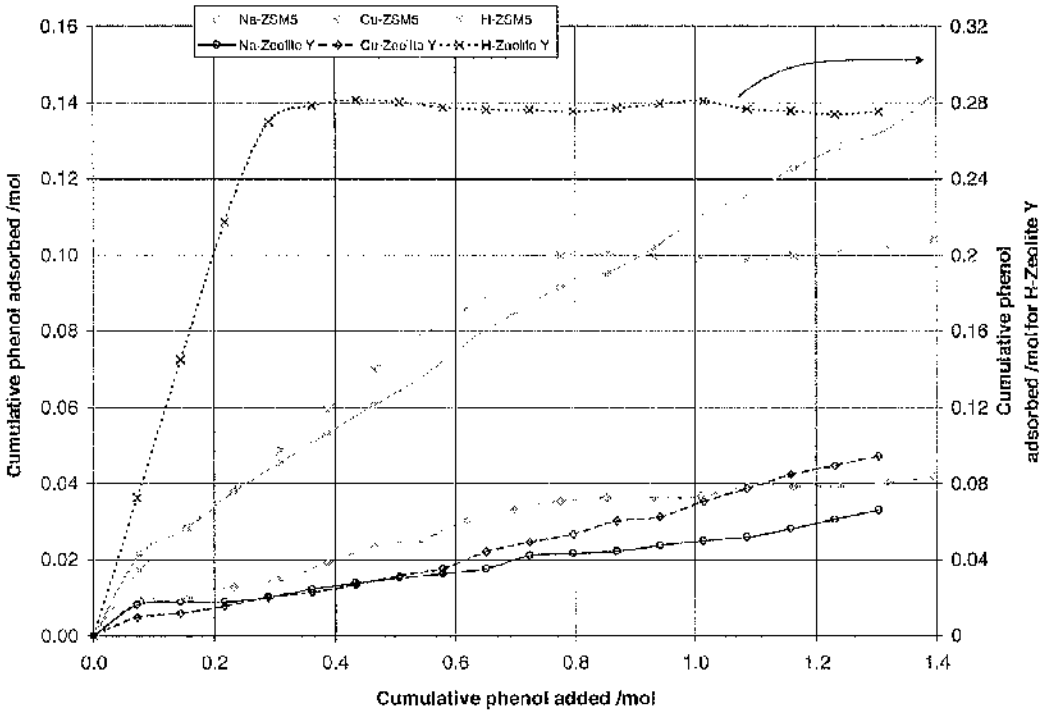

Fig. 55 Adsorption of phenol over Na, H and Cu(6%)/Zeolite-Y and Na, H and Cu(4%)/ZSM-5 using a 0.08 mol L^{-1} phenol in chloroform solution.

The catalyst H/Zeolite-Y adsorbed the most phenol, displaying a well-defined Type I adsorption isotherm. The adsorption corresponded to >6 mol of phenol per kilogram of catalyst which equated to ca. 100% occupation of the theoretical sites of positive charge or Cation Exchange Capacity (CEC). The Cu(6%)/Zeolite-Y catalyst only

adsorbed half the amount of phenol compared to H/Zeolite-Y and not much more than the Na/Zeolite-Y.

The liquid phase adsorption of phenol over Na, H and Cu(5%)/Attapulgite and Na, H and Cu(6%)/Montmorillonite (Figure 56) was also studied using the chloroform solution.

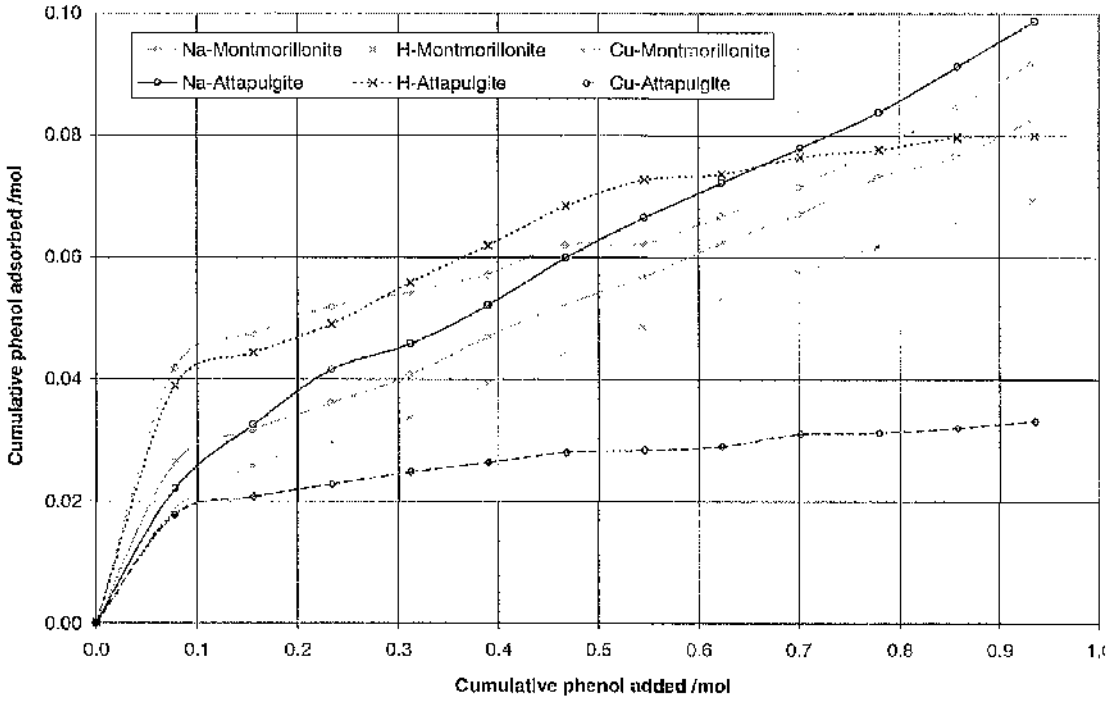

Fig. 56 Adsorption of phenol over Na, H and Cu(6%)/Montmorillonite and Na, H and Cu(5%)/Attapulgite using a 0.08 mol L^{-1} phenol in chloroform solution.

The adsorption isotherms were similar for all clay catalysts, except for Cu-Attapulgite that adsorbed less phenol than the other five catalysts.

The total amount of phenol adsorbed by the zeolite and clay catalysts was similar, at least within the same order of magnitude, with the exception of H/Zeolite-Y. The amount of phenol adsorbed by the clays corresponded to as many as fourteen phenol molecules per cation exchange site, or theoretical adsorption site. The H/Zeolite-Y

catalyst adsorbed more than twice the phenol adsorbed by the other zeolite catalysts. This equated to one phenol molecule per cation exchange site.

The concentration of phenol solution was intentionally kept constant at 0.08 mol L^{-1}. This meant that the ratio of phenol molecules to cation exchange sites in Zeolite-Y, ZSM-5, Montmorillonite and Attapulgite varied for each catalyst studied.

3.1.1.1 Phenol concentration

The adsorption of phenol over Cu(6%)/Zeolite-Y (Figure 57) and Cu(5%)/Attapulgite (Figure 58) was studied using three different concentrations of phenol solution. Despite the increased adsorption of phenol by H/Zeolite-Y (Section 3.1.1), the adsorption using different concentrations of phenol solution was studied using the copper exchanged zeolites and clays. In the literature it had been reported that Cu/MCM-41 was catalytically active in the liquid phase oxidation of 2,6-di-*tert*-butylphenol.[55, 62]

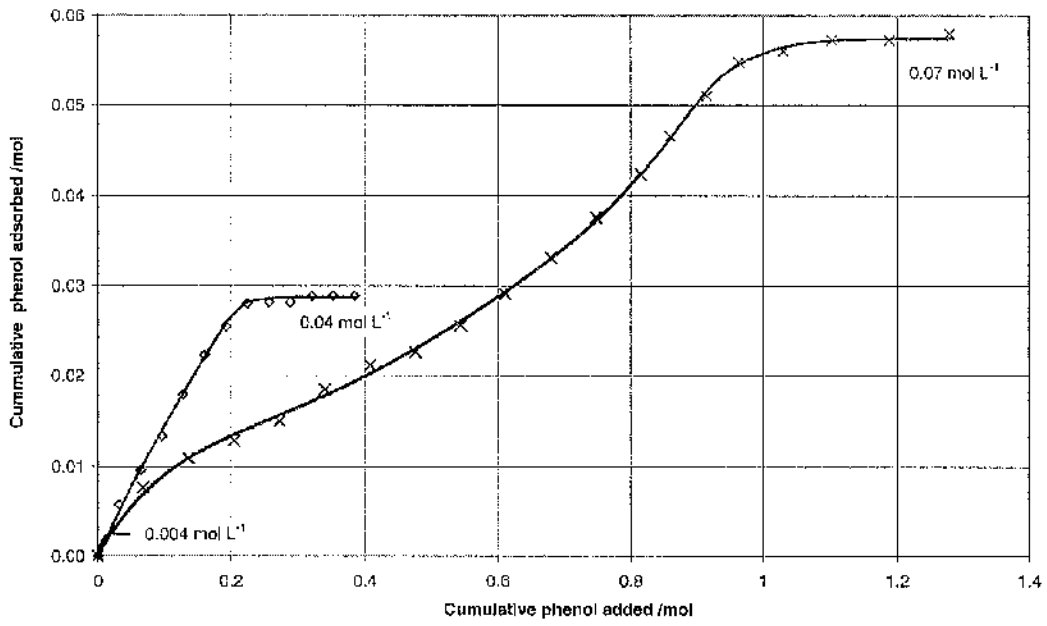

Fig. 57 Adsorption of phenol over Cu(6%)/Zeolite-Y using different concentrations of phenol in chloroform solution.

As the concentration of phenol was increased so also the total amount of phenol adsorbed by Cu(6%)/Zeolite-Y increased. The number of cation-exchange sites potentially occupied by phenol molecules has been calculated. At 0.004 mol L^{-1} only 2.1% of the total CEC could have been occupied, suggesting adsorption only at external sites. At 0.04 mol L^{-1} the coverage was 24.5% and at 0.07 mol L^{-1} it increased to 35.9%. A Type I adsorption isotherm is characteristic of a microporous material. The relatively low volume within the channels and pores means that only a monolayer of molecules can adsorb.

The adsorption of phenol at 0.004, 0.04 and 0.08 mol L^{-1} over Cu(5%)/Attapulgite was studied.

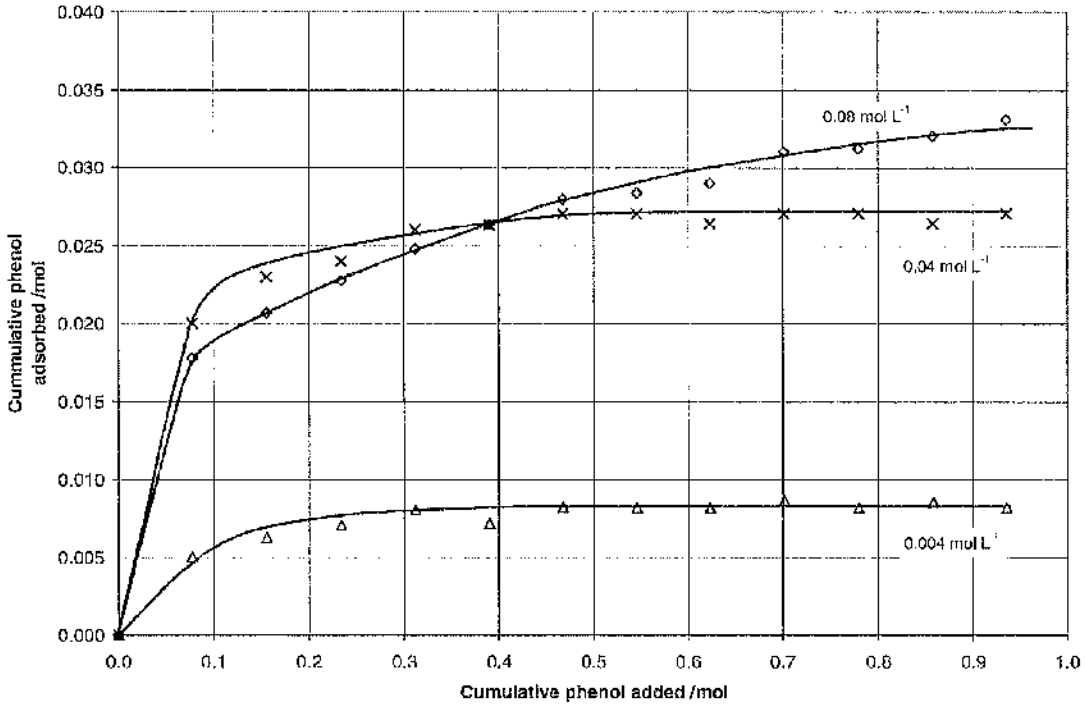

Fig. 58 Adsorption of phenol over Cu(5%)/Attapulgite using different concentrations of phenol in chloroform solution.

Adsorption at 0.04 mol L^{-1} displayed a well-defined Type I adsorption isotherm. Using the 0.08 mol L^{-1} solution the initial adsorption of phenol was reduced and then

recovered, suggesting continued adsorption. Using the 0.004 mol L^{-1} solution, adsorption was significantly less.

3.1.1.2 Adsorption from other solvents

Having established the small number of solvents ultimately suitable for the direct and oxidative polymerisation of phenol, the adsorption of phenol over of the zeolite and clay catalysts was studied using solutions of phenol in acetonitrile, chloroform and water. The solvent used affected the adsorption of phenol; indeed only chloroform could be used to study the adsorption of phenol over Cu(6%)/Zeolite-Y (Figure 59) and Cu(5%)/Attapulgite. These catalysts were chosen because of their potential catalytic activity (Section 3.1.1.1).

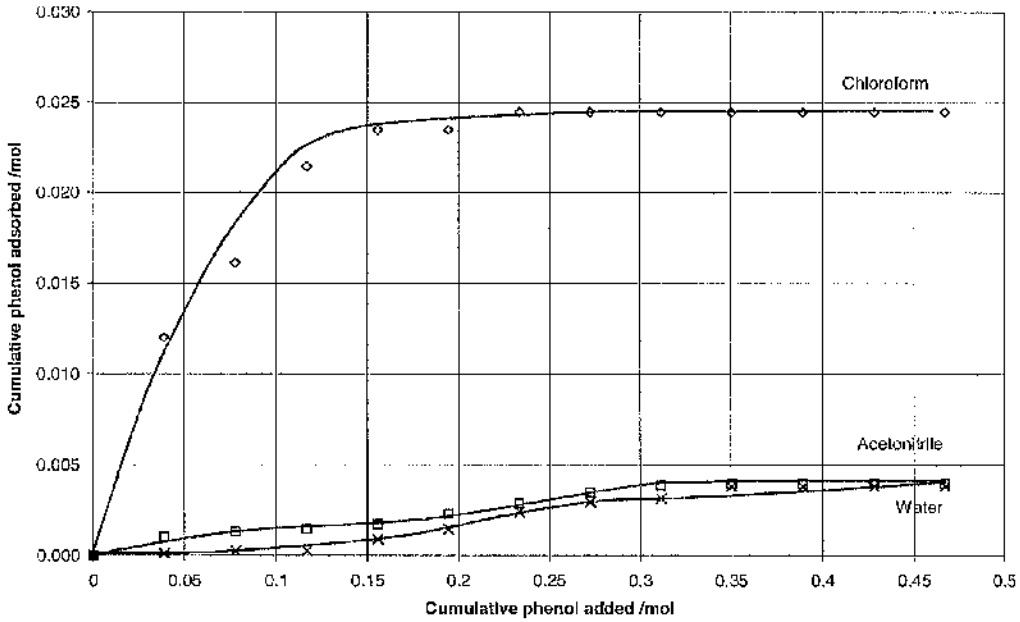

Fig. 59 Adsorption of phenol over Cu(6%)/Zeolite-Y using 0.04 mol L^{-1} solutions of phenol in chloroform, acetonitrile or water.

The adsorption of phenol over Cu(6%)/Zeolite-Y from chloroform was greater than that from the acetonitrile or water solution. The adsorption of phenol over Cu(5%)/Attapulgite could only be recorded using chloroform as the solvent. When acetonitrile and water solutions were used the pressure drop across the catalyst bed exceeded 100 bar g. It was not possible to operate the flooded bed reactor at these

pressures. To try and overcome this Cu(5%)/Attapulgite was first wetted with acetonitrile or water before being loaded into the reactor. A similar pressure drop was however observed when the flow of phenol was initiated.

3.1.2 Adsorption of 4,4'-biphenol

The adsorption of 4,4'-biphenol over Na, H and Cu/ZSM-5 and Na, H, and Cu/Zeolite-Y (Figure 60) was studied. An acetonitrile solution of 4,4'-biphenol was used because the solubility of 4,4'-biphenol in chloroform was poor.

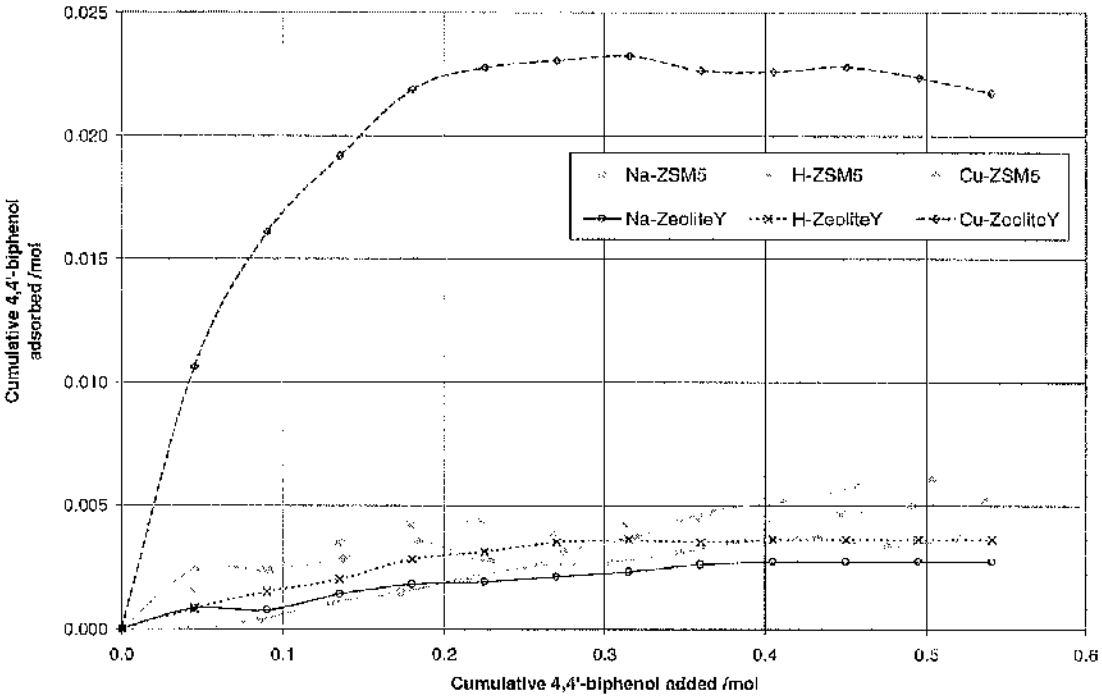

Fig. 60 Adsorption of a 0.04 mol L^{-1} 4,4'-biphenol solution in acetonitrile.

The adsorption of 4,4'-biphenol over Cu(6%)/Zeolite-Y was five times greater than the adsorption over the other Na, H and Cu exchanged zeolites. A well-defined Type I adsorption isotherm was observed. The adsorption of 4,4'-biphenol was compared to the adsorption of phenol over Cu(6%)/Zeolite-Y (Figure 61).

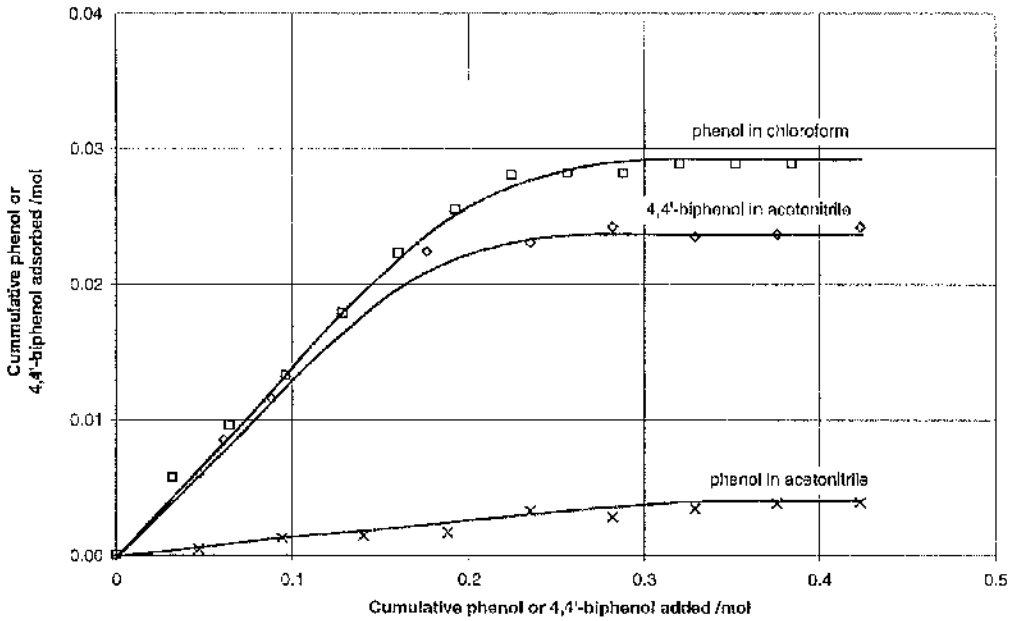

Fig. 61 Adsorption of phenol and 4,4'-biphenol over Cu(6%)/Zeolite-Y using 0.04 mol L^{-1} solutions.

The adsorption of phenol from the acetonitrile solution over Cu(6%)/Zeolite-Y was five times less compared to the adsorption from the chloroform solution. The adsorption of 4,4'-biphenol from acetonitrile was much greater than the adsorption of phenol from acetonitrile.

The adsorption of 4,4'-biphenol over Cu(5%)/Attapulgite was studied using a chloroform solution. The literature had reported copper exchanged clays as catalytically active for aniline alkylation[15] and copper exchanged zeolites were known to be catalytically active in the liquid phase oxidation of 2,6-di-*tert*-butylphenol.[55, 62] A solution of 4,4'-biphenol in chloroform was used because it had been established that acetonitrile solutions would not flow through clay catalysts. The maximum obtainable concentration of 4,4'-biphenol in chloroform was 0.004 mol L^{-1}. The adsorption of 4,4'-biphenol from chloroform has been compared to the absorption of phenol from chloroform over Cu(5%)/Attapulgite (Figure 62).

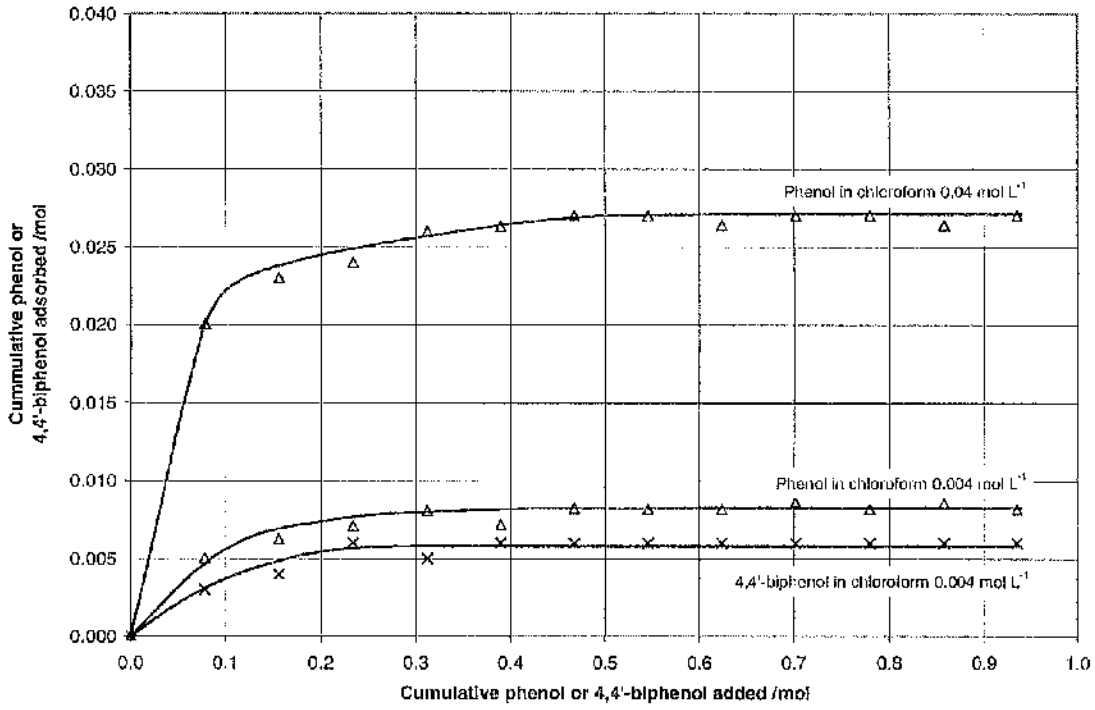

Fig. 62 Adsorption of phenol and 4,4'-biphenol over Cu(5%)/Attapulgite.

The adsorption of phenol from the 0.004 mol L^{-1} chloroform solution was greater than the adsorption of 4,4'-biphenol from the 0.004 mol L^{-1} chloroform solution.

3.1.3 Comparison of 4,4'-biphenol, 2,2'-biphenol and 4-phenoxyphenol

The adsorption of 4,4'-biphenol, 2,2'-biphenol and 4-phenoxyphenol over Cu(6%)/Zeolite-Y (Figure 63) was compared.

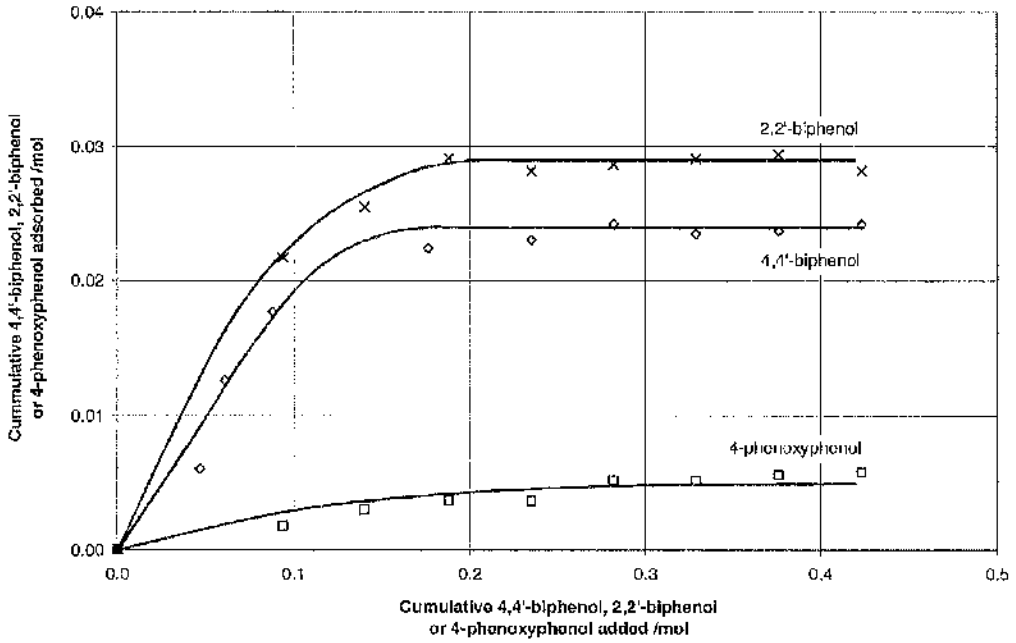

Fig. 63 Adsorption of 4,4'-biphenol, 2,2'-biphenol or 4-phenoxyphenol over Cu(6%)/Zeolite-Y using 0.04 mol L^{-1} acetonitrile solutions.

The adsorption of all three phenolic dimers from an acetonitrile solution followed a Type I adsorption isotherm. The adsorption of 4-phenoxyphenol was least, the adsorption of 2,2'-biphenol was greatest.

The adsorption of 4,4'-biphenol, 2,2'-biphenol and 4-phenoxyphenol over Cu(5%)/Attapulgite (Figure 64) was compared.

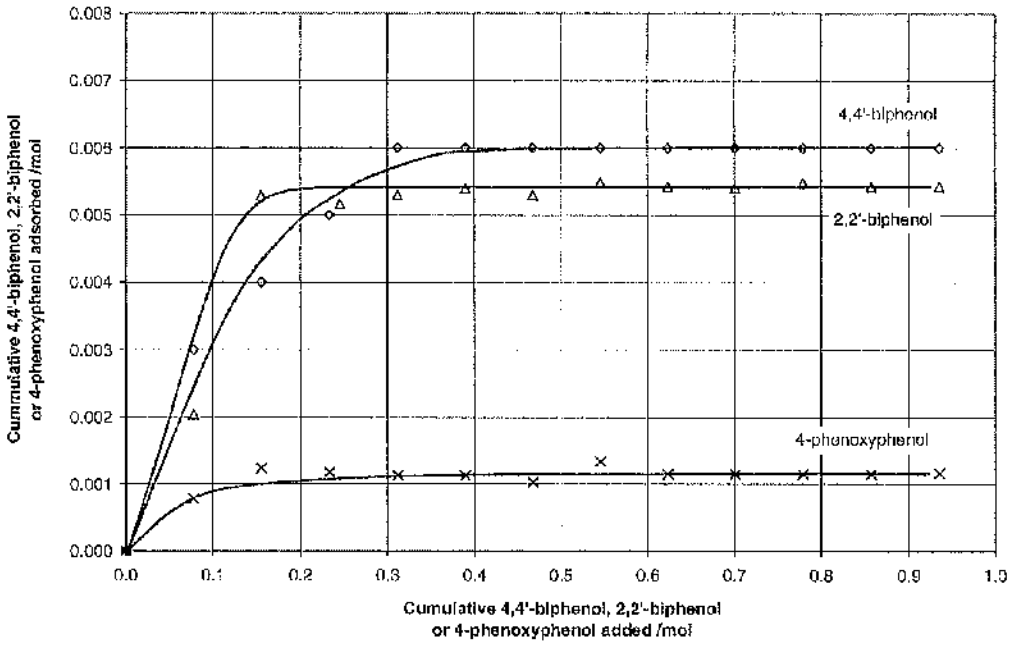

Fig. 64 Adsorption of 4,4'-biphenol, 2,2'-biphenol or 4-phenoxyphenol over Cu(5%)/Attapulgite using 0.004 mol L^{-1} chloroform solutions.

The adsorption of 4,4'-biphenol and 2,2'-biphenol from a chloroform solution was similar. The adsorption of 4-phenoxyphenol was five times less.

3.2 Gibbs free energy of phenol dimerisation

Published entropy values (S°) for 4,4'-biphenol, 2,2'-biphenol and 4-phenoxyphenol were not available. Values were therefore estimated from the known entropy values for phenol and biphenyl. The Gibbs free energies ($\Delta G°$) of phenol dimerisation to 4,4'-biphenol and 2,2'-biphenol were calculated using the molar enthalpies of formation reported by Verevkin.[107] The effect of temperature on entropy was not accounted for.

3.2.1 Phenol to 4,4'-biphenol

Assuming the value of S° for 4,4'-biphenol was 150 $JK^{-1}mol^{-1}$

(From the entropy value of phenol: 146 $JK^{-1}mol^{-1}$)

For direct dehydrogenation

$\Delta H_f°_{total}$ = 9.7 $kJmol^{-1}$ endothermic

$\Delta G°$ = 13.07 $kJmol^{-1}$ and $K = 5.1 \times 10^{-3}$ at 298K

$\Delta G°$ = 17.32 $kJmol^{-1}$ and $K = 4.5 \times 10^{-2}$ at 673K

For oxidative dehydrogenation

$\Delta H_f°_{total}$ = -525.3 $kJmol^{-1}$ exothermic

$\Delta G°$ = -455.82 $kJmol^{-1}$ and $K = 8.0 \times 10^{79}$ at 298K

$\Delta G°$ = -368.39 $kJmol^{-1}$ and $K = 3.9 \times 10^{28}$ at 673K

Assuming the value of $\Delta S°$ for 4,4'-biphenol was 200 $JK^{-1}mol^{-1}$

(From the entropy value of biphenyl: 209 $JK^{-1}mol^{-1}$)

For direct dehydrogenation

$\Delta H_f°_{total}$ = 9.7 $kJmol^{-1}$ endothermic

$\Delta G°$ = -1.83 $kJmol^{-1}$ and $K = 2.1 \times 10^{0}$ at 298K

$\Delta G°$ = -16.33 $kJmol^{-1}$ and $K = 1.9 \times 10^{1}$ at 673K

For oxidative dehydrogenation

$\Delta H_f°_{total}$ = -525.3 $kJmol^{-1}$ exothermic

$\Delta G°$ = -470.72 $kJmol^{-1}$ and $K = 3.3 \times 10^{82}$ at 298K

$\Delta G°$ = -402.04 $kJmol^{-1}$ and $K = 1.6 \times 10^{31}$ at 673K

3.2.2 Phenol to 2,2'-biphenol

Assuming the value of S° for 2,2'-biphenol was 150 $JK^{-1}mol^{-1}$

(From the entropy value of phenol: 146 $JK^{-1}mol^{-1}$)

For direct dehydrogenation

$\Delta H_f^\circ{}_{total}$ = 36.1 $kJmol^{-1}$ endothermic

ΔG° = 39.47 $kJmol^{-1}$ and $K = 1.2 \times 10^{-7}$ at 298K

ΔG° = 43.72 $kJmol^{-1}$ and $K = 4.0 \times 10^{-4}$ at 673K

For oxidative dehydrogenation

$\Delta H_f^\circ{}_{total}$ = -498.9 $kJmol^{-1}$ exothermic

ΔG° = -429.42 $kJmol^{-1}$ and $K = 1.9 \times 10^{75}$ at 298K

ΔG° = -341.99 $kJmol^{-1}$ and $K = 3.5 \times 10^{26}$ at 673K

Assuming the value of ΔS° for 2,2'-biphenol was 200 $JK^{-1}mol^{-1}$

(From the entropy value of biphenyl: 209 $JK^{-1}mol^{-1}$)

For direct dehydrogenation

$\Delta H_f^\circ{}_{total}$ = 36.1 $kJmol^{-1}$ endothermic

ΔG° = 24.57 $kJmol^{-1}$ and $K = 4.9 \times 10^{-5}$ at 298K

ΔG° = 10.07 $kJmol^{-1}$ and $K = 3.7 \times 10^{-3}$ at 673K

For oxidative dehydrogenation

$\Delta H_f^\circ{}_{total}$ = -498.9 $kJmol^{-1}$ exothermic

ΔG° = -444.32 $kJmol^{-1}$ and $K = 7.7 \times 10^{77}$ at 298K

ΔG° = -375.64 $kJmol^{-1}$ and $K = 1.4 \times 10^{29}$ at 673K

Unfortunately the molar enthalpies of formation for 4-phenoxyphenol have not been published. From the calculated values of Gibbs free energy (ΔG°) and the equilibrium constant (K) for 4,4'-biphenol and 2,2'-biphenol formation, only the oxidative dehydrogenation route is viable at either 298 or 673K. The larger the equilibrium constant the further to the right the position of equilibrium and the more products formed.

3.3 Dimerisation of phenol using zeolite catalysts

3.3.1 Chloroform solution

It was reported in Section 3.1.1.2 that the adsorption of phenol from chloroform over Cu(6%)/Zeolite-Y was greater than from an acetonitrile or water solution. The adsorption of phenol over Cu(5%)/Attapulgite could only be recorded using chloroform as the solvent. Copper exchanged zeolites were known to be catalytically active in the liquid phase oxidation of 2,6-di-*tert*-butylphenol using chloroform as the reaction solvent.[55, 62] Chloroform was therefore used as the solvent for phenol dimerisation to 4,4'-biphenol, 2,2'-biphenol and 4-phenoxyphenol. The poor solubility of 4,4'-biphenol in chloroform was recognised and so to encourage the removal of the dimer from the catalyst, the system was periodically flushed with acetonitrile.

Often only trace (*t*) amounts of 4,4'-biphenol, 2,2'-biphenol and 4-phenoxyphenol were detected from the dimerisation of phenol using a chloroform solution. Although chloroform would therefore not be the best solvent for industrial scale dimerisation of phenol, valuable data was obtained. Changing experimental conditions often altered the conversion of phenol and selectivity to one or more of the three dimers. The ability to tailor selectivity is a useful tool in industry and the data obtained has helped to develop a better understanding of the reaction mechanisms involved.

3.3.1.1 Na, H, Cu, Ag and Ni/Zeolite-Y

The catalytic activity of Na, H, Cu(6%), Ag(18%) and Ni(5%)/Zeolite-Y was investigated (Tables 12-16).

Table 12 Na/Zeolite-Y

Time (min)	Conversion (%)	Selectivity (%)		
		4,4'-biphenol	2,2'-biphenol	4-phenoxyphenol
0-5	26	t	0	0
5-10	25	t	t	0
10-15	26	0	t	0
15-30	26	t	0	0
30-45	24	t	0	0
45-50				
50-55	-	t	t	0
55-60	-	t	0	0

Table 13 H/Zeolite-Y

Time (min)	Conversion (%)	Selectivity (%)		
		4,4'-biphenol	2,2'-biphenol	4-phenoxyphenol
0-5	50	0	0	0
5-10	19	0	0	0
10-15	15	0	0	0
15-30	9	0	0	0
30-45	5	0	0	0
45-50				
50-55	-	0	0	0
55-60	-	0	0	0

Table 14 Cu(6%)/Zeolite-Y

Time (min)	Conversion (%)	Selectivity (%)		
		4,4'-biphenol	2,2'-biphenol	4-phenoxyphenol
0-5	22	t	0	t
5-10	17	t	0	t
10-15	12	t	0	2
15-30	6	t	0	1
30-45	6	t	0	2
45-50				
50-55	-	t	0	t
55-60	-	1	0	t

Table 15 Ag(18%)/Zeolite-Y

Time (min)	Conversion (%)	Selectivity (%)		
		4,4'-biphenol	2,2'-biphenol	4-phenoxyphenol
0-5	37	t	t	t
5-10	50	t	t	t
10-15	55	0	t	t
15-30	48	0	t	0
30-45	28	0	t	0
45-50				
50-55	-	t	t	t
55-60	-	t	0	0

Table 16 Ni(5%)/Zeolite-Y

Time (min)	Conversion (%)	Selectivity (%)		
		4,4'-biphenol	2,2'-biphenol	4-phenoxyphenol
0-5	100	0	0	0
5-10	100	0	0	0
10-15	100	0	t	0
15-30	70	0	t	0
30-45	30	0	t	0
45-50				
50-55	-	0	t	0
55-60	-	0	0	0

The conversion of phenol was affected by the cation-exchanged metal. Copper exchanged Zeolite-Y afforded the lowest conversion of phenol, sodium, hydrogen and silver were progressively more active whilst nickel exchanged Zeolite-Y catalysed 100% conversion of phenol between 0 and 15 min. The conversion of phenol to 4,4'-biphenol, 2,2'-biphenol and 4-phenoxyphenol was low regardless of the predominant cation present. The literature[55, 62] identified copper exchanged zeolites as active catalysts for the coupling of 2,6-di-*tert*-butylphenol. Nickel and silver exchanged Zeolite-Y catalysts were prepared and tested since these metals are in the same period or group respectively as copper and therefore have similar chemical properties.

Despite the often high conversion of phenol, only trace amounts of 4,4'-biphenol, 2,2'-biphenol or 4-phenoxyphenol were detected using any five of the catalysts studied. The reaction conditions were therefore varied in order that the conversion of phenol to 4,4'-biphenol, 2,2'-biphenol or 4-phenoxyphenol might be improved. Despite moderate conversion of phenol, the selectivity to dimers was higher for Cu(6%)/Zeolite-Y compared to the other catalysts and the activity of Cu(6%)/Zeolite-Y was regenerated after each acetonitrile flush. Each cycle of phenol in chloroform and acetonitrile flush yielded a similar phenol conversion.

3.3.1.2 Na, H and Cu/ZSM-5

The catalytic activity of Na, H and Cu(4%)/ZSM-5 was investigated (Tables 17-19). The ZSM-5 zeolite consists of a two-dimensional array of pores each with a 10-membered ring aperture.

Table 17 Na/ZSM-5

Time (min)	Conversion (%)	Selectivity (%)		
		4,4'-biphenol	2,2'-biphenol	4-phenoxyphenol
0-5	11	t	0	0
5-10	4	t	0	0
10-15	1	0	0	0
15-30	1	0	0	0
30-45	1	0	0	0
45-50				
50-55	-	t	t	0
55-60	-	0	0	0

Table 18 H/ZSM-5

Time (min)	Conversion (%)	Selectivity (%)		
		4,4'-biphenol	2,2'-biphenol	4-phenoxyphenol
0-5	14	0	0	0
5-10	15	t	t	0
10-15	14	t	0	0
15-30	12	t	0	0
30-45	10	0	0	0
45-50				
50-55	-	0	0	0
55-60	-	0	0	0

Table 19 Cu(4%)/ZSM-5

Time (min)	Conversion (%)	Selectivity (%)		
		4,4'-biphenol	2,2'-biphenol	4-phenoxyphenol
0-5	40	t	t	3
5-10	23	t	t	4
10-15	17	t	t	2
15-30	8	0	t	1
30-45	6	0	t	t
45-50				
50-55	-	t	t	t
55-60	-	0	0	0

For ZSM-5 as Zeolite-Y supported catalysts, the conversion of phenol to 4,4'-biphenol, 2,2'-biphenol or 4-phenoxyphenol was low. The activity of copper exchanged ZSM-5 was slightly better than the sodium or hydrogen forms. The coupling selectivity to 4-phenoxyphenol from phenol using Cu/ZSM-5 was between 1 and 4%. This activity was not regenerated after the acetonitrile flush unlike for Cu/Zeolite-Y for which each cycle of phenol in chloroform and acetonitrile flush yielded a similar phenol conversion. For this reason the activity and selectivity of Cu/Zeolite-Y and not Cu/ZSM-5 was further investigated.

3.3.1.3 Metal loading

Data was collected using Cu/Zeolite-Y with w/w metal loadings of 1, 5, 6 and 8% (Tables 20-23).

Table 20 Cu(1%)/Zeolite-Y

Time (min)	Conversion (%)	Selectivity (%)		
		4,4'-biphenol	2,2'-biphenol	4-phenoxyphenol
0-5	9	t	0	1
5-10	3	t	0	5
10-15	2	t	0	7
15-30	2	t	0	8
30-45	2	t	0	4
45-50				
50-55	-	t	t	t
55-60	-	t	0	t

Table 21 Cu(5%)/Zeolite-Y

Time (min)	Conversion (%)	Selectivity (%)		
		4,4'-biphenol	2,2'-biphenol	4-phenoxyphenol
0-5	22	t	0	t
5-10	16	t	0	1
10-15	11	t	0	1
15-30	4	t	0	2
30-45	4	t	1	3
45-50				
50-55	-	t	t	1
55-60	-	1	t	1

Table 22 Cu(6%)/Zeolite-Y

Time (min)	Conversion (%)	Selectivity (%)		
		4,4'-biphenol	2,2'-biphenol	4-phenoxyphenol
0-5	22	t	0	t
5-10	17	t	0	t
10-15	12	t	0	2
15-30	6	t	0	1
30-45	6	t	0	2
45-50				
50-55	-	t	0	t
55-60	-	1	0	t

Table 23 Cu(8%)/Zeolite-Y

Time (min)	Conversion (%)	Selectivity (%)		
		4,4'-biphenol	2,2'-biphenol	4-phenoxyphenol
0-5	23	0	0	t
5-10	16	t	0	2
10-15	16	t	0	1
15-30	11	t	0	1
30-45	12	t	t	1
45-50				
50-55	-	t	t	t
55-60	-	1	t	t

As metal loading was increased the conversion of phenol also increased. The increase in phenol conversion with metal loading was not linear (Figure 65). The 5, 6 and 8% copper loaded catalysts all had similar deactivation profiles which were almost linear between 0 and 30 min. The Cu(1%)/Zeolite-Y catalyst was different and conversion was maintained at 2% after 10 min of reaction.

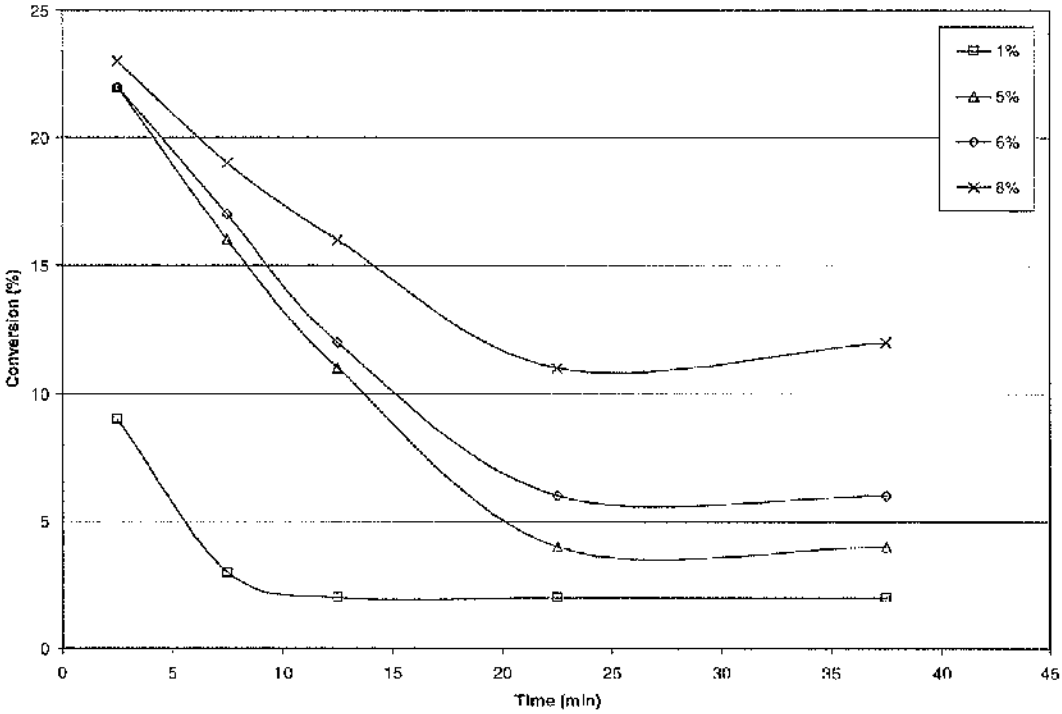

Fig. 65 Conversion of phenol using Cu/Zeolite-Y with different w/w metal loadings.

The selectivity towards 4-phenoxyphenol decreased as metal loading was increased whilst conversion of phenol to 4,4'-biphenol and 2,2'-biphenol was detected only in trace amounts.

3.3.1.4 Temperature

Data was collected at 308, 328, 348, 388 and 408 K using Cu(6%)/Zeolite-Y (Tables 24-28).

Table 24 308 K

Time (min)	Conversion (%)	Selectivity (%)		
		4,4'-biphenol	2,2'-biphenol	4-phenoxyphenol
0-5	1	1	0	15
5-10	1	1	0	24
10-15	3	t	0	6
15-30	7	t	0	2
30-45	10	0	0	1
45-50				
50-55	-	t	0	t
55-60	-	t	0	t

Table 25 328 K

Time (min)	Conversion (%)	Selectivity (%)		
		4,4'-biphenol	2,2'-biphenol	4-phenoxyphenol
0-5	10	t	0	1
5-10	7	t	0	2
10-15	6	0	0	4
15-30	6	t	0	2
30-45	5	t	0	2
45-50				
50-55	-	t	0	t
55-60	-	1	0	t

Table 26 348 K

Time (min)	Conversion (%)	Selectivity (%)		
		4,4'-biphenol	2,2'-biphenol	4-phenoxyphenol
0-5	22	t	0	t
5-10	17	t	0	t
10-15	12	t	0	2
15-30	6	t	0	1
30-45	7	t	0	2
45-50				
50-55	-	t	0	t
55-60	-	1	0	t

Table 27 388 K

Time (min)	Conversion (%)	Selectivity (%)		
		4,4'-biphenol	2,2'-biphenol	4-phenoxyphenol
0-5	12	1	0	4
5-10	25	t	0	2
10-15	16	t	t	3
15-30	8	t	1	3
30-45	6	t	1	0
45-50				
50-55	-	t	t	t
55-60	-	t	t	t

Table 28 408 K

Time (min)	Conversion (%)	Selectivity (%)		
		4,4'-biphenol	2,2'-biphenol	4-phenoxyphenol
0-5	7	t	0	3
5-10	22	t	1	2
10-15	27	0	t	2
15-30	22	t	t	1
30-45	21	t	t	1
45-50				
50-55	-	t	t	t
55-60	-	t	t	t

The effect of temperature on the conversion of phenol was complex. Plotting conversion of phenol against time for the five reaction temperatures, 308, 328, 348, 388 and 408 K helped identify three important trends (Figure 66). Uniquely, the conversion of phenol at 308 K systematically increased with Time On Stream (TOS), with no indication of deactivation. An initial period of activation was observed at 388 and 408 K that preceded the maximum conversion of phenol between 5 and 20 min. Conversion then decreased and deactivation was prominent. At 328 and 348 K the conversion of phenol decreased with TOS reaching steady state at ca. 6% conversion. This behaviour was repeated after each acetonitrile flush.

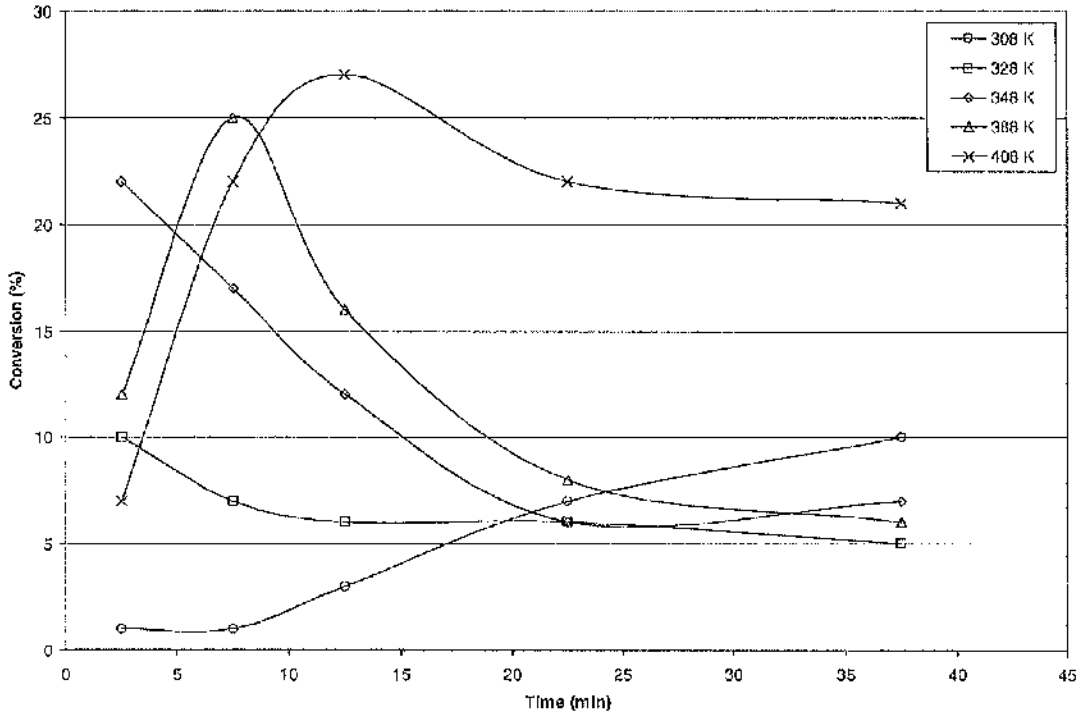

Fig. 66 Conversion of phenol against time at 308, 328, 348, 388 and 408 K.

The concentration of phenol, flow rates and therefore residence time and Weight Hourly Space Velocity (WHSV) remained constant at each temperature. There was no detectable change in selectivity to 4,4'-biphenol with temperature. The conversion of phenol to 2,2'-biphenol was however only detected at 388 and 408K. The selectivity toward 4-phenoxyphenol was greater than to either 2,2'-biphenol or 4,4'-biphenol. Selectivity remained ≤4% throughout the reactions at 328, 348, 388 and 408 K. At 308 K conversion of phenol to 4-phenoxyphenol was greatly improved. The maximum selectivity recorded was 24% between 5 and 10 min, this reduced to 6% between 10 and 15 mins and selectivity was <4% after 15 min.

3.3.1.5 Phenol concentration

Data was collected using 0.02, 0.04, 0.08, 0.16 and 0.32 mol L^{-1} solutions over Cu(6%)/Zeolite-Y (Tables 29-33).

Table 29 0.02 mol L^{-1}

Time (min)	Conversion (%)	Selectivity (%)		
		4,4'-biphenol	2,2'-biphenol	4-phenoxyphenol
0-5	43	t	0	t
5-10	37	t	0	t
10-15	37	t	0	t
15-30	30	t	0	t
30-45	26	t	0	t
45-50				
50-55	-	t	0	0
55-60	-	t	0	t

Table 30 0.04 mol L^{-1}

Time (min)	Conversion (%)	Selectivity (%)		
		4,4'-biphenol	2,2'-biphenol	4-phenoxyphenol
0-5	22	t	0	t
5-10	17	t	0	t
10-15	12	t	0	2
15-30	6	t	0	1
30-45	6	t	0	2
45-50				
50-55	-	t	0	t
55-60	-	1	0	t

Table 31 0.08 mol L^{-1}

Time (min)	Conversion (%)	Selectivity (%)		
		4,4'-biphenol	2,2'-biphenol	4-phenoxyphenol
0-5	53	t	1	t
5-10	28	t	2	t
10-15	15	t	3	t
15-30	6	t	5	t
30-45	<1	2	t	t
45-50				
50-55	-	t	1	t
55-60	-	t	1	t

Table 32 0.16 mol L^{-1}

Time (min)	Conversion (%)	Selectivity (%)		
		4,4'-biphenol	2,2'-biphenol	4-phenoxyphenol
0-5	26	t	1	1
5-10	27	t	5	1
10-15	19	t	3	1
15-30	13	t	4	t
30-45	8	t	4	t
45-50				
50-55	-	t	t	t
55-60	-	t	t	t

Table 33 0.32 mol L^{-1}

Time (min)	Conversion (%)	Selectivity (%)		
		4,4'-biphenol	2,2'-biphenol	4-phenoxyphenol
0-5	13	t	5	t
5-10	14	t	6	t
10-15	9	t	9	t
15-30	6	t	10	t
30-45	5	t	8	t
45-50				
50-55	-	t	t	t
55-60	-	t	t	t

There was no clear trend between phenol conversion and the concentration of phenol solution. At 0.08 mol L^{-1} the initial conversion was >50% which was followed by rapid catalyst deactivation resulting in a conversion of <1% within 45 min. At the other phenol concentrations conversion remained ≥5% at 45 min. Using the 0.02 mol L^{-1} solution conversion was only reduced by 17% from 43 to 26% after 45 min.

The selectivity to 4,4'-biphenol remained at *trace* levels regardless of phenol concentration. Selectivity to 4-phenoxyphenol was also largely unaffected by the concentration of phenol in chloroform solution. The selectivity to 2,2'-biphenol was notably dependent on phenol concentration. No 2,2'-biphenol was detected using 0.02 or 0.04 mol L^{-1} chloroform solution. At 0.08 mol L^{-1} 2,2'-biphenol was detected above trace amounts and selectivity then increased with concentration. The maximum selectivity recorded was 10% using the 0.32 mol L^{-1} phenol in chloroform solution.

3.3.1.6 Low temperature pre-treatment

Data was collected after the low temperature pre-treatment of Cu(6%)/Zeolite-Y in air, an oxygen rich and oxygen deficient atmosphere (Tables 34-36).

Table 34 Low temperature pre-treatment, air atmosphere.

Time (min)	Conversion (%)	Selectivity (%)		
		4,4'-biphenol	2,2'-biphenol	4-phenoxyphenol
0-5	45	0	0	0
5-10	24	t	0	0
10-15	23	t	0	t
15-30	23	0	1	t
30-45	26	0	1	t
45-50				
50-55	-	t	2	2
55-60	-	t	t	t

Table 35 Low temperature pre-treatment, N_2 atmosphere.

Time (min)	Conversion (%)	Selectivity (%)		
		4,4'-biphenol	2,2'-biphenol	4-phenoxyphenol
0-5	29	1	1	0
5-10	8	4	8	2
10-15	9	2	3	5
15-30	9	1	5	4
30-45	5	t	t	t
45-50				
50-55	-	1	2	6
55-60	-	1	0	5

Table 36 Low temperature pre-treatment, O_2 atmosphere.

Time (min)	Conversion (%)	Selectivity (%)		
		4,4'-biphenol	2,2'-biphenol	4-phenoxyphenol
0-5	60	t	0	0
5-10	16	t	2	0
10-15	11	0	13	t
15-30	10	t	10	2
30-45	10	0	12	3
45-50				
50-55	-	t	1	2
55-60	-	t	0	t

To ensure an oxygen deficient or rich atmosphere the catalyst was heated to 348 K and degassed for 30 min. All three pre-treatments increased the initial conversion of phenol compared to the standard reaction without pre-treatment (Figure 67).

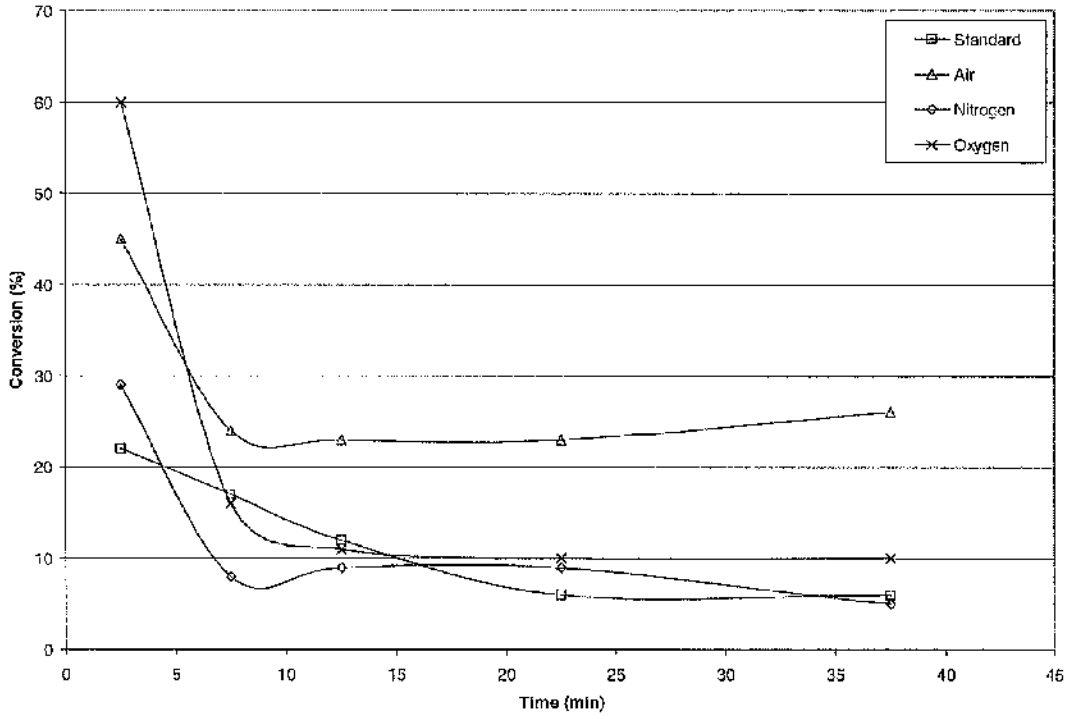

Fig. 67 Conversion of phenol against time, after low temperature pre-treatment of Cu(6%)/Zeolite-Y.

The initial conversion of phenol after low temperature pre-treatment increased as the partial pressure of oxygen was increased. Initial conversion in an oxygen rich atmosphere was 60% and was halved in an oxygen deficient atmosphere at 29%. After pre-treatment with oxygen or nitrogen conversion decreased sharply to match that of the standard reaction without pre-treatment. The catalyst pre-treated with air behaved differently; deactivation was significantly reduced and conversion stabilised after 10 min at ca. 25%.

The initial conversion of phenol after pre-treatment with nitrogen was greater than the initial conversion of the standard reaction. The partial pressure of oxygen is therefore not the only explanation for increased catalytic activity.

After pre-treatment in air, the selectivity to 4,4'-biphenol and 4-phenoxyphenol was little changed whilst 2,2'-biphenol was detected but not at selectivities >1%. After pre-treatment in nitrogen the selectivity to each dimer was increased, especially 2,2'-biphenol. After pre-treatment in oxygen the selectivity to 4,4'-biphenol and 4-phenoxyphenol remained unchanged whilst the selectivity to 2,2'-biphenol was dramatically increased to 12%. No 2,2'-biphenol was detected during the standard reaction without pre-treatment.

3.4.1.7 High temperature pre-treatment

Data was collected after the high temperature pre-treatment of Cu(6%)/Zeolite-Y at 773 K in air and nitrogen (Tables 37 and 38).

Table 37 High temperature pre-treatment in air.

Time (min)	Conversion (%)	Selectivity (%)		
		4,4'-biphenol	2,2'-biphenol	4-phenoxyphenol
0-5	100	0	0	0
5-10	99	0	0	0
10-15	80	0	0	0
15-30	13	0	0	0
30-45	2	0	0	0
45-50				
50-55	-	t	1	t
55-60	-	t	2	0

Table 38 High temperature pre-treatment in nitrogen.

Time (min)	Conversion (%)	Selectivity (%)		
		4,4'-biphenol	2,2'-biphenol	4-phenoxyphenol
0-5	66	t	0	0
5-10	53	t	0	0
10-15	42	0	0	0
15-30	29	0	0	0
30-45	8	0	0	0
45-50				
50-55	-	t	0	0
55-60	-	t	0	0

Conversion of phenol by Cu(6%)/Zeolite-Y was greatly increased after high temperature pre-treatment at 773 K in air and also increased after pre-treatment in nitrogen. The selectivity to 4,4'-biphenol, 2,2'-biphenol and 4-phenoxyphenol was however reduced to almost zero after pre-treatment with either air or nitrogen and no 2,2'-biphenol or 4-phenoxyphenol was detected.

3.3.2 Acetonitrile solution

Catalytic reactions rely on the adsorption of reactants and subsequent desorption of products. The adsorption of phenol over zeolite and clay catalysts was studied using acetonitrile, chloroform and water. Phenol adsorption was maximised using a chloroform solution and so chloroform was used as the reaction solvent. The conversion of phenol to 4,4'-biphenol, 2,2'-biphenol and 4-phenoxyphenol was however low and not greatly improved by changing for example the reaction temperature, phenol concentration or copper metal loading. The acetonitrile flush at the end of each phenol in chloroform cycle was intended to encourage removal of 4,4'-biphenol from the system since the solubility of 4,4'-biphenol in chloroform was particularly poor. The conversion of phenol to 4,4'-biphenol and the other dimers was however low enough that its solubility in chloroform would not have been a problem. Despite this the concentration of dimers in the exit stream from the reactor regularly increased during the flush. This was either because of increased solubility or an indication of increased catalytic activity when phenol and acetonitrile coexisted. Acetonitrile was therefore used as reaction solvent.

3.3.2.1 Cu, Ag and Ni/Zeolite-Y

The catalytic activity of Na, H, Cu, Ag and Ni/Zeolite-Y was investigated. Only data for the Cu, Ag and Ni/Zeolite-Y is provided in Tables 39-41.

Table 39 Cu(6%)/Zeolite-Y

Time (min)	Conversion (%)	Selectivity (%)		
		4,4'-biphenol	2,2'-biphenol	4-phenoxyphenol
0-5	16	14	0	4
5-10	17	12	1	3
10-15	12	13	1	4
15-30	6	13	1	4
30-45	4	12	2	5
45-60	3	12	2	4
60-90	2	12	2	5

Table 40 Ag(18%)/Zeolite-Y

Time (min)	Conversion (%)	Selectivity (%)		
		4,4'-biphenol	2,2'-biphenol	4-phenoxyphenol
0-5	1	10	4	8
5-10	6	3	2	4
10-15	3	5	3	9
15-30	1	t	t	t
30-45	<1	t	0	0
45-60	<1	t	0	0
60-90	<1	t	0	0

Table 41 Ni(5%)/Zeolite-Y

Time (min)	Conversion (%)	Selectivity (%)		
		4,4'-biphenol	2,2'-biphenol	4-phenoxyphenol
0-5	0	0	0	0
5-10	2	2	0	0
10-15	2	2	0	0
15-30	1	1	0	0
30-45	4	0	0	0
45-60	5	0	0	0
60-90	4	0	0	0

The sodium and hydrogen exchanged Zeolite-Y catalysts were inactive. Copper exchanged Zeolite-Y afforded the highest conversion of phenol and selectivity to 4,4'-biphenol, 2,2'-biphenol and 4-phenoxyphenol despite the relatively low adsorption of phenol from an acetonitrile solution previously reported in Section 3.1.1.2. The silver and nickel exchanged Zeolite-Y catalysts were not as active and conversion of phenol was always lower than 6%. Using Cu(6%)/Zeolite-Y the experimental conditions, for example phenol concentration, temperature and metal loading, were varied to optimise catalytic activity. The reaction data reported in Table 39 are used as a standard against which other reactions using Cu(6%)/Zeolite-Y are compared.

Deactivation of the Cu(6%)/Zeolite-Y catalyst was apparent. Conversion of phenol between 60 and 90 min was only $1/8^{th}$ of the initial conversion between 0 and 5 min. The selectivity to 4,4'-biphenol remained constant between 12 and 14%, whilst the selectivity to 2,2'-biphenol increased with TOS. The selectivity to 4-phenoxyphenol remained constant during the 90 min between 3 and 5%.

3.3.2.2 Cu/MCM-41

The activity of sodium, hydrogen and copper exchanged MCM-41 was investigated using standard experimental conditions. Only Cu(5%)/MCM-41 was active (Table 42).

Table 42 Cu(5%)/MCM-41

Time (min)	Conversion (%)	Selectivity (%)		
		4,4'-biphenol	2,2'-biphenol	4-phenoxyphenol
0-5	11	21	1	1
5-10	10	21	2	2
10-15	10	15	1	3
15-30	9	12	1	4
30-45	<1	t	t	t
45-60	<1	t	t	t
60-90	<1	t	t	t

The conversion of phenol decreased from 11 to <1% between 0 and 45 min. The deactivation between 0 and 30 min was slow with rapid deactivation between 30 and 45 min. The selectivity to 4,4'-biphenol between 0 an 30 min decreased with TOS, selectivity to 2,2'-biphenol remained constant and selectivity to 4-phenoxyphenol increased for the same TOS.

The MCM-41 classified support materials possess a regular array of hexagonal, uniform, unidimensional mesopores that can be varied in diameter from approximately 1.6 to 10 nm[12]. These materials bridge the gap between uniform microporous and amorphous mesoporous materials. For Zeolite-Y the 12-ring pore aperture has a diameter of 0.74 nm. Access and removal of phenol and dimers respectively should therefore be less hindered using the MCM-41 support. The selectivity towards 4,4'-biphenol was greater using Cu(5%)/MCM-41 compared to Cu(6%)/Zeolite-Y although the initial yield of 4,4'-biphenol was almost identical using either support.

3.3.2.3 Metal loading

Data was collected using Cu/Zeolite-Y with w/w metal loadings of 1, 5, 6 and 8% (Tables 43-46). The catalysts were prepared using different concentrations of an aqueous copper acetate solution. The copper loading was determined by HF digestion of the support and Atomic Absorption spectroscopy of the subsequent solution.

Table 43 Cu(1%)/Zeolite-Y

Time (min)	Conversion (%)	Selectivity (%)		
		4,4'-biphenol	2,2'-biphenol	4-phenoxyphenol
0-5	6	22	2	7
5-10	6	19	2	7
10-15	6	14	2	5
15-30	5	12	2	5
30-45	3	12	3	6
45-60	1	t	t	t
60-90	<1	t	t	t

Table 44 Cu(5%)/Zeolite-Y

Time (min)	Conversion (%)	Selectivity (%)		
		4,4'-biphenol	2,2'-biphenol	4-phenoxyphenol
0-5	12	18	0	4
5-10	10	15	0	3
10-15	7	20	1	4
15-30	5	13	1	3
30-45	2	8	1	1
45-60	1	5	1	0
60-90	1	3	t	0

Table 45 Cu(6%)/Zeolite-Y

Time (min)	Conversion (%)	Selectivity (%)		
		4,4'-biphenol	2,2'-biphenol	4-phenoxyphenol
0-5	16	14	0	4
5-10	17	12	1	3
10-15	12	13	1	4
15-30	6	13	1	4
30-45	4	12	2	5
45-60	3	12	2	4
60-90	2	12	2	5

Table 46 Cu(8%)/Zeolite-Y

Time (min)	Conversion (%)	Selectivity (%)		
		4,4'-biphenol	2,2'-biphenol	4-phenoxyphenol
0-5	23	11	0	4
5-10	29	9	0	5
10-15	23	9	0	7
15-30	13	11	1	8
30-45	3	10	6	3
45-60	2	11	5	4
60-90	1	19	0	6

As metal loading was increased the initial conversion of phenol also increased. Between 45 and 60 min the conversion of phenol was similar and independent of metal loading. There was a linear relationship between the initial phenol conversion and metal loading (Figure 68).

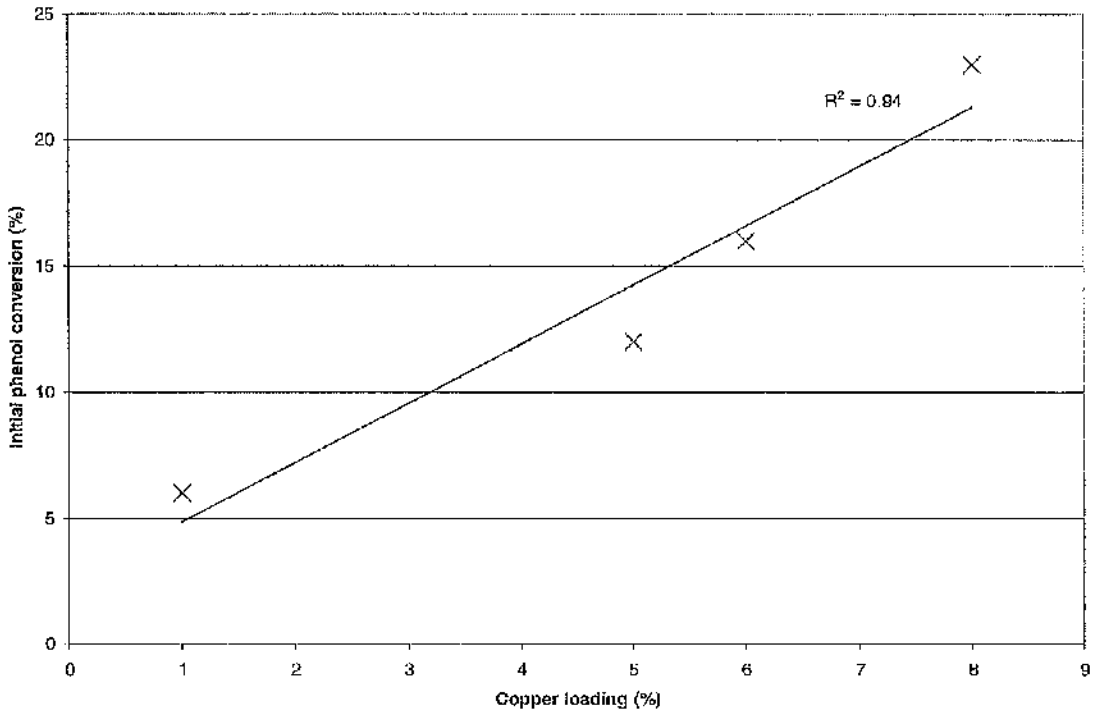

Fig. 68 Conversion of phenol against the four metal loadings: 1, 5, 6 and 8%.

The combined selectivity to 4,4'-biphenol, 2,2'-biphenol and 4-phenoxyphenol did not change significantly for loadings 5, 6 and 8%, but the selectivity to all three dimers was increased at the 1% copper loading.

3.3.2.4 Temperature

The activity of Cu(6%)/Zeolite-Y was investigated at 308, 328, 348, 388 and 408 K (Tables 47-51).

Table 47 308 K

Time (min)	Conversion (%)	Selectivity (%)		
		4,4'-biphenol	2,2'-biphenol	4-phenoxyphenol
0-5	14	4	0	t
5-10	12	9	5	1
10-15	9	10	7	2
15-30	7	6	4	1
30-45	5	6	5	1
45-60	5	2	2	t
60-90	2	2	1	t

Table 48 328 K

Time (min)	Conversion (%)	Selectivity (%)		
		4,4'-biphenol	2,2'-biphenol	4-phenoxyphenol
0-5	14	7	4	2
5-10	13	10	7	3
10-15	11	9	6	3
15-30	3	19	15	5
30-45	1	27	20	6
45-60	1	t	t	t
60-90	<1	t	t	t

Table 49 348 K

Time (min)	Conversion (%)	Selectivity (%)		
		4,4'-biphenol	2,2'-biphenol	4-phenoxyphenol
0-5	16	14	0	4
5-10	17	12	1	3
10-15	12	13	1	4
15-30	6	13	1	4
30-45	4	12	2	5
45-60	3	12	2	4
60-90	2	12	2	5

Table 50 388 K

Time (min)	Conversion (%)	Selectivity (%)		
		4,4'-biphenol	2,2'-biphenol	4-phenoxyphenol
0-5	23	5	3	3
5-10	29	4	5	3
10-15	18	4	6	3
15-30	12	3	6	3
30-45	2	t	t	t
45-60	2	t	t	t
60-90	<1	t	t	t

Table 51 408 K

Time (min)	Conversion (%)	Selectivity (%)		
		4,4'-biphenol	2,2'-biphenol	4-phenoxyphenol
0-5	14	4	3	3
5-10	30	2	4	3
10-15	21	2	4	3
15-30	8	4	5	3
30-45	3	3	3	2
45-60	2	2	4	1
60-90	1	t	t	t

Conversion of phenol did not increase linearly with temperature. This data was analogous to that obtained using a chloroform solution. Arrhenius behaviour was not observed and temperature had a complex affect on phenol conversion. An initial period of activation was observed at 388 and 408K and the maximum conversion of phenol during both reactions occurred between 5 and 10 min, not between 0 and 5 min as it did at the three lower temperatures.

Yields of the dimers 4,4'-biphenol, 2,2'-biphenol and 4-phenoxyphenol were maximised at 308 and 388 K, although catalyst deactivation was also most prominent at 388 K. The ratio of carbon-carbon/carbon-oxygen coupled dimers decreased from *14* at 308 K to *3* at 408 K.

3.3.2.5 Phenol concentration

Data was collected using 0.02, 0.04, 0.08, 0.16 and 0.32 mol L^{-1} solutions over Cu(6%)/Zeolite-Y (Tables 52-56).

Table 52 0.02 mol L^{-1}

Time (min)	Conversion (%)	Selectivity (%)		
		4,4'-biphenol	2,2'-biphenol	4-phenoxyphenol
0-5	22	7	4	1
5-10	20	10	8	2
10-15	19	16	13	3
15-30	8	21	18	5
30-45	4	26	23	7
45-60	3	25	23	8
60-90	3	20	19	6

Table 53 0.04 mol L^{-1}

Time (min)	Conversion (%)	Selectivity (%)		
		4,4'-biphenol	2,2'-biphenol	4-phenoxyphenol
0-5	16	14	0	4
5-10	17	12	1	3
10-15	12	13	1	4
15-30	6	13	1	4
30-45	4	12	2	5
45-60	3	12	2	4
60-90	2	12	2	5

Table 54 0.08 mol L^{-1}

Time (min)	Conversion (%)	Selectivity (%)		
		4,4'-biphenol	2,2'-biphenol	4-phenoxyphenol
0-5	13	10	0	4
5-10	11	11	1	4
10-15	7	11	1	4
15-30	4	10	1	4
30-45	2	17	3	7
45-60	1	14	3	6
60-90	1	19	4	9

Table 55 0.16 mol L^{-1}

Time (min)	Conversion (%)	Selectivity (%)		
		4,4'-biphenol	2,2'-biphenol	4-phenoxyphenol
0-5	9	6	0	3
5-10	10	6	1	3
10-15	9	5	1	2
15-30	4	7	1	3
30-45	<1	t	t	t
45-60	<1	t	t	t
60-90	<1	t	t	t

Table 56 0.32 mol L^{-1}

Time (min)	Conversion (%)	Selectivity (%)		
		4,4'-biphenol	2,2'-biphenol	4-phenoxyphenol
0-5	4	13	2	9
5-10	4	11	2	6
10-15	3	8	1	2
15-30	3	7	1	2
30-45	3	5	1	1
45-60	2	4	1	1
60-90	1	8	1	1

To make an accurate assessment of this data it was necessary to calculate and then compare data at a constant WHSV (Equation 5).

Equ. 5 Weight Hourly Space Velocity

$$\text{WHSV } (hr^{-1}) = \frac{\text{reactant /hour } (g\ hr^{-1})}{\text{catalyst } (g)}$$

Comparison was therefore made between the 60 – 90 min data for the 0.02 mol L^{-1} solution; 45 – 60 min for 0.04 mol L^{-1}; 15 – 30 min for 0.08 mol L^{-1}; 10 – 15 min for 0.16 mol L^{-1} and 0 – 5 min for 0.32 mol L^{-1} (Table 57). At constant WHSV the conversion of phenol using the 0.02 mol L^{-1} solution was to be compared at 120 min. This data was not available so the 60 – 90 min data point was used. Since conversion was decreasing with TOS, the conversion was expected to be <3% after 120 min (*).

Table 57 Various concentrations of phenol in acetonitrile at equivalent WHSV.

Conc.	Conversion (%)	Selectivity (%)		
		4,4'-biphenol	2,2'-biphenol	4-phenoxyphenol
0.02	<3 *	20	19	6
0.04	3	12	2	4
0.08	5	10	1	4
0.16	9	5	1	2
0.32	4	13	2	9

At equivalent WHSV the conversion of phenol increased with concentration from 0.02 to 0.16 mol L^{-1} and decreased using the 0.32 mol L^{-1} solution. The selectivity to 4,4'-biphenol, 2,2'-biphenol and 4-phenoxyphenol decreased as phenol concentration was increased and increased at 0.32 mol L^{-1}.

Calculating the order of reaction required reaction rate data. For a flow system the rate of reaction is calculated using Equation 6.

Equ. 6 Rate calculation.

$$\text{Rate (moles}^{-1}\ \text{min}^{-1}\ \text{g}^{-1}) = \frac{\text{Feed (moles min}^{-1}) \times \text{Fractional conversion}}{\text{weight of catalyst (g)}}$$

The rates of reaction (Table 58) were calculated from the initial conversion of phenol at each concentration.

Table 58 Calculated reaction rate.

Phenol concentration (mol L^{-1})	Rate of reaction (moles min^{-1} g^{-1})
0.02	3.16×10^{-6}
0.04	4.94×10^{-6}
0.08	7.50×10^{-6}
0.16	1.04×10^{-5}
0.32	7.60×10^{-6}

The rate of reaction using the 0.32 mol L^{-1} phenol solution did not compare with the calculated rates at the other four concentrations. This was also evident when conversion data was compared at constant WHSV, Table 57.

Plotting the natural log of phenol concentration against the natural log of rate gave a straight-line graph (Figure 69). The gradient of the line was 0.6 and was equal to the order of reaction with respect to phenol.

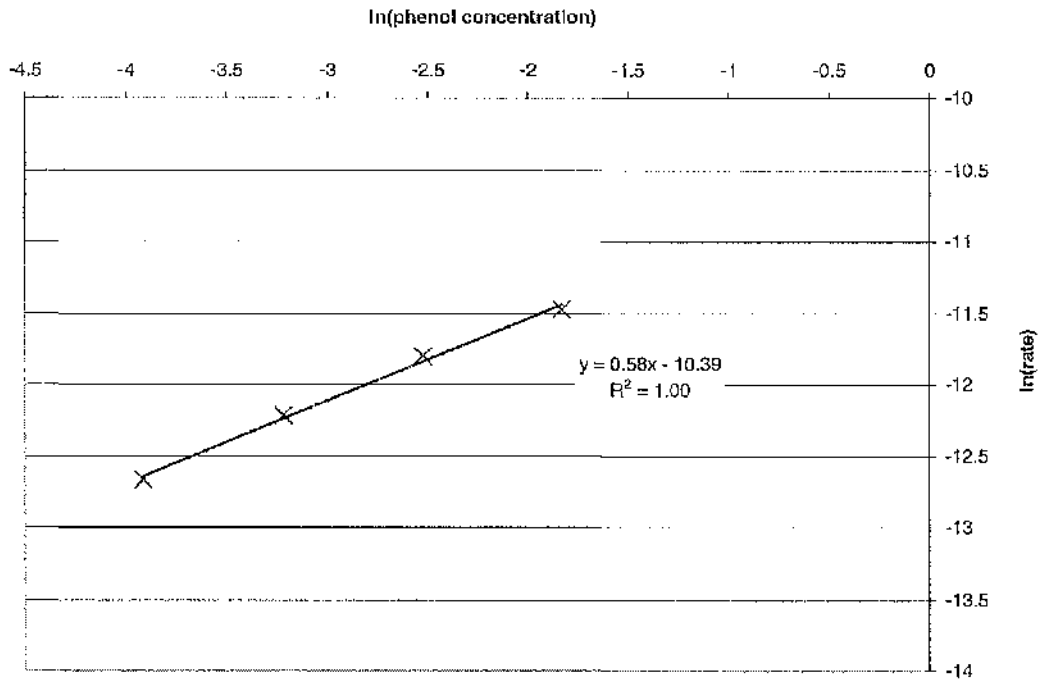

Fig. 69 Calculating the order of reaction.

3.3.2.6 Low temperature pre-treatment

Data was collected after the low temperature pre-treatment of Cu(6%)/Zeolite-Y in air, an oxygen rich and oxygen deficient atmosphere (Tables 59-61).

Table 59 Low temperature pre-treatment, air atmosphere.

Time (min)	Conversion (%)	Selectivity (%)		
		4,4'-biphenol	2,2'-biphenol	4-phenoxyphenol
0-5	16	16	1	4
5-10	10	22	1	7
10-15	4	37	3	9
15-30	2	36	4	11
30-45	<1	t	t	t
45-60	<1	t	t	t
60-90	<1	t	t	t

Table 60 Low temperature pre-treatment, nitrogen atmosphere.

Time (min)	Conversion (%)	Selectivity (%)		
		4,4'-biphenol	2,2'-biphenol	4-phenoxyphenol
0-5	17	20	0	5
5-10	9	23	0	7
10-15	5	25	0	9
15-30	3	29	5	11
30-45	2	24	5	10
45-60	2	16	4	7
60-90	1	14	3	7

Table 61 Low temperature pre-treatment, oxygen atmosphere.

Time (min)	Conversion (%)	Selectivity (%)		
		4,4'-biphenol	2,2'-biphenol	4-phenoxyphenol
0-5	20	15	1	4
5-10	8	28	1	8
10-15	6	22	2	7
15-30	2	52	6	16
30-45	1	38	5	13
45-60	1	31	5	11
60-90	1	24	4	9

There were no obvious differences in the conversion of phenol or selectivity to dimers after the three low temperature pre-treatments. The thermogravimetric analysis of Cu(6%)/Zeolite-Y heated to 348 K and held for 30 min in a nitrogen or oxygen containing atmosphere indicated only the loss of water from the catalyst irrespective of the gas used.

When compared with the standard reaction (Table 39), the selectivity to 4,4'-biphenol, 2,2'-biphenol and 4-phenoxyphenol was increased by the low-temperature pre-treatment although catalyst deactivation was also enhanced.

3.3.2.7 High temperature pre-treatment

Data was collected after the high temperature pre-treatment of Cu(6%)/Zeolite-Y at 773 K in nitrogen, air and oxygen (Tables 62 and 64).

Table 62 High temperature pre-treatment, nitrogen atmosphere.

Time (min)	Conversion (%)	Selectivity (%)		
		4,4'-biphenol	2,2'-biphenol	4-phenoxyphenol
0-5	1	10	3	2
5-10	1	5	0	1
10-15	1	3	0	4
15-30	2	1	0	0
30-45	3	1	0	0
45-60	4	t	0	0
60-90	5	t	0	0

Table 63 High temperature pre-treatment, air atmosphere.

Time (min)	Conversion (%)	Selectivity (%)		
		4,4'-biphenol	2,2'-biphenol	4-phenoxyphenol
0-5	3	27	3	7
5-10	4	9	1	4
10-15	3	10	1	3
15-30	3	6	1	2
30-45	<1	t	t	t
45-60	<1	t	t	t
60-90	<1	t	t	t

Table 64 High temperature pre-treatment, oxygen atmosphere.

Time (min)	Conversion (%)	Selectivity (%)		
		4,4'-biphenol	2,2'-biphenol	4-phenoxyphenol
0-5	4	32	3	10
5-10	4	15	2	6
10-15	4	10	2	5
15-30	3	4	1	4
30-45	1	3	2	1
45-60	1	t	t	t
60-90	1	t	t	t

High temperature pre-treatment greatly reduced the catalytic activity of Cu(6%)/Zeolite-Y. It was important to ensure the detrimental effects of water removal were minimised during heating[47]. These effects are often manifest by dealumination of the support and so the XRD analysis of fresh and spent catalysts samples was used to confirm that no dealumination of the support occurred as a result of these pre-treatments. After pre-treatment with nitrogen at 773 K the conversion of phenol uniquely increased with TOS. The selectivity to 4,4'-biphenol, 2,2'-biphenol and 4-phenoxyphenol decreased rapidly with TOS after high temperature pre-treatment. The initial selectivities were higher after any of the pre-treatments compared to the standard reaction. The selectivities to 4,4'-biphenol and 4-phenoxyphenol were proportional to the partial pressure of oxygen in the gas used for the pre-treatment. Selectivities between 0 and 10 min were at a maximum using oxygen and a minimum using nitrogen. The already reduced selectivity to 2,2'-biphenol decreased with TOS after pre-treatment, unlike the standard reaction when selectivity increased.

3.3.2.8 Pressure

The catalytic activity of Cu(6%)/Zeolite-Y was studied at four liquid pressures 0, 10, 20 and 30 bar g (Tables 65-68).

Table 65 0 bar g

Time (min)	Conversion (%)	Selectivity (%)		
		4,4'-biphenol	2,2'-biphenol	4-phenoxyphenol
0-5	16	6	4	2
5-10	13	7	5	2
10-15	8	7	5	2
15-30	2	8	6	2
30-45	2	t	t	t
45-60	1	t	t	t
60-90	1	t	t	t

Table 66 10 bar g

Time (min)	Conversion (%)	Selectivity (%)		
		4,4'-biphenol	2,2'-biphenol	4-phenoxyphenol
0-5	16	6	4	1
5-10	13	9	6	3
10-15	10	10	8	3
15-30	4	16	12	5
30-45	2	11	9	3
45-60	2	t	t	t
60-90	1	t	t	t

Table 67 20 bar g

Time (min)	Conversion (%)	Selectivity (%)		
		4,4'-biphenol	2,2'-biphenol	4-phenoxyphenol
0-5	16	14	0	4
5-10	17	12	1	3
10-15	12	13	1	4
15-30	6	13	1	4
30-45	4	12	2	5
45-60	3	12	2	4
60-90	2	12	2	5

Table 68 30bar g

Time (min)	Conversion (%)	Selectivity (%)		
		4,4'-biphenol	2,2'-biphenol	4-phenoxyphenol
0-5	13	5	3	1
5-10	25	6	4	2
10-15	18	7	5	2
15-30	8	7	6	2
30-45	4	7	6	2
45-60	4	5	5	1
60-90	3	4	4	1

In general as liquid pressure was increased the conversion of phenol also increased and deactivation reduced (Figure 70).

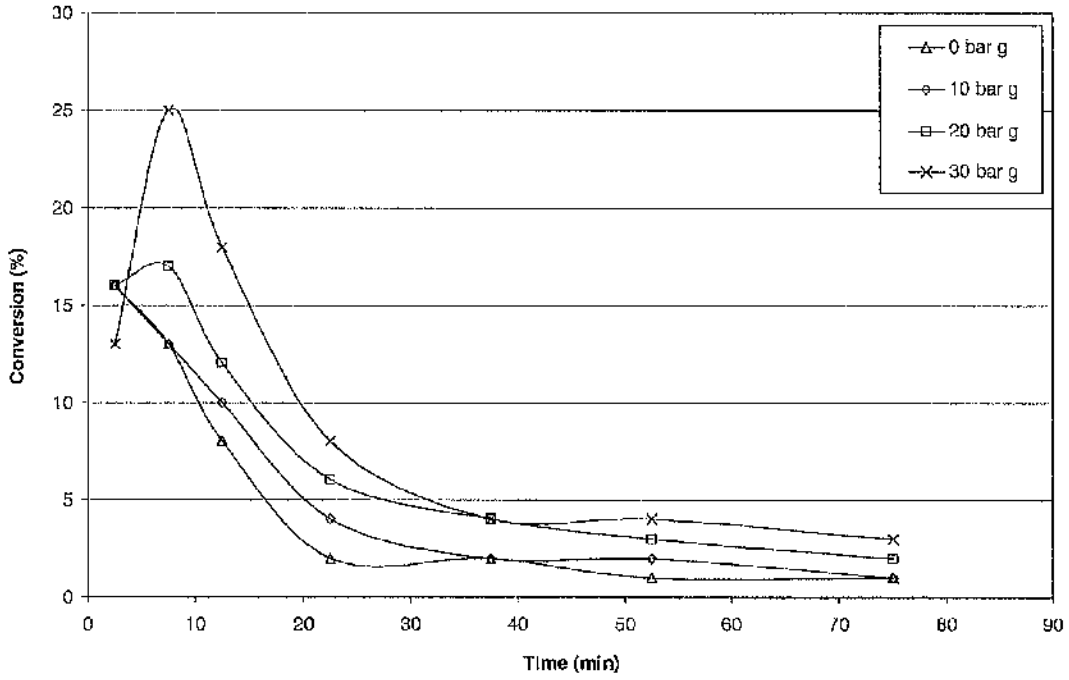

Fig. 70 Conversion of phenol at 0, 10, 20 and 30 bar g.

At 20 and 30 bar g the maximum conversion of phenol occurred between 5 and 10 min. The selectivities towards 4,4'-biphenol and 4-phenoxyphenol increased with pressure between 0 and 20 bar g and then decreased at 30 bar g. The selectivity to 2,2'-biphenol was similar at all four liquid pressures, with a small increase in selectivity at 10 bar g and decrease at 20 bar g. The XRD patterns of fresh and spent

Cu(6%)/Zeolite-Y catalysts confirmed the crystallinity of the support was unaffected by reactions at pressures between 0 and 30 bar g.

3.3.2.9 Added alkali metal

The activity of Cu(6%)/Zeolite-Y was investigated with addition of potassium acetate to the acetonitrile solution (Table 69).

Table 69 Addition of CH_3COOK.

Time (min)	Conversion (%)	Selectivity (%)		
		4,4'-biphenol	2,2'-biphenol	4-phenoxyphenol
0-5	17	15	30	36
5-10	14	15	30	30
10-15	11	14	21	18
15-30	7	21	24	20
30-45	6	25	19	17
45-60	1	23	6	25
60-90	1	0	0	0

These results are best compared against the standard reaction using Cu(6%)/Zeolite-Y (Table 70).

Table 70 Standard reaction.

Time (min)	Conversion (%)	Selectivity (%)		
		4,4'-biphenol	2,2'-biphenol	4-phenoxyphenol
0-5	16	14	0	4
5-10	17	12	1	3
10-15	12	13	1	4
15-30	6	13	1	4
30-45	4	12	2	5
45-60	3	12	2	4
60-90	2	12	2	5

The conversion of phenol was largely unaffected by the addition of potassium acetate, with almost complete deactivation within 90 min. The selectivity to 4,4'-biphenol, 2,2'-biphenol and 4-phenoxyphenol increased with the addition of the alkali metal salt. The increase in 4,4'-biphenol selectivity was noticeable after 15 min. A 20 to 30-

fold increase in the selectivity towards 2,2'-biphenol was observed between 0 and 45 min and a 5 to 10-fold increase in the selectivity towards 4-phenoxyphenol was observed between 0 and 60 min. Unfortunately, the addition of potassium acetate caused leaching of copper from the catalyst with the complete removal of all copper within 90 min.

3.3.2.10 Flow rate

Data was collected using three different flow rates of acetonitrile solution, 0.5 ml min^{-1}, 1 ml min^{-1} and 2 ml min^{-1} over Cu(6%)/Zeolite-Y (Tables 71-73).

Table 71 0.5 ml min^{-1}

Time (min)	Conversion (%)	Selectivity (%)		
		4,4'-biphenol	2,2'-biphenol	4-phenoxyphenol
0-5	16	14	0	4
5-10	17	12	1	3
10-15	12	13	1	4
15-30	6	13	1	4
30-45	4	12	2	5
45-60	3	12	2	4
60-90	2	12	2	5

Table 72 1 ml min^{-1}

Time (min)	Conversion (%)	Selectivity (%)		
		4,4'-biphenol	2,2'-biphenol	4-phenoxyphenol
0-5	13	8	0	2
5-10	13	10	1	3
10-15	7	10	1	3
15-30	6	5	1	2
30-45	5	4	1	2
45-60	2	8	1	3
60-90	1	8	1	3

Table 73 2 ml min^{-1}

Time (min)	Conversion (%)	Selectivity (%)		
		4,4'-biphenol	2,2'-biphenol	4-phenoxyphenol
0-5	10	7	0	1
5-10	10	7	1	t
10-15	8	6	1	1
15-30	3	7	t	t
30-45	1	7	t	2
45-60	1	6	t	1
60-90	1	7	t	2

The conversion of phenol decreased as flow rate was increased. The selectivities to 2,2'-biphenol and 4-phenoxyphenol halved when flow rate was increased from 0.5 to 1 ml min^{-1} and halved again between 1 and 2 ml min^{-1}. The selectivity to 4,4'-biphenol halved when the flow rate was increased from 0.5 to 2 ml min^{-1}. Changing the flow rate of phenol feedstock changed the Liquid Hourly Space Velocity (Equation 7).

Equ. 7 Liquid Hourly Space Velocity.

$$\text{LHSV}\,(\text{hr}^{-1}) = \frac{\text{solution /hour}\,(\text{cm}^3\,\text{hr}^{-1})}{\text{catalyst}\,(\text{cm}^3)}$$

3.3.2.11 Water and peroxide

The effects of adding water and peroxide to the acetonitrile solution were investigated using Cu(6%)/Zeolite-Y (Tables 74 and 75).

Table 74 Addition of H_2O

Time (min)	Conversion (%)	Selectivity (%)		
		4,4'-biphenol	2,2'-biphenol	4-phenoxyphenol
0-5	56	3	3	1
5-10	37	7	8	2
10-15	15	13	15	4
15-30	2	t	t	t
30-45	1	t	t	t
45-60	1	t	t	t
60-90	1	t	t	t

Table 75 Addition of H_2O_2

Time (min)	Conversion (%)	Selectivity (%)		
		4,4'-biphenol	2,2'-biphenol	4-phenoxyphenol
0-5	53	3	4	1
5-10	26	10	13	4
10-15	9	14	12	5
15-30	4	14	10	7
30-45	3	10	6	3
45-60	3	10	5	3
60-90	1	9	5	2

These results are best compared against the standard reaction using Cu(6%)/Zeolite-Y (Table 76).

Table 76 Standard reaction

Time (min)	Conversion (%)	Selectivity (%)		
		4,4'-biphenol	2,2'-biphenol	4-phenoxyphenol
0-5	16	14	0	4
5-10	17	12	1	3
10-15	12	13	1	4
15-30	6	13	1	4
30-45	4	12	2	5
45-60	3	12	2	4
60-90	2	12	2	5

From the available conversion and selectivity data, the affects of added water and peroxide on phenol conversion and selectivity to 4,4'-biphenol, 2,2'-biphenol and 4-phenoxyphenol were similar. A 3-fold increase in conversion was observed with the addition of H_2O or H_2O_2 during the first 10 min of reaction. After 10 min the conversion of phenol was similar to the standard reaction. The selectivity to 4,4'-biphenol and 4-phenoxyphenol increased and then decreased with TOS when H_2O or H_2O_2 were added and at their maximum were similar to the standard reaction. The selectivity to 2,2'-biphenol also increased and then decreased with TOS but was consistently higher compared to the standard reaction.

3.3.3 Characterisation of a byproduct

The dimerisation of phenol using Cu(6%)/Zeolite-Y and Ag(18%)/Zeolite-Y and chloroform or acetonitrile solutions produced 4,4'-biphenol, 2,2'-biphenol and 4-phenoxyphenol and a number of byproducts. One such byproduct was prominent in the integrator printout from the HPLC analysis of a reaction sample taken during the dimerisation of phenol over Ag(18%)/Zeolite-Y using a chloroform solution under standard conditions. The identity of the peak at 8.27 was unknown (Figure 71).

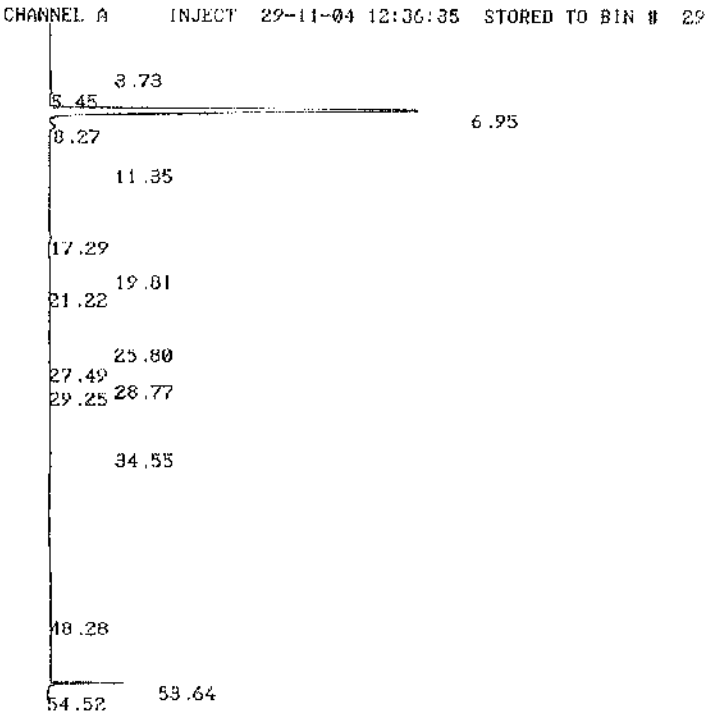

Fig. 71 Integrator printout from the HPLC analysis of a reaction sample from the dimerisation of phenol using Ag(18%)/Zeolite-Y.

Spiking the reaction sample with 4,4'-biphenol, 4,4'-dihydroxydiphenylether, 4-phenoxyphenol or 2,2'-biphenol did not confirm the identity of the compound. Additional analytical techniques were therefore used to separate, characterise and determine the structure of the compound.

During the dimerisation of phenol over Ag(18%)/Zeolite-Y using a chloroform solution, a sample of the exit solution was collected for 20 min. The chloroform was removed using rotary evaporation and the sample heated to 353 K under reduced pressure to remove most of the phenol. This increased the concentration of the

unknown compound and a sample of the remaining solid was then analysed by Mass Spectrometry (Figure 72).

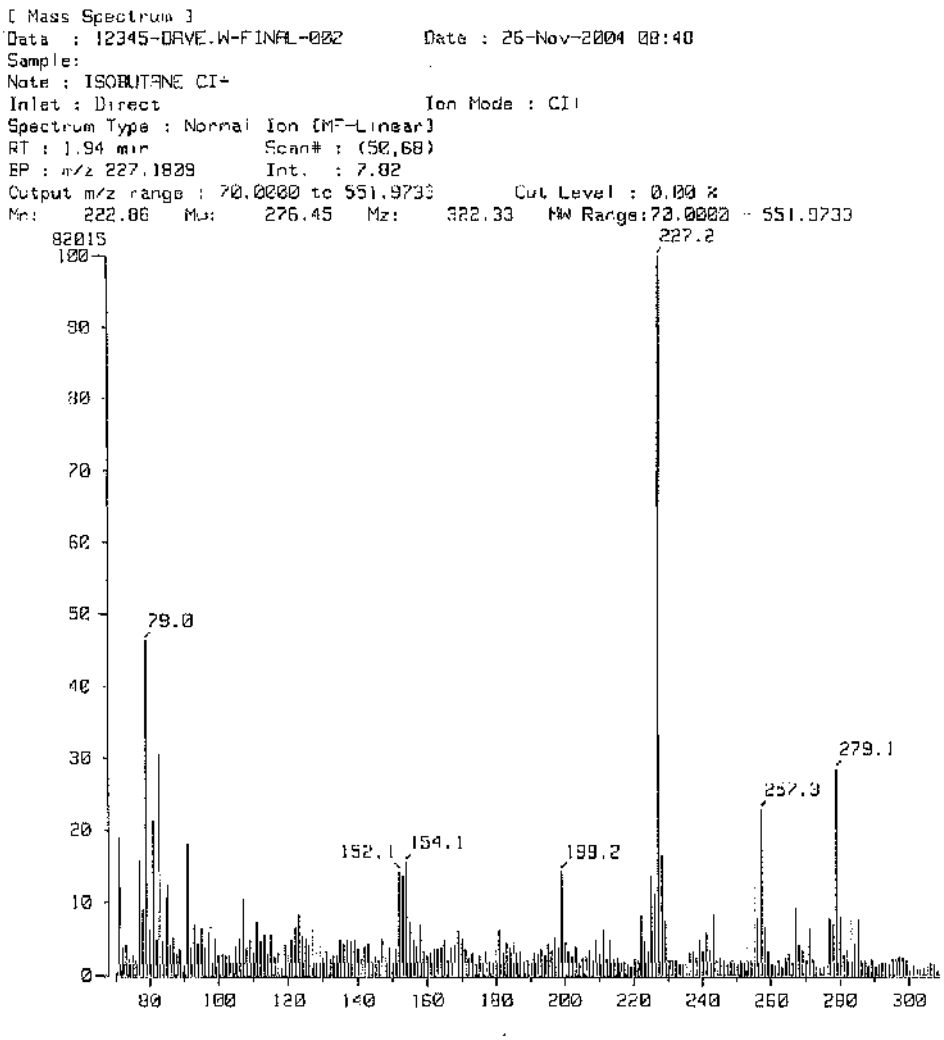

Fig. 72 Mass Spectrum of isolated compound.

The ^{1}H NMR spectra (Figures 73-75) of solutions containing 4,4'-biphenol, 4,4'-dihydroxydiphenylether and the unknown compound were obtained. The circled peaks highlight the important characteristics of 4,4'-biphenol and 4,4'-dihydroxydiphenylether which were also observed in the spectra of the unknown.

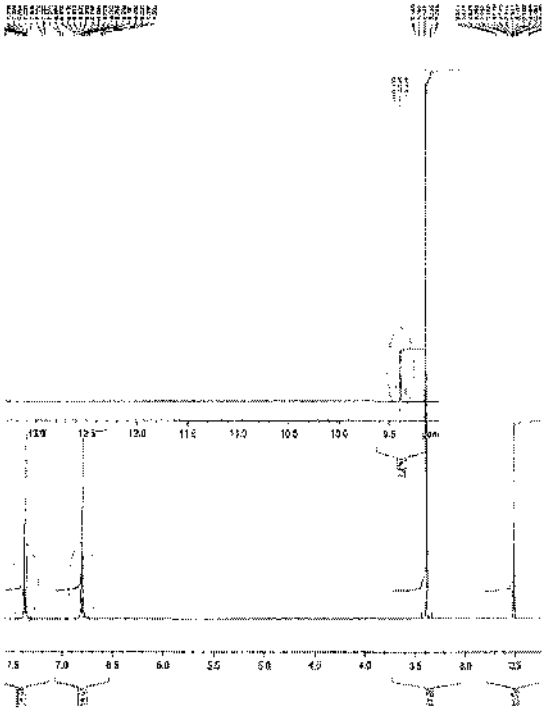

Fig. 73 ^{1}H NMR of 4,4'-biphenol

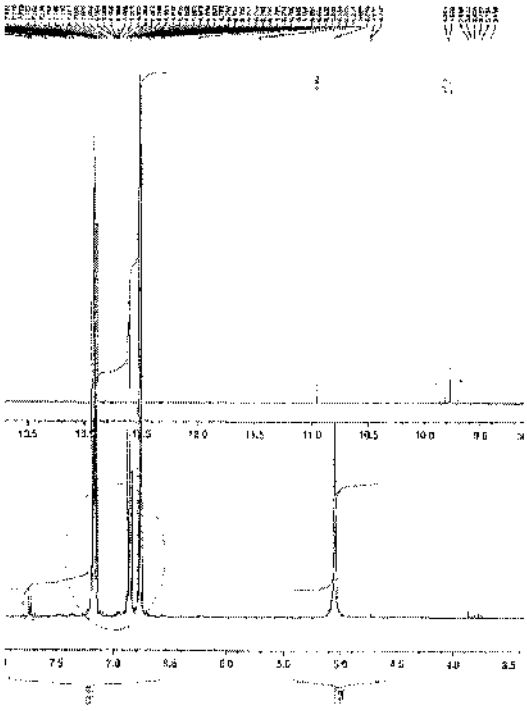

Fig. 74 ^{1}H NMR of 4,4'-dihydroxydiphenylether

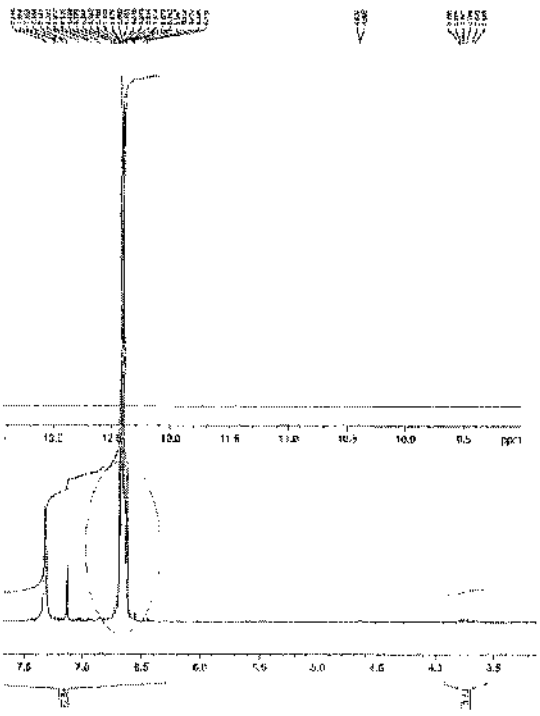

Fig. 75 ^{1}H NMR of unknown

Combining knowledge of the ion peak at m/z = 279 in the mass spectrum and the characteristics of both 4,4'-biphenol and 4,4'-dihydroxydiphenylether in the ^{1}H NMR spectrum, a phenolic trimer $C_{18}H_{14}O_3$ was proposed (Figure 76).

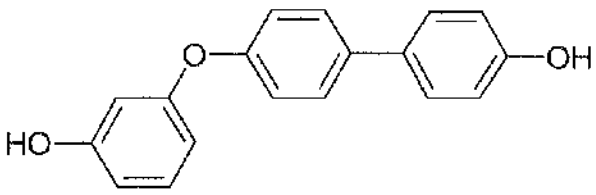

Fig. 76 Phenolic trimer

This was the only molecular formula and structure that correlated with all the analytical data collected. Molecules with this general structure are well known and were reported in a review publication by Hay[10].

3.3.4 Using other nitriles as solvents

The catalytic activity of Cu(6%)/Zeolite-Y was studied using butyronitrile and propionitrile as solvents for phenol.

3.3.4.1 Propionitrile

The dimerisation of phenol using a propionitrile solution was studied over Cu(6%)/Zeolite-Y (Table 77). Data from the standard reaction in acetonitrile has been included for comparison (Table 78).

Table 77 Propionitrile

Time (min)	Conversion (%)	Selectivity (%)		
		4,4'-biphenol	2,2'-biphenol	4-phenoxyphenol
0-5	42	5	0	1
5-10	15	9	1	2
10-15	7	14	2	4
15-30	5	9	1	3
30-45	3	12	2	5
45-60	1	18	3	7

Table 78 Acetonitrile

Time (min)	Conversion (%)	Selectivity (%)		
		4,4'-biphenol	2,2'-biphenol	4-phenoxyphenol
0-5	16	14	0	4
5-10	17	12	1	3
10-15	12	13	1	4
15-30	6	13	1	4
30-45	4	12	2	5
45-60	3	12	2	4
60-90	2	12	2	5

The conversion of phenol between 0 and 5 min was tripled using a propionitrile solution. Conversion after 5 min was comparable in either solvent. The selectivity towards 4,4'-biphenol and 4-phenoxyphenol using a propionitrile solution started lower but matched the selectivity using acetonitrile after 15 min. The selectivity to 2,2'-biphenol was similar using either solution.

3.3.4.2 Butyronitrile

The dimerisation of phenol using a propionitrile solution was studied over Cu(6%)/Zeolite-Y (Table 79).

Table 79 Butyronitrile

Time (min)	Conversion (%)	Selectivity (%)		
		4,4'-biphenol	2,2'-biphenol	4-phenoxyphenol
0-5	46	2	t	1
5-10	12	13	1	5
10-15	5	30	3	8
15-30	3	29	4	10
30-45	2	28	4	9
45-60	1	28	3	9

The conversions of phenol using butyronitrile and propionitrile solutions were comparable. The selectivity to 4,4'-biphenol and 4-phenoxyphenol started lower but after 15 min had increased to twice the selectivity obtained using acetonitrile. The selectivity to 2,2'-biphenol was consistently higher using the butyronitrile solution compared to the acetonitrile or propionitrile solutions.

3.3.5 Chloroform and acetonitrile mixed solution

The dimerisation of phenol to 4,4'-biphenol, 2,2'-biphenol and 4-phenoxyphenol was studied using Cu(6%)/Zeolite-Y and a mixed chloroform and acetonitrile solution. Solutions of phenol in chloroform were prepared with a 1:1, 10:1, 100:1 and 1000:1 molar ratio of acetonitrile to phenol added.

The conversion of phenol and selectivity to 4,4'-biphenol, 2,2'-biphenol and 4-phenoxyphenol were unaffected by the molar ratio of acetonitrile to phenol. The results were indistinguishable from the standard reaction using Cu(6%)/Zeolite-Y and a solution of phenol in chloroform without the addition of acetonitrile (Section 3.3.1.1, Table 14).

3.3.6 Homogeneous phase reactions

Using the experimental procedure outlined in Section 2.4.3 no conversion of phenol to 4,4'-biphenol, 2,2'-biphenol, 4-phenoxyphenol or any by-product was detected.

3.4 Dimerisation of phenol using clay catalysts

3.4.1 Acetonitrile solution

Since the conversion of phenol and selectivity to 4,4'-biphenol, 2,2'-biphenol and 4-phenoxyphenol catalysed by Cu(6%)/Zeolite-Y was improved by using an acetonitrile solution, the dimerisation of phenol catalysed by Cu/Montmorillonite and Cu/Attapulgite was also to be studied using an acetonitrile solution. The adsorption of phenol over clay catalysts had already however been attempted using an acetonitrile solution. It had been established that the flow of an acetonitrile solution was possible through Cu/Montmorillonite but not through Cu/Attapulgite since the pressure drop across the bed exceeded 100 bar g. The activity of Cu/Montmorillonite was therefore investigated using an acetonitrile solution and a mixed acetonitrile/chloroform solution used to study the activity of Cu/Attapulgite.

3.4.1.1 Cu/Montmorillonite

The catalytic activities of Cu(6%)/Montmorillonite and Cu(9%)/Montmorillonite were studied using an acetonitrile solution (Tables 80 and 81).

Table 80 Cu(6%)/Montmorillonite

Time (min)	Conversion (%)	Selectivity (%)		
		4,4'-biphenol	2,2'-biphenol	4-phenoxyphenol
0-5	3	11	2	5
5-10	1	22	3	6
10-15	1	24	2	5
15-30	1	15	0	4
30-45	1	12	0	1
45-60	1	17	0	7
60-90	<1	t	0	t

Table 81 Cu(9%)/Montmorillonite

Time (min)	Conversion (%)	Selectivity (%)		
		4,4'-biphenol	2,2'-biphenol	4-phenoxyphenol
0-5	8	2	t	1
5-10	8	2	t	1
10-15	11	1	t	t
15-30	13	t	t	t
30-45	15	t	0	t
45-60	13	t	0	t
60-90	1	t	0	0

The conversion of phenol increased with metal loading. The selectivity to 4,4'-biphenol, 2,2'-biphenol and 4-phenoxyphenol was unfortunately reduced to trace amounts at the higher metal loading.

3.4.1.2 Cu/Attapulgite

Since it had been established that the flow of an acetonitrile solution through Cu/Attapulgite was not possible, a mixed acetonitrile/ chloroform solution was proposed. After investigation it was found that a 40:60 volume ratio of acetonitrile/ chloroform was the maximum amount of acetonitrile that would pass through Cu/Attapulgite at a flow rate of ≤ 0.5 ml min^{-1}.

3.4.2 Chloroform and acctonitrile mix as the solvent

In order that the catalytic activity of Cu/Attapulgite and Cu/Montmorillonite could be compared, the 40:60 volume ratio of acetonitrile/ chloroform solution was used to study the activity of both catalysts.

3.4.2.1 Na, H and Cu/Montmorillonite

The catalytic activity of Na, H and Cu/Montmorillonite was studied. Only Cu/Montmorillonite catalysed the dimerisation of phenol (Table 82).

Table 82 Cu(6%)/Montmorillonite

Time (min)	Conversion (%)	Selectivity (%)		
		4,4'-biphenol	2,2'-biphenol	4-phenoxyphenol
0-5	3	5	0	5
5-10	3	8	0	6
10-15	2	7	0	2
15-30	2	7	0	1
30-45	1	11	0	12
45-60	1	9	0	5
60-90	<1	t	0	0

Conversion of phenol was low, as was selectivity toward 4,4'-biphenol and 4-phenoxyphenol. No 2,2'-biphenol was detected.

3.4.2.2 Na, H and Cu/Attapulgite

The catalytic activity of Na, H and Cu/Attapulgite was studied. Only Cu/Attapulgite catalysed the dimerisation of phenol (Table 83).

Table 83 Cu(5%)/Attapulgite

Time (min)	Conversion (%)	Selectivity (%)		
		4,4'-biphenol	2,2'-biphenol	4-phenoxyphenol
0-5	24	29	1	2
5-10	30	23	1	2
10-15	23	20	t	1
15-30	9	24	t	2
30-45	2	21	0	5
45-60	1	12	0	4
60-90	1	4	0	4

The selectivity to 4,4'-biphenol was high, whilst selectivity to the other carbon-carbon coupled dimer, 2,2'-biphenol was ca. 1%. The selectivity to 4-phenoxyphenol was also low. Both conversion of phenol and selectivity to 4,4'-biphenol decreased with TOS. Despite this the yield of 4,4'-biphenol between 0 and 10 min using Cu(5%)/Attapulgite and the acetonitrile/chloroform mixed solution was 7%. Using Cu(6%)/Zeolite-Y and an acetonitrile solution the yield of 4,4'-biphenol between 0 and 10 min was only 2%. For Attapulgite a copper loading of 5% w/w was equivalent to more than five times the theoretical Cation Exchange Capacity (CEC) of the clay.

The selectivity toward and also yield of 4,4'-biphenol was greater using Cu(5%)/Attapulgite than under any of the experimental conditions studied using Cu(6%)/Zeolite-Y or Cu(6%)/Montmorillonite. There was almost no dimerisation of phenol to 2,2'-biphenol using Cu(5%)/Attapulgite. After communication from the project sponsors, the aim of this research project was widened to investigate the potential use of zeolites and clays as catalysts for phenol dimerisation to 4,4'-biphenol, 2,2'-biphenol and 4-phenoxyphenol. The original research proposal was however for the production of 4,4'-biphenol from phenol. The selective dimerisation of phenol to 4,4'-biphenol was possible using Cu(5%)/Attapulgite.

3.4.2.3 Metal loading

Data was collected using Cu/Attapulgite with w/w metal loadings of 1, 3 and 5% (Tables 84-86).

Table 84 Cu(1%)/Attapulgite

Time (min)	Conversion (%)	Selectivity (%)		
		4,4'-biphenol	2,2'-biphenol	4-phenoxyphenol
0-5	5	1	0	2
5-10	3	5	0	1
10-15	1	10	0	3
15-30	1	8	0	0
30-45	1	6	0	0
45-60	<1	t	t	t
60-90	<1	t	t	t

Table 85 Cu(3%)/Attapulgite

Time (min)	Conversion (%)	Selectivity (%)		
		4,4'-biphenol	2,2'-biphenol	4-phenoxyphenol
0-5	14	2	0	1
5-10	11	2	0	1
10-15	11	1	0	1
15-30	11	1	0	t
30-45	7	1	0	t
45-60	7	1	0	t
60-90	3	1	0.0	1

Table 86 Cu(5%)/Attapulgite

Time (min)	Conversion (%)	Selectivity (%)		
		4,4'-biphenol	2,2'-biphenol	4-phenoxyphenol
0-5	24	29	1	2
5-10	30	23	1	2
10-15	23	20	t	1
15-30	9	24	t	2
30-45	2	21	0	5
45-60	1	12	0	4
60-90	1	4	0	4

The initial conversion of phenol increased with metal loading. At a copper loading of 1% conversion of phenol was low, at 3 and 5% loadings the total conversion of phenol was similar (Figure 77). At 5% loading the initial conversion was higher but deactivation more rapid.

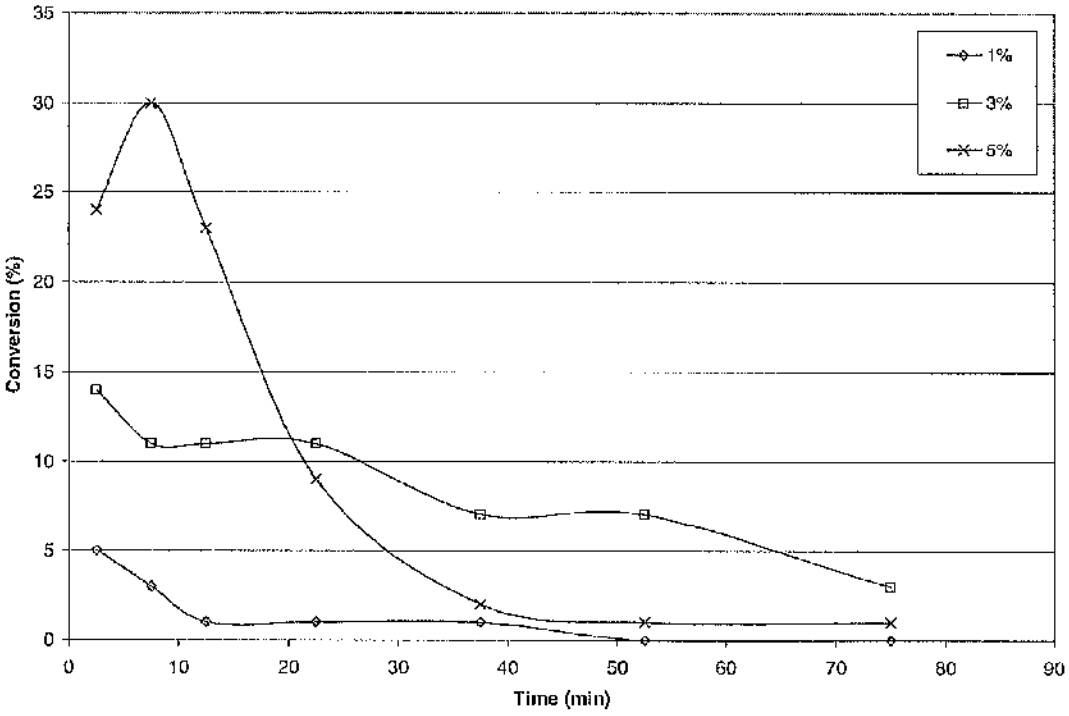

Fig. 77 Conversion of phenol using Cu/Attapulgite with 1, 3 and 5% metal loading.

The selectivity to 4,4'-biphenol, 2,2'-biphenol and 4-phenoxyphenol was much higher at the 5% copper loading compared to the 1 and 3% loadings. The yield of 4,4'-biphenol using Cu(3%)/Attapulgite was <0.5% between 0 and 10 min, at 5% copper loading the yield was 7%.

3.4.2.4 Temperature

Data was collected at 328, 348, 388 and 408 K over Cu(5%)/Attapulgite (Tables 87-90).

Table 87 328 K

Time (min)	Conversion (%)	Selectivity (%)		
		4,4'-biphenol	2,2'-biphenol	4-phenoxyphenol
0-5	30	22	1	7
5-10	22	28	t	7
10-15	12	30	0	4
15-30	2	39	0	5
30-45	2	16	0	3
45-60	1	15	0	7
60-90	<1	13	0	7

Table 88 348 K

Time (min)	Conversion (%)	Selectivity (%)		
		4,4'-biphenol	2,2'-biphenol	4-phenoxyphenol
0-5	24	29	1	2
5-10	30	23	1	2
10-15	23	20	t	1
15-30	9	24	t	2
30-45	2	21	0	5
45-60	1	12	0	4
60-90	1	4	0	4

Table 89 388 K

Time (min)	Conversion (%)	Selectivity (%)		
		4,4'-biphenol	2,2'-biphenol	4-phenoxyphenol
0-5	36	13	2	1
5-10	24	11	2	3
10-15	15	7	t	3
15-30	10	3	0	4
30-45	7	2	0	4
45-60	5	2	0	5
60-90	4	2	0	6

Table 90 408 K

Time (min)	Conversion (%)	Selectivity (%)		
		4,4'-biphenol	2,2'-biphenol	4-phenoxyphenol
0-5	95	2	t	0
5-10	91	7	1	1
10-15	47	9	1	1
15-30	20	8	1	2
30-45	8	6	0	3
45-60	3	9	0	5
60-90	2	4	0	1

Conversion of phenol at 328, 348 and 388 K was similar whilst initial conversion was almost tripled when the temperature was increased from 388 to 408 K. Arrhenius behaviour was not observed and temperature had a complex affect on phenol conversion. The combined selectivity to 4,4'-biphenol, 2,2'-biphenol and 4-phenoxyphenol reduced as temperature was increased.

3.4.2.5 Phenol concentration

Data was collected using 0.02, 0.04 and 0.08 mol L^{-1} solutions of phenol in a 40:60 volume ratio of acetonitrile/ chloroform over Cu(5%)/Attapulgite (Tables 91-93).

Table 91 0.02 mol L^{-1}

Time (min)	Conversion (%)	Selectivity (%)		
		4,4'-biphenol	2,2'-biphenol	4-phenoxyphenol
0-5	50	15	2	1
5-10	81	12	6	5
10-15	55	14	4	4
15-30	25	15	3	4
30-45	10	11	2	3
45-60	4	16	1	6
60-90	2	17	1	5

Table 92 0.04 mol L^{-1}

Time (min)	Conversion (%)	Selectivity (%)		
		4,4'-biphenol	2,2'-biphenol	4-phenoxyphenol
0-5	24	29	1	2
5-10	30	23	1	2
10-15	23	20	t	1
15-30	9	24	t	2
30-45	2	21	0	5
45-60	1	12	0	4
60-90	1	4	0	4

Table 93 0.08 mol L^{-1}

Time (min)	Conversion (%)	Selectivity (%)		
		4,4'-biphenol	2,2'-biphenol	4-phenoxyphenol
0-5	13	7	t	4
5-10	15	14	t	6
10-15	5	21	t	10
15-30	2	24	0	10
30-45	2	8	0	2
45-60	1	9	0	3
60-90	<1	t	0	t

Conversion of phenol decreased as phenol concentration was increased (Figure 78).

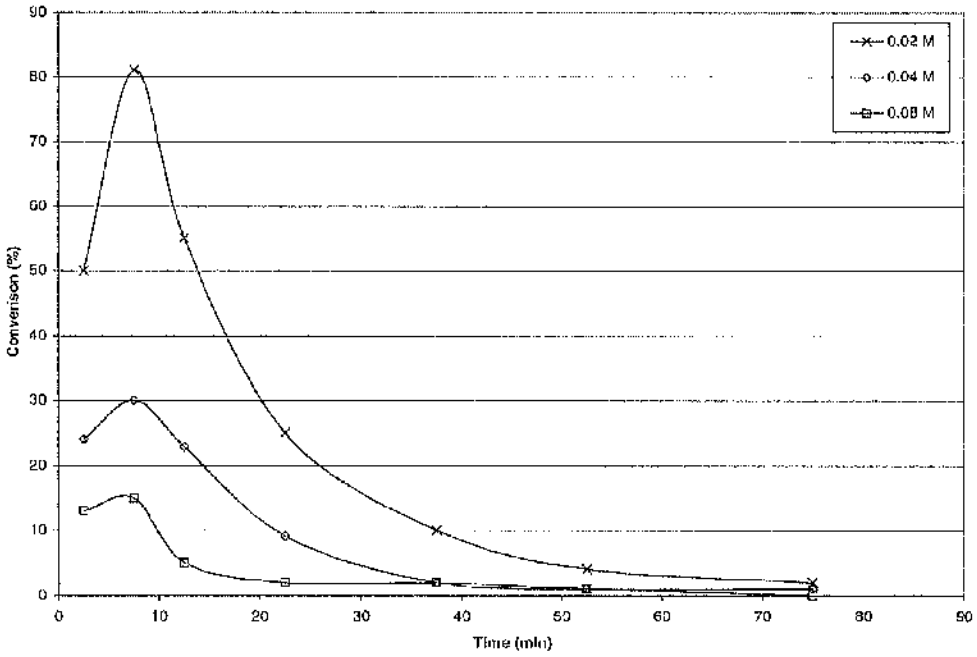

Fig. 78 Conversion of phenol using 0.02, 0.04 and 0.08 mol L^{-1} phenol solutions.

When using any of the three solutions an initial period of activation was observed before almost complete deactivation within 60 min. The selectivities to 4,4'-biphenol and 4-phenoxyphenol were unaffected by the concentration of phenol solution. The conversion of phenol to 2,2'-biphenol was however only detected above trace amounts using the 0.02 mol L^{-1} solution. The overall selectivity to dimers was greatest when using the 0.04 mol L^{-1} phenol solution.

The concentration of phenol affected the WHSV. For an accurate analysis of the affects of concentration the 45 – 60 min data for the 0.02 mol L^{-1} solution was compared with the 15 – 30 min data for 0.04 mol L^{-1} solution and the 10 – 15 min data for the 0.08 mol L^{-1} solution (Table 94).

Table 94 Various concentrations of phenol at equivalent WHSV.

Conc. (mol L^{-1})	Conversion (%)	Selectivity (%)		
		4,4'-biphenol	2,2'-biphenol	4-phenoxyphenol
0.02	4	16	1	6
0.04	9	24	t	2
0.08	5	21	t	10

The conversion of phenol and selectivity toward 4,4'-biphenol, 2,2'-biphenol and 4-phenoxyphenol varied with concentration at comparable values of WHSV.

Calculating the order of reaction required reaction rate data. For a flow system the rate of reaction was calculated using Equation 2, Section 3.3.2.5. The rates of reaction (Table 95) were calculated from the initial conversion of phenol at each concentration. Plotting the natural log of phenol concentration against the natural log of rate gave a straight-line graph (Figure 79). The gradient of the line was *zero* and was equal to the order of reaction with respect to phenol.

Table 95 Calculated reaction rate.

Phenol concentration (mol L^{-1})	Rate of reaction (moles min^{-1} g^{-1})
0.02	7.17×10^{-6}
0.04	7.47×10^{-6}
0.08	7.61×10^{-6}

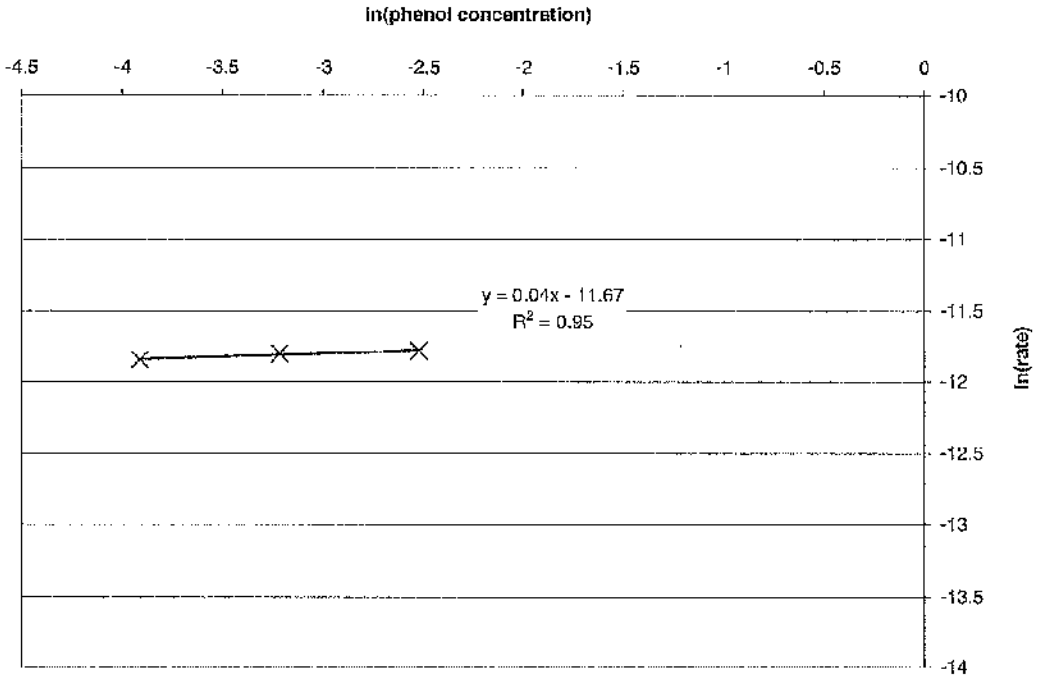

Fig. 79 Calculating the order of reaction.

3.4.2.6 Low temperature pre-treatment

Data was collected after the low temperature pre-treatment of Cu(5%)/Attapulgite in air, an oxygen rich and oxygen deficient atmosphere (Tables 96-98).

Table 96 Low temperature pre-treatment, air atmosphere.

Time (min)	Conversion (%)	Selectivity (%)		
		4,4'-biphenol	2,2'-biphenol	4-phenoxyphenol
0-5	57	15	1	9
5-10	36	20	1	5
10-15	22	23	2	6
15-30	13	24	2	6
30-45	7	15	1	5
45-60	3	21	0	7
60-90	2	5	0	3

Table 97 Low temperature pre-treatment, nitrogen atmosphere.

Time (min)	Conversion (%)	Selectivity (%)		
		4,4'-biphenol	2,2'-biphenol	4-phenoxyphenol
0-5	68	14	1	6
5-10	34	15	1	3
10-15	15	14	t	2
15-30	9	5	0	1
30-45	7	3	0	1
45-60	3	3	0	0
60-90	2	3	0	0

Table 98 Low temperature pre-treatment, oxygen atmosphere.

Time (min)	Conversion (%)	Selectivity (%)		
		4,4'-biphenol	2,2'-biphenol	4-phenoxyphenol
0-5	49	20	1	6
5-10	32	22	1	5
10-15	16	22	t	4
15-30	3	27	0	6
30-45	3	8	0	2
45-60	2	7	0	3
60-90	1	5	0	3

The conversion of phenol after low temperature pre-treatment of the catalyst at 348 K using air, nitrogen or oxygen has been compared against the standard reaction without pre-treatment (Figure 80).

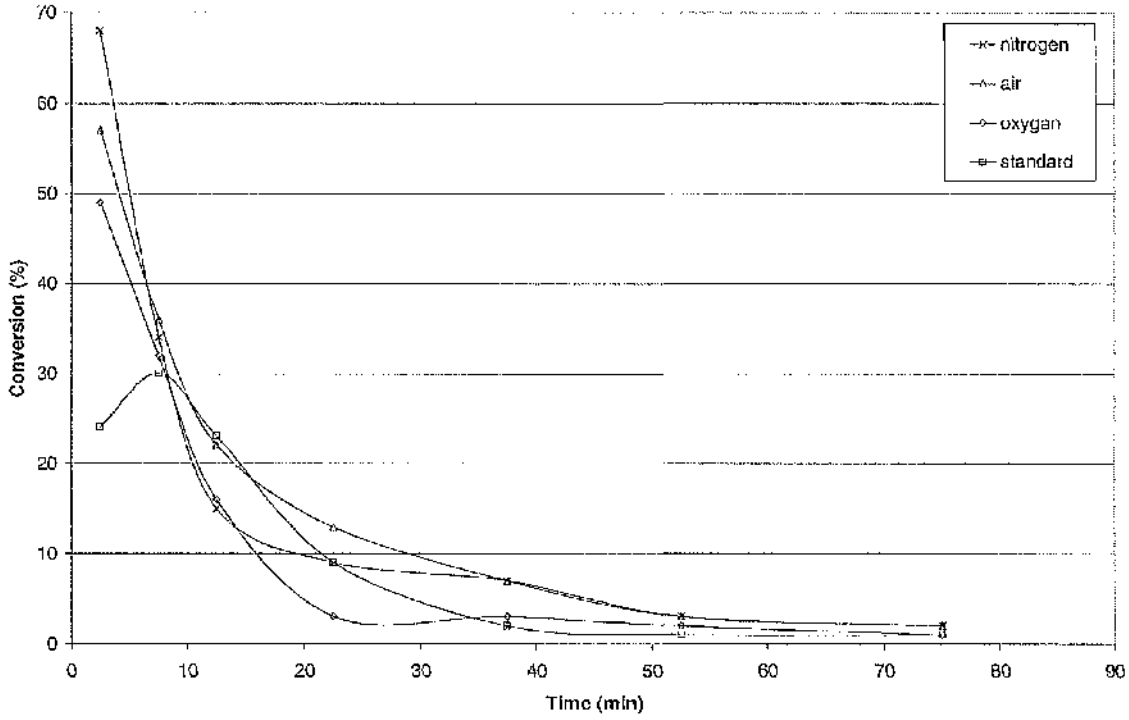

Fig. 80 Conversion of phenol after low temperature pre-treatment compared to the standard reaction.

Low temperature pre-treatment at 348 K increased the conversion of phenol between 0 and 10 min. Conversion increased as the partial pressure of oxygen decreased. The characteristic activation between 0 and 10 min observed using standard reaction conditions was not observed after pre-treatment.

The selectivities to 4,4'-biphenol, 2,2'-biphenol and 4-phenoxyphenol were increased by pre-treatment of the catalyst. The yields of 4,4'-biphenol and 4-phenoxyphenol were increased by pre-treatment but largely unaffected by the partial pressure of oxygen. The yield of 2,2'-biphenol remained low with or without pre-treatment of the catalyst.

3.4.2.7 High temperature pre-treatment

Data was collected after the high temperature pre-treatment of Cu(5%)/Attapulgite at 773 K in nitrogen, air and oxygen (Tables 99 to 101).

Table 99 High temperature pre-treatment, nitrogen atmosphere.

Time (min)	Conversion (%)	Selectivity (%)		
		4,4'-biphenol	2,2'-biphenol	4-phenoxyphenol
0-5	1	11	0	3
5-10	1	9	0	3
10-15	3	8	0	2
15-30	4	4	0	1
30-45	7	2	0	1
45-60	9	1	0	1
60-90	8	0	0	0

Table 100 High temperature pre-treatment, air atmosphere.

Time (min)	Conversion (%)	Selectivity (%)		
		4,4'-biphenol	2,2'-biphenol	4-phenoxyphenol
0-5	7	17	0	6
5-10	5	18	0	5
10-15	3	11	0	4
15-30	2	10	0	3
30-45	1	8	0	3
45-60	1	8	0	0
60-90	1	4	0	0

Table 101 High temperature pre-treatment, oxygen atmosphere.

Time (min)	Conversion (%)	Selectivity (%)		
		4,4'-biphenol	2,2'-biphenol	4-phenoxyphenol
0-5	9	19	0	7
5-10	8	16	0	4
10-15	4	16	0	3
15-30	2	9	0	3
30-45	2	8	0	2
45-60	2	8	0	1
60-90	1	5	0	1

Conversion of phenol was reduced by high temperature pre-treatment of the catalyst at 773 K. After pre-treatment in air or oxygen the subsequent phenol conversions were similar. When nitrogen was used to pre-treat Cu(5%)/Attapulgite the conversion of phenol increased with TOS, as it did for Cu(6%)/Zeolite-Y (Section 3.3.2.7).

The selectivities to 4,4'-biphenol and 4-phenoxyphenol reduced with TOS regardless of the pre-treatment conditions. Nitrogen pre-treatment caused the lowest selectivity to 4,4'-biphenol. The dimerisation of phenol to 2,2'-biphenol went undetected after all of the pre-treatments.

3.5 Catalyst deactivation and regeneration

3.5.1 Metal-ion leaching

The metal-ion leaching of copper from Cu(6%)/Zeolite-Y and silver from Ag(18%)/Zeolite-Y was investigated using the procedure described in Section 2.4.4. The AAS of reaction samples confirmed only background levels of these ions in solution. No metal-ion leaching from either catalyst support was detected.

3.5.2 Oxidation state of copper

The diffuse reflectance UV spectrum of Cu(6%)/Zeolite-Y displayed a distinctive band at 13,000 cm^{-1} (760 nm) (Figure 81).

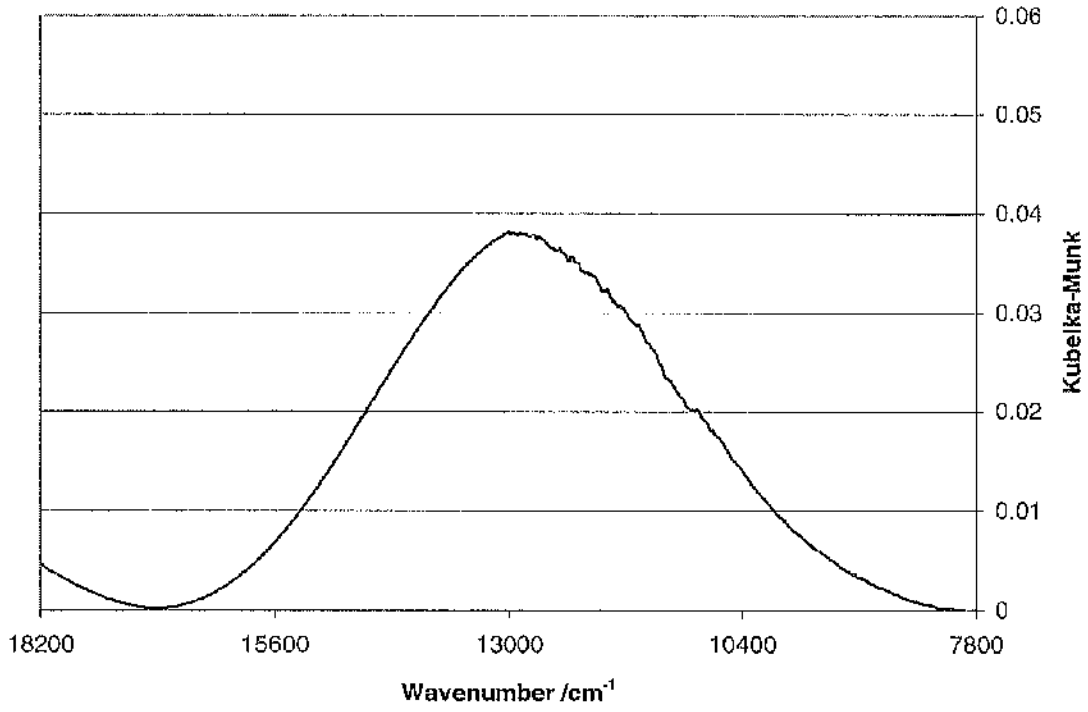

Fig. 81 The diffuse reflectance UV spectrum of Cu(6%)/Zeolite-Y.

This spectrum was measured at room-temperature although when *in situ* the catalyst temperature ranged from 308 to 408 K. Temperature was however unlikely to affect the oxidation state of copper below ca. 400 K.[38] This confirmed Cu^{2+} species were present in Cu(6%)/Zeolite-Y.

The diffuse reflectance UV spectrum of Cu(5%)/Attapulgite (Figure 82) also displayed a distinctive band at 13,000 cm^{-1}.

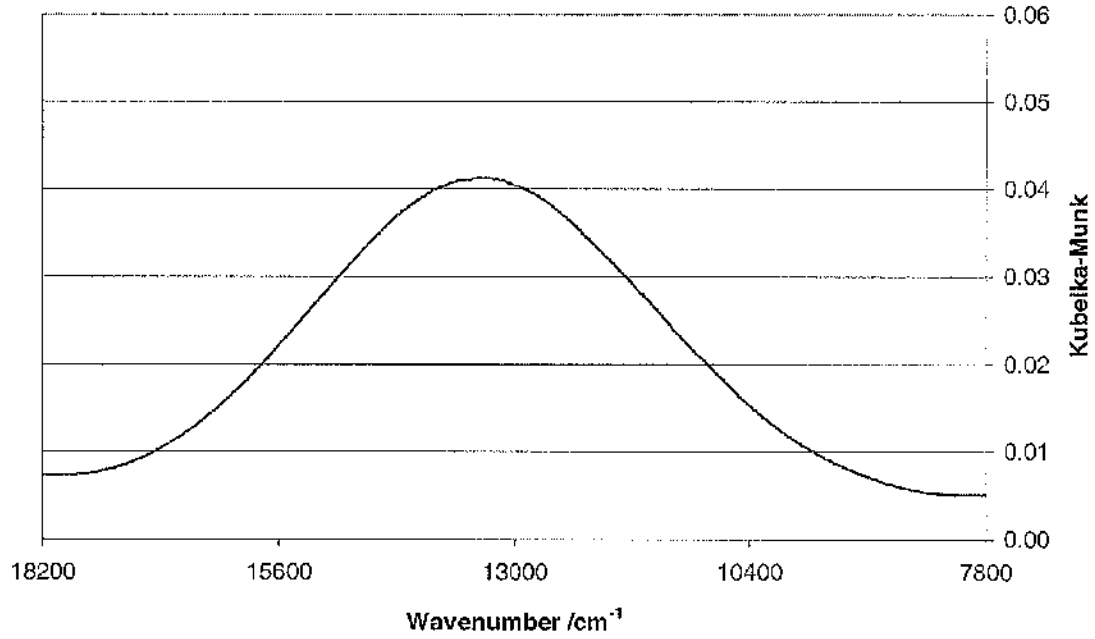

Fig. 82 The diffuse reflectance UV spectrum of Cu(5%)/Attapulgite.

The diffuse reflectance UV spectra of Cu(6%)/Zeolite-Y and Cu(5%)/Attapulgite were of *fresh* catalyst. The spectra of both catalysts after reaction were indistinguishable from those in Figures 81 and 82.

3.5.3 Surface Area

The Brunauer Emmett Teller (BET) analysis of zeolites and clays can be used only to compare the surface area and average pore diameter of the catalysts, in this case before and after reactions (Table 102).

Table 102 BET of Cu(6%)/Zeolite-Y and Cu(5%)/Attapulgite.

Catalyst		*Surface area /m^2g^{-1}*	*Ave. Pore Diameter /nm*
Cu(6%)/Zeolite-Y	Fresh	580 ±23.3	2.29
	Spent	518 ±19.7	2.29
Cu(5%)/Attapulgite	Fresh	125 ±2.4	4.91
	Spent	104 ±2.5	4.11

The surface area of both catalysts was lower after reaction. There was an 11% decrease in surface area for Cu(6%)/Zeolite-Y and a 17% decrease for Cu(5%)/Attapulgite. The average pore diameter of Cu(6%)/Zeolite-Y was unaffected by the dimerisation of phenol. The average pore diameter of Cu(5%)/Attapulgite decreased by 16%.

3.5.4 Crystalline structure

The X-ray Diffraction (XRD) patterns of various Zeolite-Y catalysts were measured and matched with those published in the literature for Zeolite-Y[108] (Figure 83).

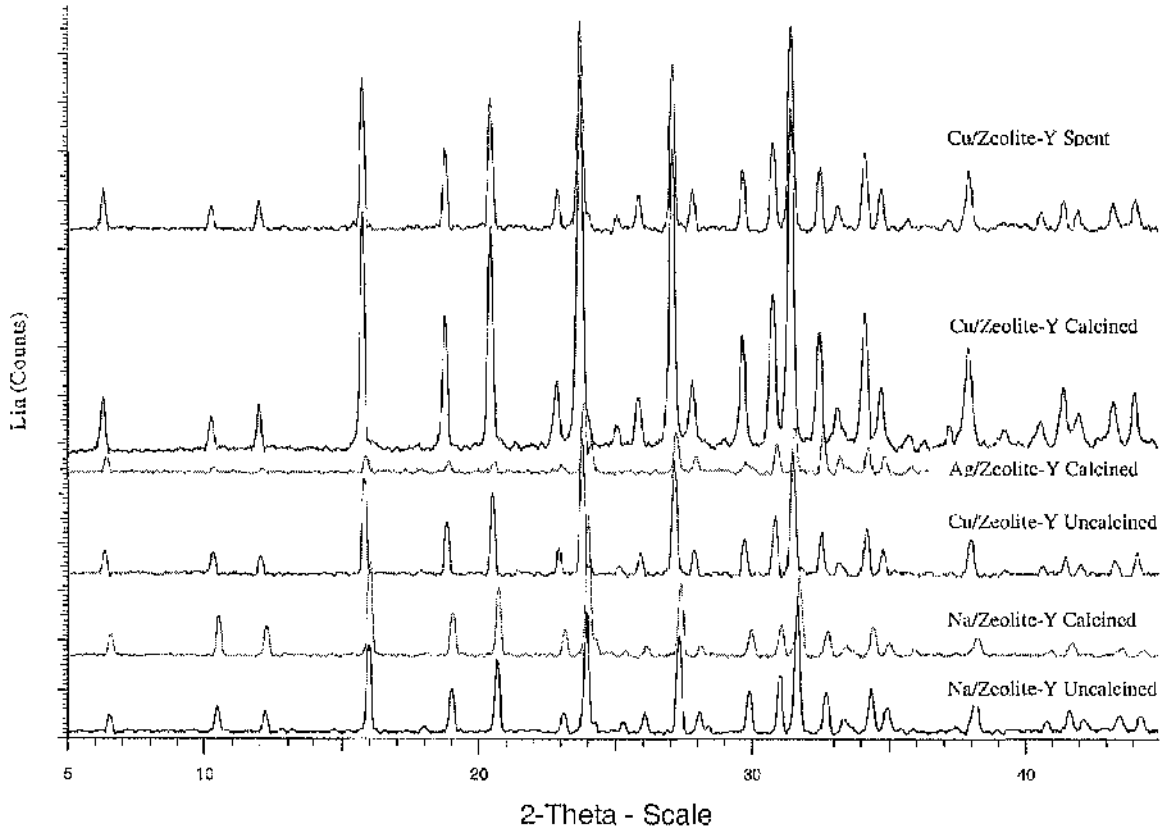

Fig. 83 XRD patterns of various Zeolite-Y samples.

The positions of all peaks were comparable for the *fresh* and *spent* catalyst samples. Peak intensities were however lower for the *spent* Cu(6%)/Zeolite-Y sample compared to the *fresh*. The left-shift of peaks after cation-exchange of sodium for copper or silver ions indicated dealumination of Zeolite-Y. Dealumination is the removal of tetrahedrally coordinated aluminiums from the zeolite framework. This affects the physiochemical, ion-exchange and catalytic properties of the material.

The X-ray Diffraction (XRD) patterns of various Attapulgite catalysts were measured (Figure 84).

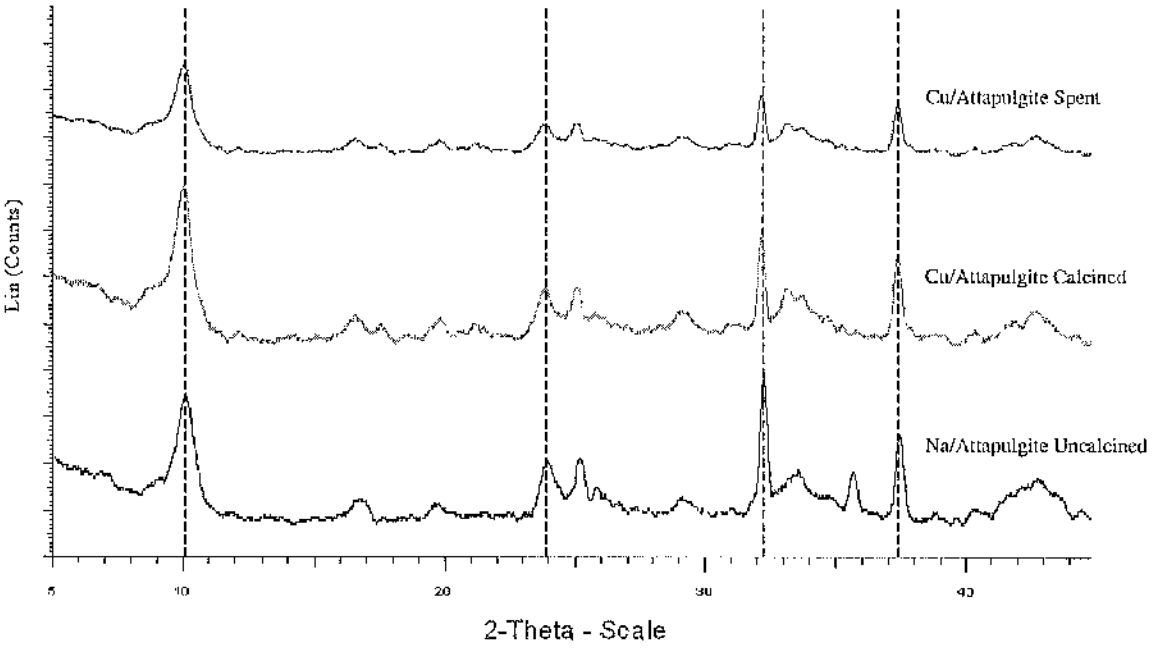

Fig. 84 XRD patterns of various Attapulgite samples.

The positions of all peaks were comparable for the *fresh* and *spent* catalyst samples. Peak intensities were lower for the *spent* Cu(5%)/Attapulgite sample compared to the *fresh*. Peak positions were similar before and after cation-exchange of sodium for copper suggesting limited dealumination of Attapulgite.

3.5.5 Pre-treatment with the reaction products

The catalytic activity and selectivity of Cu(6%)/Zeolite-Y were investigated after pre-treatment of the catalyst with acetonitrile and 4,4'-biphenol, 2,2'-biphenol and 4-phenoxyphenol in acetonitrile. Cu(6%)/Zeolite-Y was capable of catalysing the conversion of the biphenol compounds back to phenol. Subsequent dimerisation of this phenol and/or isomerisation of compounds was also possible. The catalyst was pre-treated for 30 min using a 1 ml min^{-1} flow of acetonitrile. After pre-treatment the flow of acetonitrile was changed for the standard 0.04 mol L^{-1} phenol in acetonitrile solution (Table 103).

Table 103 Pre-treated with acetonitrile.

Time (min)	Conversion (%)	Selectivity (%)		
		4,4'-biphenol	2,2'-biphenol	4-phenoxyphenol
0-5	100	t	0	t
5-10	97	1	t	1
10-15	60	4	t	1
15-30	15	8	1	2
30-45	4	15	2	2
45-60	2	19	3	4
60-90	2	17	3	3

The conversion of phenol was considerably increased by pre-treatment of the catalyst with acetonitrile. In comparison to the standard reaction (Table 104), conversion of phenol was only similar after 30 min TOS.

Table 104 Standard reaction.

Time (min)	Conversion (%)	Selectivity (%)		
		4,4'-biphenol	2,2'-biphenol	4-phenoxyphenol
0-5	16	14	0	4
5-10	17	12	1	3
10-15	12	13	1	4
15-30	6	13	1	4
30-45	4	12	2	5
45-60	3	12	2	4
60-90	2	12	2	5

Selectivity to 2,2'-biphenol was largely unaffected by pre-treatment. Conversion to 4,4'-biphenol and 4-phenoxyphenol was reduced at first, only recovering after ca. 60 min. The yields of 4,4'-biphenol and 4-phenoxyphenol were reduced from ≤7% and ≤1% respectively to ≤2% and ≤1% after pre-treatment.

During the conversion of phenol after pre-treatment with 4,4'-biphenol, 2,2'-biphenol or 4-phenoxyphenol (Tables 106, 108 and 110), the selectivity to the dimer used for pre-treatment (*) was always >100%. Yield data cannot therefore be calculated from this conversion and selectivity data. The catalyst was not flushed after pre-treatment and so was saturated with the dimer when the phenol in acetonitrile flow was started. This meant more dimer products were leaving the system than could have been produced by phenol dimerisation, hence >100% selectivity. The total number of moles of 4,4'-biphenol, 2,2'-biphenol or 4-phenoxyphenol removed from the reactor during the feed of phenol in acetonitrile after pre-treatment equated to ca. 15% of the dimer *unaccounted for* during the pre-treatment. All of the dimer retained by the catalyst could be recovered using HF digestion and accounted for using CHN analysis. The pre-treatment of Cu(6%)/Zeolite-Y with each dimer reduced the yield of the other dimers produced during subsequent phenol dimerisation to ca. 20% of the yield obtained during a standard reaction without pre-treatment.

Fresh Cu(6%)/Zeolite-Y catalyst was pre-treated for 30 min using a 1 ml min^{-1} flow of 4,4'-biphenol in acetonitrile (Table 105).

Table 105 Conversion of 4,4'-biphenol.

Time (min)	Conversion (%)	Selectivity (%)		
		Phenol	2,2'-biphenol	4-phenoxyphenol
0-5	93	14	t	0
5-10	38	4	t	t
10-15	9	8	t	1
15-30	3	3	t	2

The conversion of 4,4'-biphenol was high although most of this conversion was to byproducts and/or coke. The dimers 2,2'-biphenol and 4-phenoxyphenol were detected but selectivity to phenol was much higher, the maximum yield of phenol was 13%.

After pre-treatment the flow of 4,4'-biphenol in acetonitrile was changed for the standard 0.04 mol L^{-1} phenol in acetonitrile solution (Table 106).

Table 106 Reaction after pre-treatment with 4,4'-biphenol in acetonitrile.

Time (min)	Conversion (%)	Selectivity (%)		
		4,4'-biphenol *	2,2'-biphenol	4-phenoxyphenol
0-5	100	170	t	t
5-10	97	138	t	t
10-15	36	123	2	t
15-30	4	313	12	2
30-45	<1	t	t	t
45-60	<1	t	t	t
60-90	<1	t	t	t

The conversion of phenol after pre-treatment with 4,4'-biphenol in acetonitrile was similar to the conversion of phenol after pre-treatment with only acetonitrile. Conversions were identical between 0 and 10 min although the catalyst then deactivated more rapidly after the 4,4'-biphenol in acetonitrile pre-treatment between 10 and 90 min. The acetonitrile only pre-treatment (Table 103) reduced the conversion of phenol to 4,4'-biphenol, 2,2'-biphenol and 4-phenoxyphenol compared with the standard reaction. Pre-treatment with 4,4'-biphenol reduced to trace levels the selectivity to 2,2'-biphenol and 4-phenoxyphenol.

Fresh Cu(6%)/Zeolite-Y catalyst was pre-treated for 30 min using a 1 ml min^{-1} flow of 2,2'-biphenol in acetonitrile (Table 107).

Table 107 Conversion of 2,2'-biphenol.

Time (min)	Conversion (%)	Selectivity (%)		
		4,4'-biphenol	Phenol	4-phenoxyphenol
0-5	92	1	10	t
5-10	47	t	6	t
10-15	20	1	6	1
15-30	8	1	4	2

The conversion of 2,2'-biphenol catalysed by Cu(6%)/Zeolite-Y was greater than the conversion of 4,4'-biphenol. The selectivity to phenol was similar and as before, trace amounts of the other two dimers, in this case 4,4'-biphenol and 4-phenoxyphenol were detected.

After pre-treatment the flow of 2,2'-biphenol in acetonitrile was changed for the standard 0.04 mol L^{-1} phenol in acetonitrile solution (Table 108).

Table 108 Reaction after pre-treatment with 2,2'-biphenol in acetonitrile.

Time (min)	Conversion (%)	Selectivity (%)		
		4,4'-biphenol	2,2'-biphenol *	4-phenoxyphenol
0-5	100	t	172	t
5-10	84	t	158	t
10-15	24	1	152	t
15-30	8	1	113	1
30-45	<1	t	t	t
45-60	<1	t	t	t
60-90	<1	t	t	t

The conversion of phenol and selectivity to 4,4'-biphenol, 2,2'-biphenol and 4-phenoxyphenol after pre-treatment of Cu(6%)/Zeolite-Y with 2,2'-biphenol in acetonitrile were similar to those after pre-treatment with 4,4'-biphenol in acetonitrile and only acetonitrile.

Finally, fresh Cu(6%)/Zeolite-Y catalyst was pre-treated for 30 min using a 1 ml min^{-1} flow of 4-phenoxyphenol in acetonitrile (Table 109).

Table 109 Conversion of 4-phenoxyphenol.

Time (min)	Conversion (%)	Selectivity (%)		
		4,4'-biphenol	2,2'-biphenol	Phenol
0-5	100	t	t	3
5-10	57	t	t	7
10-15	30	t	t	11
15-30	10	t	t	13

The conversion of 4-phenoxyphenol was even greater than the conversion of 2,2'-biphenol or 4,4'-biphenol. The selectivity to phenol increased with TOS.

After pre-treatment the flow of 4-phenoxyphenol in acetonitrile was changed for the standard 0.04 mol L^{-1} phenol in acetonitrile solution (Table 110).

Table 110 Reaction after pre-treatment with 4-phenoxyphenol in acetonitrile.

Time (min)	Conversion (%)	Selectivity (%)		
		4,4'-biphenol	2,2'-biphenol	4-phenoxyphenol*
0-5	99	t	0	147
5-10	77	1	t	150
10-15	18	1	1	137
15-30	2	4	1	238
30-45	<1	t	t	t
45-60	<1	t	t	t
60-90	<1	t	t	t

The affects of Cu(6%)/Zeolite-Y pre-treatment with 4-phenoxyphenol in acetonitrile were similar to those observed after pre-treatment with 4,4'-biphenol or 2,2'-biphenol in acetonitrile or only acetonitrile. The initial conversion of phenol was increased, whilst pre-treatment with 4-phenoxyphenol reduced to trace levels the selectivity to 4,4'-biphenol and 2,2'-biphenol.

3.5.6 Thermal analysis

Figures 85 to 89 provide the Thermogravimetric analysis (TGA) of *fresh* and *spent* samples of Cu(6%)/Zeolite-Y in a flow of 2%O_2/Ar.

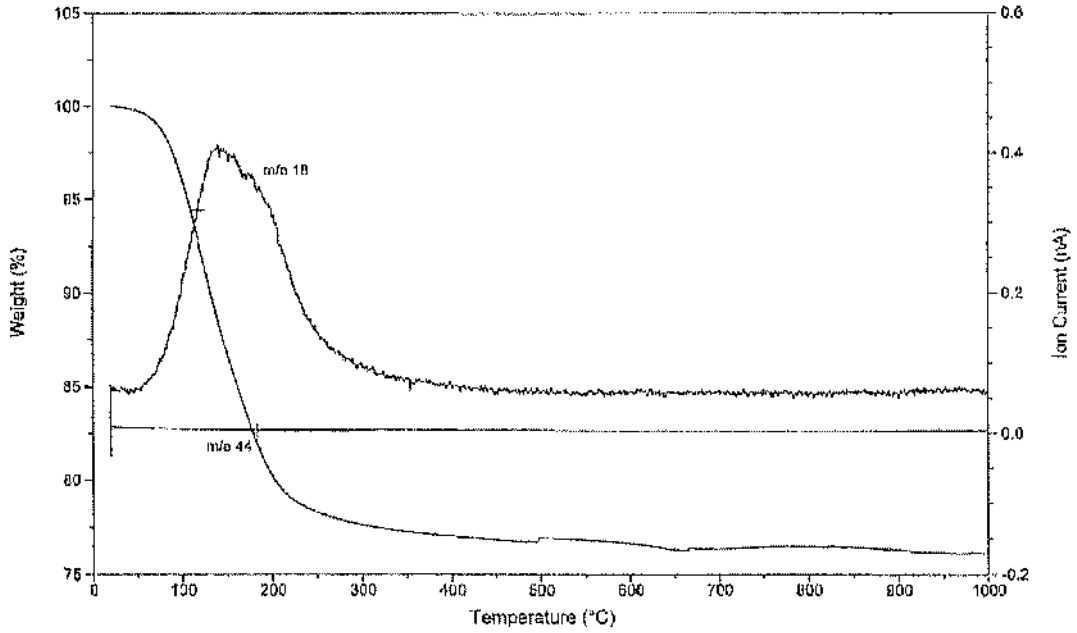

Fig. 85 TGA of *fresh* Cu(6%)/Zeolite-Y.

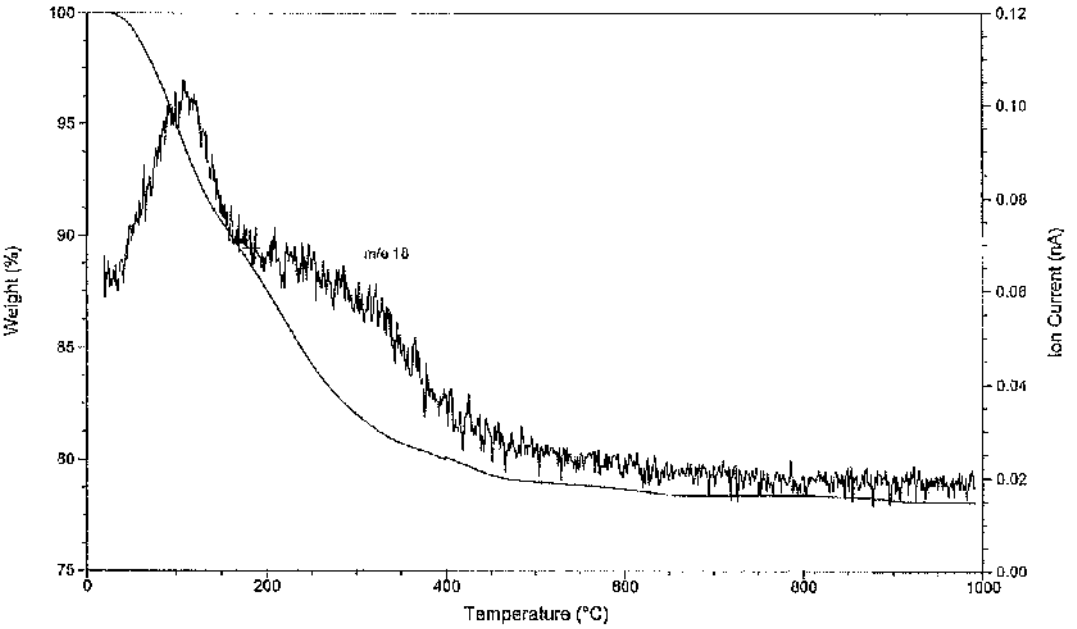

Fig. 86 TGA of *spent* Cu(6%)/Zeolite-Y (I).

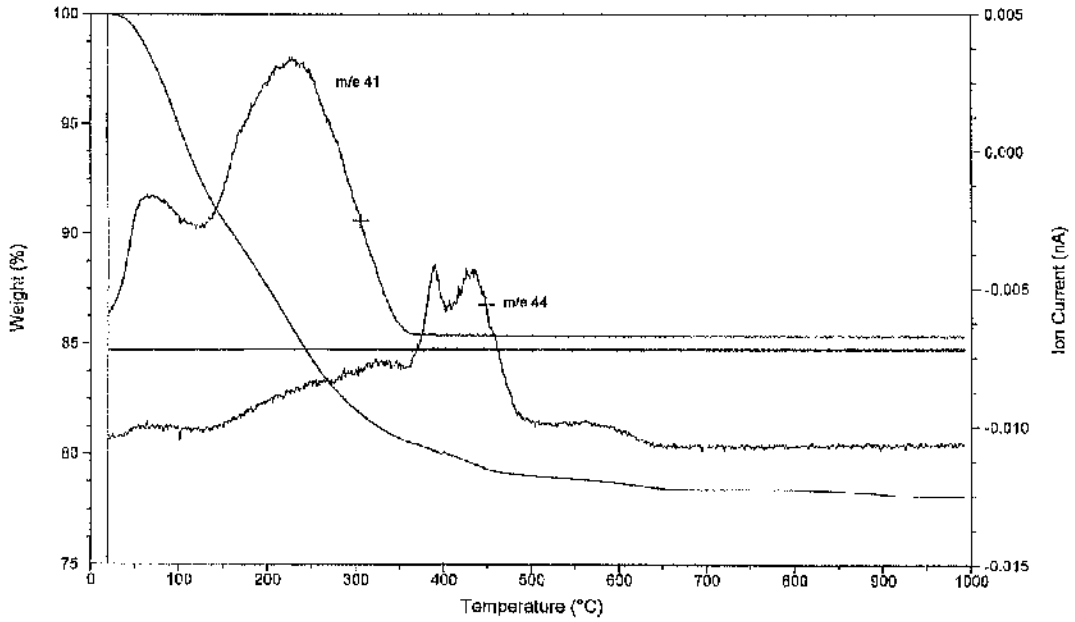

Fig. 87 TGA of *spent* Cu(6%)/Zeolite-Y (II).

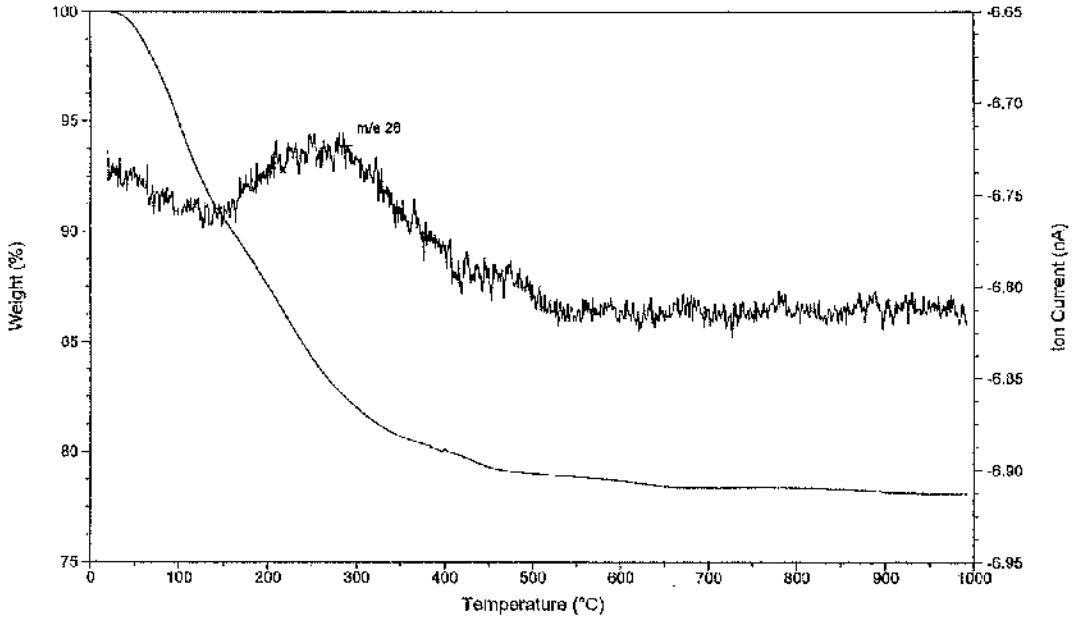

Fig. 88 TGA of *spent* Cu(6%)/Zeolite-Y (III).

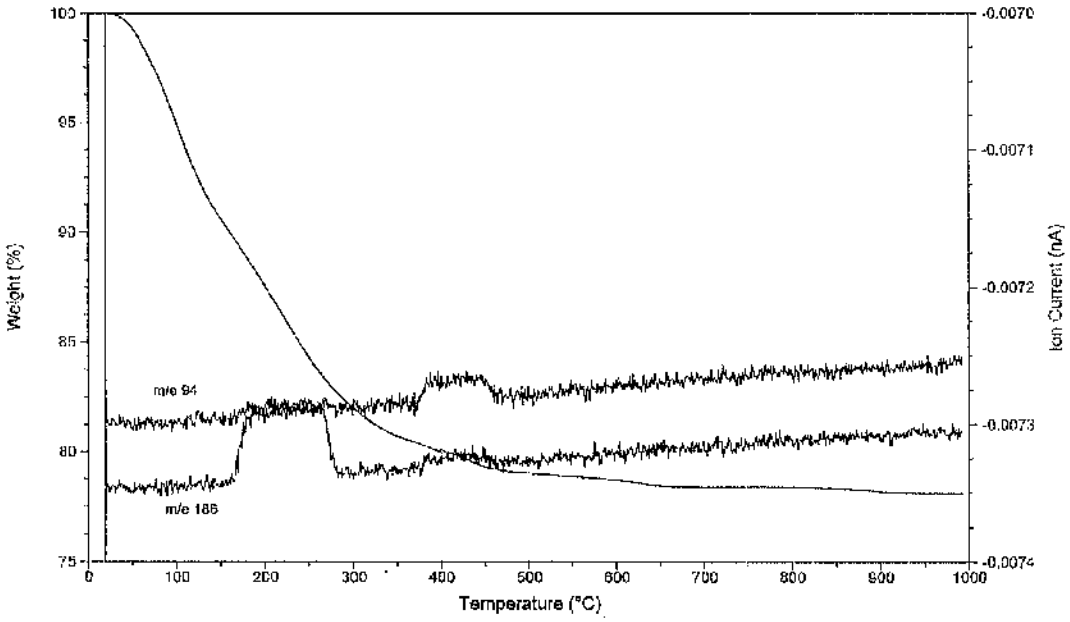

Fig. 89 TGA of *spent* Cu(6%)/Zeolite-Y (IV).

The thermal analysis of *fresh* Cu(6%)/Zeolite-Y confirmed only water was removed during heating to 1273 K at 10^{o} min^{-1}. The *spent* Cu(6%)/Zeolite-Y catalyst liberated carbon monoxide (m/e = 28), carbon dioxide (m/e = 44), acetonitrile (m/e = 41), phenol (m/e = 94), biphenol (m/e = 186) and water (m/e = 18). The mass spectra confirmed two distinguishable peaks for water and acetonitrile and at least four peaks in the mass spectrum trace for carbon dioxide. The removal of all species with the exception of carbon dioxide was confirmed below 773 K. The mass spectrum signal for carbon dioxide returned to its baseline at 923 K.

Figures 90 to 91 provide the Thermogravimetric analysis (TGA) of *fresh* and *spent* samples of Cu(5%)/Attapulgite.

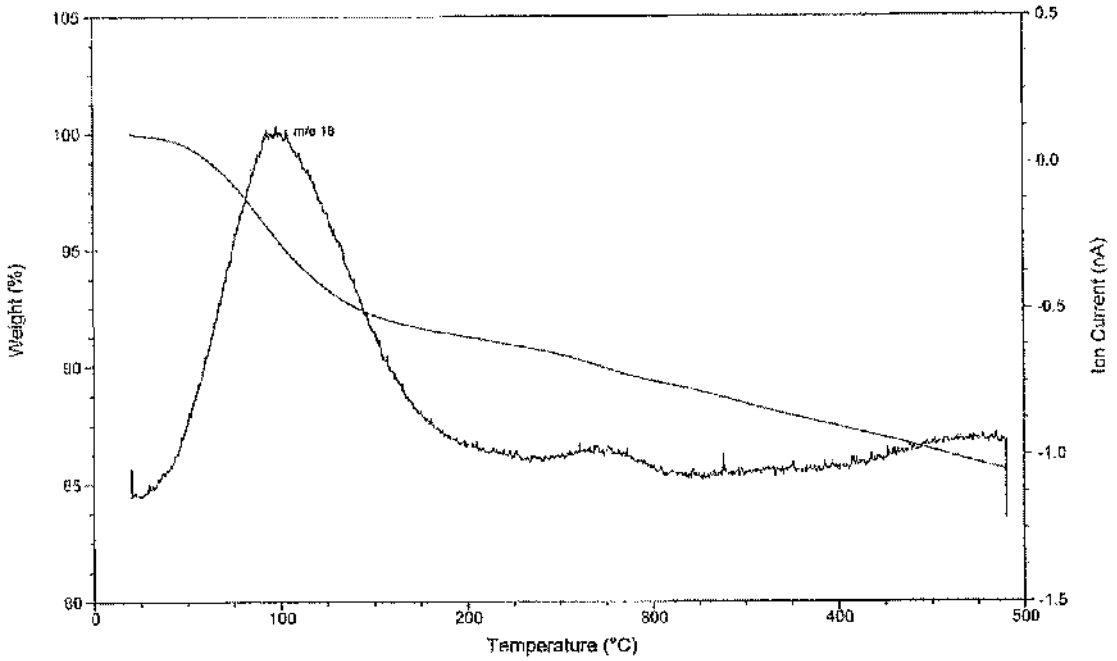

Fig. 90 TGA of *fresh* Cu(5%)/Attapulgite.

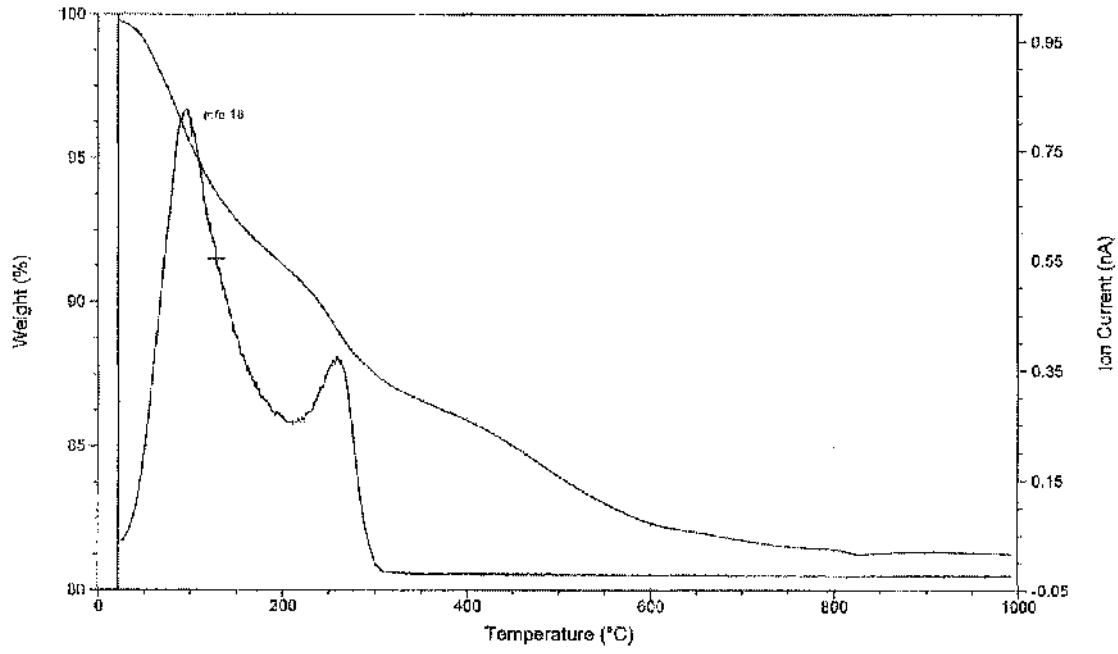

Fig. 91 TGA of *spent* Cu(5%)/Attapulgite (I).

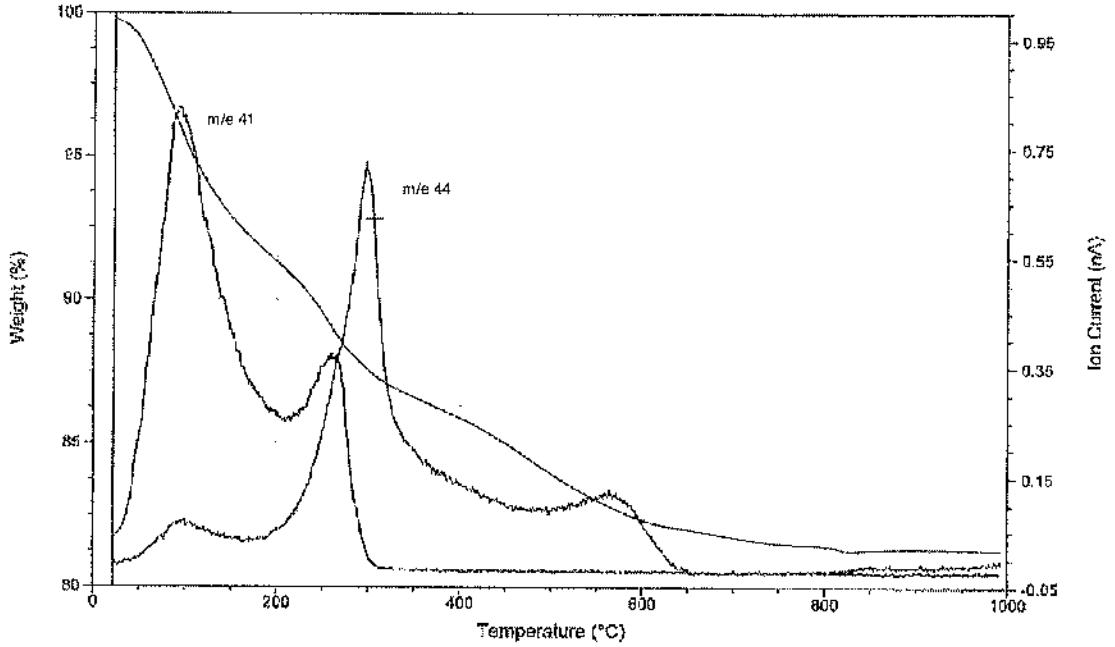

Fig. 92 TGA of *spent* Cu(5%)/Attapulgite (II).

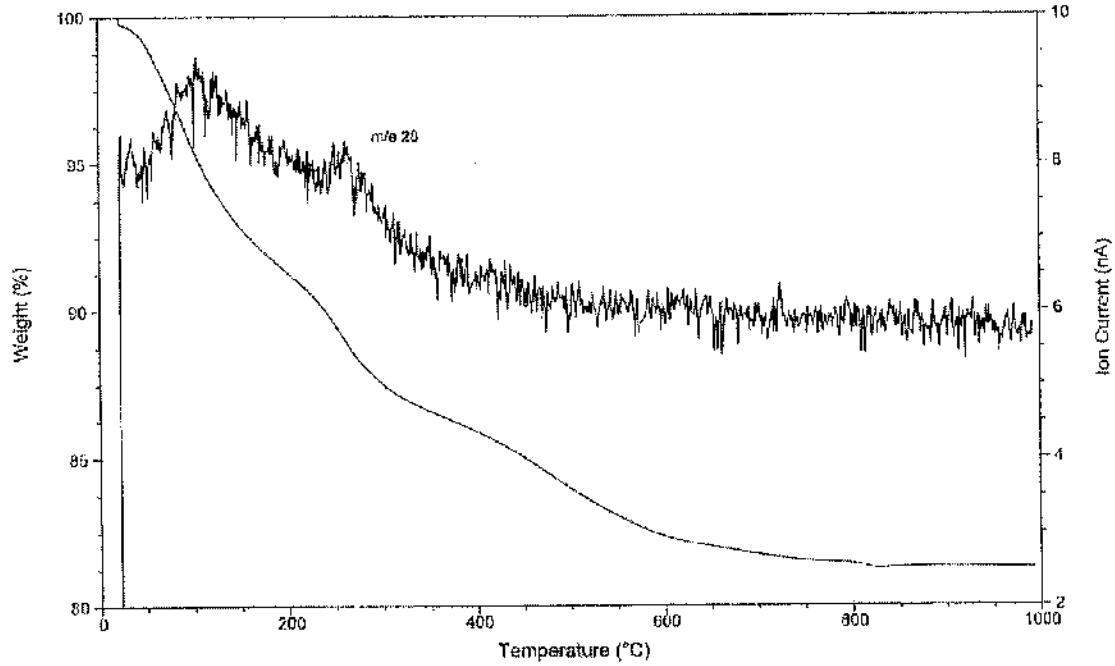

Fig. 93 TGA of *spent* Cu(5%)/Attapulgite (III).

The thermal analysis of *fresh* Cu(5%)/Attapulgite confirmed only water was removed during heating to 1273 K at 10^{o} min^{-1}. The *spent* Cu(5%)/Attapulgite catalyst liberated carbon monoxide (m/e = 28), carbon dioxide (m/e = 44), acetonitrile (m/e = 41) and water (m/e = 18). The mass spectra confirmed two distinguishable peaks for water and acetonitrile and three peaks in the mass spectrum trace for carbon dioxide. The removal of all species with the exception of carbon dioxide was confirmed below 773 K. The mass spectrum signal for carbon dioxide returned to its baseline at 923 K.

3.5.7 *In situ* and *ex situ* catalyst regeneration

The TGA of a *spent* Cu(6%)/Zeolite-Y had confirmed the removal of carbon monoxide, carbon dioxide, acetonitrile, phenol, biphenol and water below 773 K. The TGA of Cu^{I} oxide (Figure 94) confirmed the uptake of oxygen (m/e = 32) started at 573 K and continued above 873 K. The up-take of oxygen indicated the oxidation of Cu^{I} to Cu^{II}.

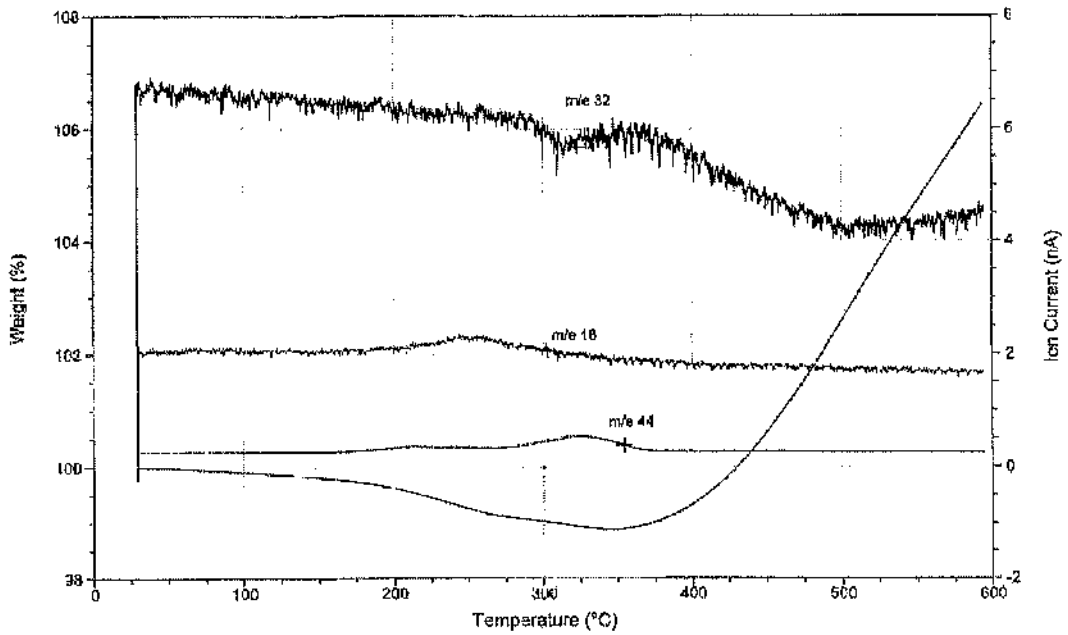

Fig. 94 TGA of Cu_2O in a flow of 2% oxygen in argon.

The *in situ* regeneration of Cu(6%)/Zeolite-Y was not successful. Activity of the regenerated catalyst was similar to activity after the *in situ* high temperature pre-treatment in air (Table 63).

The *ex situ* regeneration of Cu(6%)/Zeolite-Y confirmed that catalyst activity could be regenerated (Table 111).

Table 111 *Ex situ* regenerated.

Time (min)	Conversion (%)	Selectivity (%)		
		4,4'-biphenol	2,2'-biphenol	4-phenoxyphenol
0-5	87	2	1	t
5-10	41	7	8	1
10-15	15	11	13	3
15-30	7	11	13	4
30-45	2	17	19	7
45-60	2	20	22	9
60-90	1	16	18	8

Table 112 Standard

Time (min)	Conversion (%)	Selectivity (%)		
		4,4'-biphenol	2,2'-biphenol	4-phenoxyphenol
0-5	16	14	0	4
5-10	17	12	1	3
10-15	12	13	1	4
15-30	6	13	1	4
30-45	4	12	2	5
45-60	3	12	2	4
60-90	2	12	2	5

The conversion of phenol by the regenerated catalyst was higher than the conversion of phenol by the *fresh* catalyst. The combined yield of 4,4'-biphenol, 2,2'-biphenol and 4-phenoxyphenol was 18% over the 90 min reaction using the regenerated catalyst, compared to 11% during the standard reaction. Selectivity to 4,4'-biphenol, 4-phenoxyphenol and especially 2,2'-biphenol was increased using the regenerated catalyst and increased with TOS.

3.5.8 HF digestion of spent catalyst

The coke content of spent Cu(6%)/Zeolite-Y and Cu(5%)/Attapulgite catalyst was determined using HF digestion of the Zeolite-Y and Attapulgite support. The soluble coke was then analysed by HPLC and the insoluble by CHN analysis. Tables 113 and 114 are the conversion and selectivity data for standard reactions using Cu(6%)/Zeolite-Y and Cu(5%)/Attapulgite.

Table 113 Standard reaction using Cu(6%)/Zeolite-Y.

Time (min)	Conversion (%)	Selectivity (%)		
		4,4'-biphenol	2,2'-biphenol	4-phenoxyphenol
0-5	16	14	0	4
5-10	17	12	1	3
10-15	12	13	1	4
15-30	6	13	1	4
30-45	4	12	2	5
45-60	3	12	2	4
60-90	2	12	2	5

Table 114 Standard reaction using Cu(5%)/Attapulgite.

Time (min)	Conversion (%)	Selectivity (%)		
		4,4'-biphenol	2,2'-biphenol	4-phenoxyphenol
0-5	24	29	1	2
5-10	30	23	1	2
10-15	23	20	t	1
15-30	9	24	t	2
30-45	2	21	0	5
45-60	1	12	0	4
60-90	1	4	0	4

The selectivity to 4,4'-biphenol, 2,2'-biphenol and 4-phenoxyphenol using Cu(6%)/Zeolite-Y summed to ca. 20%. The remaining 80% was conversion of phenol to byproducts and coke. A typical integrator printout from the HPLC analysis of reaction samples (Section 2.5.2, Figure 63) had five or six peaks between 6 and 15 min that corresponded to byproducts of the dimerisation reaction. Examples of the possible byproducts were given in Section 2.5.2, Figure 64.

In addition to byproducts, some phenol was converted to coke retained in the catalyst support during a reaction. The HPLC integrator printout from the analysis of the soluble coke is reproduced in Figure 95. The CHN analysis of the insoluble coke is summarised in Tables 115 and 116.

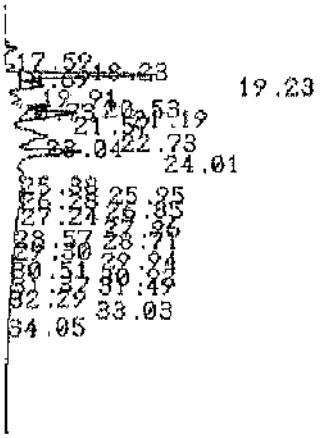

Fig. 95 HPLC integrator printout of soluble coke from Cu(6%)/Zeolite-Y.

Table 115 CHN analysis of insoluble coke from Cu(6%)/Zeolite-Y.

Element	Result (wt %)
C	4.83
	4.71
H	3.52
	3.43

Table 116 CHN analysis of insoluble coke from Cu(5%)/Attapulgite.

Element	Result (wt %)
C	4.87
	5.02
H	3.75
	3.85

Of the phenol converted by either Cu(6%)/Zeolite-Y or Cu(5%)/Attapulgite, between 20 and 30% was converted to the dimers 4,4'-biphenol, 2,2'-biphenol and 4-phenoxyphenol, between 20 and 30% was converted to byproducts and the remaining 50% was converted to coke that was tetramers and pentamers of phenol.

4 Discussion

In the discussion section I will provide an explanation of the results communicated in Section 3 and evaluate the literature reviewed in Section 1. I will first address the adsorption studies and then comment on the regioselective dimerisation of phenol.

4.1 Phenol and biphenol adsorption

For a successful heterogeneous catalytic reaction reactants must be transported to the catalyst and products away from it. For porous catalysts like zeolites and clays, molecules must be transported through the pores of the material to the active sites. Catalysis must always be preceded by the adsorption of reactants allowing reaction between the adsorbates and desorption of the products. An interaction between phenol, the aluminosilicate surface and exchanged ions was therefore essential for the catalysed dimerisation of phenol to 4,4'-biphenol, 2,2'-biphenol and 4-phenoxyphenol and so the liquid phase adsorption of phenol from solution was studied. In a two-component liquid system the solute and solvent may or may not compete for adsorption sites, this is referred to as competitive and non-competitive adsorption respectively. Some solvents have a poisoning effect which is also well documented.[13]

There are many liquid phase catalytic systems for which the solvent is not simply a medium for dissolving the reactants and products. The hydrogenation of many hydrocarbons over Rh/SiO_2 is enhanced by the H-donor characteristics of secondary alcohols.[13] Solvents can also be used to modify the properties of a catalyst surface and so studying the adsorption of phenol was fundamental for an improved understanding of the mechanism by which phenol was dimerised to 4,4'-biphenol, 2,2'-biphenol and 4-phenoxyphenol.

Adsorption from the liquid phase has been summarised by Giles and co-workers.[109] The authors divided the large number of published isotherms into four main classes. The 'S' class is convex and the 'L' or Langmuir is concave with respect to the concentration axis. The 'H' or 'high affinity' isotherm does not go through the origin and the 'C' class is 'constant' (Figure 96).

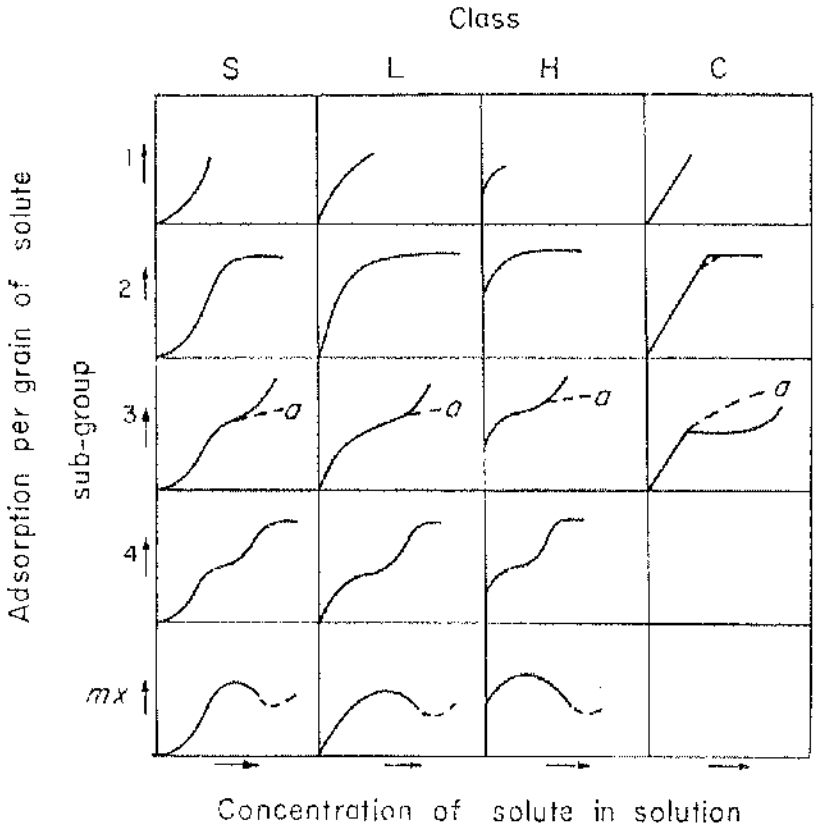

Fig. 96[109] Classification of isotherms for adsorption from solution.

The shape of the adsorption isotherm depends on the unique adsorbate and adsorbent combination, although adsorbate molecules are generally classed as ionic or non-ionic. The literature[54] reports that in general the sorption of non-ionic organic compounds follows a linear (C) isotherm whilst ionic adsorbates form a monolayer and so follow the Langmuir (L) isotherm. Phenol is non-ionic but the deprotonated phenolate ion ($Ph\text{-}O^-$) is ionic. The adsorption isotherms of phenol over H/Zeolite-Y and H/ZSM-5 followed the linear (C) isotherm, the adsorption of phenol (phenolate) over Na/Zeolite-Y, Cu/Zeolite-Y, Na/ZSM-5 and Cu/ZSM-5 followed the Langmuir (L) isotherm (Section 3.1.1).

The observed Langmuir isotherms suggest the adsorption of phenolate ions over Na/Zeolite-Y, Cu/Zeolite-Y, Na/ZSM-5 and Cu/ZSM-5 catalysts. Phenol is a weak acid with a pK_a = 10.0, the hydrogen of the hydroxyl group can dissociate in the presence of a base, in this case the aluminosilicate surface of the zeolite. Phenol is

most likely to adsorb with the oxygen atom of the hydroxyl group H-bonded to the cation and the hydrogen coordinated to the neighbouring basic oxygen atom of the zeolite or clay framework (Figure 97).

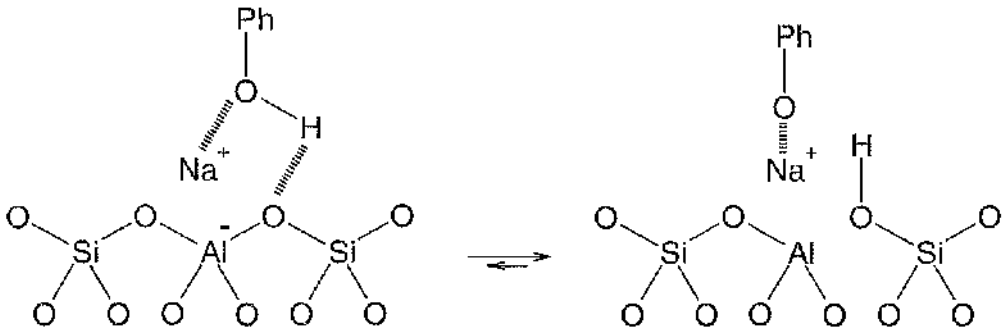

Fig. 97 Phenol adsorption and deprotonation over a cation exchanged aluminosilicate surface.

Of the adsorption studies reported in Section 3.1.1 the atypical result was the isotherm obtained using Na/ZSM-5, for which the adsorption of phenol was increased by the relatively high hydrophobicity of Na/ZSM-5.[55] The high Si/Al ratio of ZSM-5 means more silicon and less aluminium sites. Cations are associated with every aluminium site for charge balance and with each cation there is water of hydration. In general if the water content of a catalyst is reduced, the adsorption capacity is increased and so the adsorption of phenol by Na/ZSM-5 was increased.[110]

A Brønsted acid site on a hydrogen exchanged zeolite or clay and the adsorption of phenol at that site is illustrated Figure 98.[60] There were no cations in H/Zeolite-Y or H/ZSM-5 and as a result phenol was not deprotonated by adsorption to the aluminosilicate surface. The water content of H/Zeolite-Y and H/ZSM-5 catalysts was reduced by the lack of cations available for H-bonding to the oxygen of water.

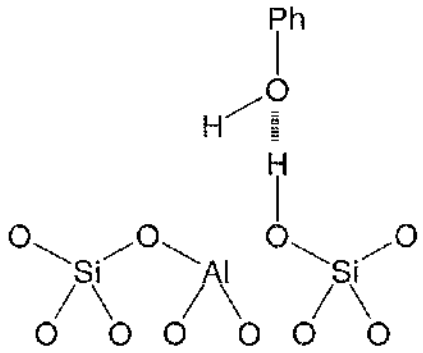

Fig. 98 Brønsted acid site on aluminosilicate surface and phenol adsorption.

Adsorption of phenol by H/Zeolite-Y was increased because the water content of the catalyst was reduced, so reducing the competitive adsorption between phenol and water. The adsorption of phenol over H/Zeolite-Y equated to one phenol molecule at half the cation exchange sites. Only half the sites were accessible to phenol however, suggesting the adsorption of one phenol molecule per active site.[111]

The effects of ion exchange were not limited to an interaction between phenol and the exchanged cation. A Cu^{2+} ion has a diameter of only 0.07 nm but the associated hydration sphere can increase the effective diameter to >0.4 nm. This can cause pore blocking and limit the access of phenol molecules to adsorption sites. The charge of Cu^{2+} might be expected to promote twice the adsorption of phenol or phenolate ions compared to Na^{+}. Indeed the adsorption of two phenol molecules at one cation exchange site is sterically feasible using the supports Zeolite-Y, Montmorillonite or Attapulgite but there is no evidence that cation charge controls adsorption. The *Mulliken* electronegativity of oxygen is 3.22, aluminium 1.37 and silicon 2.03. Oxygen is more electronegative than aluminium or silicon and so has a stronger 'pull' on the electrons from the Al – O or Si – O bonds. In practice, the negative charge on aluminium is delocalised over the oxygen framework (Figure 99).

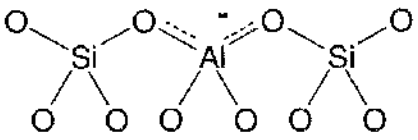

Fig. 99 Surface of an aluminosilicate after isomorphous substitution of Si for Al.

The adsorption of phenol over Montmorillonite and Attapulgite catalysts was studied (Section 3.1.1, Figure 56). The amount of phenol adsorbed by Montmorillonite and Attapulgite catalysts was similar despite different aluminosilicate structures and cation-exchange capacities, suggesting the systems were under diffusion control. Maximum phenol adsorption corresponded to fourteen phenol molecules per cation exchange site and therefore it was assumed that adsorption occurred at sites not associated with the exchanged cations.

The authors Beutel *et al.*[60] and Fitch *et al.*[112] used ^{29}Si MAS NMR to confirm the aromatic hydrogen atoms of phenol and phenolate ions could associate with framework oxygen atoms within the Na/Zeolite-X supercage (Section 1.3.1). The ability of phenol and phenolate ions to locate close enough to the framework oxygen atoms to hydrogen bond was limited in Zeolite-X and so also Zeolite-Y by the size of the supercage. In contrast, the lamellar structure of the clays allows close association between the adsorbate and framework oxygen atoms. The aluminosilicate surfaces of clays can be represented in the same way as zeolites. with adsorption of phenol and phenolate ions via the aromatic ring increasing with the adsorption capacity of the system regardless of the cation-exchange capacity (CEC).

The adsorption of phenol over Cu/Attapulgite (Section 3.1.1, Figure 56) was less than the other five clay catalysts studied. The associated hydration sphere of copper is much greater than that of sodium. The exchanged cation can therefore limit the access of phenol molecules to other adsorption sites. Montmorillonite is classified as a smectite clay, whose aluminosilicate structure is capable of swelling or expanding. Attapulgite has a constant basal spacing not affected by solvent and so is a non-swelling clay. The exchange of sodium for copper cations and the increase in associated cation hydration sphere within Attapulgite therefore limits the access of

phenol molecules to other adsorption sites. The Montmorillonite clay swells to accommodate the larger cation and maintain the adsorption capacity despite diffusion control.

The concentration of phenol solution was constant at 0.08 mol L^{-1} which meant the ratio of phenol molecules to cation exchange sites in Zeolite-Y, ZSM-5, Montmorillonite and Attapulgite varied for each catalyst. The adsorption of phenol over Cu/Zeolite-Y and Cu/Attapulgite was also investigated using different concentrations of phenol in solution. The adsorption of phenol over Cu(6%)/Zeolite-Y (Section 3.1.1.1, Figure 57) displayed Langmuir type isotherms at 0.004, 0.04 and 0.07 mol L^{-1} which was characteristic of adsorption within the channels and pores of a microporous material. The relatively limited volume within the channels and pores of Zeolite-Y meant that only a monolayer of molecules could adsorb. The cumulative concentration at which adsorption reached a maximum increased with the concentration of the adsorbate, suggesting that additional sites were utilised at the higher concentrations or that more phenol molecules entered the supercage.

The unique and limited adsorption of phenol over the clay catalyst Cu(5%)/Attapulgite using a 0.08 mol L^{-1} solution of phenol has been discussed. A similar isotherm was recorded using a 0.04 mol L^{-1} solution but adsorption was reduced when using a 0.004 mol L^{-1} solution (Section 3.1.1.1, Figure 58). The adsorption of phenol from 0.08 and 0.04 mol L^{-1} solutions was similar because the access of phenol to adsorption sites remained limited. Phenol was in competition with acetonitrile for adsorption sites and so at the lower phenol concentration adsorption was reduced by the competitive adsorption between phenol and acetonitrile, not by the access of molecules to active sites.

Zeolite is from the Greek meaning 'boiling stone.' When first discovered, zeolites were heated and appeared to boil as water was removed. As mentioned, aluminosilicates contain charge-compensating ions that have high affinities for polar molecules such as water.[87, 113] Water is hydrogen bonded to the cations via the oxygen atom and it is also possible for water to hydrogen bond via the hydrogen atoms to the framework oxygen atoms of the aluminosilicate surface (Figure 100). The Thermogravimetric analysis of Cu(6%)/Zeolite-Y confirmed a significant weight loss

associated with water which corresponded to more than ten water molecules per copper cation.

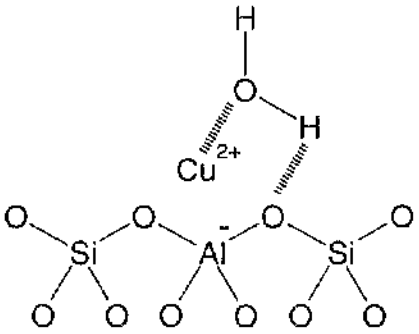

Fig. 100 Hydrogen bonded water to copper and neighbouring oxygen atom on aluminosilicate surface.

The adsorption of phenol over Cu(6%)/Zeolite-Y was maximised using chloroform as the solvent, the adsorption of phenol from an acetonitrile or water solution was much less. Chloroform is hydrophobic and the solubility of water in chloroform is <1%, whilst acetonitrile and water are fully miscible. The adsorption of phenol over the zeolite and clay catalysts was studied at room temperature with no pre-treatment of the catalyst. The preparation of every catalyst involved calcination at 773 K to remove carrier molecules, for example acetate. This removed from the catalyst all the water associated with the cations but upon cooling and storage the material re-adsorbed this water, which was present during the adsorption studies.

Water molecules are ligands, donating a pair of electrons to empty orbitals of the metal ion and forming a coordination complex. Ligands are Lewis bases, defined as molecules that can donate an electron pair, water and acetonitrile are labile ligands for copper, chloroform is not[79]. Acetonitrile like water has a lone pair of electrons capable of occupying the empty electronic orbitals of a metal ion. The chlorine atoms of chloroform also have lone pairs of electrons but are unable to donate these electrons to a central metal ion. Using acetonitrile or water as the solvent, the adsorption of phenol from solution was low since acetonitrile, phenol and water competed for adsorption sites as ligands surrounding the copper cation. Chloroform did not compete with phenol and therefore more of the water ligands were replaced with phenol. The

adsorption of phenol from acetonitrile or water related to no more than one phenol molecule per available copper exchanged site in Cu/Zeolite-Y. The adsorption of phenol from chloroform suggested more than one phenol molecule per copper cation.

Clays were first used in industry to remove the oil from sheep's wool prior to dying and spinning. This historical use of clay relied upon the same preferential adsorption of organic molecules over clay that the catalysed polymerisation of phenol depends on. 'The habitat of clay minerals is essentially that of *humans*, the very thin surface of contact between air, water and earth. The clays belong to the earth but owe most of their characteristics to the interaction of water and air, so do *humans*.'[114] Adsorption of phenol over Cu(5%)/Attapulgite could only be recorded using chloroform as the solvent. All clays attract water to their surfaces through adsorption, some incorporate water into their structure, referred to as absorption. The sepiolite-palygorskites (attapulgite) contain water within the channels of the aluminosilicate structure known as *zeolitic* water, which is easily removed upon heating. Sepiolite-palygorskites absorb water but do not swell and so pore and channel blocking is a potential problem, causing an increased pressure drop across the catalyst bed.[114] Using a chloroform solution the adsorption of phenol over Cu(5%)/Attapulgite was not hindered by the competitive adsorption of the solvent, using acetonitrile the solvent competed for adsorption sites. The non-expansion of Attapulgite meant that the larger copper cation and associated hydration sphere of acetonitrile blocked the access of phenol to other adsorption sites which caused the increased pressure drop.

The adsorption of 4,4'-biphenol over the zeolite and clay catalysts was reported in Section 3.1.2 using an acetonitrile solution since the solubility of 4,4'-biphenol in chloroform was poor. The adsorption of 4,4'-biphenol over Cu(6%)/Zeolite-Y was much greater than the adsorption of phenol from acetonitrile over the same catalyst, suggesting the internal pore and cage structure of Zeolite-Y was well matched to the molecular dimensions of 4,4'-biphenol. The adsorption of 4,4'-biphenol from acetonitrile solution was five times greater than the adsorption of phenol from acetonitrile. The low adsorption of 4,4'-biphenol by Na and H-forms of Zeolite-Y advocates the lack of subsequent catalytic activity. All catalytic reactions require the adsorption of reactants and importantly the desorption of products. The relatively low yield of the dimer 4,4'-biphenol reported in Section 3.3.2 is explained by its strong

adsorption and subsequent self-poisoning effect. The strength of 4,4'-biphenol adsorption over any aluminosilicate surface will be increased if the molecule is adsorbed at more than one apex. The interaction between the hydroxyl group of phenol with cations and neighbouring oxygen atoms will be discussed but it is possible that these interactions occur at both hydroxyl groups of 4,4'-biphenol, indeed this interaction must be viable for the dimerisation of phenol utilising two adsorption sites, one phenol molecule at each site. The exchange between 4,4'-biphenol and acetonitrile was less labile than phenol and acetonitrile.

The adsorption of 4,4'-biphenol and phenol was also compared over Cu(5%)/Attapulgite. It had already been established (Section 3.1.1.2) that acetonitrile could not be used as a solvent with the clay catalysts. Chloroform was therefore used but the concentration of solution lowered to accommodate the reduced solubility of 4,4'-biphenol in chloroform. In chloroform neither phenol or 4,4'-biphenol were labile with the solvent and consequently adsorption was similar. Adsorption of 4,4'-biphenol was slightly less than phenol which reflected the increased steric hindrance involved in 4,4'-biphenol entering the pores and cavities of Cu(5%)/Attapulgite.

Adsorption of the three dimers 4,4'-biphenol, 2,2'-biphenol and 4-phenoxyphenol was compared over Cu(6%)/Zeolite-Y and Cu(5%)/Attapulgite (Section 3.1.3). The adsorption of 4,4'-biphenol and 4-phenoxyphenol was similar, the adsorption of 2,2'-biphenol was much less. The adsorption of 2,2'-biphenol simultaneously at two adjacent copper exchanged sites required distortion of the molecule. The distortion of 2,2'-biphenol meant the molecule probably adsorbed at only one site, increasing its lability and altering the equilibrium between adsorbed and desorbed 2,2'-biphenol molecules.

4.2 Dimerisation of phenol using Cu/Zeolite-Y and Cu/Attapulgite

Copper has been used as a catalyst for cross-coupling reactions since the pioneering work of Ullmann and Goldberg at the beginning of the last century.[115] In 1956 Hay and his co-workers[4] discovered that 2,6-dimethylphenol could be oxidatively polymerised to poly(phenylene oxide) (PPO) at room temperature in an oxygen atmosphere using a copper(I)/amine complex as a catalyst. The C-C coupled diphenoquinone was detected in small amounts but became the dominant product at reaction temperatures above 373 K. Xu *et al.*[95] reported in 1998 that basic copper and basic copper/amine catalytic systems were active for the liquid-phase, oxidative coupling of 2,6-disubstituted phenols. Fujiyama *et al.*[55] reported the para-coupling of 2,6-di-*tert*-butylphenol for which the mesopores of MCM-41 offer a substantially preferable reaction field in comparison to the bulk solution. Research by Gillard and co-workers,[66] published in 1988 suggested that with the right catalyst the oxidative dehydrogenation of pyridine could be adapted for the production of 4,4'-bipyridyl (Section 1.3.2). A suitable catalyst for the para-coupling of 2,6-di-*tert*-butylphenol, pyridine or phenol must be capable of supporting transition metals and be shape selective. Transition metal ions, especially copper have been reported[56, 87] as catalytically active for the liquid phase oxidation of phenol derivatives. Zeolite and clay catalysts are currently the subject of great interest because of their shape selective, ion exchange and adsorption properties.

The mechanism of these coupling reactions has been the subject of much discussion since the 1960's and several mechanistic proposals have been made accordingly, many of the which suggest bifunctional catalysis.[69] Catalytic activity is controlled by the redox properties of the copper ions,[35] which themselves control the acid site strength allowing catalyst selectivity to be 'fine-tuned'.[2] The redox properties of exchanged copper ions in any zeolite or clay catalyst are controlled by the local geometry of the ligand field and the total delocalised negative framework charge, compensated by cations. The framework charge is controlled by the concentration of aluminium in the framework and exchangeable cations. The cations contribute to framework stabilisation and act as coordination centres for adsorbed molecules. The exchangeable cations in dehydrated zeolites are generally located at sites that offer the optimum coordination with structural oxygens. The coordination is controlled by the geometry of the oxygen ring surrounding one or two aluminium ions.

The acid-base properties of alkali metal exchanged zeolites and clays are attracting increasing attention, 'the basicity of the framework oxygen atoms renders these solids suitable for base catalysed reactions in organic fine chemistry.'[60] The active sites in ion exchanged zeolite and clay catalysts are characterised by the combination of metal ion and framework oxygen atoms. Access by phenol molecules to these active sites varies between catalysts and depends ultimately on the aluminosilicate pore structure. The active sites in Zeolite-Y can be located in the relatively small sodalite cages or much larger supercages. The two-dimensional layered structure of Attapulgite offers potentially better reactant and product access but reduced shape selectivity.

4.2.1 Location of active sites

The selectivity of phenol dimerisation catalysed by Cu/Zeolite-Y and Cu/Attapulgite was controlled by the position of copper cations. Many authors including Schoonheydt[116], Marra *et al.*[111] and Bulanek *et al.*[35] have proposed models for copper siting in Cu/Zeolite-Y. The models have been adapted and improved over the last decade inline with continued research. There is however no singularly accepted model, Figure 101 is a plausible combination of models from the literature and will be used as a working model for understanding the selectivity of phenol dimerisation.

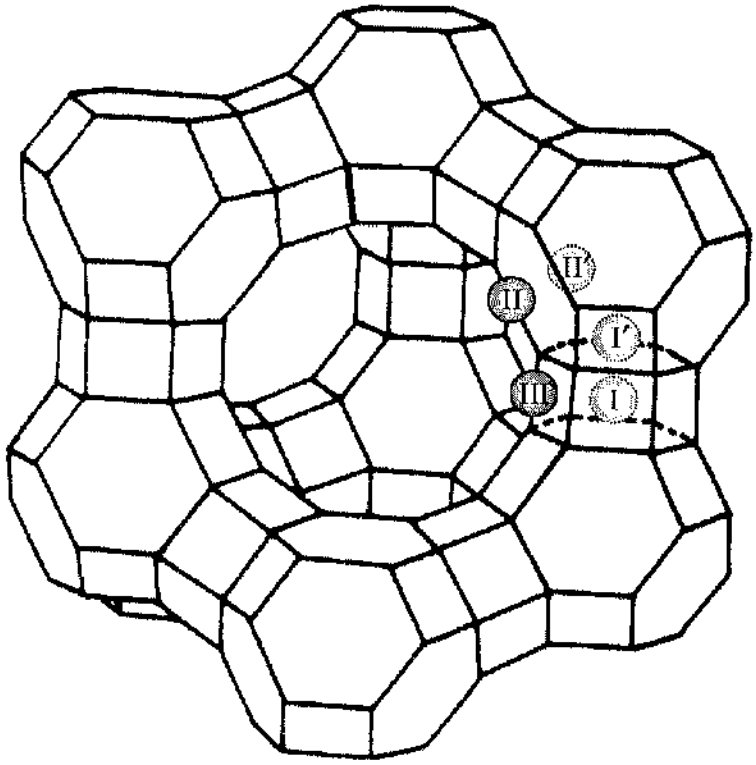

Fig. 101 Copper siting in Cu/Zeolite-Y.

Figure 101 illustrates the supercage and surrounding sodalite cages of Zeolite-Y. Each line represents a Si – O – Si, Si – O – Al or Al – O – Al bond; the silicon or aluminium atoms or ions are positioned where three or four lines intersect. Connecting the sodalite units with hexagonal prisms creates the three-dimensional structure of Zeolite-Y. Five copper sites are proposed, I, I′, II, II′ and III for which there is evidence of the coordination of copper at each site. Site I is located at the

centre of the hexagonal prism, inaccessible to guest molecules and therefore cannot contribute to catalytic activity. This site is highly populated due to its high coordination and therefore increased stability. Site I′ is inside the sodalite cage, surrounded by the oxygens at the top of the hexagonal prism. Access to this site is restricted to molecules that can penetrate the six-membered ring of the sodalite cage, for example H_2. Other small molecules, for example CO and N_2 are however too big and so catalytic activity at this site is also prohibited. The simultaneous occupation of sites I and I′ is forbidden because of Coulombic repulsion. Sites II and II′ are associated with the six-membered ring forming the frontier between the sodalite cage and supercage. Site II′ is inside the sodalite cage, site II is also inside the supercage and so can contribute to catalytic activity. The simultaneous occupation of sites II and II′ is also forbidden. The cation at site III is coordinated to only four framework oxygen atoms and so has the highest coordinative unsaturation and is therefore least occupied. Site III is however located in the supercage and can therefore contribute with site II to catalytic activity.[111] The number of sites II and III per supercage is determined by the Si/Al ratio of the framework and copper loading.

The coordination of copper at site III can be square pyramidal or square planar and is determined by the number of AlO_2^- units with which the copper cation is associated. The square pyramidal coordination is associated with a pair of AlO_2^- units, of which there are two arrangements with units adjacent or opposite (Figure 102).

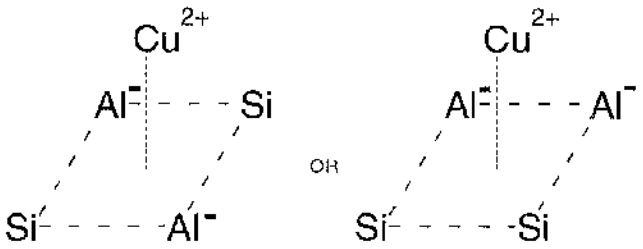

Fig. 102 Square pyramidal coordination of copper at site III.

The square planar coordination of copper is characterised by its association with a single framework Al atom, as illustrated in figure 103.

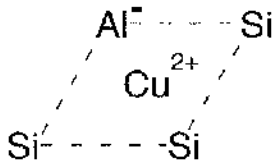

Fig. 103 Square planar coordination of copper at site III.

The cations in square planar geometry are more easily reduced and are responsible for most catalytic activity.[35, 117] The number of these sites increases with copper loading and as the concentration of aluminium is reduced. This coordination is more common when copper acetate is used as the precursor.

Clays have a two-dimensional layered aluminosilicate structure and so the geometry of cation sites is controlled less by the framework structure. Although less well characterised, the catalytic activity of clays should not be underestimated. Clays are classified according to their swelling properties, type and number of structural cations and the distance between the sheet layers of the crystal structures, referred to as the *basal spacing*. The charged surfaces and cation exchange sites of the clay interact strongly with polar molecules for example water, although these interactions are complex, understanding is improved if the movement of exposed hydrogens is traced between organic molecules and the surface of the clay and vice versa.

The selectivity of Cu/Attapulgite for phenol dimerisation to 4,4'-biphenol is explained by the ordered spacing of exchangeable cations present in the interlayer. There are two types of cations in clay minerals, (i) exchangeable cations present in the interlayer and (ii) non-exchangeable, coordinated trivalent and divalent cations, eg. Al^{3+} and Mg^{2+}.[2] The exchangeable cations can be mono or divalent and are normally surrounded by water molecules.[114] Only Cu/Attapulgite catalysed the dimerisation of phenol, Na and H/Attapulgite were inactive. The coordinated, non-exchangeable cations were therefore not the primary source of catalytic activity. For zeolites the

exchangeable cations are also charge-compensating ions, necessary because of framework ion substitution but the exchangeable cations represent nearly all of the cation exchange capacity.[114] The linear, needle-like morphology of palygorskite (attapulgite) is best visualised in Figure 104.

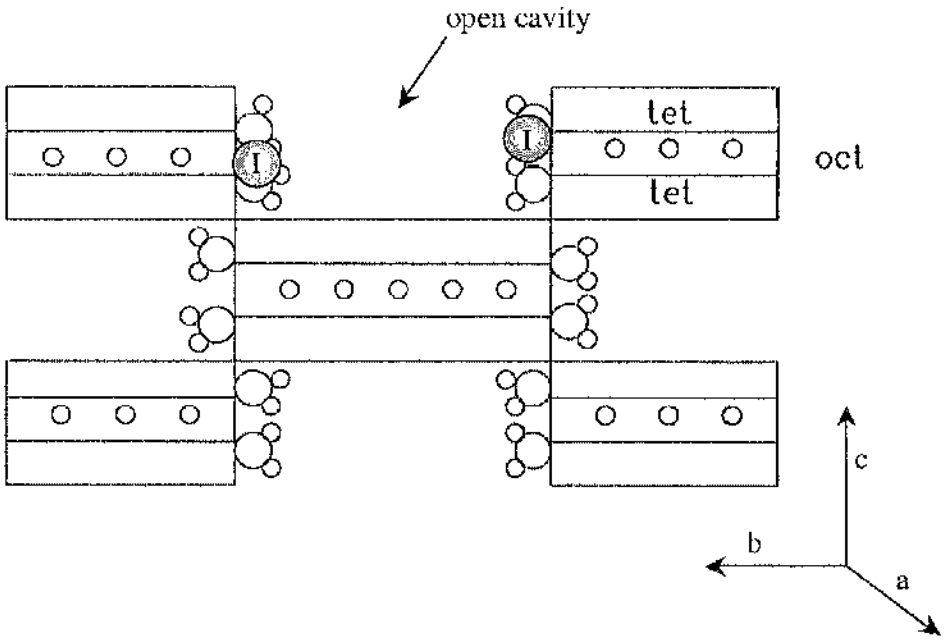

Fig. 104 Copper exchanged sites in Cu/Attapulgite.

The fundamental building block of palygorskite is a 2:1 tetrahedral and octahedral unit. The units are however not linked to form the more common sheet structure but a ribbon, extending in Figure 104 perpendicular to the page (axis a). The open cavities are similar to those in zeolites, in which water and interlayer exchanged ions can be accommodated. The dimension of these cavities is approximately b = 0.96 nm, c =1.04 nm[114] and a = ∞; a close match to the dimension of 4,4'-biphenol, with a distance between oxygen atoms of 0.99 nm. As for Zeolite-Y the distance between cation exchange sites determines the catalytic activity and dimerisation selectivity.

4.2.2 Catalyst selectivity

The shape selectivity of reactions catalysed by zeolites and clays was discussed in Section 1.2.1 and can be provided by reactant selectivity, two types of product selectivity and restricted transition-state selectivity.[19] The successful regioselective dimerisation of phenol by zeolite and clay catalysts would be best controlled by restricted transition-state selectivity and not the size-exclusion of products. Catalysts affect the kinetics of chemical reactions and can therefore be designed to direct selectivity.[82] Kodayashi *et al.*[6] suggested that if a catalyst generates and regenerates only a nucleophilic active oxygen intermediate, which then reacts with phenols to give *controlled* radicals without formation of *free* radicals, the stereoselectivity of the subsequent coupling may be entirely regulated.

Phenol adsorption occurs at copper sites and as suggested by Beutel *et al.*,[60] formation of a Brønsted acid site is concurrent with phenolate ion formation. Skeletal transformations of hydrocarbons and subsequent coke formation depend essentially on Brønsted acidity,[41, 90] although it is possible to convert Brønsted acid sites back to Lewis basic sites using a base.[113] The dimerisation of phenol over crystalline aluminosilicates used water as the base. There was more water present when using the acetonitrile solution of phenol compared to the chloroform solution which was why coke formation was more prominent when using a chloroform solution.

The coordination of phenol to copper via the oxygen atom was necessary for phenol activation by deprotonation and radical formation. For zeolite and clay catalysts using an acetonitrile, chloroform or a mixed phenol solution, other dimerisation products were detected. The dimerisation of phenol to 4,4'-biphenol is possible when two phenol molecules, adsorbed via the oxygen at copper sites opposite one another interact. The *para*-carbon atoms of both phenol molecules are therefore in proximity and radical coupling possible. There are then three mechanisms by which the dimerisation of phenol to 4-phenoxyphenol and 2,2'-biphenol can be rationalised, (i) resonance structures of adsorbed phenol, (ii) the adsorption of phenol at cation exchange sites next to rather than opposite one another, (iii) desorption of a radical and coupling with a coordinated radical. There is evidence in the literature[6, 69, 113] for each of these proposals.

The adsorption of phenol via the oxygen to copper can be considered as one of a number of resonance structures. The most likely coordination will be via the oxygen atom but resonance structures can exist with coordination to the carbon atoms of the aromatic ring, especially carbon-4 in the *para*-position. This makes the C-O dimerisation of phenol to 4-phenoxyphenol and coupling to 2,2'-biphenol feasible when two phenols are activated at cation exchange sites opposite one another. More than one phenol maybe adsorbed per site, as was suggested for phenol adsorption from a chloroform solution but only one phenol can be activated per site before desorption and regeneration of Cu^{2+} from Cu^{1+}.

Cation exchange sites are distributed throughout the crystalline structures of Cu/Zeolite-Y and Cu/Attapulgite, sites maybe opposite or next to a neighbouring site. Phenol molecules adsorbed at sites 90° apart can dimerise to yield 2,2'-biphenol and 4-phenoxyphenol (Figure 105).

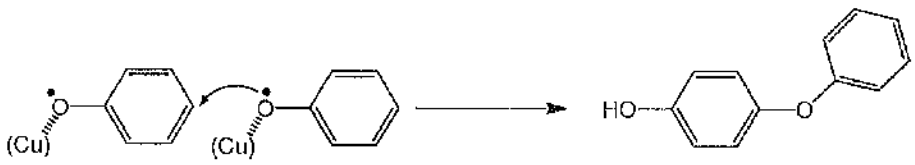

Fig. 105[6] Dimerisation of phenol to yield 4-phenoxyphenol.

The third proposal is that a phenol radical desorbs and couples to another phenol radical still adsorbed at an active site, although the most plausible rational for the controlled coupling of phenol to 4-phenoxyphenol and 2,2'-biphenol using Cu/Zeolite-Y and Cu/Attapulgite catalysts is proposal (ii), the location of cation exchange sites. If copper exchanged sites were opposite then selectivity was directed towards 4,4'-biphenol, if sites were next to one another then 4-phenoxyphenol and 2,2'-biphenol were produced. The yield of 4,4'-biphenol was greatest because adsorption of phenol at opposite sites was less sterically hindered. The acetonitrile ligands on copper and acetonitrile coordinated to Brønsted acid sites reduced the ability of phenol to move closer to neighbouring active sites, hindering conversion of phenol to 4-phenoxyphenol and 2,2'-biphenol. Using chloroform, the relatively small water ligands allowed phenol molecules to move more freely towards neighbouring sites.

The resonance structure of a phenoxy radical suggests that the single electron is most often associated with the oxygen atom. The C-O coupling was therefore favoured over C-C coupling since one of the phenol molecules had the radical species associated with the oxygen. For phenol dimerisation to 4,4'-biphenol the radical on both phenoxy molecules must be located at carbon-4. This reduced selectivity to 4,4'-biphenol unless adsorbed molecules had the correct orientation.

Catalyst deactivation was ultimately due to coke formation whilst the conversion of phenol was similar using either a chloroform or acetonitrile solution since the rate-limiting step was the dimerisation of phenol.[78] Only one phenol activation could be performed per cation exchange site before regeneration was required.

4.3 Zeolite catalysts

The activity of the zeolite catalysts was investigated using chloroform, acetonitrile, butyronitrile and propionitrile solutions of phenol. In response to the adsorption studies the dimerisation of phenol was first attempted using a chloroform solution, although subsequently the yields of 4,4'-biphenol, 2,2'-biphenol and 4-phenoxyphenol were improved using the nitrile solvents.

The calculated Turn Over Number (TON) of phenol molecules over copper sites was ca. 1, although this assumed the access of phenol to all cation exchange sites. Phenol could not however enter the sodalite cage of Zeolite-Y and so access to sites I, I′ and II′ was prohibited. Sites II and III are inside the supercage and therefore accessible to phenol but sites II and II′ cannot co-exist. The literature[35, 117] suggests that the only catalytically active copper sites are those with square planar coordination at site III. It is not possible therefore to calculate an accurate TON of phenol over copper sites but the number is greater than one.

Water was an important component of reactions catalysed by Cu/Zeolite-Y. The adsorption of phenol from a chloroform solution was greater than the adsorption from acetonitrile solution because in chloroform phenol only replaced the water ligands, in acetonitrile phenol competed with water and acetonitrile molecules for adsorption sites. It has recently been reported that the coupling of organic molecules using copper catalysts is accelerated by an optimal amount of water and that the role of water is complex.[115] The selectivity of phenol dimerisation catalysed by Cu/Zeolite-Y was due to competitive adsorption between water, the solvent and phenol at copper exchanged sites. The conversion of phenol to 4,4'-biphenol, 2,2'-biphenol and 4-phenoxyphenol by Cu/Zeolite-Y was greatly improved using acetonitrile as the solvent for phenol and as a catalyst modifier. The authors Baesjou *et al.*[69] suggested that with limited amine present conditions were acidic, owing to the Lewis-acidity of the copper(II) ion. In excess amine the acidity was reduced and carbon-oxygen coupling was favoured (Section 1.4.2).

4.3.1 Chloroform solution

Chloroform did not complex with the copper cations and therefore the exchange of water ligands for chloroform was not labile. The catalytic activity of Na, H, Cu, Ag and Ni/Zeolite-Y was investigated and with the exception of H/Zeolite-Y all were catalytically active for the dimerisation of phenol. Activity increased Cu < Na < Ag < Ni which correlated with the lability and inertness of complexes, copper being the most labile.[113] There was no evidence for any catalytic activity over H/Zeolite-Y, instead the apparent conversion of phenol was the result of phenol adsorption without reaction which correlates to the adsorption of phenol over H/Zeolite-Y reported in Section 4.1. The generation of a phenoxy radical requires a Lewis acid to accept an electron and so the metal cations, Na, Ag and Ni were all catalytically active. The most active metal was the least labile as this limited the adsorption of phenol. Increasing the number of strong phenol ligands weakened the Lewis acid and reduced the ability of the cation to generate phenoxy radicals.

The conversion of phenol decreased with Time On Stream (TOS) using all catalysts. The activity of Zeolite-Y supported catalysts was regenerated after each acetonitrile flush between phenol in chloroform cycles. The pore diameter of Zeolite-Y is 0.74 nm, ZSM-5 is 0.55 – 0.60 nm and the maximum width of the dimers 4,4'-biphenol, 4-phenoxyphenol and 2,2'-biphenol is 0.56 nm. The removal of dimers from ZSM-5 was feasible but restricted, although the removal of larger polymeric species would have been severely hindered. As a result coking and subsequent pore blocking of ZSM-5 was prominent whilst flushing the system with acetonitrile removed little of the byproducts from phenol dimerisation. In contrast the larger pore diameters of Zeolite-Y assisted removal of the larger compounds.[118]

Conversion of phenol increased with the metal loading of Zeolite-Y although the increase was not linear. The metal loading of Zeolite-Y is more complex than the loading of other high surface area materials for example γ-alumina. Although simplified these materials have surfaces upon which metal species can be loaded which are generally accessible to a wide variety of molecules and increasing the metal loading increases the number of available active sites. Although there are different types of active site on γ-alumina, there are five well defined cation exchange sites for

Zeolite-Y, see Figure 101. Thomas and Thomas[118] have reported that Ca^{2+} ions preferentially occupy Type I sites and until all these sites are occupied, Ca^{2+} ions will not exchange with Na^{+} to occupy sites in the supercage that are accessible to molecules larger than hydrogen.[118] Increasing the metal loading of Cu/Zeolite-Y does not therefore directly increase the number of available active sites; the large increase in phenol conversion between the 1% and higher metal loadings of 5, 6 and 8% indicates the population by Cu^{2+} ions at cation exchange sites in the supercage. The number of phenol molecules per supercage was however limited as was the rate of phenol dimerisation.

The rate of this reaction was limited by the rate of phenol dimerisation and so the conversion of phenol increased with metal loading. Coke formation was the ultimate cause of catalyst deactivation and so an increase in the number of active sites capable of phenol dimerisation before the blockage of zeolite pores by coke, meant an increase in the conversion of phenol. The selectivity of phenol dimerisation to 4,4'-biphenol and 2,2'-biphenol was only measured in trace amounts at all four metal loadings, the selectivity to 4-phenoxyphenol was similar at 5, 6 and 8% but much higher at 1% metal loading. At the lowest metal loading there were fewer adsorbed phenol molecules per supercage and their movement was less sterically hindered, increasing the possibility of C-O coupling. At lower metal loadings there were however fewer accessible copper ions for the adsorption and activation of phenol.

Reaction temperature had a complex affect on phenol conversion and the selectivity of dimer products. At higher temperatures more phenol molecules had at least the activation energy required for coupling. As reaction temperature was increased the rate of product desorption also increased and the equilibrium between reactant adsorption and desorption was altered, as summarised in Figure 106.

$$A \underset{k_{-a}}{\overset{k_{+a}}{\rightleftharpoons}} A_{(ads)} \quad \text{adsorption}$$

$$\xrightarrow{k_r} P_{(ads)} \quad \text{reaction}$$

$$\xrightarrow{k_d} P \quad \text{desorption}$$

Fig. 106[1] A general mechanism for heterogeneously catalysed monomolecular reactions.

The extremes of reaction temperature were the most informative, the data for 328, 348 and 388 K suggests phenol conversion and dimer selectivity were influenced by the controlling factors at 308 and 408 K. Uniquely, the conversion of phenol at 308 K systematically increased with TOS and selectivity to 4-phenoxyphenol was high. At 308 K few phenol molecules would have had the energy required for activation but of those molecules that did, many reacted to produce 4-phenoxyphenol. The C-O selectivity was due to the relatively free movement of adsorbed phenol towards neighbouring copper sites. Once reacted, desorption of the products was slow and detection in the exit stream from the reactor was delayed. Conversion was expected to increase and plateau as the dimerisation of phenol matched desorption of the products. Phenolic dimers and byproducts were the precursors to polyphenolic coke compounds so at 308 K lower phenol conversion reduced coke formation and subsequent catalyst deactivation. At 408 K conversion was increased as more phenolic byproducts were formed. Byproducts and phenolic dimers remained the precursors to coke but at 408 K the desorption of these compounds was increased and so coke formation was minimised. With less coke formation deactivation was reduced and conversion sustainable at >20%.

The conversion of phenol to 2,2'-biphenol was only detected at 388 and 408 K, suggesting the activation energy required for the coupling of two phenol molecules to 2,2'-biphenol was greater than that for 4,4'-biphenol or 4-phenoxyphenol production. The enthalpy of formation for 2,2'-biphenol was greater than that for 4,4'-biphenol (Section 3.2).

The conversion of phenol and selectivity to 2,2'-biphenol varied with the concentration of phenol in chloroform solution. The moles of phenol initially converted between 0 and 5 min using phenol solutions of 0.02 and 0.04 mol L^{-1} were identical, as were the moles of phenol initially converted using 0.08, 0.16 and 0.32 mol L^{-1} solutions. Using the number of moles converted, the conversion of phenol doubled between 0.04 and 0.08 mol L^{-1} which correlated to the production of 2,2'-biphenol. At the higher phenol concentrations more phenol molecules were adsorbed per cation exchange site as confirmed by the adsorption studies (Section 4.1). With more phenol molecules coordinated to copper, phenoxy radicals on neighbouring sites were less able to orientate for C-O coupling to form 4-phenoxyphenol. The C-C coupling of phenol to 2,2'-biphenol under standard reaction conditions was viable therefore only when phenoxy radicals were forced closer together by increased phenol adsorption. Without coordination from the solvent, dimerisation of phenol to 4,4'-biphenol remained unfavourable. The increased conversion of phenol at concentrations ≥0.08 mol L^{-1} is therefore rationalised by the dimerisation of phenol to 2,2'-biphenol and polymerisation of phenol to 2,2-coupled byproducts.

Biffis and co-workers[115] recently reported the role of water for the coupling of organic molecules using copper catalysts could be more complex than previously thought. Since water and chloroform were not labile, most of the water ligands around copper cations remained and so under standard reaction conditions the Cu/Zeolite-Y catalytic system was saturated with water. The thermogravimetric analysis of fresh Cu(6%)/Zeolite-Y confirmed the loss of water from Cu/Zeolite-Y below 373 K. The removal of some of this water by low temperature pre-treatment of the catalyst prior to reaction increased the adsorption of phenol and therefore also the initial conversion of phenol. Increasing the adsorption of phenol was analogous to increasing the concentration of phenol solution and favoured the dimerisation of phenol to 2,2'-biphenol. The initial conversion of phenol was then a function of the partial pressure of oxygen used for degassing. The regeneration of active sites required oxygen and water and so increasing the concentration of oxygen in the feed stream increased the rate at which sites could be regenerated before coke formation limited conversion at 10 min.

After high temperature pre-treatment of Cu/Zeolite-Y at 773 K the apparent conversion of phenol was increased to a maximum 100%. With all water removed from the catalyst adsorption of phenol was maximised but catalytic activity was destroyed. There was almost no dimerisation of phenol to 4,4'-biphenol, 2,2'-biphenol or 4-phenoxyphenol or polymerisation of phenol to byproducts and coke. Apparent deactivation was therefore a function of reduced adsorption capacity rather than coke formation. Reedijk *et al.*[74] and Challa *et al.*[69] reported using a copper(II) nitrate/ N-methylimidazole catalyst for the homogeneous phase oxidative polymerisation of 2,6-dimethylphenol. Both authors concluded that 2,6-dimethylphenol did not react with the complex in the absence of water. High temperature pre-treatment removed all the water from Cu/Zeolite-Y and the ability of copper to activate phenol.

4.3.2 Acetonitrile solution

Acetonitrile and water were labile ligands for all accessible metal cations and acetonitrile also bound directly to the aluminosilicate surface via Brønsted acid sites formed by the deprotonation of phenol upon adsorption. Copper was the most active metal when using an acetonitrile solution. The activity decreased: Cu > Ag > Ni, the opposite trend to when a chloroform solution was used. Water, acetonitrile and phenol were all labile ligands for the metal cations and so as the lability of the metal increased so also the likelihood of phenol adsorption, activation and dimerisation increased. Copper was the most labile and therefore the most active metal catalyst for the dimerisation of phenol. Conversion of phenol was the same in acetonitrile as it had been in chloroform, although the selectivity of phenol dimerisation to 2,2'-biphenol, 4-phenoxyphenol and especially 4,4'-biphenol was greatly improved. Selectivity to 4,4'-biphenol was a function of the acetonitrile used as a solvent for phenol and depended less on the metal cation, as explained in Section 4.2.2.

The active metal sites in Cu(5%)/MCM-41 were located along the length of unidimensional mesopores. Without the intersecting pore and cage system of Cu(6%)/Zeolite-Y the majority of active sites in MCM-41 were too far apart for dimerisation of phenol to 2,2'-biphenol, unlike the more elongated 4,4'-biphenol and 4-phenoxyphenol. The Cu(6%)/Zeolite-Y catalyst yielded ca. 10% more 4,4'-biphenol over the 90 min compared to Cu(5%)/MCM-41. Using either catalyst the initial yield of 4,4'-biphenol was similar but Cu(5%)/MCM-41 quickly deactivated. The pore diameters of Cu(5%)/MCM-41 were larger and so the dimerisation of phenol was less sterically hindered. Conversion of phenol by Cu(5%)/MCM-41 was increased at the expense of dimer selectivity and the polymerisation of phenol to byproducts, the precursors to coke caused rapid catalyst deactivation.

As the metal loading of Cu/Zeolite-Y was increased the conversion of phenol also increased. In acetonitrile the number of phenol molecules adsorbed at each copper site was limited by the competitive adsorption of phenol with acetonitrile and water. As metal loading was increased, so also the number of copper sites increased on which a phenol molecule could adsorb and be activated, enhancing phenol conversion. Selectivity to 4,4'-biphenol, 2,2'-biphenol and 4-phenoxyphenol decreased as copper loading was increased since as the number of activated phenol molecules per unit

volume of catalyst increased, the likelihood of secondary reactions and subsequent coke formation also increased, reducing selectivity to phenolic dimers.

Reaction temperature had a complex affect on the catalytic dimerisation of phenol using a solution of phenol in acetonitrile. Temperature affected the relative adsorption and desorption rates of phenol, acetonitrile, water and the products of phenol dimerisation. Higher reaction temperatures increased the desorption rate of acetonitrile from Brønsted acid sites on the aluminosilicate surface adjacent to copper cations. This reduced the selectivity to 4,4'-biphenol and as a result increased the number of active sites at which C-O coupling was viable which enhanced byproduct formation. A period of activation was identified at 388 and 408 K, when the maximum conversion of phenol was not between 0 and 5 min but between 5 and 10 min. After the catalyst was pre-heated to reaction temperature, phenol solution at room temperature was introduced into the reactor. This cooled the catalyst bed, reducing phenol conversion until the furnace reheated the reactor and catalyst to reaction temperature. At lower temperatures the cooling effect was less and the furnace maintained a constant catalyst bed temperature. The general affect of temperature was to increase conversion since at elevated temperatures more phenol molecules had at least the activation energy required for coupling.

Increasing the concentration of phenol solution between 0.02 and 0.16 mol L^{-1} increased the conversion of phenol and decreased the selectivity to 4,4'-biphenol, 2,2'-biphenol and 4-phenoxyphenol. Using a solution of phenol in acetonitrile the number of phenol molecules adsorbed per active site was limited. It was possible that some of the copper sites accessible to phenol had only acetonitrile and water adsorbed at the metal. Increasing phenol concentration therefore increased the number of sites at which phenol was adsorbed. As the number of activated phenol molecules per unit volume was increased so also phenol polymerisation to byproducts and coke increased. This reduced the selectivity of phenol dimerisation to 4,4'-biphenol, 2,2'-biphenol and 4-phenoxyphenol. Using a 0.32 mol L^{-1} phenol solution the conversion of phenol was reduced and selectivity to phenolic dimers improved. At 0.32 mol L^{-1} the number of phenol molecules adsorbed at cation exchange sites in each supercage was increased. This sterically hindered the polymerisation of phenol, increasing the selectivity to phenolic dimers but reducing the rate of reaction as less phenolic dimers

were removed from the catalyst before deactivation. The order of reaction with respect to phenol was calculated as +0.6 confirming phenol concentration had a direct affect on the rate of reaction.

The low temperature pre-treatment of Cu(6%)/Zeolite-Y did not affect the initial conversion of phenol between 0 and 5 min but did cause more rapid deactivation of the catalyst. Deactivation was independent of the partial pressure of oxygen in the gas used for degassing the system prior to reaction. Under standard reaction conditions using a solution of phenol in acetonitrile, Cu(6%)/Zeolite-Y was water deficient for optimum *in situ* catalyst regeneration. When some of the water in a fresh sample of catalyst was removed prior to reaction, the rate of deactivation was increased as there was less water available for the generation of active sites before coking blocked catalyst pores and prevented any further conversion of phenol. The selectivity to phenolic dimers was increased as the competitive adsorption between water and acetonitrile was reduced. With more acetonitrile adsorbed at cation exchange sites and neighbouring Brønsted acid sites the selectivity to 4,4'-biphenol was increased. Less water also meant more phenol adsorption which increased conversion of phenol to 4-phenoxyphenol and in particular 2,2'-biphenol.

The effects of high and low temperature pre-treatment on the conversion of phenol by Cu(6%)/Zeolite-Y and selectivity to 4,4'-biphenol, 2,2'-biphenol and 4-phenoxyphenol were similar. After high temperature pre-treatment however the initial conversion of phenol was reduced to <4%, after the low-temperature pre-treatment the initial phenol conversion was similar to a standard reaction. Rapid deactivation was caused by a shortage of water for active site regeneration. During the pre-treatment of Cu(6%)/Zeolite-Y at 773 K the water ligands were removed and not replaced, altering the coordination environment of copper and reducing the ability of copper to activate phenol. The reduction of Cu^{2+} to Cu^{1+} was caused by pre-treatment with nitrogen at 773 K after which the conversion of phenol uniquely increased with TOS as oxygen was introduced into the system by incomplete degassing of the feedstock solution, reoxidising Cu^{1+} to Cu^{2+} and generating catalytic activity.

The conversion of phenol increased with liquid pressure as the movement of phenol within the pores of Zeolite-Y was improved. Gas and liquid pressures are not synonymous since liquids are almost incompressible. The ability of a liquid to enter a void or pore is controlled largely by the size of the opening, the contact angle and the liquid-gas interface, which is affected by the pressure of the liquid. The surface tension below which wetting of the solid surface occurs, increases with liquid pressure. At 30 bar g more of the zeolite pores and supercage have their internal surfaces wetted by phenol solution increasing the chance of phenol adsorption and subsequent phenol dimerisation.

Copper acetate was used to prepare Cu(6%)/Zeolite-Y from Na/Zeolite-Y. Adding potassium acetate to the feedstock solution facilitated the ion-exchange of copper for potassium and subsequent removal of copper acetate from the system. Most of the copper in a fresh sample of Cu(6%)/Zeolite-Y had been leached within 90 min. Conversion of phenol was largely unaffected by the addition of potassium acetate, but copper was mobilised by the addition, substantially increasing the selectivity to 2,2'-biphenol and 4-phenoxyphenol as all dimerisations became equally viable. The number of possible phenol activations per cation before reoxidation of the metal did not increase. Fujiyama *et al.*[55] and Kohara *et al.*[62] reported the addition of alkali metals into the feedstock solution or onto the Cu-Na/MCM-41 catalyst surfaces increased catalytic activity for phenol oxidation. Neither Fujiyama *et al.*[55] or Kohara *et al.*[62] provided an explanation for the increased catalytic activity observed. Hayashibara and co-workers[93] also studied the effect of alkali promoters but on Cu-Na/ZSM5 catalysts for the oxidation of benzyl alcohol and suggested that the alkali forced Cu ions within the zeolite to locate at sites more accessible to reactant molecules. Using an *open* flow reactor the addition of potassium acetate to the feedstock leached all copper from the system. The *closed* batch reactors used by Fujiyama *et al.*[55], Kohara *et al.*[62] and Hayashibara *et al.*[93] ensured all copper and potassium compounds were in constant contact with the catalyst and reactants. No recognition was made by any of the authors that the dimerisation reactions could be taking place outside the aluminosilicate support and were therefore homogeneous.

At a constant Liquid Hourly Space Velocity (LHSV) the conversion of phenol increased with flow rate. As flow rate was increased the residence time of phenol and phenolic dimers in the cages and pores of Cu(6%)/Zeolite-Y was reduced which meant subsequent phenol polymerisation to the larger coke molecules was less likely. This slowed the rate of deactivation and so conversion of phenol at a constant LHSV increased.

Using standard reaction conditions and a solution of phenol in acetonitrile, Cu(6%)/Zeolite-Y was water deficient for optimum *in situ* catalyst regeneration. Catalyst activity and the rate of deactivation were reported by Girotti *et al.*[87] to depend on the water content of the liquid phase fraction of the reaction mixture. Acetonitrile and water were labile ligands for copper and so some of the water in fresh Cu(6%)/Zeolite-Y was removed by the flow of phenol in acetonitrile solution. Adding water to the feedstock enhanced active site regeneration, increasing phenol conversion. Lucas *et al.*[90] demonstrated that water could reduce the deactivation rate of H/ZSM-5 catalysts by converting Brønsted acid sites into Lewis acid sites so by reducing coke formation. Adding water to the catalytic system altered the equilibrium between water, acetonitrile and phenol, with less acetonitrile more phenol was adsorbed which made the dimerisation of phenol to 2,2'-biphenol viable. In the presence of a metal, peroxide (H_2O_2) decomposes to water and oxygen. The coupling of phenol to phenolic dimers using Cu(6%)/Zeolite-Y with H_2O_2 added to the feedstock was increased by the controlled *in situ* generation of water and oxygen required for active site regeneration.

4.3.3 Other solutions

The dimerisation of phenol to 4,4'-biphenol, 2,2'-biphenol and 4-phenoxyphenol was studied using Cu(6%)/Zeolite-Y and a mixed chloroform and acetonitrile solution. Different molar ratios of acetonitrile to phenol were used but even at a 1:1 molar ratio the results were indistinguishable from the standard reaction using a solution of phenol in chloroform. More acetonitrile was required if the coordination of acetonitrile to copper and the aluminosilicate surface was to direct the dimerisation of phenol.

The dimerisation of phenol over Cu(6%)/Zeolite-Y was also studied using solutions of phenol in propionitrile and butyronitrile. The conversions of phenol using propionitrile and butyronitrile solutions were comparable at ca. 45% between 0 and 5 min. After 5 min the conversion of phenol in either solution was similar and matched the conversion obtained in acetonitrile solution. The initial increase in conversion using propionitrile and butyronitrile was due to increased phenol adsorption. Propionitrile and butyronitrile were less labile ligands and so there was less competition between phenol and the solvent for adsorption sites. This was analogous to increasing phenol concentration which increased conversion and reduced dimer selectivity. After 5 min when the initial conversion reduced, the extended hydrocarbon chain of butyronitrile adsorbed on copper and the aluminosilicate surface had even greater control on the orientation of activated phenol molecules, directing the dimerisation of phenol to 4,4'-biphenol.

4.4 Clay catalysts

The activity of the clay catalysts was investigated using a mixed chloroform and acetonitrile solution of phenol. Since the conversion of phenol and selectivity to 4,4'-biphenol, 2,2'-biphenol and 4-phenoxyphenol catalysed by Cu(6%)/Zeolite-Y had been improved using an acetonitrile solution, the dimerisation of phenol catalysed by Cu/Montmorillonite and Cu/Attapulgite was also to be studied using an acetonitrile solution. It had however already been established that it was not possible to flow an acetonitrile solution through Cu/Attapulgite since the pressure drop across the bed exceeded 100 bar g. The activity of Cu/Montmorillonite and Cu/Attapulgite was therefore investigated using a mixed acetonitrile/chloroform solution.

The yield of 4,4'-biphenol was controlled by the position of active sites and therefore adsorbed phenoxy radicals. For Cu/Attapulgite the cation exchange sites are located along the walls of the open cavities. The distance across the cavity is well matched to the distance between the oxygen atoms of 4,4'-biphenol. Montmorillonite is classified as a dioctahedral layered smectite clay with interlayer spacings between 1.0 and 1.5 nm.[2] The exchangeable cations in Cu/Montmorillonite are located in the interlayer adjacent to the aluminosilicate surfaces. Using Cu/Zeolite-Y, a high yield of 4,4'-biphenol was recorded because adsorption of phenol at opposite sites in the supercage was least sterically hindered. For the same reason dimerisation of phenol using sites on opposite sides of the Attapulgite cavities was least sterically hindered and so 4,4'-biphenol formation was favoured. With an interlayer spacing of between 1.0 and 1.5 nm, the dimerisation of phenol using Cu/Montmorillonite was affected less by the steric constraints of the support and so C-C and C-O coupling were equally viable. When the interlayer space was >1 nm the interaction between activated phenolate ions across the interlayer was minimised, increasing the selectivity to 4-phenoxyphenol. The rate-limiting step using Cu/Attapulgite like Cu/Zeolite-Y was the dimerisation of phenol, whilst coke formation was the ultimate cause of deactivation. The activity of Cu/Attapulgite relied upon the access of phenol molecules to two exchangeable cations opposite one another on either side of an open cavity. As for Cu/Zeolite-Y the dimerisation of phenol by copper exchanged Attapulgite was a catalytic not stoichiometric reaction since only a small fraction of copper cations were catalytically active.[114]

4.4.1 Chloroform and acetonitrile mixed solution

As the metal loading of Cu/Attapulgite was increased so also the conversion of phenol increased. Assuming the even distribution of interlayer cations, as metal loading was increased the average distance between copper cations decreased. At 1 and 3% loading few active sites were close enough for the dimerisation of phenol. At 5% loading the average distance was reduced and coupling of phenol to 4,4'-biphenol was viable. As the initial conversion of phenol was increased so also the rate of coke formation and catalyst deactivation increased.

The effect of temperature on the conversion of phenol by Cu/Attapulgite and selectivity to phenolic dimers was complex, Arrhenius behaviour was not observed. Phenol conversion at 328, 348 and 388 K was similar, at 408 K conversion between 0 and 10 min was increased to >90%. Selectivity to 4,4'-biphenol, 2,2'-biphenol and 4-phenoxyphenol decreased as reaction temperature was increased, particularly when the temperature was raised from 388 to 408 K. The marked increase in conversion at 408 K was accompanied by a decrease in dimer selectivity and increased coke formation. The precursors to coke were phenolic dimers and trimers and at higher temperatures more phenol molecules had at least the activation energy required for coupling to phenolic dimers and coke. Temperature also affected the rate of phenol adsorption and the desorption rate of phenol and reaction products. The water content of the catalyst was also affected by reaction temperature as was the stability of the acetonitrile and water complex with copper cations. As temperature was increased the lability of the copper, acetonitrile and water complex was increased which reduced the steric control that acetonitrile ligands had on the dimerisation of phenol, so reducing selectivity to phenolic dimers, in particular 4,4'-biphenol.

The same number of moles of phenol were converted between 0 and 5 min at the three concentrations of phenol solution 0.02, 0.04 and 0.08 mol L^{-1}. The order of reaction with respect to phenol concentration was calculated as zero, suggesting a mass transfer limited reaction. Mass transfer or diffusion control describes a system when the movement of reactants to the active sites limits the rate of reaction.[119] Attapulgite is a non-swelling clay and the flow of reactants and products through the mesopores of any clay can be restricted by the seemingly unordered arrangement of aluminosilicate sheets or ribbons. Diffusion control was not observed using

Cu/Zeolite-Y which had an ordered, three-dimensional structure of sodalite units connected through hexagonal prisms. The maximum conversion of phenol using Cu/Attapulgite was recorded between 5 and 10 min at each concentration, another indication that the system was diffusion controlled. Regardless of phenol concentration the conversion of phenol increased with TOS as the local concentration of phenol at cation exchange sites increased before conversion of phenol was decreased due to catalyst deactivation. The maximum conversion of phenol using Cu/Zeolite-Y as the catalyst was sometimes recorded between 5 and 10 min but not using standard experimental conditions or as a function of phenol concentration.

The selectivity of phenol dimerisation to 4,4'-biphenol, 2,2'-biphenol and 4-phenoxyphenol was affected by phenol concentration. The yield of 4,4'-biphenol was the highest at all three phenol concentrations. At 0.02 mol L^{-1} there was significant conversion of phenol to 2,2'-biphenol and 4-phenoxyphenol. If phenol was adsorbed at active sites on opposite sides of the cavity then selectivity was directed towards 4,4'-biphenol, if sites were next to one another then 4-phenoxyphenol and 2,2'-biphenol were produced, as discussed in Section 4.2.2. In Cu/Zeolite-Y neighbouring sites were 90° apart, hindering the adsorption of phenol molecules simultaneously at both sites. For Cu/Attapulgite the cation exchange sites were located down the length of open cavities at 180° to one another. Simultaneous adsorption of phenol at neighbouring sites was therefore not sterically hindered although the dimerisation of phenol to 4,4'-biphenol remained favourable because of the well matched distance between the cavity walls and the dimensions of 4,4'-biphenol. As the concentration of phenol was increased from 0.02 to 0.04 mol L^{-1} the yield of 4,4'-biphenol doubled as more phenol molecules adsorbed at sites opposite one another. As a result the selectivities to 2,2'-biphenol and 4-phenoxyphenol were reduced. At 0.08 mol L^{-1} the local concentration of phenol increased and so the opportunity for phenol polymerisation increased which reduced in particular the selectivity to 4,4'-biphenol.

Low temperature pre-treatment illustrated the sensitivity of the catalytic system to experimental conditions. The low temperature pre-treatment of Cu/Attapulgite removed some of the adsorbed water, as confirmed by the thermal analysis of fresh catalyst (Section 3.5.6). Removing some of this water increased phenol adsorption by reducing the competitive adsorption from water and subsequently increased phenol

conversion. Using standard reaction conditions with no pre-treatment the catalyst contained excess water and so low temperature pre-treatment using nitrogen, air or oxygen for degassing increased the conversion of phenol. The initial conversion of phenol increased as the partial pressure of oxygen decreased, which was unique to the low temperature pre-treatment of Cu/Attapulgite. The catalytic activity of Cu/Attapulgite was greater than the activity of Cu/Zeolite-Y and so using nitrogen for the low temperature pre-treatment of Cu/Attapulgite reduced the rate of active site regeneration. This reduced the polymerisation of phenol to coke, thus reducing pore blocking and increasing the initial conversion of phenol. This is better described as slowing the rate of catalyst deactivation rather than increasing conversion.

High temperature pre-treatment of Cu/Attapulgite removed most of the adsorbed water and reduced the conversion of phenol. Like the pre-treatment of Cu(6%)/Zeolite-Y at 773 K ligands surrounding the copper cations in Cu/Attapulgite were removed and not replaced and so the coordination environment around the copper cations was altered, reducing the ability of copper to activate phenol. Again like Cu/Zeolite-Y, the reduction of Cu^{2+} to Cu^{1+} was possible by pre-treatment with nitrogen at 773 K and the conversion of phenol by Cu/Attapulgite increased with TOS as oxygen was introduced into the system by incomplete degassing of the feed stock solution. The yield of 4,4'-biphenol, 2,2'-biphenol and 4-phenoxyphenol increased with the partial pressure of oxygen after low temperature pre-treatment of Cu/Attapulgite. This substantiated evidence that the polymerisation of phenol was an oxidative dehydrogenation process.

4.5 Catalyst deactivation and regeneration

There are four reasons for the deactivation of zeolite and clay catalysts during commercial processes.[41] Carbonaceous deposits or coke are the principal cause of deactivation for processes involving the conversion of hydrocarbons. The rate of deactivation depends not only on the relative rate but also the mode of coke formation. The effect of coke is more pronounced when deactivation is due to pore blockage compared to active site coverage[42]. There are four modes of pore blockage defined by Guisnet and co workers,[41] summarised in Figure 13, Section 1.2.6.1. The regeneration of catalyst activity is an important aspect of any catalytic system since deactivation by coke is reversible. Coke is generally removed by oxidation and the re-calcination in $2\%O_2/Ar$ and air of Cu/Zeolite-Y and Cu/Attapulgite removed all carbonaceous deposits and re-oxidised any Cu^{1+} species back to Cu^{2+}, regenerating catalytic activity. The Carbon/Hydrogen/Nitrogen (CHN) analysis of insoluble coke from a standard reaction using fresh Cu(6%)/Zeolite-Y confirmed that the coke consisted of various tetramers and pentamers of phenol.

The UV/Vis/NIR spectra of copper exchanged Zeolite-Y were obtained by Mesu[39] for a range of copper loadings, Section 1.2.5. The measured spectra of fresh Cu(6%)/Zeolite-Y and Cu(5%)/Attapulgite presented the characteristic d-d transition band of Cu^{2+} between wavelengths of 12,500 and 15,300 cm^{-1}. Deactivation of Cu(6%)/Zeolite-Y and Cu(5%)/Attapulgite would have occurred if Cu^{1+} ions could not be reoxidised to Cu^{2+} ions and so confirming the oxidation state of copper in fresh and spent samples of catalyst helped to identify the causes of catalyst deactivation. The UV/Vis/NIR spectra of spent Cu(6%)/Zeolite-Y and Cu(5%)/Attapulgite catalyst after reaction using standard conditions also presented the characteristic d-d transition band with equal intensity. This suggested that the reoxidation of copper was not the cause of catalyst deactivation. The spectra were obtained *ex situ*, having removed the catalyst from the reactor it was dried at room temperature in nitrogen. The thermal analysis of Cu^{1+} oxide in a flow of $2\%O_2/Ar$ confirmed the uptake of oxygen indicative of the oxidation of Cu^{1+} to Cu^{2+}, only at temperatures above 573 K. Therefore even when the catalyst was briefly exposed to oxygen at room temperature, this was unlikely to affect the oxidation state of copper.

The metal ion leaching of copper from Cu(6%)/Zeolite-Y and Cu(5%)/Attapulgite was investigated and no significant leaching was observed, certainly not enough to justify the observed loss of catalyst activity. This data therefore agrees with the investigation by Norena-Franco and co-workers[28] which reported no significant leaching of copper from Cu/MCM-41 used for the hydroxylation of phenol (Section 1.2.3). Like Norena-Franco and co-workers[28] the dimerisation of phenol was studied using an acetonitrile solution of phenol and the catalysts prepared using a hydrothermal method of exchange.

Another potential cause of catalyst deactivation was coking, resulting in any or all of the four modes of pore blockage suggested by Guisnet and co-workers[41] discussed in the introduction, Section 1.2.6.1. Deactivation depends not only on the relative rate but also the mode of coke formation. The effect of coke is more pronounced when deactivation is due to pore blockage compared to active site coverage[42]. Coking, deactivation rates and the composition of coke depend on the pore structure of the zeolite or clay. Coke can be characterised by its hydrogen/carbon ratio, whether it is soluble or insoluble in for example methylene chloride[42] and by the temperature at which it forms[44]. The dimerisation of phenol using Cu(6%)/Zeolite-Y and Cu(5%)/Attapulgite was sensitive to reaction temperature. Arrhenius behaviour was not observed for any of the combinations of catalyst and phenol solution which meant it was not possible to calculate for example the activation energy for phenol dimerisation. The complex effect of temperature on phenol conversion and selectivity to 4,4'-biphenol, 2,2'-biphenol and 4-phenoxyphenol may have been the result of coke formation. The hydrogen to carbon ratio of the coke formed within Cu(6%)/Zeolite-Y and Cu(5%)/Attapulgite catalysts was 0.78, close to that of phenol which is 1.

From the XRD patterns of *fresh* and *spent* catalyst samples the crystalline structure of catalysts remained intact during the dimerisation of phenol. The literature[42, 45, 46] reports that *ex situ* X-ray powder diffraction can be used to confirm the deposition of coke within aluminosilicate structures. Peak intensities were less for the spent Cu/Zeolite-Y sample compared to the fresh and Adebajo *et al.*[120] suggest that this is due to X-ray shielding caused by the absorption of radiation by carbonaceous material in the zeolite pores. Lucas *et al.*[45] used XRD to correlate the decreasing intensity of a shoulder on the main reflection with increasing coke content. The decrease in surface

area after reaction, observed for both Cu(6%)/Zeolite-Y and Cu(5%)/Attapulgite confirmed by BET analysis also suggested the deposition of coke within the pores of the catalysts although the coke did not affect the pore diameter of the catalysts. The pore dimensions of Cu(6%)/Zeolite-Y and the dimensions of the open cavities of Cu(5%)/Attapulgite are similar to the dimensions of the phenolic dimers, especially 4,4'-biphenol which explains why these materials were catalytically active and shape selective but also why deactivation was a problem. Removal of phenolic dimers from within these pores and cavities was restricted by their size and so many of the phenolic polymers with three of more phenol moieties were trapped inside the aluminosilicate framework.

The thermal analysis of fresh Cu(6%)/Zeolite-Y confirmed only water was removed during heating to 1273 K at 10° min^{-1}. The fresh catalyst was therefore free from residual acetate molecules used for catalyst preparation. The spent Cu(6%)/Zeolite-Y catalyst liberated CO (m/e = 28), CO_2 (m/e = 44), acetonitrile (m/e = 41), phenol (m/e = 94), biphenol (m/e = 186) and water (m/e = 18). The CO and CO_2 were combustion products of coke, the acetonitrile and phenol were the feedstock for the reaction and the removal of biphenol suggested that not all dimeric products had been flushed from the system. The water removed from fresh Cu(6%)/Zeolite-Y was liberated at 398 K, above the boiling point of water suggesting that water ligands were strongly bound to metal copper cations. More than one peak in the mass spectrum trace of a single mass/charge (m/e) ratio implies more than one type of that species. The mass spectrum of water liberated from spent Cu(6%)/Zeolite- Y therefore indicated two types of water. There was a peak at 398 K, also observed in the analysis of fresh catalyst and another peak at 573 K that was assigned to the conversion of Brønsted acid sites back to basic Lewis sites. This conversion was possible in the presence of a base, as discussed in Section 4.2.2 but in the absence of any base heating the catalyst can drive the conversion, with the liberation of water. Conversion of Brønsted to Lewis acid sites at 673 K was mentioned in Section 1.4.1, but the sites on Cu(6%)/Zeolite-Y were originally Lewis base sites, which accounts for the discrepancy in conversion temperature.

The liberation of acetonitrile from spent Cu(6%)/Zeolite-Y samples suggested two modes of adsorption. The less strongly adsorbed acetonitrile was liberated at the

boiling point of acetonitrile, 353 K. Water is reportedly a stronger ligand for copper, compared to acetonitrile[28] and the thermal analysis of spent Cu(6%)/Zeolite-Y confirmed that water was liberated above its boiling point at 398 K whilst acetonitrile was liberated at its boiling point. The peak at 498 K observed in the acetonitrile trace was assigned to the removal of acetonitrile adsorbed on the aluminosilicate surfaces, Section 4.2.2. This acetonitrile was strongly bound to the surface which vindicates the ability of acetonitrile to direct the selectivity of phenol dimerisation. This type of acetonitrile was not removed using standard reaction conditions or at any other reaction temperature studied. There were multiple peaks in the mass spectrum of carbon dioxide (m/e = 44) and at least two peaks for carbon monoxide (m/e = 28). The CO and CO_2 were combustion products of coke suggesting many different types of coke and byproducts. The desorption of phenolic dimers occured between 448 and 548 K, under the boiling point of 4,4'-biphenol, 2,2'-biphenol and 4-phenoxyphenol but before the temperature of decomposition at ca. 573 K. Phenol desorbed between 648 and 723 K, above the boiling point of phenol at 455 K, suggesting phenol was also strongly adsorbed to the aluminosilicate surface and copper cation.

The thermal analysis of fresh Cu(5%)/Attapulgite catalyst confirmed the removal of water whilst spent Cu(5%)/Attapulgite liberated CO (m/e = 28), CO_2 (m/e = 44), acetonitrile (m/e = 41) and water (m/e = 18). As before the CO and CO_2 were combustion products of coke, acetonitrile and phenol were the feedstock for the reaction. From the lack of mass spectrum traces at m/e = 94 and 186 the removal of phenol and biphenol from spent Cu(5%)/Attapulgite could not be detected. The mass spectrum trace of water liberated from spent Cu(5%)/Attapulgite suggested two types of water removed at 373 and 523 K, assigned again to the ligands surrounding copper cations and to the conversion of Brønsted acid sites back to basic Lewis sites. The aluminosilicate structure of Attapulgite (Section 4.2.1, Figure 104) illustrated the relative ease at which phenol and water could access the cation exchange sites in the open cavities. The removal of phenol and biphenol from the catalyst prior to thermal analysis supports this hypothesis.

The liberation of acetonitrile from spent Cu(5%)/Attapulgite catalyst suggested two modes of adsorption. The peaks were assigned to acetonitrile coordinated to copper and acetonitrile adsorbed on the aluminosilicate surface. The acetonitrile liberated at

373 K did so above its boiling point (353 K) whilst water ligands were liberated at the boiling point of water 373 K. The opposite trend was recorded for Cu(6%)/Zeolite-Y suggesting the strength of ligand adsorption was affected by the aluminosilicate support structure. The thermal analysis of Cu(5%)/Attapulgite and Cu(6%)/Zeolite-Y highlighted the subtly different coordination environments of copper.

Heating Cu(6%)/Zeolite-Y to 723 K at 10^{o} min^{-1} removed all the coke deposited in the pores and channels of the aluminosilicate structure. This helped to design a procedure for catalyst regeneration but it was also important to establish the effects of 4,4'-biphenol, 2,2'-biphenol and 4-phenoxyphenol had on the conversion of phenol. The activity of Cu(6%)/Zeolite-Y was studied after pre-treatment with the phenolic dimers in acetonitrile and acetonitrile on its own although the effect of pre-treating the catalyst with acetonitrile masked the affects of the three dimers. The acetonitrile pre-treatment generated a catalyst apparently capable of maximum conversion of phenol from an acetonitrile solution for the first 10 min of reaction. In Section 4.3.2 the conversion of phenol was also reportedly increased by the addition of water or peroxide as this aided the regeneration of active sites and so pre-treatment with acetonitrile should have decreased the conversion of phenol by removing most of the water, already in short supply. The addition of acetonitrile did decrease the conversion of phenol to phenolic dimers, but increased the apparent overall conversion of phenol. Pre-treating the catalyst with acetonitrile removed all but trace amounts of water, present as ligands surrounding the copper cations. The increased conversion of phenol by pre-treatment with acetonitrile was therefore the result of a change to the copper cation active site. Water is reportedly a stronger and so less labile ligand for copper compared to acetonitrile.[28] After pre-treatment with acetonitrile the adsorption of phenol was maximised by the need for phenol to replace only acetonitrile molecules. Acetonitrile was therefore not only a solvent for phenol but also a catalyst modifier. After pre-treatment with acetonitrile or any of the phenolic dimers in acetonitrile the catalysts activity was limited by the lack of water but the adsorption of phenol was maximised so increasing the apparent conversion of phenol.

The affect of acetonitrile on the conversion of phenol masked the individual affects of the three dimers 4,4'-biphenol, 2,2'-biphenol and 4-phenoxyphenol. Despite this the decomposition of each dimer to phenol and the isomerisation to the other two dimers

was confirmed over Cu(6%)/Zeolite-Y. Phenol was the major product of each pre-treatment with 4,4'-biphenol, 2,2'-biphenol or 4-phenoxyphenol in acetonitrile. The yield of phenol from the decomposition of 4,4'-biphenol over Cu(6%)/Zeolite-Y was six times more than the yield of 4,4'-biphenol from the dimerisation of phenol over the same catalyst and therefore the back reaction during the standard dimerisation of phenol was cause for a significant loss in the yield of 4,4'-biphenol. The planar conformation of 4,4'-biphenol confirmed by Das[80] meant that the negative charge from one deprotonation was delocalised over the whole molecule and this stabilised the ion, resisting a second deprotonation. The effect was not as prominent for the twisted and non-linear structures of 4-phenoxyphenol and 2,2'-biphenol respectively but the decomposition of all three of these molecules to phenol over Cu(6%)/Zeolite-Y was equally viable. The relative ease at which 4,4'-biphenol was decomposed ratifies the catalytic activity of Cu/Zeolite-Y.

The *ex situ* regeneration of Cu(6%)/Zeolite-Y confirmed that catalyst activity could be regenerated. The initial conversion of phenol using the regenerated catalyst was more than five times greater than conversion of phenol recorded using the fresh catalyst. After the spent catalyst was calcined it was left exposed to atmosphere for one week before being reloaded into the reactor. The conversion of phenol by Cu(6%)/Zeolite-Y and selectivity to 4,4'-biphenol, 2,2'-biphenol and 4-phenoxyphenol was known to be affected by the water content of the catalyst. The hydration of the regenerated catalyst was not the same as the fresh sample that had been stored under ambient conditions for months not days. The author Mesu[39] confirmed the d-d transition band of Cu/Zeolite-Y was sensitive to the hydration state of the zeolite and Cu^{2+} loading suggesting the presence of at least two different Cu^{2+} species. The selectivities to 4,4'-biphenol, 2,2'-biphenol and 4-phenoxyphenol using the regenerated catalyst were similar to those recorded using a 0.02 mol L^{-1} solution of phenol in acetonitrile and fresh Cu(6%)/Zeolite-Y. The increased conversion of phenol reduced the local concentration of phenol, mimicking the selectivity to dimers using the less concentrated phenol solution. The increased conversion of phenol by the regenerated catalyst was a result of changing the adsorption equilibrium between water, acetonitrile and phenol causing rapid coke formation and catalyst deactivation.

5 Conclusions

The polymerisation of 2,6-dimethylphenol for the production of C-C and C-O coupled biphenol compounds is catalysed on an industrial scale using homogeneous phase copper/diamine complexes. These homogeneous systems are however unable to yield useful polymers from phenols with only one or no *ortho*-substituent; the polymers yielded are branched and highly coloured compounds,[5] the same group of polyphenols responsible for the colour of a cup of black tea. The stereoselective polymerisation of 2- and/or 6-unsubstituted phenols has been a challenge since Hay's pioneering work in the late 1950's.[5]

The aim of this research project has been to develop a shape selective catalyst capable of the regioselective dimerisation of phenol to 4,4'-biphenol, 2,2'-biphenol and 4-phenoxyphenol, exploiting the different molecular dimensions of the phenolic dimers. Unlike the homogeneous phase process the direct dimerisation of phenol to 4,4'-biphenol, 2,2'-biphenol and 4-phenoxyphenol is atom efficient. *Green chemistry* requires good atom economy using synthetic methods that maximise the incorporation of material used in the process into the final product. The authors Kubota *et al.*[77] commented in 2004 that it was 'difficult to control the regioselectivity of the oxidative polymerisation of 2- and/or 6-unsubstituted phenols using conventional catalysts.' This investigation has demonstrated that the regioselective dimerisation of phenol can be realised using metal-ion exchanged zeolites and clays as catalysts.

The reaction scheme (Figure 107) suggested by Fujiyama *et al.*[55] and Kohara *et al.*[62] for the polymerisation of 2,6-dimethylphenol has been used to better understand the reaction mechanism for the regioselective dimerisation of phenol (Figure 108). The use of zeolites and clays as catalysts for the regioselective dimerisation of phenol has not previously been investigated. The findings of this research project combined with those reported in the literature regarding the polymerisation of 2,6-dimethylphenol provide evidence for each step of the newly proposed reaction scheme. Over the last four decades many researchers have investigated the coupling of phenoxy radicals and concluded that at least one radical is coordinated to the catalyst complex.[70-72] Other researchers[6, 78] have proposed a cyclic reaction scheme for the regeneration of active sites (Section 1.3.3) but have concentrated less on the reaction mechanism.

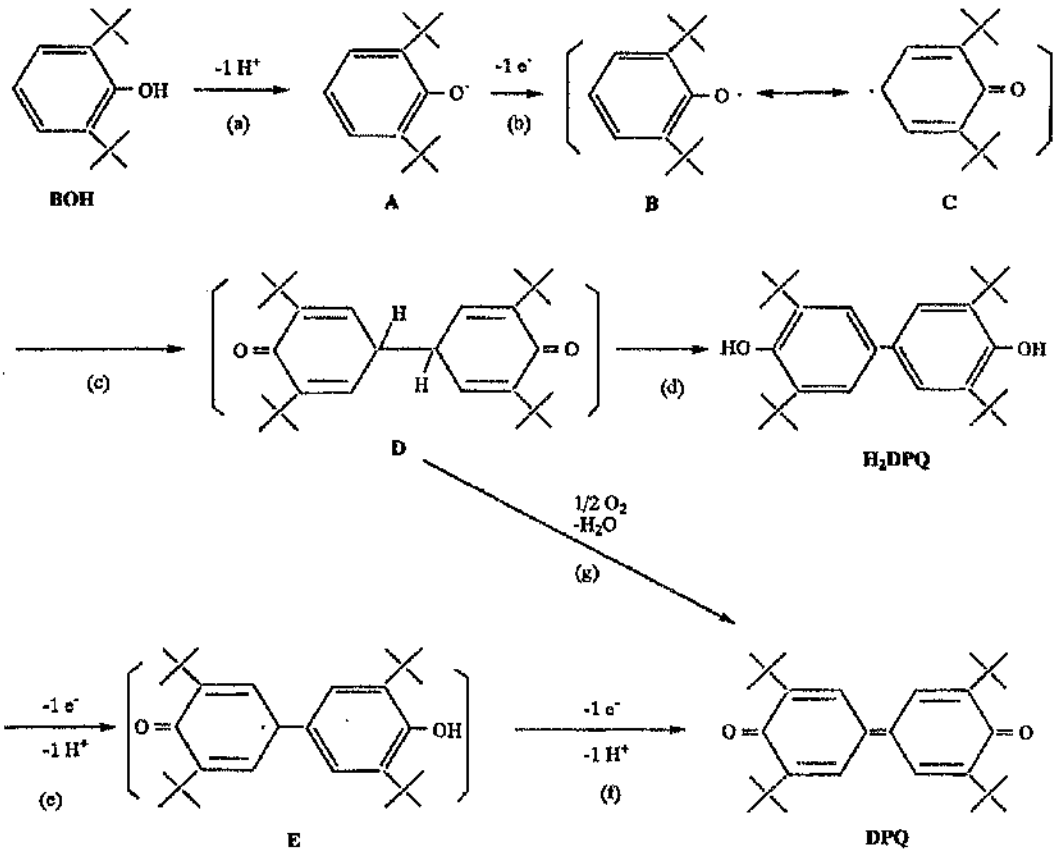

Fig. 107[55] Reaction mechanism for the dimerisation of phenol derivatives.

A recent review paper by Kodayashi *et al.*[6] in 2003 focused on the homogeneous catalysed oxidative polymerisation of phenols. The authors proposed three reaction mechanisms for the C-O selective dimerisation of 2,6-dimethylphenol, (i) the coupling of free phenoxy radicals, (ii) coupling of phenoxy radicals coordinated to the catalyst and (iii) coupling of phenoxonium cations with phenol (Section 1.3.3). The systems are not however fully understood and no single reaction mechanism has yet been universally accepted. The results from this research project provide evidence for the coupling of phenoxy radicals coordinated to the catalyst, proposal (ii). A new reaction mechanism (Figure 108) has been proposed which includes both water and oxygen. The oxygen was required to oxidise Cu^{1+} back to Cu^{2+} and water used to convert Brønsted acid sites back to Lewis base sites[113] in order to complete the catalytic cycle. Beutel *et al.*[60] have been amongst those to report the adsorption of phenol to protonate a basic framework oxygen atom and yield a phenolate ion. The authors[60] reported that catalytic activity was increased in the presence of a base, but

the same reaction has been reported active without added base.[55, 62] The added base enhanced activity because the active site was more readily regenerated not because the base deprotonated phenol.

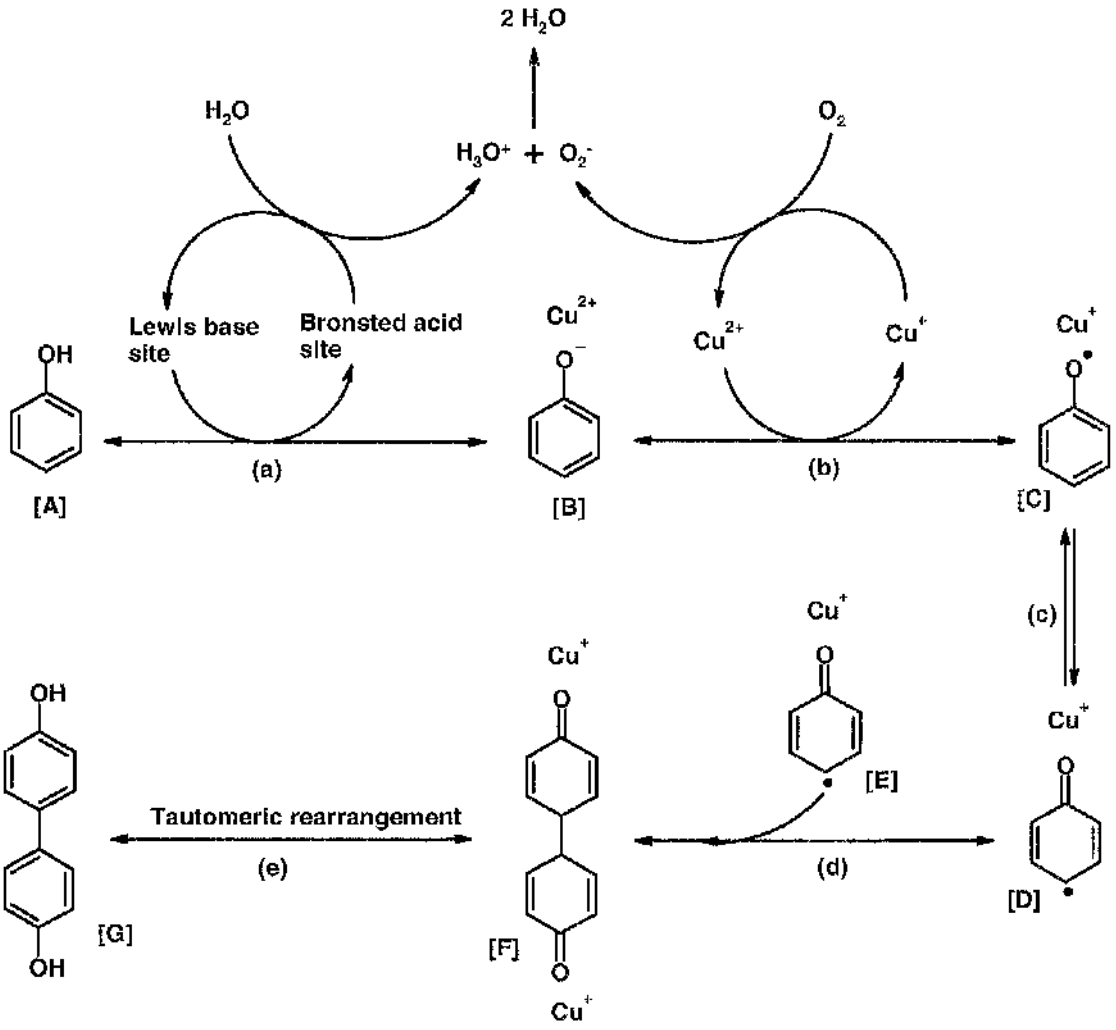

Fig. 108 Reaction mechanism for the regioselective dimerisation of phenol.

Phenol [A] was converted (step (a)) to a phenolate ion [B] by adsorption to a copper cation and an electronegative oxygen atom on the surface of the aluminosilicate support (Figure 97, Section 4.1). This produced a Bronsted acid site that was converted back to a Lewis base site via the protonation of water. Step (b) was the one electron transfer between the phenolate ion and metal. Electron transfer relied on the reduction potential of the metal complex exceeding the oxidation potential of phenolate. Radical [C] remained coordinated to the Cu^{1+} cation, allowing the

migration of the radical from the oxygen to the carbon atoms of the aromatic ring (Step(c)). The donation of electrons from oxygen into the aromatic ring meant that the radical was most likely to be positioned at carbon-4, molecule [D]. The regioselective dimerisation of phenol was governed by the adsorbed orientation of molecule [E], as discussed in Section 4.2.2. If copper exchanged sites were opposite then selectivity was directed towards 4,4'-biphenol, if sites were next to one another then 4-phenoxyphenol and 2,2'-biphenol were produced. Step (d) was the coupling of phenoxy radicals and the rate-determining step. Tautomeric rearrangement (Step (e)) of molecule [F] to molecule [G] generated 4,4'-biphenol, 2,2'-biphenol or 4-phenoxyphenol depending on molecule [F]. The byproducts of this reaction were H_3O^+ and O_2^- or $2H_2O$ and so dehydrogenation was oxidative. This was an atom efficient, *green* process with environmentally benign byproducts; the challenge now is to reduce the formation of byproducts and coke.

The solvents used to dissolve phenol had a considerable impact on the selectivity of phenol dimerisation. The effects of solvent have previously not been investigated; acetonitrile was not only a solvent but also a catalyst modifier. The solvent used did not affect the rate of reaction, rate-determining step or conversion of phenol. The selectivity of phenol dimerisation catalysed by Cu/Zeolite-Y or Cu/Attapulgite was due to the competitive adsorption between water, the solvent and phenol at copper exchanged sites. Chloroform did not coordinate to the copper or aluminosilicate surface and therefore did not replace any water. This allowed free movement of phenol towards neighbouring sites and so the less controlled dimerisation of phenol. The conversion of phenol to 4,4'-biphenol, 2,2'-biphenol and 4-phenoxyphenol by Cu/Zeolite-Y was greatly improved using acetonitrile as the solvent for phenol and as a catalyst modifier, although adsorption of phenol at copper exchanged sites opposite one another was the least sterically hindered. The acetonitrile ligands around copper and acetonitrile coordinated to Brønsted acid sites reducing the ability of phenol to move closer to neighbouring active sites, hindering conversion of phenol to 4-phenoxyphenol and 2,2'-biphenol. The yield of 4,4'-biphenol was controlled by the position of active sites and therefore adsorbed phenoxy radicals. For Cu/Attapulgite the distance across the open cavities and between cation exchange sites was well matched to the distance between the oxygen atoms of 4,4'-biphenol.

[1] R. J. Wijngaarden, A. Kronberg and K. R. Westerterp in *Industrial Catalysis, Optimising Catalysts and Processes*, (1998) Wiley-VCH, Germany.
[2] R. S. Varma, *Tetrahedron*, **58** (2002) 1235-1255
[3] P. E. Laszlo in *Preparative Chemistry Using Supported Reagents*, (1987) Academic, San Diego, CA.
[4] A. S. Hay, *Progress in Polymer Science*, **24** (1999) 45-80
[5] A. S. Hay, *Journal of Organic Chemistry*, (1968) 1160-1161
[6] S. Kobayashi and H. Higashimura, *Progress in Polymer Science*, **28** (2003) 1015-1048
[7] F. Boccuzzi, G. Martra, C. P. Papalia and N. Ravasio, *Journal of Catalysis*, **184** (1999) 327-334
[8] M. Jonsson, J. Lind and G. Merenyi, *Journal of Physical Chemistry A*, **106** (2002) 4758-4762
[9] P. R. Ashton, D. Joachimi, N. Spencer, J. F. Stoddart, C. Tschierske, A. J. P. White, D. J. Williams and K. Zab, *Angewandte Chemie-International Edition in English*, **33** (1994) 1668-1668
[10] *Examined patent application*, (JP06-74227)
[11] M. Michio, Y. Toyofumi and U. Kazuto, *IHARA CHEMICAL IND CO*, (1989) JP1042449
[12] P. I. Ravikovitch, D. Wei, W. T. Chueh, G. L. Haller and A. V. Neimark, *Journal of Physical Chemistry B*, **101** (1997) 3671-3679
[13] R. L. Augustine in *Heterogeneous Catalysis for the Synthetic Chemist*, (1996) Marcel Dekker, USA, 195.
[14] T. Christie, B. Thompson and B. Brathwaite, *Institute of Geological and Nuclear Sciences*, Table 2
[15] S. Narayanan and K. Deshpande, *Applied Catalysis a-General*, **199** (2000) 1-31
[16] A. Szegedi, Z. Konya, D. Mehn, E. Solymar, G. Pal-Borbely, Z. E. Horvath, L. P. Biro and I. Kiricsi, *Applied Catalysis a-General*, **272** (2004) 257-266
[17] M. Karthik, A. K. Tripathi, N. M. Gupta, A. Vinu, M. Hartmann, M. Palanichamy and V. Murugesan, *Applied Catalysis a-General*, **268** (2004) 139-149
[18] A. Corma, M. J. Diaz-Cabanas, F. Rey, S. Nicolooulas and K. Boulahya, *Chemical Communications*, (2004) 1356-1357
[19] C. E. Webster, R. S. Drago and M. C. Zerner, *Journal of Physical Chemistry B*, **103** (1999) 1242-1249
[20] M. W. Anderson and J. Klinowski, *Journal of the American Chemical Society*, **112** (1990) 10-16
[21] I. Sobczak, M. Ziolek, M. Renn, P. Decyk, I. Nowak, M. Daturi and J. C. Lavalley, *Microporous and Mesoporous Materials*, **74** (2004) 23-36
[22] J.-H. Lee, J.-G. Kim, J.-K. Lee and J.-H. Kim, *Catalysis Today*, **87** (2003) 35-42
[23] T. Baba, Y. Tohjo, T. Takahashi, H. Sawada and Y. Ono, *Catalysis Today*, **66** (2001) 79-86
[24] N. U. Zhanpeisov, G. Martra, W. S. Ju, M. Matsuoka, S. Coluccia and M. Anpo, *Journal of Molecular Catalysis A: Chemical*, **201** (2003) 237-246
[25] Y. J. Li and C. Y. Liu, *Journal of Electroanalytical Chemistry*, **517** (2001) 117-120
[26] B. Biskup and B. Subotic, *Separation and Purification Technology*, **37** (2004) 17-31
[27] H. Van Bekkum, E. M. Flanigen, J. C. Jansen and R. P. Townsend, *Studies in Surface Science and Catalysis*, **58** (1991) 359-390
[28] L. Norena-Franco, I. Hernandez-Perez, P. Aguilar and A. Maubert-Franco, *Catalysis Today*, **75** (2002) 189-195
[29] K. S. Triantafyllidis, L. Nalbandian, P. N. Trikalitis, A. K. Ladavos, T. Mavromoustakos and C. P. Nicolaides, *Microporous and Mesoporous Materials*, **75** (2004) 89-100
[30] F. Boccuzzi, S. Coluccia, G. Martra and N. Ravasio, *Journal of Catalysis*, **184** (1999) 316-326
[31] I. Langmuir, *Journal of the American Chemical Society*, **38** (1916) 2221
[32] S. J. Gregg and K. S. W. Sing, *Adsorption, Surface Area and Porosity*, (1982) 54-211
[33] J. S. J. Hargreaves, *Crystallography Reviews*, **11** (2005) 21-34

[34] Y. Oumi, S. Nemoto, S. Nawata, T. Fukushima, T. Teranishi and T. Sano, *Materials Chemistry and Physics*, **78** (2002) 551-557
[35] R. Bulanek, B. Wichterlova, Z. Sobalik and J. Tichy, *Applied Catalysis B-Environmental*, **31** (2001) 13-25
[36] J. Sarkany, J. L. d'Itri and W. M. H. Sachtler, *Catalysis Letters*, **16** (1992) 241
[37] R. R. S. Reddy, S. L. Reddy, G. S. Reddy and B. J. Reddy, *Crystal Research and Technology*, **37** (2002) 485-490
[38] G. T. Palomino, P. Fisicaro, S. Bordiga, A. Zecchina, E. Giamello and C. Lamberti, *Journal of Physical Chemistry B*, **104** (2000) 4064-4073
[39] J. G. Mesu, *Host-Guest Chemistry of Zeolite-encaged Cu2+/Histidine complexes, Utrecht University -PhD Thesis* (2005) 121-144
[40] J. Sarkany, *Journal of Molecular Structure*, **410-411** (1997) 137-140
[41] M. Guisnet, P. Magnoux and D. Martin in *Roles of acidity and pore structure in the deactivation of zeolites by carbonaceous deposits*, **111** (1997) ELSEVIER SCIENCE PUBL B V, Amsterdam, 1-19.
[42] M. Guisnet and P. Magnoux, *Applied Catalysis*, **54** (1989) 1-27
[43] L. D. Rollmann and D. E. Walsh, *Journal of Catalysis*, **56** (1979) 139-140
[44] M. Guisnet and P. Magnoux, *Applied Catalysis A-General*, **212** (2001) 83-96
[45] A. deLucas, P. Canizares, A. Duran and A. Carrero, *Applied Catalysis A-General*, **156** (1997) 299-317
[46] M. Guisnet, *Journal of Molecular Catalysis a-Chemical*, **182** (2002) 367-382
[47] M. Guisnet and P. Magnoux, *Catalysis Today*, **36** (1997) 477-483
[48] A. P. Antunes, M. F. Ribeiro, J. M. Silva, F. R. Ribeiro, P. Magnoux and M. Guisnet, *Applied Catalysis B-Environmental*, **33** (2001) 149-164
[49] D. R. Armstrong, C. Cameron, D. C. Nonhebel and P. G. Perkins, *Journal of the Chemical Society-Perkin Transactions 2*, (1983) 563-568
[50] T. G. Stone and W. A. Waters, *Journal of the Chemical Society*, **1** (1964) 213
[51] I. Flemming in *Frontier Orbitals and Organic Chemical Reactions*, (1976) Wiley, London, 195.
[52] F. H. Allen, *Acta Crystallogr., B*, **58** (2002) 380-388
[53] V. R. Choudhary and T. V. Choudhary, *Chemical Engineering Science*, **52** (1997) 3543-3552
[54] M. Ghiaci, A. Abbaspur, R. Kia and F. Seyedeyn-Azad, *Separation and Purification Technology*, **40** (2004) 217-229
[55] H. Fujiyama, I. Kohara, K. Iwai, S. Nishiyama, S. Tsuruya and M. Masai, *Journal of Catalysis*, **188** (1999) 417-425
[56] N. Roostaei and F. H. Tezel, *Journal of Environmental Management*, **70** (2004) 157-164
[57] Y.-H. Shen, *Colloids and Surfaces A: Physicochemical and Engineering Aspects*, **232** (2004) 143-149
[58] D. W. Ming and J. B. Dixon, *Clays and clay minerals*, **35** (1987) 463-468
[59] G. M. Haggerty and R. S. Bowman, *Environmental Science & Technology*, **28** (1994) 452-458
[60] T. Beutel, M. J. Peltre and B. L. Su, *Colloids and Surfaces A-Physicochemical and Engineering Aspects*, **187** (2001) 319-325
[61] J. Perez-Ramirez, G. Mul, F. Kapteijn, J. A. Moulijn, A. R. Overweg, A. Domenech, A. Ribera and I. Arends, *Journal of Catalysis*, **207** (2002) 113-126
[62] I. Kohara, H. Fujiyama, K. Iwai, S. Nishiyama and S. Tsuruya, *Journal of Molecular Catalysis A: Chemical*, **153** (2000) 93-101
[63] J. S. Reddy, P. Liu and A. Sayari, *Applied Catalysis A: General*, **148** (1996) 7-21
[64] G. V. Smith, R. Song and J. R. E. Malz, *Catalysis of Organic Reactions*, (1988) 335-342
[65] R. F. Dalton, D. A. Dowden and G. H. Lang, *Imperial Chemical Industries Limited*, (1971) GB1377213
[66] R. D. Gillard and D. P. J. Hall, *Chemical Communications*, (1988) 1163-1164
[67] Y. Soma, M. Soma and I. Harada, *Journal of Physical Chemistry*, **89** (1985) 738-742

[68] M. J. Tricker, D. T. B. Tennakoon, J. M. Thomas and S. H. Graham, *Nature*, **253** (1975) 110-111
[69] P. J. Baesjou, W. L. Driessen, G. Challa and J. Reedijk, *Journal of the American Chemical Society*, **119** (1997) 12590-12594
[70] H. Finkbeiner, A. S. Hay, H. S. Blanchard and G. F. Endres, *Journal of Organic Chemistry*, **31** (1966) 549
[71] C. C. Price and K. Nakaoka, *Macromolecules*, **4** (1971) 363-&
[72] E. Tsuchida, M. Kaneko and H. Nishide, *Makromol Chem*, **151** (1972) 221
[73] J. Kresta, A. Tkac, R. Prikryl and L. Malik, *Makromol Chem*, **176** (1975) 157
[74] P. J. Baesjou, W. L. Driessen, G. Challa and J. Reedijk, *Journal of Molecular Catalysis A-Chemical*, **110** (1996) 195-210
[75] H. Turk and Y. Cimen, *Journal of Molecular Catalysis A: Chemical*, **234** (2005) 19-24
[76] W. G. B. Huysmans and W. A. Waters, *Journal of Chemistry Society, B*, (1967) 1163
[77] M. Kubota, A. Shiga, H. Higashimura, K. Fujisawa, Y. Moro-oka, H. Uyama and S. Kobayashi, *Bulletin of the Chemical Society of Japan*, **77** (2004) 813-818
[78] H. Higashimura, K. Fujisawa, M. Kubota and S. Kobayashi, *Journal of Polymer Science Part a-Polymer Chemistry*, **43** (2005) 1955-1962
[79] P. Gamez, C. Simons, R. Steensma, W. L. Driessen, G. Challa and J. Reedijk, *European Polymer Journal*, **37** (2001) 1293-1296
[80] T. N. Das, *Journal of Physical Chemistry: A*, **105** (2001) 5954-5959
[81] H. Pal and T. N. Das, *Journal of Physical Chemistry A*, **107** (2003) 5876-5877
[82] M. V. Landau, S. B. Kogan, D. Tavor, M. Herskowitz and J. E. Koresh, *Catalysis Today*, **36** (1997) 497-510
[83] W. J. Mortier in *Complication of Extra Framework Sites in Zeolites*, (1982) Butterworth, London.
[84] B. C. Gates, L. Guczi and H. Knozinger, *Studies in Surface Science and Catalysis, Metal Clusters in Catalysis*, **29** (1986) 357-414
[85] A. T. Aguayo, A. G. Gayubo, J. Ortega, M. Olazar and J. Bilbao, *Catalysis Today*, **37** (1997) 239-248
[86] C. N. Satterfield, *Heterogeneous Catalysis in Industrial Practice*, (1991) 209-266
[87] G. Girotti, F. Rivetti, S. Ramello and L. Carnelli, *Journal of Molecular Catalysis A: Chemical*, **204-205** (2003) 571-579
[88] S. C. Larsen, A. Aylor, A. T. Bell and J. A. Reimer, *Journal of Physical Chemistry*, **98** (1994) 11533-11540
[89] R. N. Yong, S. Desjardins, J. P. Farant and P. Simon, *Applied Clay Science*, **12** (1997) 93-110
[90] A. de Lucas, P. Canizares and A. Duran, *Applied Catalysis A: General*, **206** (2001) 87-93
[91] J. Das and A. B. Halgeri, *Applied Catalysis a-General*, **194** (2000) 359-363
[92] J. H. Clark, A. P. Kybett and D. J. Macquarrie, *Supported Reagents, Preparation, Analysis and Applications*, (1992) 49-53, 58, 59, 73-75
[93] H. Hayashibara, S. Nishiyama, S. Tsuruya and M. Masai, *Journal of Catalysis*, **153** (1995) 254-264
[94] N. Idaka, S. Nishiyama and S. Tsuruya, *Physical Chemistry Chemical Physics*, **3** (2001) 1918-1924
[95] J. Xu, M. Ekblad, S. Nishiyama, S. Tsuruya and M. Masai, *Journal of the Chemical Society-Faraday Transactions*, **94** (1998) 473-479
[96] S. Sueto, S. Nishiyama, S. Tsuruya and M. Masai, *Journal of the Chemical Society-Faraday Transactions*, **93** (1997) 659-664
[97] K. R. Reddy, K. Ramesh, K. K. Seela, V. V. Rao and K. V. R. Chary, *Catalysis Communications*, **4** (2003) 112-117
[98] R. F. Parton, J. M. Jacobs, H. V. Ooteghem and P. A. Jacobs, *Studies in Surface Science and Catalysis*, (1989) 163
[99] J. W. Niemantsverdriet in *Spectroscopy in Catalysis, An Introduction*, (1995) VCH Verlagsgesellschaft mbH, Weinheim, 288.

[100] H. H. Willard, L. L. J. Merritt, J. A. Dean and F. A. J. Settle in *Instrumental Methods of Analysis*, (1988) Wadsworth Publishing Company, Belmont, California.
[101] J. Wills in *Cary, Praying Mantis Accessory Instructuion Manual*, (1992) Varian.
[102] R. G. Heidenreich, E. G. E. Krauter, J. Pietsch and K. Kohler, *Journal of Molecular Catalysis A-Chemical*, **182** (2002) 499-509
[103] G. Christian in *HPLC Tips and Tricks*, (1990) Alden Press, Oxford.
[104] Waters in *Waters 717plus Autosampler, Operator's Manual*, (1993) Waters Corporation, USA.
[105] tsp in *SpectraSYSTEM UV/Vis Detectors, Reference Manual*, (1994) Thermo Separation Products Inc., USA.
[106] I. Wilson, C. Poole and M. Cooke in *Encyclopedia of Separation Science*, (2000) Academic Press.
[107] S. P. Verevkin, *Journal of Chemical Thermodynamics*, **30** (1998) 389-396
[108] B. O. Hincapie, L. J. Garces, S. Gomez, R. Ghosh and S. L. Suib, *Catalysis Today*, **110** (2005) 323-329
[109] C. H. Giles, T. H. MacEwan, S. N. Nakhwa and D. Smith, *Journal of the Chemical Society*, (1960) 3973
[110] E. G. Derouane (Ed.) in *A Molecular View of Heterogeneous Catalysis, Proceedings of the First Francqui Colloquium*, (1996) DeBoeck Universite, Brussels.
[111] G. L. Marra, A. N. Fitch, A. Zecchina, G. Ricchiardi, M. Salvalaggio, S. Bordiga and C. Lamberti, *Journal of Physical Chemistry B*, **101** (1997) 10653-10660
[112] A. N. Fitch, H. Jobic and A. Renouprez, *Journal of Physical Chemistry*, **90** (1986) 1311
[113] D. F. Shriver and P. W. Atkins in *Inorganic Chemistry*, (1999) Oxford University Press, Belgium.
[114] B. Velde in *Introduction to Clay Minerals*, (1992) Chapman and Hall, Cambridge, 198.
[115] A. Biffis, M. Gardan and B. Corain, *Journal of Molecular Catalysis A-Chemical*, **250** (2006) 1-5
[116] R. A. Schoonheydt, *Catalysis Reviews-Science and Engineering*, **35** (1993) 129-168
[117] J. Dedecek, Z. Sobalik, D. Tvaruzkova, D. Kaucky and B. Wichterlova, *Journal of Physical Chemistry*, **99** (1995) 16327-16337
[118] J. M. Thomas and W. J. Thomas in *Principles and Practice of Hetergeneous Catalysis*, (1997) VCH, Germany.
[119] B. Cornils, W. A. Herrmann, R. Schlogl and C.-H. Wong, *Catalysis from A to Z: A Concise Encyclopedia*, 124, 163, 419, 635-639
[120] M. O. Adebajo, M. A. Long and R. L. Frost, *Spectrochimica Acta Part a-Molecular and Biomolecular Spectroscopy*, **60** (2004) 791-799